University of Strathclyde
Strathclyde Institute of Pharmacy and Biomedical Sciences

Determining the impact of neocortex size changes on information processing: Implications for neurodevelopmental disorders

Mirna Merkler

A thesis submitted in partial fulfilment of the requirements for the degree of Doctor of Philosophy

March 2021

Declaration of Authenticity and Author's Rights

This thesis is the result of the author's original research. It has been composed by the author and has not been previously submitted for examination which has led to the award of a degree.

Signed:  Date: 22.03.2021.

Acknowledgements

I would first like to thank my supervisor, Dr Shuzo Sakata, for giving me this opportunity and encouraging me to learn, be curious and grow as a scientist. All the advice and support over the years were truly invaluable. Many thanks also to our collaborator Prof. Nancy Ip for her inputs on the project and the posters.

I would also like to thank all the previous and current members of Sakata lab, especially Aimee Bias and Daniel Lynholm for the training in electrophysiological and surgical techniques, as well as the support when I first started programming in Matlab. Furthermore, Aimee Bias and Amisha Patel - my PhD experience would not be the same without you. Thank you for your words of encouragement, the everyday silly jokes and rants, and all the gaming sessions.

Additionally, I would like to thank my dear colleagues on the SIPBS 4th floor, especially Carolina Locatelli and Gines Martinez Cano. I am happy to have met you two amazing people at the very start and shared this whole journey with you. Thanks also goes to my friends in Croatia, my mom and my sister for their endless support through this endeavour.

An extra special thanks goes to Kristijan Ivančić for being my biggest cheerleader and moving to Scotland with me. I also really cannot thank you enough for motivating me to write my thesis during the lockdown and pandemic.

Finally, I would like to thank the BPU technical staff for their advice and help in care of the mice used in this project.

Abstract

Development of the cerebral cortex is highly regulated by genetically programmed sequential events. Alterations in this process by genetic or non-genetic factors can lead to over- or underproduction of cortical neurons and abnormal connectivity, resulting in neurodevelopmental disorders, such as autism spectrum disorder (ASD). Although ASD patients often exhibit atypical sensory processing, the relationship between abnormal cortical size and sensory processing is still unclear.

Here we hypothesise that abnormal cortical expansion during development leads to atypical sensory processing. To test this hypothesis, we utilized a recently established mouse model, in which the number of superficial cortical excitatory neurons is increased pharmacologically during embryonic development. This mouse model is also known to exhibit macrocephaly and autism-like phenotypes. In this project, we assessed their auditory perception behaviourally and evaluated neuronal population activity in the auditory cortex and medial geniculate nucleus through high-density *in vivo* electrophysiological recording.

Our results indicate that the overproduction of superficial cortical excitatory neurons negatively affects auditory processing. Treated mice exhibited hyposensitivity to near-threshold auditory stimuli during behavioural auditory detection assessment. Further, their cortical neurons showed lower spontaneous and auditory evoked activity as well as delayed peak response latency. We also observed atypical cortical functional connectivity.

Overall, our study suggests that abnormal cortical expansion during development results in atypical auditory processing, and provides further insights into the neural basis of perceptual deficits in neurodevelopmental disorders such as ASD.

Table of contents

List of figures and tables

List of abbreviations

A1	Primary auditory cortex
AAF	Anterior auditory field
ABR	Auditory brainstem responses
ASD	Autism spectrum disorder
CCG	cross-correlogram
CGE	Caudal ganglionic eminence
CN	Cochlear nucleus
CP	Cortical plate
CSD	Current source density
DAPI	4’,6-diamidino-2-phenylindole
DAQ	Data aquisition board
dB	Decibel
DTI	Diffusion tensor imaging
E9,11...	Embryonic day 9, 11...
E-I	Excitatory-inhibitory
EEG	Electroencephalograpy
EMG	Electromyography
ERP	Event-related potentials
FA	False alarm
fMRI	Functional magnetic resonance imaging
GW	Gestational week

HC	Head circumference
IC	Inferior colliculus
IPs	Intermediate progenitors
iPSCs	Induced pluripotent stem cells
IZ	Intermediate zone
L I,II/III...	Cortical layer 1, 2/3...
LFP	Local field potential
LLN	Nuclei of the lateral lemniscus
MEG	Magnetoencephalography
MGB	Medial geniculate body/nucleus
MGE	Medial ganglionic eminence
MIA	Maternal immune activation
MUA	Multi-unit activity
MZ	Marginal zone
NPCs	Neural progenitor cells
P2,21...	Postnatal day 2, 21...
PBS	Phosphate buffered saline
PBST	Phosphate buffered saline with Triton-X
PCs	Principal component space
PFA	Paraformaldehyde
POA	Preoptic area
PSTH	Peristimulus time histogram

SNR	Signal to noise ratio
SOC	Superior olivary complex
SUA	Single-unit activity
SVZ	Subventricular zone
VPA	Valproic acid
VZ	Ventricular zone

1. Introduction

In the course of mammalian evolution, brain size has significantly changed. The most drastic increase was in the cerebral cortex, caused by the emergence and expansion of superficial cortical layers (Finlay and Darlington, 1995; Smart, 2002; Mihrshahi, 2006; Herculano-Houzel *et al.*, 2007, 2014; Herculano-Houzel, 2009). This growth in the number of cortical neurons and their high density is correlated with higher information processing demands (Herculano-Houzel *et al.*, 2007; Collins *et al.*, 2010; Olkowicz *et al.*, 2016).

Although this expansion is evolutionarily advantageous, on the scale within human species increased number of neurons can cause macrocephaly (Vaccarino *et al.*, 2009), which is often found in neurodevelopmental disorders such as autism (Fombonne *et al.*, 1999; Fatemi *et al.*, 2002; Lainhart *et al.*, 2006; Brunetti-Pierri *et al.*, 2008). In autism spectrum disorder (ASD) sensory perception abnormalities are very common (Marco *et al.*, 2011; Robertson and Baron-Cohen, 2017). Differences in sensory processing may actually cause core features of autism, such as language delay and difficulty with reading emotion from faces (Rapin and Dunn, 2003; Bonnel *et al.*, 2010).

This brings us to the key questions of this project: is there a connection between increased cortical size and sensory processing abnormalities in ASD? Could an increase in the number of neurons cause changes in neural activity and connections, leading to sensory difficulties such as auditory perception?

To understand how and when can human brain enlarge abnormally, we will first need to look at brain development and specific processes it includes. Then, I will give an overview of ASD and summarize the studies on sensory processing in ASD. Since we are looking at auditory processing specifically, chapter 1.3. will describe the layout of the auditory pathway as well as functions of auditory areas, with a primary focus on the auditory cortex. Further, I will summarize the methods for assessing sensory

perception and techniques for examining neural activity. Finally, in chapter 1.6. I will lay out the hypothesis and aims of this thesis.

1.1. Neurodevelopment and cortical expansion in mammals

In this subchapter, I will define the main events during neurodevelopment and go through the timeline of these events in humans and mice. Then, I will talk about the cortical expansion that occured in mammalian evolution and the potential mechanisms driving this expansion. Finally, I will describe some of the signalling pathways involved in neurodevelopment, and identify their potential roles in cortical size abnormalities.

1.1.1. Brain development

Brain development in humans starts *in utero*, with the formation of the neural tube in the 3rd gestational week (GW3) (Stiles and Jernigan, 2010; Budday *et al.*, 2015; Jiang and Nardelli, 2016). A single layer of neural progenitor cells (NPCs) is lining the hollow neural tube. As the embryo develops further, the cavity inside of the neural tube becomes more complex, eventually forming ventricles. The epithelial tissue that surrounds the ventricles, rich with NPCs is called the ventricular zone (VZ). The role of these cells and VZ in the production of neurons (neurogenesis) will be explained in more details later in this chapter. Neurogenesis in humans starts in GW6, marking as well the onset of cerebral cortex development (corticogenesis)(Stiles and Jernigan, 2010; Lui *et al.*, 2011; Budday *et al.*, 2015).

By GW4, the two hemispheres of the brain are formed and neural tube expands into three vesicles, prosencephalon, mesencephalon and rhombencephalon, precursors of the forebrain, midbrain and hindbrain (Figure 1.1.). These vesicles further divide by GW7, forming telencephalon and diencephalon from prosencephalon, and metencephalon and myelencephalon from rhombencephalon. All major compartments of the nervous system are outlined by GW8 (Stiles and Jernigan, 2010).

Development of a healthy brain is dependent on gene expression as well as inputs from the environment (Jiang and Nardelli, 2016). Since the brain develops in the caudo-rostral direction, the prefrontal cortex is the last region of the brain to develop, which occurs well into adulthood (Huttenlocher, 1990; Huttenlocher and Dabholkar, 1997; Teffer and Semendeferi, 2012).

The main events of brain development during embryogenesis are preserved across mammalian species (Workman *et al.*, 2013). In mice, which are the most commonly used experimental animal model and the model used in this project, the neural tube formation onset is around embryonic day 9 (E9) (Goffinet and Rakic, 2000; Semple *et al.*, 2013), while corticogenesis starts around E11 and continues until the end of gestation (around E19) (Dehay and Kennedy, 2007).

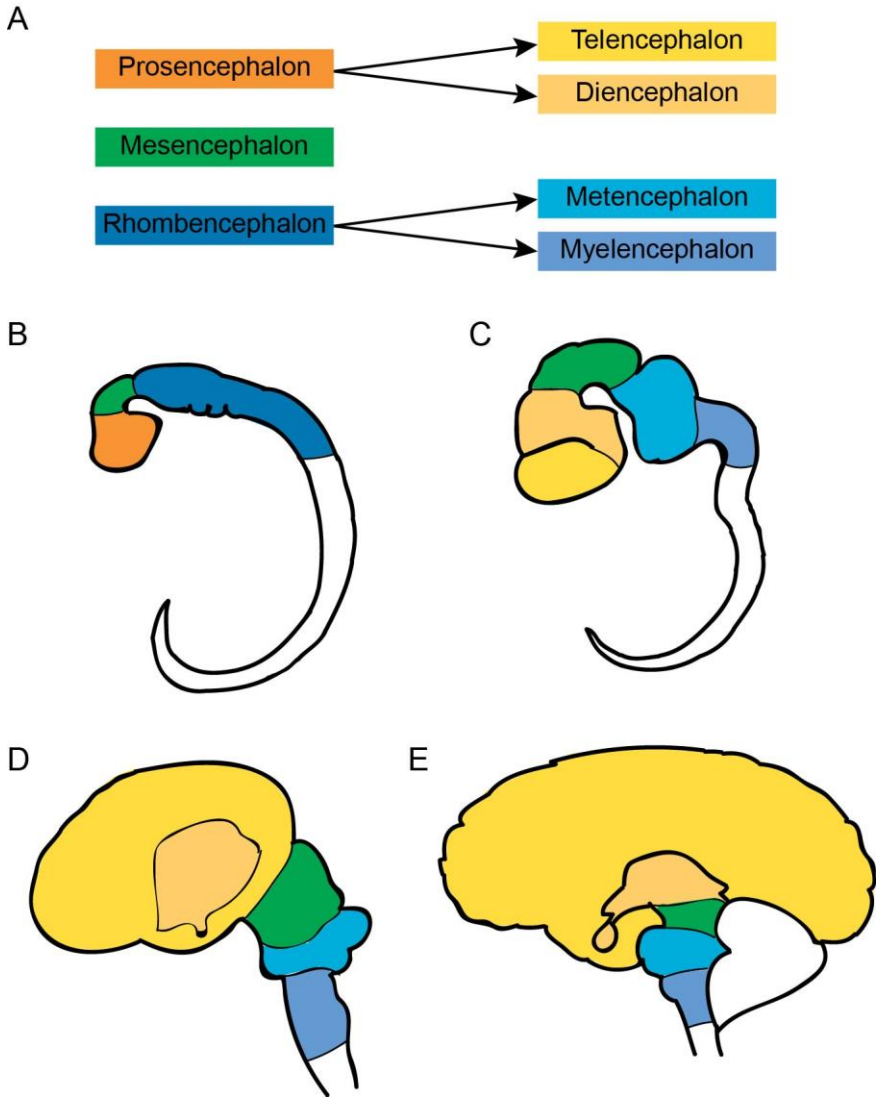

Figure 1.1. Human brain development. **A**- Schematics of three initial embryonic brain regions splitting into five. **B**- Embryonic brain at GW4 (3 vesicles + spinal cord). **C**- Brain of an embryo at GW7 (5 vesicles + spinal cord). **D**- Brain at GW13 (cortex is in development). **E**- Human brain around birth (~GW40). Brain regions in B-E are colour-coded according to A.

1.1.2. Neurogenesis and corticogenesis

Production of neurons, or neurogenesis, is regulated by the rate of amplification and differentiation of NPCs. In the cortex, two main types of neurons are excitatory glutamatergic pyramidal neurons (~80%) and inhibitory GABAergic interneurons (~20%) (Markram *et al.*, 2008a; Harris and Shepherd, 2015).

Excitatory neurons of the cerebral cortex are generated in the proliferative zones of the dorsal telencephalon (pallium) from two types of NPCs, radial glial cells (RGs) and intermediate progenitor cells (IPs) (Figure 1.2.) (Molyneaux *et al.*, 2007; Fame *et al.*, 2011; Greig *et al.*, 2013). Radial glial cells are located in the VZ and they divide asymmetrically into a radial glial cell and an intermediate progenitor cell. In some cases, RGs divide into a radial glial cell and a neuron. Intermediate progenitor cells then migrate to subventricular zone (SVZ) where they divide symmetrically for several cycles, producing more IPs, before eventually differentiating into neurons. The balance between amplification of IPs and their differentiation into neurons is therefore crucial for the production of the correct amount of neurons and formation of the cerebral cortex, and it requires spatiotemporal coordination (Fang *et al.*, 2013; Flore *et al.*, 2016).

In primates, SVZ can be divided into inner and outer subventricular zone (iSVZ and oSVZ). It is considered that the emergence of oSVZ is responsible for the increased production of supragranular neurons in the primate cortex (Lui *et al.*, 2011; Dehay *et al.*, 2015; Kennedy *et al.*, 2021).

Neurons use radial glial cells as a scaffold to migrate through the intermediate zone (IZ) and form the cortical plate (CP) above it (Molyneaux *et al.*, 2007; Stiles and Jernigan, 2010; Fame *et al.*, 2011; Greig *et al.*, 2013). They migrate in an inside-out gradient, forming the laminar structure of the cortex. First layers created form the

pre-plate, which is the first stage of corticogenesis, prior to the formation of the cortical plate. As cortical plate appears, the pre-plate is split into the outer marginal zone (MZ) and an inner subplate (SP), with the cortical plate in between the two. New neurons formed later on migrate in a radial fashion, past the neurons already in the cortical plate and settle just beneath the marginal zone (MZ). After neurogenesis is completed, NPCs differentiate into glial cells (astocytes and oligodendrocytes) (Alvarez-Buylla *et al.*, 2001; Greig *et al.*, 2013; Yamaguchi *et al.*, 2016).

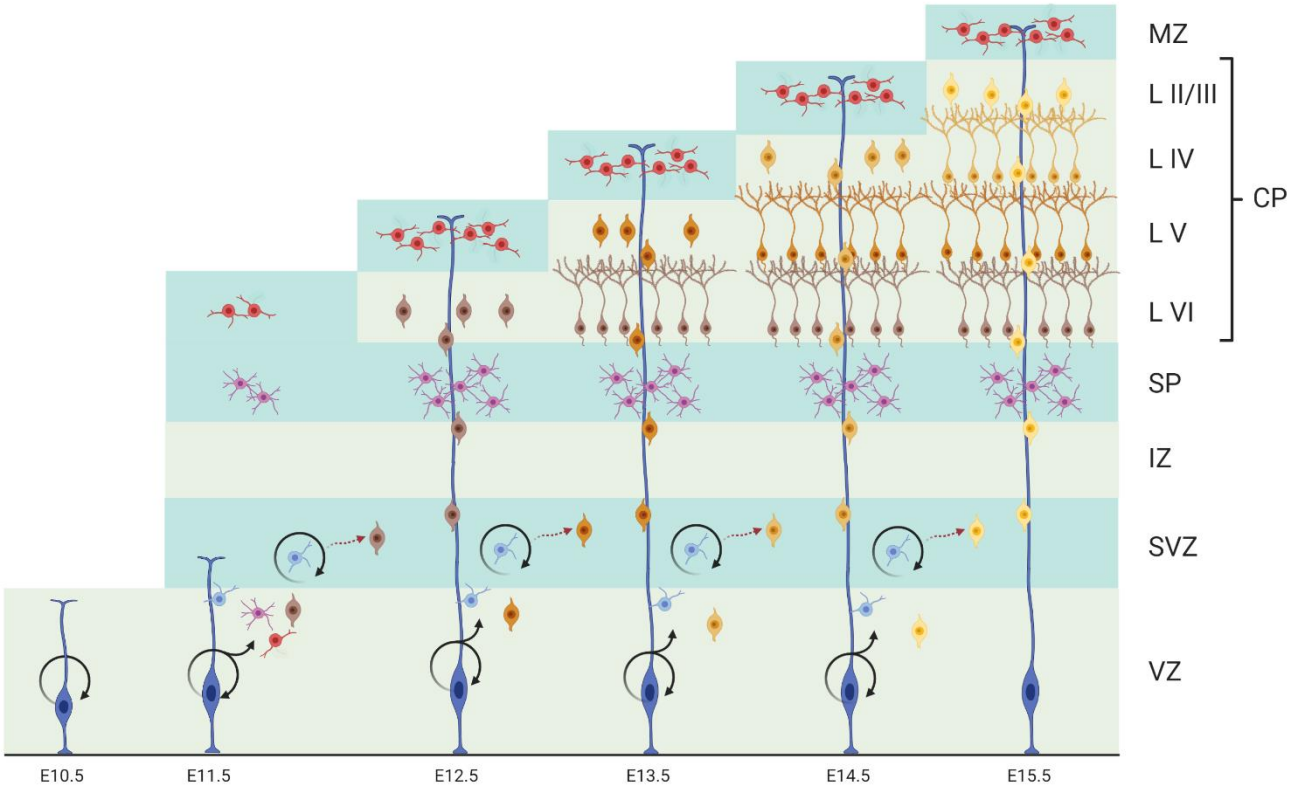

Figure 1.2. Overview of the neurogenesis in the mouse neocortex. Around E11.5 radial glial cells (dark blue) in the ventricular zone start dividing asymmetrically, producing more radial glia as well as intermediate progenitor cells (light blue), subplate neurons (purple) and Cajal-Retzius cells (red). CR cells settle in MZ. IP cells migrate to SVZ, where they amplify and differentiate into neurons (dark brown). Newborn neurons (generated from RGs or IPs) migrate from VZ or SVZ along the RG fibres, forming the layers of the cerebral cortex. The oldest neurons (dark brown) settle in layer VI, while the newest (yellow) form layer II/III. Layer I develops from MZ. VZ – ventricular zone, SVZ – subventricular zone, IZ – intermediate zone, SP – subplate, CP – cortical plate, MZ – marginal zone, L VI-II/III – cortical layers. Time on the bottom of the figure: embryonic day (E) 10.5-15.5.

Cortical inhibitory neurons are born from progenitor cells in the ventral telencephalon (subpallium), more specifically from the medial ganglionic eminence (MGE), caudal ganglionic eminence (CGE) and preoptic area (POA) (Figure 1.3.) (Anderson *et al.*, 1997; Lim *et al.*, 2018). These three regions generate different types of interneurons, and their high diversity is a result of various transcriptional programs (Lim *et al.*, 2018; Mayer *et al.*, 2018). According to their morphological, biochemical and electrophysiological properties interneurons can be divided into three major classes: parvalbumin expressing (PV+), somatostatin expressing (SST+) and serotonin receptor 3a expressing (5HT3aR+) cells (Rudy *et al.*, 2011; Tremblay *et al.*, 2016). PV+ and SST+ are produced in the POA and MGE, while 5HT3aR+ are generated in CGE. In the MGE, progenitor cells first produce SST+ followed by PV+. Similar to excitatory neurons, most of the interneurons also follow an inside-out gradient to populate the cortex, so their laminar distribution is dependent on the time of neurogenesis (Valcanis and Tan, 2003; Rymar and Sadikot, 2007; Lim *et al.*, 2018).

Interneurons migrate in a tangential fashion towards neocortex via two routes, one leading through MZ, used by most interneurons, and the other one through SVZ (Marín and Rubenstein, 2001; Wichterle *et al.*, 2001; Lim *et al.*, 2018). After pyramidal cells form a certain cortical layer, interneurons migrate into it radially. Interneuronal radial migration onset and final location are suspected to be influenced by intrinsic mechanisms as well as molecular signals coming from pyramidal cells (Inamura *et al.*, 2012).

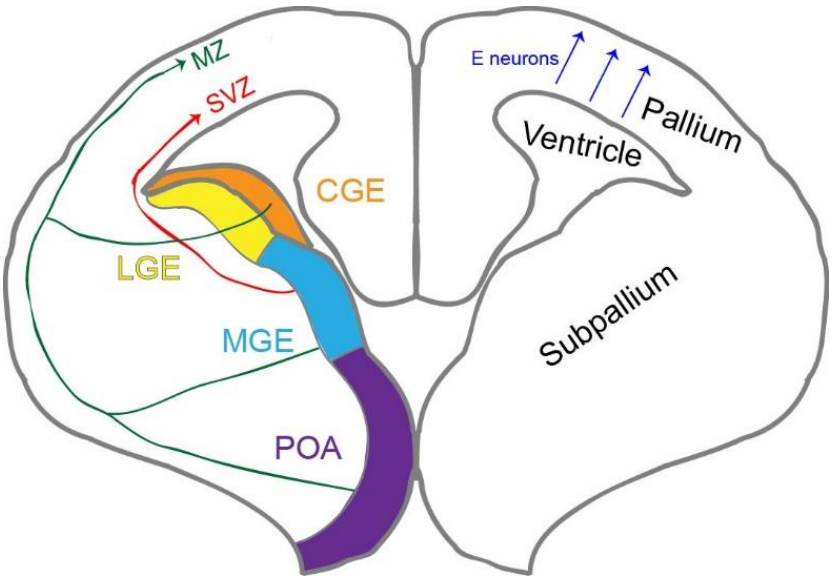

Figure 1.3. Emergence and migration of cortical excitatory and inhibitory neurons in the developing mouse brain. The left half of the brain shows inhibitory pathways. Excitatory neurons are produced in the pallium and migrate radially to the cortical plate (blue arrows). Inhibitory neurons are generated in the subpallium and migrate tangentially, following two routes ending in MZ or SVZ of the developing cortex (green and red arrows). MZ – marginal zone, SVZ – subventricular zone, LGE – lateral ganglionic eminence, CGE – caudal ganglionic eminence, MGE – medial ganglionic eminence, POA – preoptic area.

At the end of corticogenesis, the neocortex is composed of 6 layers (Figure 1.4.). Layer I, which develops from the marginal zone, and layer VI, the earliest developed from the cortical plate, contain the oldest neurons (Stiles and Jernigan, 2010; Greig *et al.*, 2013). Subplate neurons largely disappear though apoptosis, while the rest form interstitial cells in the white matter or integrate into layer VI (Torres-Reveron and Friedlander, 2007; Marx *et al.*, 2015). The remaining layers follow the inside-out gradient, layer V being the oldest after layer I and VI, and layer II being the most recent. The six-layered cortex is also divided into functionally defined cortical areas based on their distinct cytoarchitectural organization, called Brodmann areas (Falk and Gibson, 2001). Each of these areas is in charge of specific cognitive and behavioural functions.

During neurogenesis and corticogenesis, more neurons are produced than is ultimately needed, thus causing neurons to go through apoptosis during the early postnatal period. In mice, excitatory neurons first go through apoptotic wave between P2 and P5, followed by inhibitory neurons from P7 to P8 (Wong *et al.*, 2018). Remaining cortical neurons undergo dendritic pruning, thus eliminating unused and weak synapses (Stiles and Jernigan, 2010; Semple *et al.*, 2013; Budday *et al.*, 2015). This results in an increase in their response efficiency and specialization. Remaining connections are further strengthened through myelination, allowing quicker and more efficient progression of neural signals. In humans, most of the brain wiring is established before birth (Ball *et al.*, 2014; Qiu *et al.*, 2015; van den Heuvel *et al.*, 2015). Rapid human brain maturation through grey-matter growth and myelination occurs during the first 2 years (Gilmore *et al.*, 2018). Afterwards, the brain matures at a slower pace.

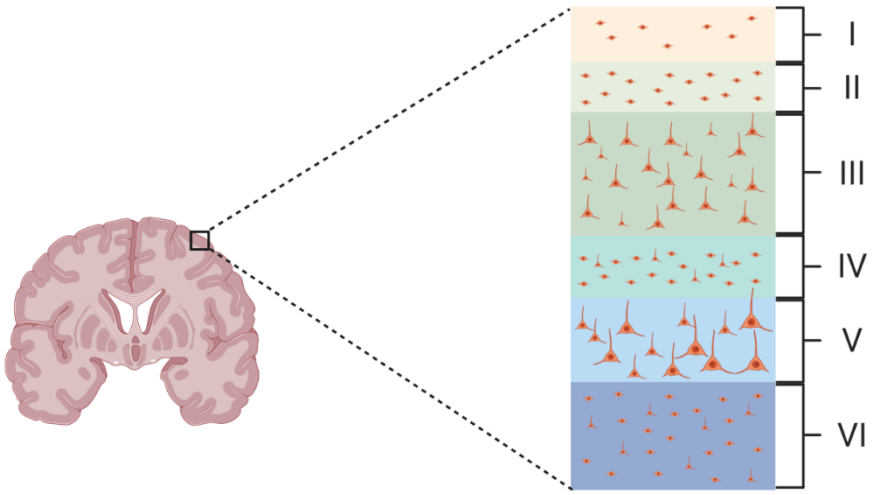

Figure 1.4. Layers of the cerebral cortex (adapted from (Ranson and Clark, 1959)).

1.1.3. Evolutionary cortical expansion

Cerebral cortex is vital for higher-order functions such as perception, cognition, memory and language (O'Rahilly and Müller, 2008; Friederici, 2011; Roth and Dicke, 2012; Teffer and Semendeferi, 2012). In humans, cortex makes up to ~80% of total brain mass (Herculano-Houzel, 2009; Van Essen *et al.*, 2018). As mentioned earlier,

there was a drastic increase in the size of the cerebral cortex during evolution (Figure 1.5.).

The six-layered cortex is a feature specific for mammals (Lui *et al.*, 2011). While reptiles have a three-layered cortex within the pallium, which is evolutionary related to mammalian cortical layers I, V and VI (Lui *et al.*, 2011; Molnár, 2011; Briscoe and Ragsdale, 2018), birds do not have cortical layers. However, neuronal circuitry in the avian pallium is similar to that of mammalian neocortex (Briscoe and Ragsdale, 2018). Cortical layers II and III are evolutionary new. They are indistinguishable in rodents, but dissimilar in primates (Fame *et al.*, 2011). These superficial layers have expanded considerably more during the evolution of mammals than the deep cortical layers (Smart, 2002; Mihrshahi, 2006; Molnár *et al.*, 2006). Their increase could be a consequence of the duration of neurogenesis, changes in cell cycle parameters or expression of genes in charge of neural growth or survival (Groszer *et al.*, 2001; Lukaszewicz *et al.*, 2005; Dehay and Kennedy, 2007; Pilaz *et al.*, 2009; Georgala *et al.*, 2011).

In the cortex, excitatory neurons can be divided into 3 subclasses depending on where they extend their axons: intratelencephalic (IT) neurons (projecting axons within the telencephalon), pyramidal tract (PT) neurons (projecting to subcerebral areas) and corticothalamic (CT) neurons (projecting to ipsilateral thalamus) (Harris and Shepherd, 2015). Some of the IT neurons are projecting to the contralateral cortex through corpus callosum or anterior commissure. These callosal projection neurons enable communication between 2 hemispheres of the mammalian cortex and have an important role in higher-order functions. Around 80% of callosal projection neurons are found in the superficial layers (LII and III) of the primate cortex, and if we compare their abundancy across mammalian species, they have gone through an extensive increase in numbers (Figure 1.5.) (Molyneaux *et al.*, 2007; Fame *et al.*, 2011). Therefore, it might be possible that these neurons in primates have gone through additional rounds in cell proliferation during embryonic cortical development (Rakic, 1995), causing the cortical expansion.

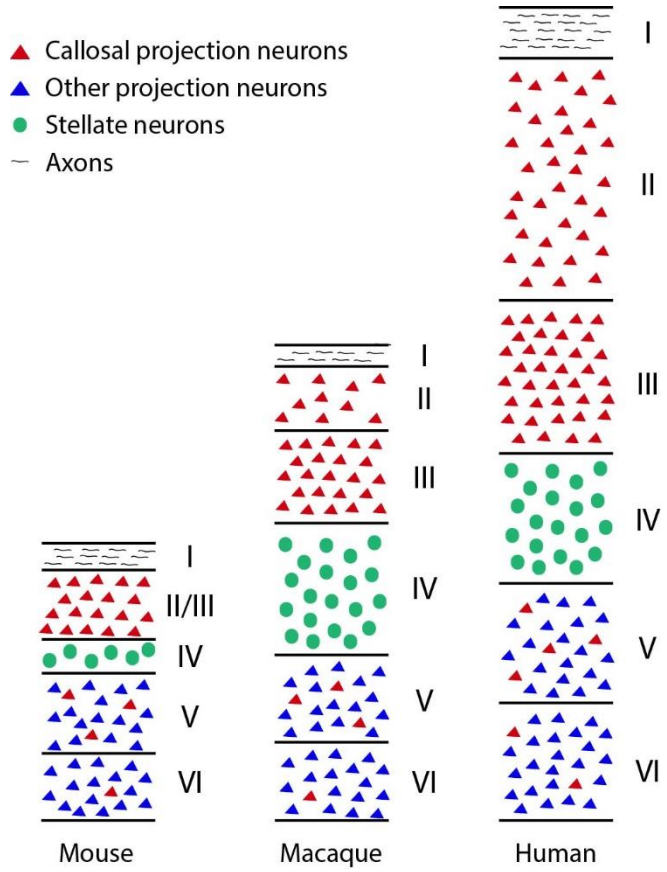

Figure 1.5. Schematic comparison of an adult mouse, macaque and human neocortex. I-VI represent cortical layers. Superficial layers of human neocortex have noticeably expanded and callosal projection neurons have increased in numbers. Adapted from (Molnár *et al.*, 2006; Fame *et al.*, 2011).

Large number of superficial cortical neurons and high cortical density has been suggested as the basis of increased cognitive abilities in mammals, which would be useful in complex social dynamics (Roth and Dicke, 2005; Olkowicz *et al.*, 2016; Herculano-Houzel, 2017). Primates were probably more efficient in hunting for food and defending from predators because they were able to communicate better (Barrett and Henzi, 2005). Reduced mortality could have caused longer sexually active periods and enhanced reproductive success of primates with larger cortex, therefore propagating this trait (Rakic, 1995). Cortical expansion was also associated with better visual acuity (Fang and Yuste, 2017), meaning a potential increase in information processing capacity (Dicke and Roth, 2016).

The volume of white matter also increases through evolution (Zhang and Sejnowski, 2000; Schoenemann *et al.*, 2005). In large mammalian brains, longer neuronal fibers are necessarry to connect the neurons.

To fit a larger number of neurons as well as a larger surface around subcortical nuclei, mammalian brains developed many gyri (folds) and sulci (grooves). This convolution of the cortex is a feature only of larger brains, such as those of chimpanzees and humans, while smaller mammals, such as rodents, have a smooth (lissencephalic) brain surface.

1.1.4. Signalling pathways in neurodevelopment

Brain development is highly complex, and many signalling pathways are involved in its regulation. Errors in control mechanisms of these pathways can cause abnormalities in neuronal production during brain development (Hidalgo and Ffrench-Constant, 2003; Jiang and Nardelli, 2016). Some of the neurodevelopmental signalling pathways I will mention here are Wnt/β-catenin, Hedgehog (Hh) and Retinoic Acid (RA), mainly because disruptions in these pathways are often found in ASD (Kumar *et al.*, 2019; Baranova *et al.*, 2020).

Hedgehog (Hh) signalling pathway has important regulatory roles in neurogenesis, neural phenotype determination, stem cell maintenance, cell cycling and apoptosis (Machold *et al.*, 2003; Gulino *et al.*, 2007; Belgacem *et al.*, 2016; Lu *et al.*, 2017; Antonelli *et al.*, 2019; Baranova *et al.*, 2020). Suppression of this pathway during embryogenesis is lethal, while abnormalities in it are known to cause severe birth defects.

Retinoic Acid (RA) signalling pathway is involved in neuronal patterning, proliferation, differentiation (specifically GABAergic, dopaminergic and motor neurons), and the establishment of neurotransmitter systems (Siegenthaler *et al.*, 2009; Webb, 2009; Podleśny-Drabiniok *et al.*, 2017; Zieger and Schubert, 2017; Kumar *et al.*, 2019; Baranova *et al.*, 2020). RA signalling depends on the concentrations of its precursor, retinol (vitamin A), and reductions in it can cause disruptions in RA signalling.

Wnt/β-catenin signalling pathway contains important regulatory molecules for neuronal development, including differentiation of NPCs, neuronal migration, dendritogenesis and synaptogenesis (Hirabayashi *et al.*, 2004; Teo *et al.*, 2005; Prasad and Clark, 2006; Srahna *et al.*, 2006; Zechner *et al.*, 2007; Munji *et al.*, 2011; Varela-Nallar and Inestrosa, 2013). This complex pathway is highly regulated and evolutionary preserved (Klaus and Birchmeier, 2008). It is usually divided into canonical, or β-catenin dependent pathway, and non-canonical pathway. Canonical Wnt pathway stabilizes β-catenin, a protein acting as a transcription factor and modulating the expression of target genes. It has been shown that overexpression of *Wnt3a* enhances the activity of β-catenin and causes premature IP differentiation, leading to cortical dysplasia (Otero *et al.*, 2004; Munji *et al.*, 2011). On the other hand, downregulation with pathway inhibitor *Dkk1* hinders neuronal production (Munji *et al.*, 2011). Additionally, stabilization of β-catenin in trangenic mice caused an increase in amplification of NPCs and an increase in the cerebral cortex size (Chenn and Walsh, 2002).

One of the regulatory molecules in Wnt/β-catenin pathway is axin. Axin has several important roles in neurogenesis. In vitro, axin was shown to regulate neuronal differentiation and morphogenesis. It has a role in axon formation, cytoskeletal regulation, as well as gene expression during neurogenesis (Heisenberg *et al.*, 2001; Guo *et al.*, 2008; Fang *et al.*, 2011, 2013; Ye *et al.*, 2015). Axin is also a scaffold protein for various proteins involved in neurogenesis (Luo and Lin, 2004) and it has been demonstrated to regulate proliferation and differentiation of IPs (Fang *et al.*, 2013), thus modulating developmental steps in corticogenesis. Recently, an experimental approach has been established for changing the cortical neuronal number in mice by manipulating levels of axin (Fang *et al.*, 2014; Fang and Yuste, 2017).

Axin controls the intermediate progenitor cell population during neurogenesis through regulation of β-catenin concentration (Figure 1.6.) (Fang *et al.*, 2013). In the presence of neurogenic signals (Wnt, RA or TGFβ), Cdk5 is activated and phosphorylates cytoplasmatic axin, triggering its translocation into the nucleus.

Reduction in cytoplasmatic axin causes an increase in β-catenin concentration and its transfer to the nucleus. In the nucleus, phosphorylated axin and β-catenin form a complex with TCF/Lef which initiates gene transcription and induces neuronal differentiation. Both axin and β-catenin are required in the nucleus of NPCs for the signal transduction of Wnt, RA and TGF-β to induce neuronal differentiation (Hirabayashi *et al.*, 2004; Otero *et al.*, 2004; Zhang *et al.*, 2010).

In the absence of neurogenic signals or in the presence of proliferating (e.g. Shh), β-catenin is first phosphorylated by CKIα (Liu *et al.*, 2002). It then forms a complex with axin, GSK-3β and APC, the β-catenin destruction complex. GSK-3β mediated phosphorylation of β-catenin triggers ubiquitin-directed proteolysis and β-catenin degradation. Thus, β-catenin mediated transcription and GSK-3β activity are inhibited, which stimulates Shh signalling and promotes amplification of intermediate progenitor cells.

Hence, we can suspect that overexpression of axin in the cytoplasm of NPCs would cause an increase in the concentration of β-catenin destruction complex, a rise in the amplification rate of IP cells and lead to macrocephaly. Several studies have reported this outcome when overexpressing axin through its degradation inhibition (Fang *et al.*, 2013, 2014; Fang and Yuste, 2017). Similarly, it was also shown that mutations in the GSK-3β axin-binding site result in microcephalic brains (Heisenberg *et al.*, 2001), plausibly through the inability to form the destruction complex. Further, axin knockdown results in a premature neuronal differentiation due to early cell-cycle exit, ultimately leading to a reduced number of neurons (Fang *et al.*, 2013).

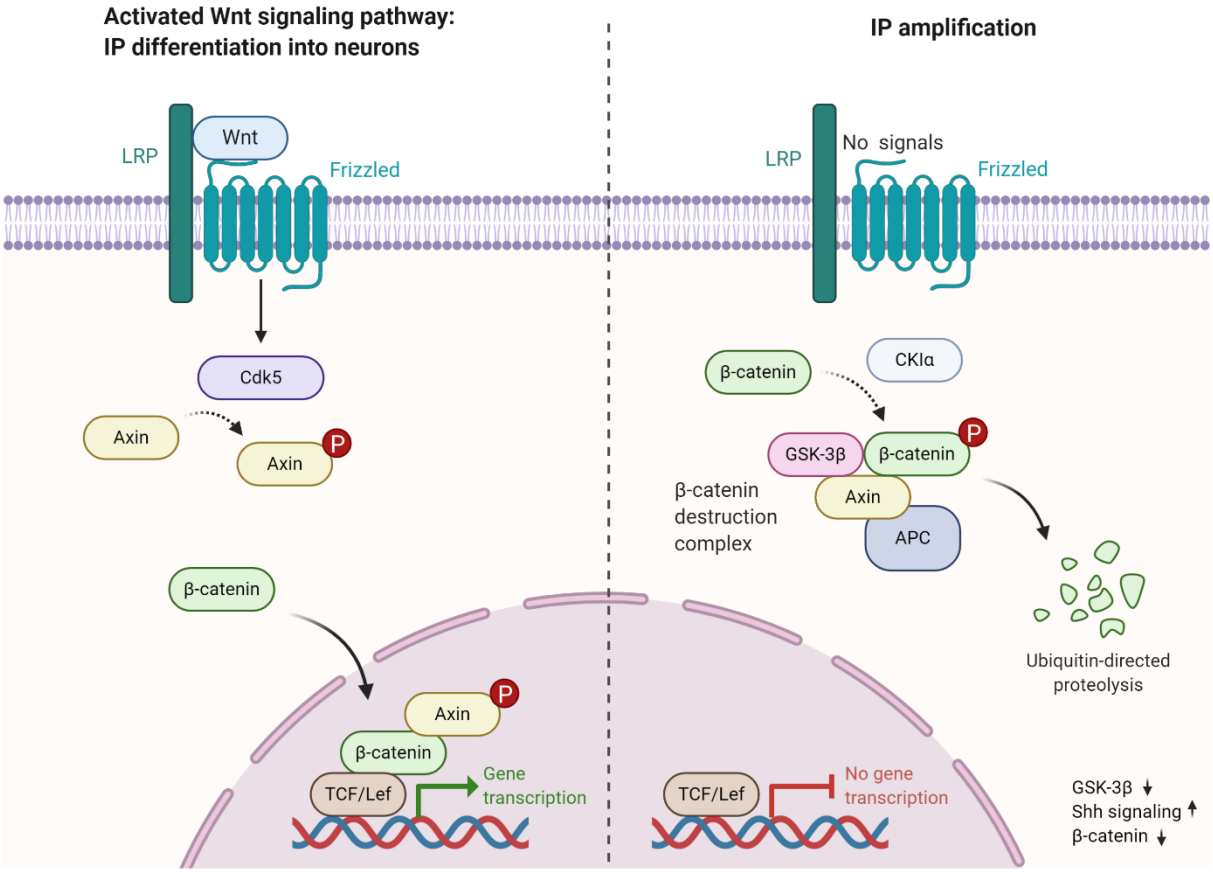

Figure 1.6. Axin dependent IP amplification and differentiation. The left side of the figure shows activated Wnt pathway, resulting in gene transcription and neuronal differentiation. The right side shows β-catenin proteolysis via β-catenin destruction complex activity, resulting in amplification of intermediate progenitor cells.

To summarize, proper control of neurogenesis is essential to ensure typical brain development. Minor changes in the amplification or differentiation ratio of IPs can lead to a shift in the number of neurons and therefore differences in the size of the cerebral cortex, causing micro- or macrocephaly (Caviness *et al.*, 1995, 2003; Rakic, 1995; Chenn and Walsh, 2002; Dehay and Kennedy, 2007; Vaccarino *et al.*, 2009; Gilmore and Walsh, 2013). Variation in neuronal number can lead to abnormal brain function and appearance of neurodevelopmental disorders, such as autism spectrum disorder (Fombonne *et al.*, 1999; Fatemi *et al.*, 2002; Brunetti-Pierri *et al.*, 2008; Fang *et al.*, 2014).

1.2. Autism spectrum disorder

During the 1940s, Drs. Leo Kanner and Hans Asperger first characterized autism as emotional and communication disorder different than schizophrenia, present in children from birth (Kanner, 1943; Asperger, 1944). In the present day, autism spectrum disorder (ASD) refers to a range of developmental disorders characterized by repetitive behaviour, abnormal sensory processing and difficulties in communication and social interaction (American Psychiatric Association, 2013). Disorder severity greatly varies, with some individuals exhibiting speech difficulties and language development delay, repetitive behaviour, theory of mind deficits, seizures, significant deviations in brain size or intellectual disability, while others have normal to even above average intelligence (Baron-Cohen *et al.*, 1985; Cain and Oakhill, 2007; Canitano, 2007; Richler *et al.*, 2007; Simonoff *et al.*, 2008; Esbensen *et al.*, 2009; Fein, 2011; Moran *et al.*, 2011; Rommelse *et al.*, 2015; Sacco *et al.*, 2015; Frye *et al.*, 2016). According to the 5th edition of Diagnostic and Statistical Manual of Mental Disorders from American Psychiatric Association (DSM-5), ASD includes childhood autism (autistic disorder), Asperger Syndrome and Pervasive Developmental Disorder not otherwise specified (PPD-NOS) (American Psychiatric Association, 2013). ASD is mostly diagnosed in early childhood, between 12 and 24 months of age, however, some people do not get diagnosed until adulthood (Johnson *et al.*, 2007; Pierce *et al.*, 2011, 2019; Russell *et al.*, 2011). Because diagnostic criteria changes frequently and the disorder has a very versatile phenotype, it is difficult to track its prevalence. According to the official national statistics, the prevalence of ASD in the UK in 2012 was 1.1%, with a higher occurrence in men than women (2% and 0.3%, respectively)(NHS, 2012). Since ASD is very heterogeneous in symptoms and the cause is still unknown, pharmacological treatment is currently focused on containing the most impairing individual symptoms, such as hyperactivity, aggression, repetitive behaviour and self-harming (Myers *et al.*, 2007; Posey *et al.*, 2008; Huffman *et al.*, 2011).

Most common early symptoms of ASD are abnormalities in sensory perception, occurring in infants as young as 6 months (Baranek *et al.*, 2013; Estes *et al.*, 2015).

Atypical sensory processing is also more prominent in families with higher genetic probability for autism, with several ASD occurrences within the family (Donaldson *et al.*, 2017). Further, studies have found changes in the neural circuitry of many primary sensory cortical areas, dedicated to perceptual processing (Marco *et al.*, 2012; Matsuzaki *et al.*, 2012; Robertson *et al.*, 2014). Since the neural basis of sensory processing is well studied and evolutionary conserved, investigating sensory processing in ASD has the potential to provide insights into differences in neural circuitry and origins of autistic features (Heeger *et al.*, 2017).

1.2.1. Sensory processing in ASD

Over 90% of children with ASD express hypo- or hypersensitivity to certain stimuli, most commonly sight, sound and touch (Dakin and Frith, 2005; Leekam *et al.*, 2007; Tomchek and Dunn, 2007; Ben-Sasson *et al.*, 2009; O'Connor, 2012; Tavassoli *et al.*, 2014; Mikkelsen *et al.*, 2018). Abnormal stimulus sensitivity is not unique to ASD, but it occurs more frequently than in other neurodevelopmental disorders. Since ASD as a disorder is very diverse, it is difficult to compare the studies on sensory abnormalities. Another drawback is that studies vary in patients age, gender, IQ and severity of the disorder, as well as research conditions and techniques used. Further, sensory processing is a sequence involving several levels: sensory input is transformed into electrical information, which is then transferred and processed in targeted brain regions. Abnormalities in any part of these pathways could lead to abnormal sensory processing, with different manifestations. Another anomaly to consider when looking into results of sensory processing in ASD is that individuals with ASD are thought to have a local processing bias. More precisely, studies suggest that they are better at processing details, or "local" information, than understanding the wider, "global" meaning ("Can't see the forest for the trees")(Happé, 1999; Happé and Frith, 2006). Local processing bias has been reported in perceptual, visuospatial, auditory, and verbal domains (Shah and Frith, 1983, 1993; Mottron *et al.*, 2000; Bertone *et al.*, 2005a; Vulchanova *et al.*, 2012; Bouvet *et al.*, 2014). Depending on task demands, this type of processing can be advantageous or disadvantageous. ASD patients often detect single shapes in groups of objects faster than control

individuals, but at the same time, they show relatively poor results in estimating the direction of objects moving as a group. Since temporal processing of local sensory signals in ASD is slower and noisier, It is thought that the global processing in ASD isn't disrupted, but slower, causing issues in perception of weak stimuli and perception of stimuli within short time windows (Brock *et al.*, 2002; McPartland *et al.*, 2004; Szelag *et al.*, 2004; Kwakye *et al.*, 2011; Stevenson *et al.*, 2014b).

This local processing bias is referred to in three main theories. “Weak central coherence theory“ which was developed in 1989 by Uta Frith, “Hierarchization deficit hypothesis“ proposed by Laurent Mottron and Sylvie Belleville in 1993 and “Enhanced perceptual functioning model“ proposed by Laurent Mottron and Jake Burack in 2001 (Frith, 1989; Mottron and Belleville, 1993; Mottron and Burack, 2001). According to the original weak central coherence theory, local bias stems from a detail-focused processing style. This theory suggests a deficit in global processing and it explains the superior performance of ASD individuals in tasks that require focusing on details, as well as the lack of understanding and use of context in tasks. It accounts for enhanced and diminished perceptual functioning in autism. This theory has since been updated and it now suggests that local processing bias is the key factor, not a deficit in global processing, and the local bias can be overcome when specifically global processing is required for a task.

Hierarchization deficit hypothesis builds on the weak central coherence theory, and it suggests that local and global processing function normally in ASD, but the interaction between them is abnormal. According to this theory patients with ASD struggle to distinguish between local and global levels and they cannot switch easily between them, compared to neurotypical individuals.

Finally, the more recent theory for local bias is the enhanced perceptual functioning model. It suggests that the local bias stems from an enhanced low-level perception and locally oriented processing which can negatively affect higher-level cognition and behaviour. This does not suggest necessary difficulties on a global level. ASD individuals are better in detecting simple stimuli while the perception of complex

stimuli is either normal or impaired. Complex stimuli processing involves more neurons while distinguishing between different stimuli demands more processing resources. According to this theory, increasing neuronal complexity will disrupt the performance in perceptual tasks.

Another interesting theory on sensory processing in autism is the "Perceptual load theory in autism", which was developed by Anna Remington in 2009 (Remington *et al.*, 2009). It is considered that each task has a certain perceptual load which dictates the extent to which stimuli are processed. If a task has a high perceptual load, there is no capacity left to process irrelevant information. However, a task with a low perceptual load wouldn't use the full resource capacity, resulting in processing irrelevant information until the saturation is achieved. Since patients in ASD exhibit superior results in certain tasks, but they are more affected by distractions and noise in others, it is suggested by this theory that perceptual capacity is higher in ASD.

I will now try to summarize the current knowledge from clinical studies on tactile, visual and auditory abnormalities in ASD.

Tactile processing

Tactile abnormalities most commonly described for ASD are hypersensitivity to light touch and certain clothing. However, clinical studies have reported both hyposensitivity in children (Ben-Sasson *et al.*, 2007; Tomchek and Dunn, 2007; Ashburner *et al.*, 2008; Foss-Feig *et al.*, 2012), and hypersensitivity in children (Rogers *et al.*, 2003; Cascio *et al.*, 2016) and adults (Crane *et al.*, 2009; Tavassoli *et al.*, 2014).

Reports on tactile detection thresholds in ASD vary. Some studies show lower detection thresholds (hypersensitivity) to thermal stimuli and 200Hz vibration in adults (Blakemore *et al.*, 2006; Cascio *et al.*, 2008), but these findings were not replicated in children using 250Hz vibration stimulus (Güçlü *et al.*, 2007). Higher thresholds were found for sinusoidal static detection using 25Hz flutter in children (Puts *et al.*, 2013, 2014), while other studies showed no difference for 40Hz flutter stimulus (Blakemore *et al.*, 2006; Güçlü *et al.*, 2007). Since vibrations and flutter

stimuli are processed by different mechanoreceptors, tactile abnormalities in ASD might be restricted to certain pathways. This could account for some of the observed differences in the reported results, although different paradigms were also used across these studies. One difference that is well-replicated across several studies is the detection of dynamic thresholds. Gradually increasing stimuli in amplitude into detectable range results in worse detection threshold compared to static stimuli in control subjects, however, detection threshold in individuals with ASD is not impaired with this gradual increase (Tommerdahl *et al.*, 2008; Puts *et al.*, 2014; Tavassoli *et al.*, 2016).

Neuronal responses to tactile stimuli in ASD have been found altered in several studies. In adolescents, somatosensory cortical map encoding differences and a decreased connectivity in finger regions was found (Coskun *et al.*, 2009, 2013). Electroencephalography (EEG) and magnetoencephalography (MEG) studies show lower amplitude responses to stimuli in children as well as earlier and increased peak responses to stimulation (Hashimoto *et al.*, 1986; Miyazaki *et al.*, 2007; Marco *et al.*, 2012). Functional magnetic resonance imaging (fMRI) studies report an increased trial-by-trial variability (Dinstein *et al.*, 2012; Haigh *et al.*, 2015). Finally, diffusion tensor imaging (DTI) study looking into connectivity between motor and somatosensory cortex reported abnormalities in ASD patients (Thompson *et al.*, 2017).

Results from tactile processing studies in ASD indicate that this sensory domain is affected. Various abnormalities in neuronal connectivity, activity and behavioural responses have been reported. Unfortunately, the studies are scarce and involve a smaller number of participants compared to visual and auditory processing. Furthermore, findings are often contradictory and inconclusive.

Visual processing

Visual hypo- and hypersensitivity have been reported in individuals with ASD. Visual sensitivity assessments for static stimuli, such as contrast discrimination, orientation processing, visual acuity, crowding and flicker detection, have all been reported as

typical in autism (Bertone *et al.*, 2005b; Pellicano *et al.*, 2005; De Jonge *et al.*, 2007; Kéïta *et al.*, 2010; Koh *et al.*, 2010b; Tavassoli *et al.*, 2011; Grubb *et al.*, 2013; Freyberg *et al.*, 2016), although there are studies showing impairments in object boundary detection, crowding paradigms and decreased contrast-detection ability in static and moving stimuli (Sanchez-Marin and Padilla-Medina, 2008; Vandenbroucke *et al.*, 2008; Baldassi *et al.*, 2009; Kéïta *et al.*, 2010). However, processing of dynamic visual stimuli has often been shown as atypical in ASD individuals (Spencer *et al.*, 2000; Blake *et al.*, 2003; Koh *et al.*, 2010a). Taking into consideration that local-global processing is abnormal in ASD, the following results from clinical studies confirm the existence of local processing bias.

ASD patients demonstrate enhanced discrimination and perception of details in the visual domain, particularly for simple stimuli, which is supported through their superior results in visual search tasks, where the goal is to detect shapes within a larger complex picture (Shah and Frith, 1983, 1993; Jolliffe and Baron-Cohen, 1997; Plaisted *et al.*, 1998; O'Riordan and Plaisted, 2001; O'Riordan *et al.*, 2001).

On the other hand, individuals with ASD exhibit deficits in the visual processing of complex stimuli. Impairment in face processing is widespread and present from an early age in ASD (Dawson *et al.*, 2002, 2005). Further, they have lower detection thresholds for local motion (Chen *et al.*, 2012; Manning *et al.*, 2015), yet higher thresholds for the perception of coherent motion (Spencer *et al.*, 2000; Milne *et al.*, 2002; Robertson *et al.*, 2012, 2014). Processing of basic stimulus features, such as contour and texture, have also been found negatively affected in ASD (Bertone *et al.*, 2005b; Pei *et al.*, 2009).

Studies combining fMRI and visual perceptual or cognitive tasks have found an increase in neuronal activity across visual cortical areas in patients with ASD (Ring *et al.*, 1999; Hubl *et al.*, 2003; Lee *et al.*, 2007b; Manjaly *et al.*, 2007; Soulières *et al.*, 2009; Damarla *et al.*, 2010). This increase in visual areas often goes along with reduced activity in the frontal cortex, amygdala and fusiform gyrus (Ring *et al.*, 1999; Schultz *et al.*, 2000; Dalton *et al.*, 2005; Lee *et al.*, 2007b; Manjaly *et al.*, 2007).

EEG studies in ASD show atypical processing in visual cortex. Increased activity in lateral occipital sites during texture segregation task suggests neuronal abnormalities in low-level visual processing. Event-related potentials (ERP) study in a visual oddball task shows abnormally large early-stage visual cortical responses to task-irrelevant stimuli, as well as shorter latencies to the response. Latencies to later-stage visual cortical responses to task-relevant stimuli were longer in ASD. Hyperreactivity in early-stage visual processing could disturb discrimination between irrelevant and relevant stimuli in ASD since the behavioural error rate was also significantly higher in ASD subjects.

An MEG study on temporal processing in ASD, using embedded figures task, demonstrates that ASD individuals recruit different brain areas when distinguishing letters surrounded by irrelevant context, compared to controls (Neumann *et al.*, 2011). Primary visual cortex was most active during the early time window in ASD subjects, in contrast to superior parietal lobe in controls. This suggests a difference in processing global and local information between ASD and neurotypical individuals, with ASD subjects relying more on early visual processing and not utilizing higher-order functions as much as controls.

Gamma band activity, important for perceptual and cognitive functions, and in the visual domain for biding separate visual information into a whole, is altered during face processing (Grice *et al.*, 2001; Wright *et al.*, 2012). Even though face orientation change was detected, as confirmed by ERP, the gamma bursts did not differ between upright and inverted face presentation in ASD patients. In contrast, gamma bursts in controls were modulated by the orientation of the stimulus, with larger values in upright compared to the inverted condition (Grice *et al.*, 2001). In another study, looking at gamma responses during facial emotions presentation, gamma response was absent from occipital areas of ASD patients during face presentations and the subjects took longer to identify the emotions (Wright *et al.*, 2012).

Altogether these results are an indication of altered functional connectivity within and between different brain areas in ASD. Visual cortical areas seem to have

increased activity while long-range connectivity seems to be impaired. Results also suggest that there is a local processing bias with superior processing of details along with an impairment in more complex tasks, as well as a potential inhibitory - excitatory imbalance.

Auditory processing

Several aspects of auditory processing in ASD are atypical. Children show a preference to music stimuli over speech, and they often have a better pitch perception compared to neurotypical individuals (Blackstock, 1978; Heaton *et al.*, 1998, 1999; Mottron *et al.*, 2000; Bonnel *et al.*, 2003; Heaton, 2003). They are also more accurate in identifying and recalling pitch (Heaton *et al.*, 1998; Heaton, 2003; Järvinen-Pasley and Heaton, 2007; Järvinen-Pasley *et al.*, 2008a, 2008b). A small percentage of adolescents and adults with ASD demonstrate superior pitch perception as well as frequency discrimination, especially individuals showing more prominent language-related impairments (Heaton *et al.*, 2008; Jones *et al.*, 2009; Bonnel *et al.*, 2010). The connection between linguistic deficits and superior pitch perception in ASD is unknown. Superior pitch perception could be a consequence or even a cause of decreased attention to social stimuli (O'Connor, 2012). Enhanced pitch perception during development could result in hypersensitivity and avoidance of certain sounds, hence diminishing typical maturation of communication. On the other hand, communication deficits could further enhance sensory deprivation due to hearing loss and language impairment. Hearing disorders are reported in 33-46% of autism cases (Klin, 1993).

Further, hypersensitivity to loud sounds, or hyperacusis, is often reported in ASD. Children show loudness sensitivity at lower sound intensity levels for pure tones and click stimuli (Rosenhall *et al.*, 1999; Khalfa *et al.*, 2004). This sensitivity decreases with age and it is no longer significantly different from control subjects in adulthood (Kern *et al.*, 2006). Sound intensity discrimination studies in adolescents and adults found similar results in controls and ASD subjects for intensity change discrimination of simple and complex tones (Jones *et al.*, 2009; Bonnel *et al.*, 2010). This decrease in

sensitivity could be a consequence of either a later maturation of auditory regions or the emergence of coping mechanisms.

On the other hand, individuals with ASD exhibit difficulties with speech and non-speech stimuli perception in noisy environments, with higher perception thresholds and slower as well as less accurate stimulus direction identification (Alcántara *et al.*, 2004; Teder-Sälejärvi *et al.*, 2005). This suggests there might be some abnormalities in ASD with suppressing irrelevant auditory stimuli. One of the involuntary auditory responses in humans is head-turning towards the sound direction, which most likely exists in order to enhance the processing of the sound source. In children with ASD this response is less common, with the difference especially prominent in responses to social stimuli (Dawson *et al.*, 1998, 2004). ASD patients also have difficulties in specifying the order of tones if they are presented closely in time (Kwakye *et al.*, 2011). These temporal difficulties could be coming from a longer latency in auditory evoked neuronal responses, which has been observed for pure tones and speech (Bruneau *et al.*, 2003; Oram Cardy *et al.*, 2008; Whitehouse and Bishop, 2008; Roberts *et al.*, 2010, 2011; Edgar *et al.*, 2015). Additionally, a reduction in activity was observed in auditory cortex and cerebellum of ASD patients during sound processing, specifically during non-verbal processing (Novick *et al.*, 1980; Oades *et al.*, 1988; Courchesne *et al.*, 1989; Ciesielski *et al.*, 1990; Buchwald *et al.*, 1992; Lincoln *et al.*, 1993; Müller *et al.*, 1999; Bruneau *et al.*, 2003).

Auditory processing in the cortex is commonly examined using EEG and MEG while presenting auditory stimuli and looking at event-related potentials (ERPs). Neuronal responses are collected over multiple sound presentation trials and averaged to get information on the temporal and spatial features of responses. EEG and MEG studies show atypical neuronal activity in primary auditory cortex and longer latencies to activity in primary and association auditory cortex areas (Bruneau *et al.*, 2003; Oram Cardy *et al.*, 2008; Whitehouse and Bishop, 2008; Roberts *et al.*, 2010, 2011; Edgar *et al.*, 2015). However, some studies have found faster responses (Martineau *et al.*, 1984; Ferri *et al.*, 2003). Studies included patients of different age and severity of the

disorder, as well as different techniques that were used, which can possibly explain the discrepancies in results. In MEG studies, abnormalities were also found in gamma-band oscillations in children and adolescents with ASD (Wilson *et al.*, 2007; Rojas *et al.*, 2008; Edgar *et al.*, 2015)

Studies on auditory brainstem responses (ABR) also report longer and less consistent latencies in children and adolescents with ASD (Rosenhall *et al.*, 2003; Kwon *et al.*, 2007; Russo *et al.*, 2008, 2009). More specifically, there is a longer conduction time between cranial nerve VIII and lateral lemniscus. These brainstem abnormalities suggest there are differences in processing complex stimuli in early auditory pathways, however, they cannot account for all the deficits found in individuals on the spectrum. Early pathway abnormalities could also be a result of atypical top-down modulations in ASD (Whitehouse and Bishop, 2008).

MRI studies found neuroanatomical differences in auditory brain regions of ASD patients. In neurotypical individuals, there are hemispheric asymmetries in planum temporale, a part of the temporal lobe considered to be involved in speech and language processing. This structure is usually larger in the left hemisphere. In individuals with ASD this asymmetry is not present, possibly because of the reduced grey matter volume in the left planum temporale (Rojas *et al.*, 2002, 2005; Gage *et al.*, 2009). A couple of MRI studies found larger grey matter volumes across brain areas in ASD patients. To name a few, increased volume was found in auditory areas such as Heschl's gyri, the brain structure containing primary auditory cortex in humans, and superior temporal gyrus, as well as the frontal lobes, visual and parietal cortex (Courchesne *et al.*, 2003; Lotspeich *et al.*, 2004; Gage *et al.*, 2009; Hyde *et al.*, 2010; Wang *et al.*, 2017; Pierce *et al.*, 2019).

Diffusion tensor imaging (DTI) studies looking into white matter connectivity found reduced integrity, aberrant connectivity and atypical hemispheric asymmetry throughout auditory areas of ASD individuals (Barnea-Goraly *et al.*, 2004; Lee *et al.*, 2007a; Cheng *et al.*, 2010; Lange *et al.*, 2010). Altered connectivity could result in a deficit in information integration. Spectro-temporally complex sound perception

requires proper communication between multiple brain regions, such as auditory core and belt, as well as auditory core and inferior colliculus (Scott and Johnsrude, 2003; Semple and Scott, 2003; Chi *et al.*, 2005). This is necessary for noise elimination and language comprehension and it wouldn't be efficient in case of reduced connectivity (Prat, 2011; Verly *et al.*, 2014).

Abnormal local-global processing can be found in the auditory domain as well. Superior results in local processing are visible with pitch perception (Blackstock, 1978; Heaton *et al.*, 1998, 1999; Mottron *et al.*, 2000; Bonnel *et al.*, 2003; Heaton, 2003) and better matching of sentences with their pitch graphic shape (Järvinen-Pasley *et al.*, 2008a), while diminished global processing is visible in matching these sentences with their meaning (Järvinen-Pasley *et al.*, 2008a). In another study showing diminished global processing, rearranging random words into meaningful groups haven't affected the recall in children with ASD, in contrast to control individuals (Järvinen-Pasley *et al.*, 2008b).

Auditory stimuli can be simple or complex on the spectral and temporal level. Spectrally, a pure tone is simple because it contains energy on one frequency, while speech is complex since it has several frequency components. Temporally, complex stimuli have sound sequences or changes in amplitude between onset and offset. As suggested by the enhanced perceptual functioning model, spectrally complex stimuli require larger neuronal complexity than simple stimuli (Mottron *et al.*, 2006). In neurotypical individuals, increasing spectral complexity of sounds results in increased activation in primary auditory cortex (“auditory core“) and surrounding auditory regions (secondary and tertiary cortex, or “belt“ and “parabelt“, respectively), while simple stimuli activate mainly the primary auditory cortex (Scott and Johnsrude, 2003).

As listed earlier, ASD individuals show superior performance in tasks that use spectrally simple stimuli and low-level operations such as pitch discrimination. In contrast, they display a deficit in tasks combining complex spectro-temporal stimuli with complex or even with low-level operations. Spectral processing in these tasks

has been shown as intact while temporal was impaired (Alcántara *et al.*, 2004; Järvinen-Pasley *et al.*, 2008b; Groen *et al.*, 2009). In a task targeting strictly temporal processing of sounds, ASD individuals exhibit poor long-sound and normal short-sound discrimination (Järvinen-Pasley *et al.*, 2008b). This is suggesting that the processing of temporal characteristics of sounds in ASD is abnormal, which concurs with MRI anatomical findings of deficits in the left hemisphere, implicated to process rhythm, duration and other temporal characteristics of sensory signals.

Taken together, atypical processing and altered connectivity found across auditory pathway could affect acquisition and differentiation of sounds as well as integration with higher-order functions. Elucidating the potential causes of abnormal auditory sensory processing in ASD is essential for understanding the appearance of language and communication impairments as well as developing the treatments for auditory hypo and hypersensitivities.

Multisensory processing

On everyday basis humans process multiple unisensory modalities simultaneously (e.g. visual and auditory), and combining information from different sensory modalities improves perception (Sumby and Pollack, 1954; Stein *et al.*, 1962; Lovelace *et al.*, 2003; Diederich and Colonius, 2004).

Multisensory processing occurs in paralel with unisensory processing (Calvert and Thesen, 2004), and several brain areas have been implicated in multisensory integration, such as superior colliculus, superior temporal cortex and posterior parietal cortex (Meredith and Stein, 1986; Stricanne *et al.*, 1996; Kadunce *et al.*, 2001; Cohen and Andersen, 2002; Avillac *et al.*, 2005; Loveland *et al.*, 2008; Redcay, 2008; Stevenson *et al.*, 2011).

In ASD, deficits in multisensory integration have been reported (Mongillo *et al.*, 2008; Donohue *et al.*, 2012; Charbonneau *et al.*, 2013; Collignon *et al.*, 2013; Stevenson *et al.*, 2014a, 2014b; Foxe *et al.*, 2015). Children with ASD do not seem to benefit from combined information of multiple modalities (Charbonneau *et al.*, 2013; Collignon *et*

al., 2013; Stevenson *et al.*, 2014a). It was also reported that ASD patients are less efficient in discriminating both uni- and multisensory emotion expression (Charbonneau *et al.*, 2013). Audiovisual speech processing seems to be specifically impaired (Mongillo *et al.*, 2008; Stevenson *et al.*, 2014b; Foxe *et al.*, 2015), which could stem from poor temporal acquity (Stevenson *et al.*, 2014b, 2016). Indeed, other studies found abnormal temporal multisensory processing of auditory and visual modalities, depending on ASD symptom severity (Foss-Feig *et al.*, 2010; Donohue *et al.*, 2012; de Boer-Schellekens *et al.*, 2013). Donohue *et al.* reported that when auditory stimuli occured before visual, ASD participants with more severe symptoms described them more often as simultaneous. However, this could be a result of altered auditory temporal processing found in ASD (Kwakye *et al.*, 2011).

These multisensory deficits could be caused by changes in functional connectivity between brain areas, specifically in areas involved in social information and communication processing. DTI studies reported decreased connectivity in parieto-occipital and temporal tracts, as well as white matter changes in the superior temporal gyrus and temporal stem, regions important for multisensory integration, language and social function (Lee *et al.*, 2007a; Chang *et al.*, 2014). Underconnectivity was also found between voice-selective cortex and brain structures involved in reward and emotion (Abrams *et al.*, 2013). fMRI studies found differences in activity of parietofrontal region, frontal and temporal association cortices, fronto-limbic areas and superior temporal region during audiovisual emotional matching tasks (Loveland *et al.*, 2008; Doyle-Thomas *et al.*, 2013). Lower activation synchronization was found across cortical areas during sentence comprehension, as well as an abnormal activity in Wernicke's and Brocka's area (Just *et al.*, 2004). Further, EEG studies reported abnormal amplitude and latency of responses to multisensory stimuli (Courchesne *et al.*, 1985, 1989; Russo *et al.*, 2010, 2012; Brandwein *et al.*, 2013, 2015).

In conclusion, difficuties in social communication and emotion recognition found in ASD patients could stem from abnormalities in multisensory processing. Studies have

found altered connectivity and abnormal activity during mutisensory stimuli presentation in brain regions relevant for communication and emotion. Further, since altered temporal processing of unimodal stimuli has been reported, mutisensory processing issues could stem from abnormal temporal binding of multiple unimodal stimuli (Robertson and Baron-Cohen, 2017). Investigating the potential causes of these functional differences could lead to better understanding of ASD and its emergence.

1.2.2. Theories on potential causes

Several factors have been linked with the development of ASD in children, including neuroanatomical changes such as cortical expansion and excitatory-inhibitory imbalance, as well as genetic predisposition and environmental influences. Some of these anomalies could also be connected and have a causal relationship, e.g. genetic mutations causing an increase in excitatory neuron number and with it an abnormal excitatory-inhibitory ratio.

Cortical expansion

In his 1943 paper on autism, Dr. Leo Kanner first reported macrocephaly in children. Since then, this feature has been extensively described in many papers.

Approximately 20% of children with autism spectrum disorder (ASD) have macrocephaly (Fombonne *et al.*, 1999; McCaffery and Deutsch, 2005), an enlargement of head size greater than 2 standard deviations above the population mean (Mirzaa and Dobyns, 2017). Macrocephaly is often indicative of an increase in brain volume, megalencephaly (McCaffery and Deutsch, 2005; Casanova *et al.*, 2006; Courchesne *et al.*, 2011). Macrocephaly in neurotypical children is usually found due to an increase in cerebrospinal fluid volume, while in ASD macrocephaly is connected to accelerated brain growth (Vaccarino *et al.*, 2009). Combining head circumference (HC) measurements with MRI assessments of brain volume revealed that HC is an accurate indication of brain volume in children, but not in adults (Aylward *et al.*, 2002; Bartholomeusz *et al.*, 2002).

Histological and neuroimaging studies in children with ASD have found a significant increase in the cortical volume, with the effect being nonuniform across different regions and varying between studies (Piven *et al.*, 1995, 1996; Courchesne *et al.*, 2001, 2003, 2011; Carper *et al.*, 2002; Sparks *et al.*, 2002; Lotspeich *et al.*, 2004; Carper and Courchesne, 2005; Wegiel *et al.*, 2010). Increase in grey as well as the white matter was reported in children with ASD, with percentages varying across studies and most likely depending on the age of the subjects (Courchesne *et al.*, 2001, 2003; Carper *et al.*, 2002; Herbert *et al.*, 2003; Lotspeich *et al.*, 2004; Simms *et al.*, 2009; Oblak *et al.*, 2011). Significant differences were found for frontal and temporal lobe grey matter and frontal, temporal and parietal lobe white matter, while occipital lobe seems to have typical values.

Grey matter increase is indicative of an increase in neuronal number, and on average 67% more neurons were found in the prefrontal cortex of ASD children (Courchesne *et al.*, 2011). This increase is thought to occur during the first postnatal years, then the expansion severely slows down and cortex reaches normal dimensions by adolescence and adulthood. Combined MRI and HC studies of brain volume in toddlers and young children up to 4 years old with ASD revealed an early excessive brain growth (10% higher brain volume than in neurotypical), followed by an abnormally reduced growth rate (Courchesne *et al.*, 2001; Sparks *et al.*, 2002). Another HC study in children with ASD describes normal HC at birth, followed by an increase starting at 6-14 months of age and finishing by 2nd year of life (Courchesne *et al.*, 2003). However, since the increase in cortical volume is reported to be nonuniform across different regions in ASD, the difference might not be measurable within the first couple of postnatal months especially if this increase occurs in late-maturing brain regions. A recent MRI study in infants with high familial risk of ASD found hyperexpansion of cortical surface area, followed by brain volume overgrowth (Hazlett *et al.*, 2017). Interestingly, this cortical surface hyperexpansion was found in sensory processing cortical areas. Considering that cortical volume is a product of thickness and surface area, these results indicate that age-related brain volume measurements in ASD studies might be under the influence of two different things,

especially because cellular mechanisms for surface area expansion and cortical thickness are different (Panizzon *et al.*, 2009).

This abnormal brain growth in early life could have an effect on the onset of the autistic behavioural phenotype. In neurotypical individuals, the process of neural circuits formation and brain growth occurs over a period of several years and it is shaped by experiences (Quartz and Sejnowski, 1997). Repetitions of sensory inputs, emotions and actions such as speech lead to synaptic reinforcements and refining of neural circuitry. In ASD children, where this growth is limited to a very short period, neural circuitry is lacking these experiences during formation, which most likely perturbs its development (Courchesne and Pierce, 2005). It is suspected that in ASD neural connections are ineffective, with limited arborization of axons and dendrites (Courchesne *et al.*, 2005). Indeed, imaging studies found aberrant connections in infants, later diagnosed with ASD (Wolff *et al.*, 2012; Emerson *et al.*, 2017).

A study on local-global switching comparison between macrocephalic children with ASD, ASD children and neurotypical children reported difficulties in switching from local into global level specifically for children with combined ASD and macrocephaly (White *et al.*, 2009). These results suggests that macrocephaly with ASD in early life and consequently abnormal development of neural circuitry could result in poor integration of information as well as a generalisation, which could be the origin of local processing bias found in ASD.

Increase in neuronal numbers and cortical volume across different regions in ASD could reflect potential abnormalities occurring during neurogenesis, neuronal migration or brain maturation (Gould and McEwen, 1993; Bailey *et al.*, 1998). A decrease in programmed cell death could also account for abnormal neuronal numbers. For example, mutations of apoptotic genes caspase-9 and PTEN have been connected to macrocephaly (Kuida *et al.*, 1998; Ueno *et al.*, 2019).

Recently, studies of induced pluripotent stem cells (iPSC) derived from children and adults with ASD reported abnormalities in prenatal processes (Mariani *et al.*, 2015;

Marchetto *et al.*, 2017; Derosa *et al.*, 2018; Adhya *et al.*, 2021). More specifically, they found increased cell proliferation, reduced differentiation and neuronal as well as synaptic maturation, along with the reduced neuronal activity.

To summarize, there is a high incidence of macrocephaly in ASD patients and several possible causes have been proposed for this abnormal rise in cell numbers. The increase could be unequal for different cell types, causing a disbalance in the ratio of excitatory and inhibitory neurons. An increase in excitatory neuron number could account for the increase in the grey and white matter, found in ASD patients, since excitatory neurons project myelinated axons. Additionally, since a much higher proportion of cortical neurons are excitatory (around 80%), a relatively small increase in their number could have a significant effect on white and grey matter volume, even with interneuron numbers remaining unchanged.

Excitatory-Inhibitory ratio imbalance

A disturbed ratio of excitatory and inhibitory neurons would cause excitatory neurons to fire either excessively or insufficiently (Belmonte *et al.*, 2004b; Dinstein *et al.*, 2015). Epilepsy is common in ASD, with a reported prevalence rate of 5-40%, depending on the patients' age and severity of the diagnosis (Canitano, 2007). Seizures and epilepsy could stem from an increase in the excitatory-inhibitory ratio, coming from either an increase in excitation or a decrease in inhibition. Disruption in GABAergic signalling was reported in several magnetic resonance spectroscopy, genetic and histological ASD studies (Shao *et al.*, 2003; Ma *et al.*, 2005; Fatemi *et al.*, 2009; Griswold *et al.*, 2012; Foss-Feig *et al.*, 2013; Piton *et al.*, 2013; Chen *et al.*, 2014; Robertson *et al.*, 2016). Cells derived from ASD patients display reduced β-catenin transcriptional activity, increased proliferation, reduced synaptogenesis, reduced spontaneous neuronal activity and a reduction in GABAergic neurons (Marchetto *et al.*, 2017). Additionally, genetic animal models with perturbations in GABAergic neurons or GABA receptors (e.g. *Gad2, Shank3, Gabrb3* or *Mecp2* knockout mice) demonstrate autism-like behaviour (DeLorey *et al.*, 1998; Chao *et al.*, 2010; Peça *et*

al., 2011; Wiebe *et al.*, 2019). Finally, high blood glutamate levels were found in ASD patients, further indicating towards the E-I imbalance (Zheng *et al.*, 2016).

On the other hand, some animal model and cell culture studies suggest that a decrease in the excitatory-inhibitory ratio is the origin of ASD. In Mecp2 knockout mice, modelling Rett syndrome, reduced spontaneous and evoked activity of pyramidal neurons, as well as enhanced inhibition, were observed (Dani *et al.*, 2005; Nelson *et al.*, 2006). These mice also have fewer and weaker excitatory connections (Dani and Nelson, 2009). Similar findings were reported in iPSCs study from Rett syndrome patients, where derived neurons had fewer synapses, reduced spine density and smaller soma size as well as reduced spontaneous activity (Marchetto *et al.*, 2010). *Mef2c* cKO mouse model, a gene which mutations have been connected to autism, also demonstrates an increase in inhibitory and a decrease in excitatory activity, as well as autism-like behaviour. Further, a mouse model with neurexin-1β deletion demonstrates a reduction in excitation and inhibition (Rabaneda *et al.*, 2014). Neuroligin mutations, which are a trans-synaptic pair of neurexins, cause a decrease in excitatory synaptic function in mice (Etherton *et al.*, 2009; Delattre *et al.*, 2013). Both neurexin and neuroligin mutations and deletions have been connected to ASD, and these mice also demonstrate autism-like behaviour (Ju *et al.*, 2014; Rabaneda *et al.*, 2014).

The differences across ASD human and genetic models studies can be explained by compensatory mechanisms. That is, mutations can cause alterations in neural circuity during brain development, along with changes in E-I balance, which can then induce secondary changes. For example, a deficit/increase in excitation can be corrected by secondary homeostatic plasticity mechanisms down/up-regulating inhibition in order to restore the balance. These primary effects and secondary changes are often difficult to discern (Nelson and Valakh, 2015). A study in several ASD mouse models with inhibitory deficiencies (Fmr1, Cntnap2, 16p11.2 and Tsc2) found a decrease in inhibition conductance as well as a smaller decrease in excitation conductance, producing a stable and normal synaptic depolarization and spontaneous spiking in

LII/III (Antoine *et al.*, 2019). These results suggest that increased E-I is actually a compensatory mechanism, emerging as a result of altered cortical activity caused by genetic mutations.

Disrupted connectivity could also shift the E-I balance. Changes in the synapse numbers and efficacy can lead to irregular circuits and abnormal neuronal activity. Several imaging studies of white matter have reported decreased long-range and increased short-distance connectivity in ASD patients (Belmonte *et al.*, 2004a; Herbert *et al.*, 2004; Just *et al.*, 2004, 2007; Courchesne and Pierce, 2005; Zikopoulos and Barbas, 2010). Local overconnectivity was also supported through increased activity found within certain brain areas (Courchesne and Pierce, 2005; Kennedy *et al.*, 2006). As mentioned earlier, changes in the white matter most likely suggest changes in excitatory connections, therefore indicating an E-I imbalance. Additionally, an increase in dendritic spine density of cortical layer II and V pyramidal neurons was found in ASD (Hutsler and Zhang, 2010). Majority of pyramidal neurons spine synapses are excitatory, hence an increase in spine density is implying an increase in excitatory-inhibitory ratio.

Mutations affecting excitatory or inhibitory synapse function can affect cortical development. Changing the excitatory-inhibitory balance could affect the signal-to-noise ratio in cortical circuits and disrupt signal detection as well as affect the maturation of cortical regions (Rubenstein and Merzenich, 2003; Hensch and Fagiolini, 2005; Sohal and Rubenstein, 2019). This would lead to abnormal sensory processing.

Additionally, the propagation of sensory signals through sensory pathway requires a precise balance between excitation and inhibition. If the overall excitation is too low, signal propagation will fail before reaching the higher-order regions (Nelson and Valakh, 2015).

Therefore, identifying transcriptional pathways that might be affected in ASD, and are involved in neuronal development, could help in understanding the origin of

neuroanatomical changes and resulting sensory abnormalities in ASD. This could also lead to establishing the targets for potential therapeutic interventions.

Genetics

ASD is highly heritable, suggesting there is a genetic component to the disorder. Studies on twins and families report around 60-90% incidence for ASD, greater than any other psychiatric disorder (Bailey *et al.*, 1995; Lichtenstein *et al.*, 2010). According to the latest exome sequencing study, there are as much as 102 risk genes for ASD (Satterstrom *et al.*, 2020). Recent iPSC studies of ASD individuals found abnormal expression of genes involved in neuronal differentiation, axon guidance and cell migration (Derosa *et al.*, 2018; Adhya *et al.*, 2021). Since many of the high-risk genes found are upstream regulators of core neurodevelopmental signalling pathways that control different aspects of brain development, such as proliferation, neurogenesis, cell migration and synaptogenesis, any abnormalities in these key pathways may disrupt important developmental processes, leading to ASD. Thus, instead of trying to find a specific gene mutation, to understand the emergence of ASD, it would be reasonable to look at disruptions of different neurodevelopmental signalling pathways during specific times in development. Results from studies on high-risk genes and iPSCs derived from ASD patients persistently indicate towards disruptions in several major neurodevelopmental pathways (Courchesne *et al.*, 2019, 2020; Gazestani *et al.*, 2019; Kumar *et al.*, 2019; Baranova *et al.*, 2020).

As mentioned earlier, Wnt/β-catenin pathway plays an important role in brain development and synaptic function, and it has been suspected as a relevant contributor in ASD and other developmental disorders (Okerlund and Cheyette, 2011; Mulligan and Cheyette, 2016). Multiple studies have implicated that changes in Wnt pathway are frequently found in ASD, mostly mutations of high-risk genes encoding for different elements on the pathway. Mouse KO models targeting signalling molecules on this pathway have expressed ASD-like behaviour as well as molecular, cellular and electrophysiological characteristics. *GSK3-α* and *β*, *APC*, *Prickle2, TCF4, CTNNB1* and *Wnt1* are some of the most commonly studied genes on the Wnt

pathway, and all of them have been connected to ASD-related abnormalities (Zhou *et al.*, 2007; Mines *et al.*, 2010; Martin *et al.*, 2013; Sowers *et al.*, 2013; Dong *et al.*, 2016; Forrest *et al.*, 2018). Interestingly, PTEN, whose mutations have been associated with ASD and macrocephaly (McBride *et al.*, 2010; O'Roak *et al.*, 2012), is also implicated in the canonical Wnt pathway (Hodges *et al.*, 2018). β-catenin is increased in Pten+/- mouse model, and additional β-catenin gene (*CTNNB1*) mutation suppresses macrocephaly in these mice (Chen *et al.*, 2015). It has been suggested that PTEN and β-catenin function in balance, regulating brain growth, and disruptions in this balance can cause abnormalities in brain size.

Wnt also interacts with and modulates other signalling pathways, such as Hedgehog, Notch, BMP, TGF-β, RA and NF-κB pathways (Feigenson *et al.*, 2011; Osei-Sarfo and Gudas, 2014; Ma and Hottiger, 2016; Chatterjee and Sil, 2019; Pelullo *et al.*, 2019). This all could potentially imply that the ASD risk factors emerge from altered regulation in the canonical Wnt pathway.

In ASD patients, mutations were also found in a known regulator gene for Hh signalling pathway, Ptchd1. Mouse models with KO or Ptchd1 deficiency demonstrate cognitive impairments, hyperactivity, decreased dendritic arborization and a decrease in the number and functional deficits of excitatory synapses (Tora *et al.*, 2017; Ung *et al.*, 2017). Dysregulations of Sonic hedgehog (Shh), one of the ligands on the Hh pathway, have been linked to ASD (Al-Ayadhi, 2012; Bashir *et al.*, 2014; Halepoto *et al.*, 2015). Mainly, Shh, as well as Indian hedgehog (Ihh) protein levels in serum of ASD children, have been found elevated, with a positive correlation of Shh and Ihh levels with ASD severity (Bashir *et al.*, 2014; Halepoto *et al.*, 2015). On the other hand, Desert hedgehog (Dhh) levels in serum of ASD children have been found decreased (Bashir *et al.*, 2014).

RA signalling studies in rats have shown that retinol deficiency during pregnancy leads to autistic-like behaviour in rat pups (Lai *et al.*, 2018). Additionally, reduction in retinoic acid-related orphan receptor alpha (RORA) expression, as well as ALDH1A1, has been found in ASD patients (Nguyen *et al.*, 2010; Pavăl *et al.*, 2017; Sayad *et al.*,

2017). RORA regulates several ASD-linked genes, such as *NLGN1* (Sarachana and Hu, 2013).

A few other pathways implicated in ASD are RAS/ERK and PI3K/AKT/mTOR (Pinto *et al.*, 2014; Chen *et al.*, 2015; Sahin and Sur, 2015; Courchesne *et al.*, 2019). Both up and down-regulation of genes on these pathways have been linked to ASD. Some of the most studied genes are *Mecp2, PTEN, SHANK3, TSC* and *Raf1* (Buxbaum *et al.*, 2007; Moessner *et al.*, 2007; Adviento *et al.*, 2014; Vignoli *et al.*, 2015; Garg *et al.*, 2017; Wen *et al.*, 2017).

Recently, a single-cell genomics study was done in cortical tissue of ASD patients to identify transcriptomic alterations in specific cell types (Velmeshev *et al.*, 2019). This study reported alterations in synaptic and neurodevelopmental genes of L II/III cortical excitatory neurons, while dysregulation of specific genes in these cells correlated with autism severity.

To summarize, many of the genes highly associated with ASD are involved in key neurodevelopmental pathways. Therefore, alterations in these pathways have been proposed as the basis of ASD emergence. One pathway that has been researched and suggested the most is the canonical Wnt pathway. Still, further research is necessary to understand how changes in different parts of these pathways affect the ASD occurrence.

Gene-environment interactions

While genetics is very important in the occurrence of ASD, the relevance of environmental factors still shouldn't be neglected. Known ASD-related genes have been identified in only around 25% of autistic children, suggesting that environmental factors play a larger role in the incidence of ASD than previously thought (Miles, 2011). Studies in twins have shown a large difference in ASD rate between identical twins, while others also reported that non-identical twins have a significantly higher risk compared to non-twin siblings (Rosenberg *et al.*, 2009; Hallmayer *et al.*, 2011). This implies that the combination of genetic predisposition and environment during

prenatal or early postnatal development may contribute to ASD onset. Additionally, maternal exposure to stress, infection and certain medications have also been connected to increased risk of ASD in children.

Valproic acid (VPA) has been used as an anti-epileptic drug and mood stabilizer in bipolar disorder. Clinical studies have associated birth defects, developmental delay, cognitive function impairments and increased risk of autism in children with VPA use during pregnancy (Adab *et al.*, 2004; Meador, 2008; Meador *et al.*, 2009, 2011; Nadebaum *et al.*, 2011a, 2011b; Shallcross *et al.*, 2011; Christensen *et al.*, 2013). Autistic symptoms have been reported in children exposed to VPA *in utero* as well as in animal experimental models (Rasalam *et al.*, 2005; Schneider and Przewłocki, 2005; Wagner *et al.*, 2006; Markram *et al.*, 2008b; Christensen *et al.*, 2013; Nicolini and Fahnestock, 2018; Zhao *et al.*, 2019). Rodent studies on VPA offspring have reported autism-like behaviour, including social and communication deficits and repetitive behaviour (Schneider and Przewłocki, 2005; Wagner *et al.*, 2006; Roullet *et al.*, 2010).

VPA is an inhibitor of histone deacetylases, modifying cell proliferation and differentiation during development (Göttlicher *et al.*, 2001; Phiel *et al.*, 2001). Increasing the amount of acetylated histone proteins is affecting the G1 phase regulatory proteins, inhibiting cell cycle exit of neural progenitor cells and consequently causing an increase in the production of projection neurons of superficial cortical layers in embryos (Fujimura *et al.*, 2016). The thickness of superficial cortical layers in VPA treated mice measured at P21 is significantly increased, as well as the overall neocortical thickness in humans and rats exposed to VPA *in utero* (Sabers *et al.*, 2014; Wood *et al.*, 2014; Fujimura *et al.*, 2016). This excitatory neuron-specific increase in neocortex could also alter E-I balance.

Time window of exposure to VPA seems to have a large effect on the emergence of ASD traits in rodents. Mice exposed to VPA at E12.5 show strong social interaction deficits, however, this effect is absent in mice exposed to VPA at E9 or E14.5 (Kataoka *et al.*, 2013). Similarly, exposure to VPA at E12 in rats has the strongest behavioural effect (Kim *et al.*, 2011). Exposing rats to VPA on E12 also caused an upregulation of

anti-apoptotic factors and reduction of apoptotic factors, suggesting that VPA interferes with programmed cell death which leads to brain overgrowth (Go *et al.*, 2011).

Neural responses in *in utero* VPA exposed humans and animal models are abnormal, but consistent with findings in ASD patients. Comparable auditory electrophysiological studies in humans and mice reported delayed auditory evoked responses and abnormal gamma frequency oscillations in both species (Gandal *et al.*, 2010). Visual domain study in ferrets treated with VPA reported abnormal neuronal responses to orientation selectivity (Pohl-Guimaraes *et al.*, 2011).

Increasing the number of excitatory neurons in superficial cortical layers following *in utero* VPA exposure in rats has also caused alterations in neuronal excitability, an increase in dendritic arborization of pyramidal cells and an increase in local connectivity (Rinaldi *et al.*, 2007, 2008; Snow *et al.*, 2008; Walcott *et al.*, 2011). However, these connections exhibited a decrease in strength (Rinaldi *et al.*, 2007, 2008). These alterations in circuitry could cause compensatory mechanisms to emerge as development progresses, generating behavioural traits typical for ASD.

Another environmental factor implicated to increase ASD occurrence is prenatal maternal exposure to infection (Patterson, 2009, 2011; Meltzer and Van De Water, 2017). Several studies have associated an increased risk of ASD with maternal infection, although results vary depending on exposure time window, maternal immune response intensity and type of infectant (Atladóttir *et al.*, 2010b, 2010a; Goines *et al.*, 2011; Brown *et al.*, 2014; Lee *et al.*, 2015; Zerbo *et al.*, 2015; Hornig *et al.*, 2018). A large clinical study reported a significant ASD risk increase for children of mothers hospitalized for more severe viral infections in the first trimester, as well as those for bacterial infections in the second trimester (Atladóttir *et al.*, 2010b). Maternal immune activation (MIA) has since been widely tested using animal models (Patterson, 2009; Meyer, 2014; Reisinger *et al.*, 2015; Estes and McAllister, 2016).

MIA animal models are developed by exposing pregnant rodents to bacterial or viral mimetics, causing a strong immune response that affects the development of embryos (Estes and McAllister, 2016). Most commonly used agent for injections is RNA molecule polyinosinic-polycytidylic acid (poly I:C), whose presence activates toll-like receptor 3, provoking an immune response (Medzhitov, 2001; Meyer and Feldon, 2012). Time window of injection is usually during the proliferation of neuronal progenitor cells, therefore upregulating cell cycle gene expression and cell proliferation, which perturbs corticogenesis, leading to abnormal neuronal migration, and causes brain overgrowth (Soumiya *et al.*, 2011b, 2011a; Oskvig *et al.*, 2012; Smith *et al.*, 2012; Le Belle *et al.*, 2014; Lombardo *et al.*, 2018). Similar to the VPA animal model, MIA exhibits overproduction of neurons, increased cortical thickness and megalencephaly (Smith *et al.*, 2012; Le Belle *et al.*, 2014). Maternal exposure to poly I:C has also been connected to altered synaptic protein expression in pups, as well as downregulation of NMDA receptors (Soumiya *et al.*, 2011a; Forrest *et al.*, 2012; Labouesse *et al.*, 2015). Together with neuronal overproduction, this could cause abnormal changes in neuronal networks and E-I imbalance.

MIA models display social, communication, repetitive and other behavioural abnormalities typical for ASD. Mice exposed to poly I:C at E12.5 exhibited altered auditory communication through ultrasonic vocalization (USV) in young and adult age and reduced olfactory communication through urine-induced scent marking, social interaction deficits and increase in self-grooming and marble burying (Malkova *et al.*, 2012; Schwartzer *et al.*, 2013).

As in VPA exposure, changing the time window of poly I:C injection has a different effect on embryonic development. Mouse pups exposed to poly I:C at E9 demonstrate sensorimotor deficits, E12.5 pups show ASD-like behaviour, while E17 pups have problems with working memory (Meyer *et al.*, 2008; Malkova *et al.*, 2012; Schwartzer *et al.*, 2013). This demonstrates that potential maternal infection and immune activation in a different period during development can result in different outcomes.

Combining genetic mouse models with MIA increases the risk of ASD, further implicating that ASD onset is a result of an interplay between genetic predisposition and environmental factors. For example, Pten haploinsufficiency combined with MIA caused an increase in brain size up to 44%, compared to 8% increase without MIA (Le Belle *et al.*, 2014).

Drugs promoting Wnt pathway (e.g. VPA, SSRI or lithium) usually increase levels of Wnt1/2 or inhibit components of the β-catenin destruction complex, such as GSK-3β (Wexler *et al.*, 2008; Okamoto *et al.*, 2010; Wang *et al.*, 2010). However, certain drugs inhibit the pathway, either by blocking Wnt binding to receptors or by inhibiting other molecules on the pathway, thus preventing β-catenin activation (Semënov *et al.*, 2005; Henderson *et al.*, 2010; Thorne *et al.*, 2010; Grossmann *et al.*, 2012; Gurney *et al.*, 2012; Hahne and Grossmann, 2013). The effect these drug manipulations of the Wnt pathway have on ASD emergence are not well known, probably because of their different spatial and temporal activity. Different cells most likely show different effects for up/down-regulation of Wnt and the consequences of these manipulations are presumably greater during neurodevelopment than they are in the mature brain.

Recently, a new mouse model has been developed for studying alterations in the canonical Wnt pathway through prenatal injections of a small compound, XAV939 (Fang *et al.*, 2014). This compound is an inhibitor of tankyrase 1 and 2, both of which interact with a highly conserved domain of axin and stimulate its degradation (Huang *et al.*, 2009). Axin concentrations in the cytoplasm are regulated through PARylation by tankyrase, followed by ubiquitylation and degradation, for the purpose of limiting β-catenin destruction complex and fine-tuning cell responsiveness to Wnt signals. Through this inhibition of axin degradation, XAV939 is causing an increase in IP amplification which ultimately results in overproduction of cortical pyramidal neurons (Figure 1.7.) (Fang *et al.*, 2013, 2014; Fang and Yuste, 2017).

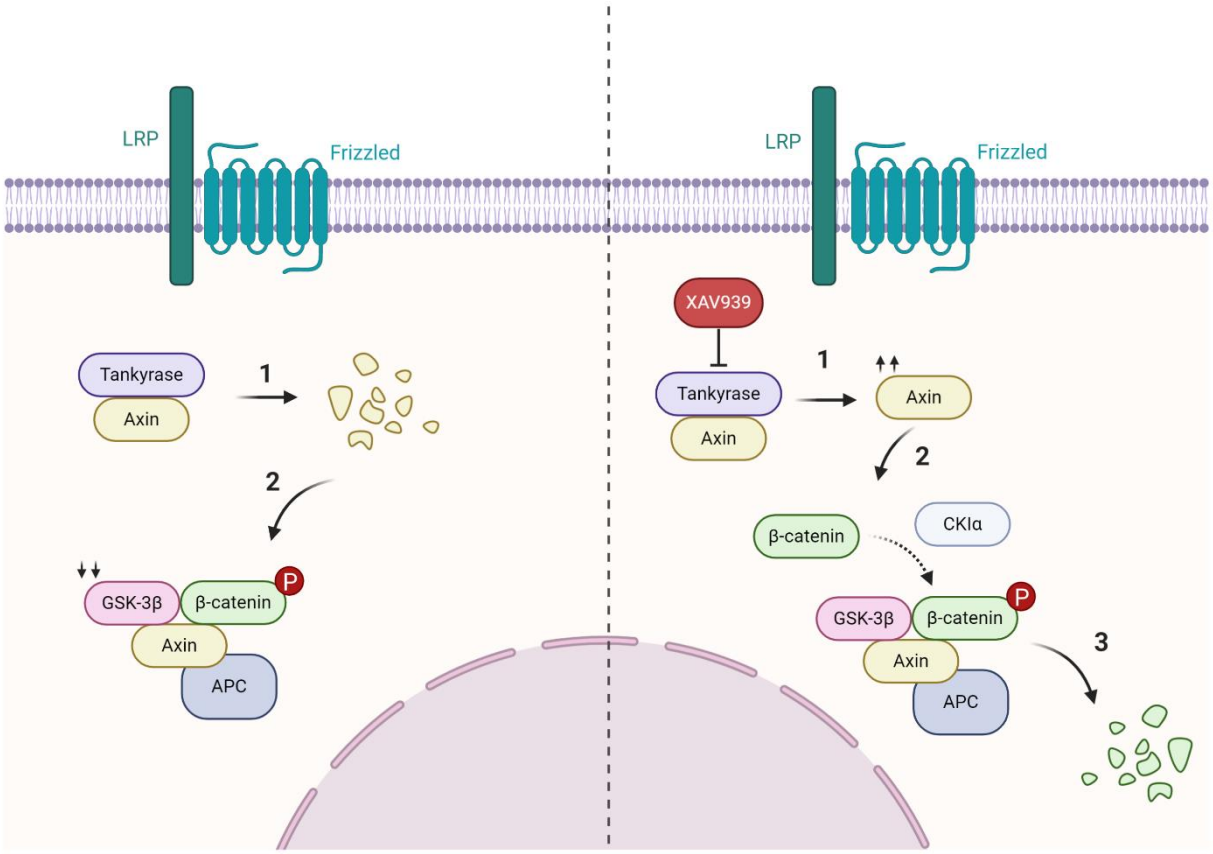

Figure 1.7. Tankyrase mediated axin degradation. In normal conditions (left), tankyrase controls β-catenin destruction complex concentrations through axin degradation. In the presence of XAV939 (right) axin degradation is inhibited, causing an elevated concentration of β-catenin destruction complex and resulting in an increase in IP amplification.

Injecting XAV939 at E13.5 increases the production of IPs in the VZ/SVZ by E15.5, which causes more upper-layer cortical neurons to develop by E17.5 (Fang *et al.*, 2013). XAV939 mice exhibit an increase in pyramidal neuron number of cortical layer II/III specifically, across all ages (Fang *et al.*, 2013, 2014; Fang and Yuste, 2017). This treatment does not alter the production of interneurons, most likely because endogenous axin levels are very low in the NPCs of subpallium (Fang *et al.*, 2014). Treatment also doesn't affect the production of microglia or astrocytes (Fang *et al.*, 2014). However, treated mice show disrupted dendritic spine development and function and altered distribution of interneurons (Fang *et al.*, 2014).

Young XAV939 treated mice exhibit altered neuronal connectivity, with a high number of excitatory and a normal number of inhibitory synapses, suggesting an E-I imbalance (Fang *et al.*, 2014). Excitatory neurons in these young mice show higher spontaneous and evoked activity. However, these differences change with time. Adult XAV939 mice have a significant reduction in the number of excitatory synapses, causing them to reach a similar number to control mice in adulthood (Fang *et al.*, 2014). On the other hand, a lot more inhibitory synapses survived in these treated mice compared to controls. Excitatory neurons in treated adult mice exhibit lower evoked activity than controls (Fang *et al.*, 2014). Since these mice had more excitatory neurons in their early development, it is possible that through compensatory mechanisms later in life the E-I balance shifted towards the stronger inhibitory environment.

Behaviourally, adult XAV939 mice display sharper orientation discrimination compared to control mice (Fang and Yuste, 2017). This suggests that the number of neurons in upper-layers of the cortex can affect perceptual discrimination of animals. XAV939 mice also demonstrate ASD-like behavioural traits, such as social deficits and repetitive behaviour (Fang *et al.*, 2014). Thus, results from this mouse model implicate that there is a causal relationship between changes in the canonical Wnt pathway during embryonic development and the emergence of ASD-like phenotypes.

In conclusion, ASD is a highly variable neurodevelopmental disorder, with many potential causes and diverse sensory processing difficulties. The emergence of this disorder could be caused by an interplay of several factors, such as genetic predisposition triggered by an environmental element. Macrocephaly is common in ASD, indicating that signalling pathways regulating neurogenesis could be involved in its emergence. With abnormal neurogenesis, an excitatory-inhibitory imbalance can arise. This imbalance would affect the processing of sensory information, alter signal-to-noise ratio and change signal detection.

1.3. Auditory pathway

As reviewed in the previous section 1.2.1, one of the most evidently affected and researched sensory modalities in ASD is hearing. Language and communication deficits found in ASD could stem from auditory abnormalities in early life (Rapin, 1997; Dawson *et al.*, 1998; Linke *et al.*, 2018). To understand the anatomical basis of abnormal auditory processing found in ASD, we should first look at the anatomy and functionality of the auditory pathway.

To perceive a sound from the environment, acoustic information has to go through several "terminals" in the nervous system, where it is transformed and processed. This whole pathway the sound information travels through can be split depending on the anatomical position of the "terminals" into the peripheral and central auditory system. Peripheral pathway consists of the outer, middle and inner ear, and their task is to collect the sound vibrations and transform them from mechanical into an electrical signal (Figure 1.8.). This signal is then relayed through the auditory nerve into the central part of the auditory pathway, comprising of different auditory regions in the brain. Some of the main regions of the central auditory pathway in mammals are the cochlear nucleus, superior olivary complex, inferior colliculus, medial geniculate body and auditory cortex (Figure 1.9.) (Fitzpatrick, 2004).

1.3.1. Peripheral auditory system

Outer Ear

The outer ear consists of the pinna (auricle) and ear canal. Sounds from the environment are collected by the pinna and channelled into the ear canal, where the sound waves travel through to the middle ear.

Middle Ear

Middle ear starts with the tympanic membrane (eardrum). This membrane is connected to the oval window of the cochlea (inner ear) though a chain of three small bones (ossicles), called the malleus, incus and stapes. Since the inner ear is a fluid-rich environment, which has a high impedance, and the stimulus travels from low impedance air environment, transferred energy needs to be amplified or it would be

lost. When sound waves vibrate the tympanic membrane, the ossicles move, amplifying the vibrations before transferring them into the inner ear (Fitzpatrick, 2004).

Inner Ear (Cochlea)

Cochlea is a fluid-filled snail-like structure, where sound waves travelling through the fluid transform into electrical signals (Fitzpatrick, 2004). It consists of the basilar and tectorial membrane and 3 larger chambers: scala vestibuli, scala media and scala tympani (Figure 1.8., enlarged section). The basilar membrane is located on top of scala tympani and it separates scala media and scala tympani. The structure of the basilar membrane allows the distinction of sound frequency. It is narrow and stiff at its basal end in the oval window of the cochlea, and getting wider and more flexible by the apical end. Sound waves arriving at the oval window cause the fluid (endolymph) to move, increasing in amplitude and decreasing velocity until stopping at a certain point. This position depends on the frequency, where lower frequencies can travel further up the membrane while higher frequencies are located at the base (von Bekesy, 1960). Distribution of frequencies along the basilar membrane is called a tonotopic map (Fitzpatrick, 2004).

Sitting on top of the basilar membrane is the most important part of scala media, the organ of Corti. It contains two types of hair cells, inner and outer, with hair-like projections called stereocilia. Inner hair cells are situated on the basilar membrane and facing the tectorial membrane, surrounded by endolymph. Travelling sound waves cause movements of the basilar membrane, creating a propagating wave that leads to lateral movement of the tectorial membrane over stereocilia (Russell, 1987). This mechanical bending of the inner hair cells in the organ of Corti results in depolarization of hair cells and release of neurotransmitters, stimulating auditory nerve endings and ultimately transferring the mechanical signal into electrical (Zdebik *et al.*, 2009).

Different hair cells are activated by different frequencies, depending on their position along the basilar membrane, thus allowing tonotopy and separation of different

frequencies in higher auditory structures. The hearing frequency range differs across species, it spans between 0.02-20kHz in humans, while in mice it is 2-100kHz (Malmierca and Ryugo, 2012).

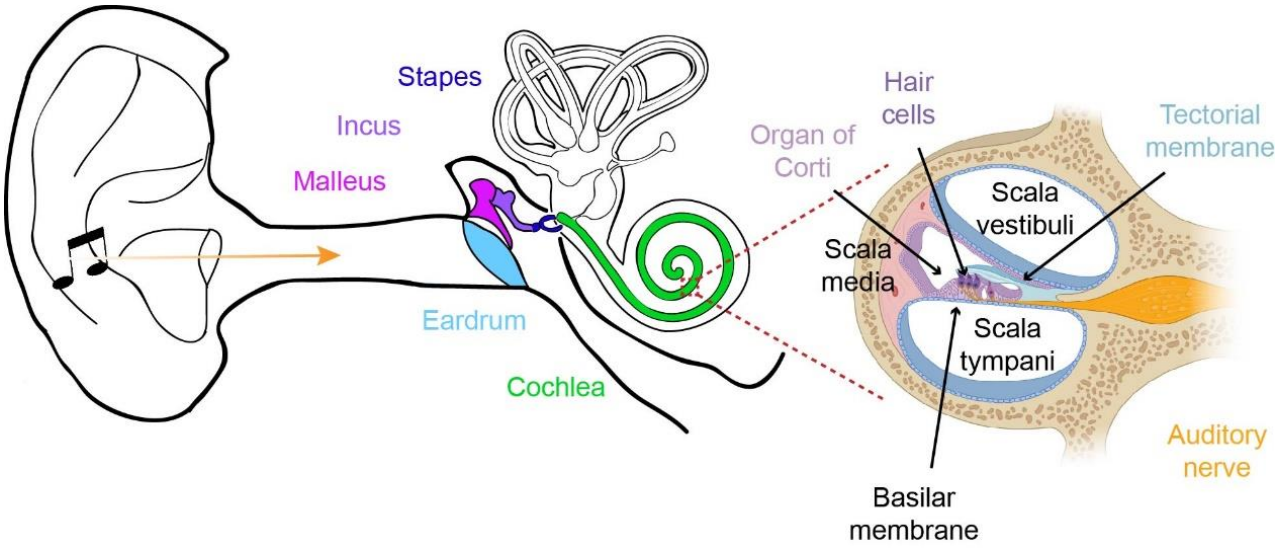

Figure 1.8. Schematic representation of the peripheral auditory system. Sound waves are coming through the ear canal, vibrate the eardrum, transmitting the signal via malleus, incus and stapes to the cochlea. Enlarged section through the cochlea shows locations of its internal structures.

1.3.2. Auditory nerve

Auditory nerve transfers the electrical signal from organ of Corti to the central auditory system, more specifically to cochlear nucleus located in the brainstem. There are 2 main types of auditory, spiral ganglion neurons. Type I (~90-95%) is bipolar, large and myelinated and it innervates a single inner hair cell through a compact bouton (Rouiller, 1997). Each inner hair cell can have connections with multiple type I spiral ganglion neurons (Meyer *et al.*, 2009). Type II (~5-10%) is unipolar, small and unmyelinated, innervating multiple outer hair cells (Benson and Brown, 2004; Weisz *et al.*, 2012).

1.3.3. Central auditory system

Most of the structures in the central auditory system are tonotopically organized, each in its specific way. There is also a hierarchy present, so as the signal progresses upstream, the extent of processing and stimulus integration increases.

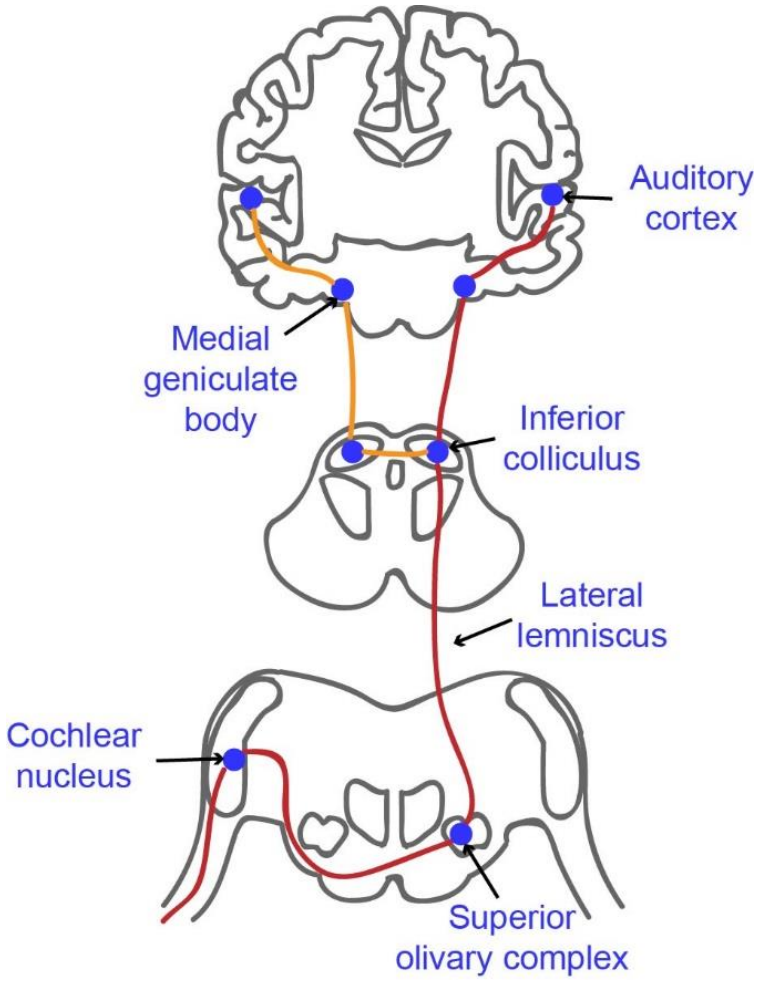

Figure 1.9. Schematic of the major connections in the central auditory pathway. The signal is transmitted from the auditory nerve into the cochlear nucleus, following an upstream pathway ending with the auditory cortex.

Cochlear Nucleus

In the brainstem, auditory nerve fibres branch into two paths – anterior and posterior. Anterior branch innervates ventral cochlear nucleus (CN), while posterior innervates dorsal CN. Ventral CN is comprised mostly of bushy cells and it is responsible for sound localization. Dorsal CN contains mostly fusiform cells and it is

responsible for more complex signal filtering, amplification and processing, such as time and frequency of the sound (Rhode and Greenberg, 1992). Dorsal CN is more distinctly laminated in rodents than in humans (Moore and Osen, 1979; Moore *et al.*, 1996).

Cochlear nucleus contains tonotopically organized isofrequency sheets. Each sheet is made of neurons responding to a specific, narrow frequency range. The frequencies contained in isofrequency sheets vary between species (Suga and Jen, 1976; Fekete *et al.*, 1984).

Right and left CN are interconnected, and CN also receives descending projections from higher auditory areas, such as inferior colliculus and auditory cortex (Malmierca and Ryugo, 2012). Most of the ascending fibres from cochlear nucleus cross over to contralateral superior olivary complex in the brainstem, while some innervate ipsilateral SOC.

Superior Olivary Complex

Signals from both ears are integrated in the superior olivary complex (SOC), creating one, binaural signal and playing a vital role in directional hearing (Schwartz, 1992; Rouiller, 1997). SOC can be further divided into lateral SOC, medial SOC and medial nucleus of the trapezoid body (Malmierca and Ryugo, 2012). Lateral SOC and medial nucleus of the trapezoid body are larger in high frequency hearing species, such as mice, while medial SOC is smaller, compared to humans. Rodents also have an additional nucleus in the SOC, the superior paraolivary nucleus. All of these nuclei are surrounded by the periolivary nuclei (Osen *et al.*, 1984). Ascending fibres from SOC pass through the nuclei of the lateral lemniscus (LLN) on their way to innervate contralateral or ipsilateral inferior colliculus (Schwartz, 1992).

Inferior Colliculus

From CN, SOC and LLN auditory information ascends into inferior colliculus (IC) in the midbrain (Oliver, 1987; Winer and Schreiner, 2005; Saldaña *et al.*, 2009). Left and right IC are interconnected, and they also receive descending projections from the

auditory cortex (González Hernández *et al.*, 1986; Doucet *et al.*, 2003). IC is a crucial relay terminal on the auditory pathway, and it can be split into the lateral, central and dorsal part.

Central nucleus of IC is the main nucleus, receiving most of the ascending fibres (Fitzpatrick, 2004). It has laminar tonotopic organization across species, meaning that neurons tuned to low-frequency range are located at the top, while high-frequency tuned neurons are found at the bottom of the structure (Meininger *et al.*, 1986; Schreiner and Langner, 1997; Ehret *et al.*, 2003). It has been suggested that the laminae also contain additional maps of sound features, such as amplitude and phase (Herrnberger *et al.*, 2002).

Lateral nucleus and dorsal cortex of IC have a poorly defined best frequency with broadly tuned neurons and longer latency to the auditory response (Aitkin *et al.*, 1975, 1981, 1994). It has been suggested that lateral nucleus of IC is involved in sound localization while dorsal cortex of IC is involved in speech detection (Aitkin *et al.*, 1975; Binns *et al.*, 1992). Both of these IC areas are also multisensory (Wong and Borst, 2019).

Medial Geniculate Body

From IC, auditory information ascends to the medial geniculate body (MGB). MGB is the main auditory center of the thalamus and the last stage of subcortical auditory processing (Malmierca and Ryugo, 2012). Higher-order information of sounds is starting to get processed in the MGB, such as speech (von Kriegstein *et al.*, 2008; Glad Mihai *et al.*, 2019). MGB is also involved in learning and memory, and projects to amygdala (Ferrara *et al.*, 2017). MGB can be divided into the ventral, medial, dorsal part.

Ventral MGB is the main nucleus, getting ascending inputs from IC and descending inputs from auditory cortex. Projections from vMGB mainly terminate in primary auditory cortical layers III and IV (Huang and Winer, 2000; Lee and Sherman, 2010). vMGB has a strong tonotopic organization, and densely packed neurons in this area

show synchronization tendency to repetitive stimuli (Imig and Morel, 1985; Rodrigues-Dagaeff *et al.*, 1989). In primates, approximately 25% of neurons in vMGB are GABAergic, while the rest are glutamatergic. In rodents <1% of neurons in vMGB are GABAergic (Winer and Larue, 1996). vMGB neurons have short latencies to the auditory response and sharp frequency tuning (Bordi and LeDoux, 1994; Anderson and Linden, 2011).

Medial MGB receives inputs from the lateral nucleus of the IC as well as some non-auditory areas (Rouiller *et al.*, 1989). It also sends projections to various non-auditory cortical areas as well as the auditory cortex. mMGB shows weaker tonotopic organization, with similar frequency tuning range as vMGB but shorter latencies (Bordi and LeDoux, 1994; Anderson and Linden, 2011)

Dorsal MGB receives inputs from the dorsal cortex of IC and projects mainly to auditory belt areas. dMGB shows similar responses as the dorsal cortex of IC, with longer latencies and broader frequency tuning compared to vMGB (Winer and Schreiner, 2005; Anderson and Linden, 2011). Tonotopic organization was not found in dMGB of any species (Malmierca and Ryugo, 2012). It is thought that dMGB is involved in attention (Winer *et al.*, 2005).

Auditory Cortex

Finally, signals from MGB arrive into the auditory cortex. In mice, auditory cortex includes 5 areas: primary auditory cortex (A1), anterior auditory field (AAF), ultrasonic filed (UF), secondary auditory cortex (A2) and dorsoposterior filed (DP). A1 and AAF in mice show clear tonotopy. In A1, neurons tuned to low frequencies are located in the posterior part and high frequency tuned neurons are anterior, while AAF tuning is inverse (Stiebler *et al.*, 1997). Across species, there are differences in the number of auditory cortical areas, their connections and tonotopic organization (Reale and Imig, 1980; Seldon, 1981; Stiebler *et al.*, 1997; Saenz and Langers, 2014). Functionally, AC areas can be divided into auditory core (A1 and AAF in mice), belt (A2) and parabelt (Kaas and Hackett, 2000; Lee *et al.*, 2004). Inputs from the thalamus

mainly arrive into the core and the information is then ascending further upstream to belt and parabelt (Kaas and Hackett, 1998, 2000).

Descending (corticofugal) auditory pathways extend from auditory cortex to organ of Corti (Malmierca and Ryugo, 2012). These efferent pathways are important for feedback control and modulation (Suga, 2008). From auditory cortex, three tracts descend: corticothalamic, corticotectal and corticobulbular. Corticothalamic tract connects AC and MGB. In the MGB, vMGB receives most of the inputs from layer VI of A1 and AAF, while dMGB receives projections from layer V of A1 (Winer *et al.*, 2001; Lee and Sherman, 2010). These projections seem to be glutamatergic, however, AC stimulation has excitatory and inhibitory effects in MGB (Ryugo and Weinberger, 1976; Potashner *et al.*, 1988). Corticotectal tract terminates in IC, while corticobulbar tract terminates in SOC and CN. Cortical layer V projects directly to IC, SOC and CN (Feliciano *et al.*, 1995; Winer, 2005; Meltzer and Ryugo, 2006; Bajo *et al.*, 2007). Two tracts descend from inferior colliculus, colliculo-olivary, projecting to SOC, and colliculo-cochlear, terminating in CN (Faye-Lund, 1986; Saldaña, 1993; Malmierca *et al.*, 1996). Finally, the most peripheral, olivocochlear tract consists of SOC projections to CN and organ of Corti (Rasmussen, 1946; Ciuman, 2010).

Laminar architecture of AC is similar as in other cortical areas, with six layers (I-IV) and layer II and III merged into layer II/III in rodents (Linden, 2003; Malmierca and Ryugo, 2012). Each of the cortical layers contains specific types of neurons, with specific dendritic morphology and axonal connections, as well as distinct electrophysiological properties. As previously described, inputs from vMGB primarily go into layers III and IV, while the feedback control from AC downstream goes from layers V and VI.

Around 20% of neurons in the cortex are GABAergic, and 40% of them are PV+ interneurons (Xu *et al.*, 2010). In the auditory cortex, these inhibitory neurons are responsible for shaping the receptive fields of neurons, through controling their intensity and frequency tuning as well as their temporal precision (Wang *et al.*, 2002; Wehr and Zador, 2003; Moore and Wehr, 2013). For example, Aizenberg *et al.*

demonstrated that activation of PV+ interneurons results in narrowing receptive field of excitatory neurons in mice, while supressing PV+ interneurons had an opposite effect (Aizenberg *et al.*, 2015). PV+ interneurons in A1 are most abundant in the vMGB input layers - deep layer III and layer IV (Hendry and Jones, 1991; Ouellet and de Villers-Sidani, 2014).

Layer I is the top-most cortical layer, which contains a small number of neurons and almost all of them are inhibitory neurons (Prieto *et al.*, 1994). It receives inputs mostly from mMGB (Larkum, 2013; Lee, 2013).

Layer II/III contains inhibitory neurons and most of the pyramidal callosal projection neurons. Neurons in this layer are small and densely packed (Winer, 1984c, 1984b, 1985). Most of them locally innervate L II/III and L V, but they also have axonal projections to distant cortical regions, projecting across corpus callosum (Imig and Brugge, 1978; Lee and Winer, 2008; Hand *et al.*, 2015). Excitatory L II/III neurons are highly selective and sharply tuned to auditory stimuli (Sakata and Harris, 2009). They fire sparsely and are several-fold less active than L V excitatory neurons for both spontaneous and evoked activity.

Layer IV neurons have axons projecting to L II/III and L V and receiving auditory input from vMGB (Winer, 1984a; Lee and Winer, 2008). In other sensory cortices, L IV is mainly populated by spiny stellate cells. However, in the auditory cortex these cells are absent and L IV contains mostly small, densely packed pyramidal cells (Smiths and Populin, 2001). Main GABAergic neurons in this layer are PV+ interneurons (Ouellet and de Villers-Sidani, 2014).

Layer V consists of inhibitory and large pyramidal neurons that receive inputs from many sources, mostly upper cortical layers, and have outputs to cortical and subcortical structures (MGB, IC and pons) (Lee and Winer, 2008; Lee, 2013). L V neurons in primary auditory cortex show dense spontaneous and auditory-evoked activity (Sakata and Harris, 2009). A possible role of these large, dense-coding cells

is to receive information from many small, sparse-coding cells and then broadcasting the information to subcortical structures (Sakata and Harris, 2009; Kim *et al.*, 2015).

Layer VI is the deepest and oldest cortical layer. It contains corticothalamic neurons, which project primarily to the ipsilateral MGB (Lee, 2013; Harris and Shepherd, 2015). It receives inputs from mMGB and L I (Lee and Winer, 2008; Lee, 2013). Diversity in neuronal morphology is the largest in this cortical layer, hence the name multiform layer (Briggs, 2010; Thomson, 2010).

Auditory cortex is the final target in auditory information processing and several studies have shown it is directly involved in basic auditory processing such as tone detection and frequency discrimination (Talwar *et al.*, 2001; Jaramillo and Zador, 2011; Pai *et al.*, 2011; Kato *et al.*, 2015; Carcea *et al.*, 2017). Further, developmental changes in the cortex are suspected as the basis for the emergence of ASD phenotypes. Thus, auditory cortex should be investigated when looking into ASD-related abnormalities in auditory perception. Next, I will summarize the paradigms that can be used for assessing sensory perception.

1.4. Behavioural assessment of sensory perception

Sensory information processing starts with the reception of the stimulus, followed by transmission of stimulus information and finally, its perception. Reception and transmission of auditory stimuli have been covered in the previous subchapter, so here I will focus on perception and the methods for its assessment in rodents. Sensory perception starts with stimulus detection, followed by stimulus discrimination, identification and finally, comprehension.

The easiest and most basic level of perception is stimulus detection, meaning identification of the presence or absence of a stimulus. Usually, in behavioural detection tasks, different intensities of stimuli are used to identify the minimal detected intensity or, detection threshold (e.g. (Gillmeister and Eimer, 2007)).

Discrimination is the ability to identify the difference between two stimuli. Many behavioural discrimination tasks test to identify the smallest difference between presented stimuli that can still be recognized as separate stimuli (e.g. (Lindholm and Koriath, 1985)).

Stimulus identification requires detection and discrimination of the stimulus and then naming, or, identifying it (e.g. different tones in a sequence (Divenyi and Hirsh, 1974)). Finally, the most complex level of perception is comprehension. It requires all previous levels and understanding the meaning of the stimulus (e.g. musical instrument (Handel, 1995)).

Since rodents are the most prevalent experimental animal models, behavioural tasks were designed to investigate their sensory perception. Here, I will go through the main aspects to consider when planning a sensory assessment in rodents, followed by the paradigms used mostly for evaluation of stimulus detection or discrimination in head-fixed conditions.

1.4.1. Degree of movement

There are two main options for movement to consider when planning behavioural assessments in rodents, head-fixed and freely moving. It is also possible to combine the two, for example having an animal head-fixed while walking or running on a ball or a treadmill while presenting the stimulus in a virtual environment.

Ideally, to investigate rodent behaviour in the most natural way we would use a freely moving setup. One of the prevalent behavioural paradigms used in this condition for rats and mice is a three-port setup, where the subject is expressing their decision by poking their nose into one of the ports (Uchida and Mainen, 2003; Busse *et al.*, 2011; Raposo *et al.*, 2012). This paradigm can be combined with a limited number of methods for neural recordings, in either a wireless or tethered approach. Nevertheless, for most of the methods to assess electrophysiological activity, this option may not be ideal. Approaches for long-term chronic neuronal recordings in freely moving rodents are being developed (Voigts *et al.*, 2013; Inagaki *et al.*, 2019;

Juavinett *et al.*, 2019; Polo-Castillo *et al.*, 2019; Burton *et al.*, 2020), however acute recordings in head-fixed animals are still superior in terms of stability, SNR and precision control, making them the most prevalent choice.

Head-fixed condition is commonly used in rodents to assess neural correlates of sensory perception. This allows precise monitoring and modulation of neuronal activity, with great stability of the recordings and high SNR (Ferezou *et al.*, 2007; Komiyama *et al.*, 2010; Guo *et al.*, 2014a; Allen *et al.*, 2019; Steinmetz *et al.*, 2019). Rodents can engage with the behavioural paradigm by operating levers, turning a wheel or licking spouts with sensor beams. Head-fixed condition also allows tracking of eye movement, pupil dilation or whisker movement, all of which gives us additional information on subjects state. Recently, a head-mounted system was made for tracking eye, pupil and whisker movement in freely-moving mice, with simultaneous electrophysiological recording, making this information available in freely-moving condition as well (Meyer *et al.*, 2018).

1.4.2. Motivation

Rodents need to be motivated to learn and execute a task. Motivation can be accomplished in two ways, giving rewards as positive reinforcement or punishment as negative. Using punishment can lead to quicker learning but it also causes stress in animals, which can have a negative effect on motivation in complex tasks (Carandini and Churchland, 2013). Positive reinforcement, therefore, seems like a better choice for motivation, and it is becoming a more common choice for behavioural scientists (Busse *et al.*, 2011; Felsen and Mainen, 2012; Raposo *et al.*, 2012; Guo *et al.*, 2014b).

A typical choice for reward is either water or food pellets. To persuade rodents to perform in a task in exchange for a reward, animals in behavioural assessments are put in food or water restriction. This means that they receive a certain amount of water/food per day, typically for 5 to 7 days a week, and part of their daily intake comes from task engagement. The amount of daily intake is determined by animals weight and overall health status (Guo *et al.*, 2014b). However, occasionally, regular

water and food are not motivating enough so sucrose can be used in form of pellets or diluted in water (Guo *et al.*, 2014b).

Most commonly used methods for punishment are air puffs, mild electric shock and time-out (Letzkus *et al.*, 2011; Guo *et al.*, 2014b; Song *et al.*, 2017; Gallero-Salas *et al.*, 2021). Punishment is often used in combination with reward, i.e. giving rewards for correct behaviour and punishing unwanted behaviour.

1.4.3. Training length and timing

The length of training for a paradigm also has to be taken into account when planning the task. Naturally, subjects will take longer to learn complex tasks and short training time could cause high variability in results and a lot of errors (Carandini and Churchland, 2013). On the other hand, overtraining can cause a shift from purposeful and goal-directed behaviour to repetitive, habitual behaviour and leads to changes in neuronal plasticity and spiking dynamics (Smith and Graybiel, 2013). This could generate incorrect conclusions on the neural basis of investigated behaviour.

Another aspect to consider is the time of day for training. Rodents are nocturnal animals, meaning they are most active during the night. In order to match up their circadian rhythm with ours, researchers usually place behavioural animals into the reverse light/dark cycle (O'Connor *et al.*, 2010; Guo *et al.*, 2014b; Speed *et al.*, 2019; Rumyantsev *et al.*, 2020). In this way, after a habituation period to a new cycle, we can train and test the subjects during their most active phase.

Finally, the length of a session and number of sessions per week can also influence the length and success of the training. Ideally, sessions shouldn't be too long because the subject can get fed-up or lose interest. Too short sessions can produce misleading results if the animal is too eager or thirsty, but it can also lead to undertraining. The number of sessions per week varies among studies, but they are most often between 5 and 7. Too few session in a week can cause animals to forget the task and lead to a longer training period.

1.4.4. Paradigms for perceptual assessment in head-fixed condition

Go/No-go task

This paradigm is the simplest by design and rodents can learn it relatively quickly. The goal of this task is for the animal to perform an action in the presence of a stimulus or its specific feature ("Go") and to not engage in its absence ("No-go") (Figure 1.11A). The main problems with this paradigm are subjects motivation and impatience (Carandini and Churchland, 2013). As the session progresses, the animal can lose its motivation to perform, especially with more difficult stimuli. This would cause false-negative results, implying that the animal cannot detect the stimulus while the actual truth is that stimulus was detected but the subject did not engage in the task. On the other hand, a subject can be too eager and perform the action even without the presence of the stimulus or when it cannot detect it. This can cause false-positive results, suggesting that the subject can detect certain stimuli when that is not actually the case.

To avoid false positive and false negative results, signal detection theory is used (Carandini and Churchland, 2013). In this method catch trials are introduced as trials where the stimulus is not presented, to "catch" how often the subject engages randomly. Animals reaction during the catch trial is counted as "false alarm" while non-engagement is counted as "correct rejection". False alarm rate is then calculated as the percentage of animals reaction during catch trials and used to normalize the "hit" rate. If the animal is too eager to perform and has a large FA rate, one should consider adjusting the reward size. If the animal lacks motivation, causing low hit and FA rates, one should also adjust reward size as well as consider having shorter sessions and re-training the subject, if necessary.

A true, objective measure of animals responses, independent of their strategy bias is discriminability (detectability) index (d'). D-prime is an estimation of the signal (stimulus) strength relative to no-signal condition (Figure 1.10.). It is calculated as:

$$d' = Z(\text{hit rate}) - Z(\text{false alarm rate}),$$

where Z is inverse of the standard normal cumulative distribution function (Green and Swets, 1966). Higher d' means better discriminability between signal and no-signal condition.

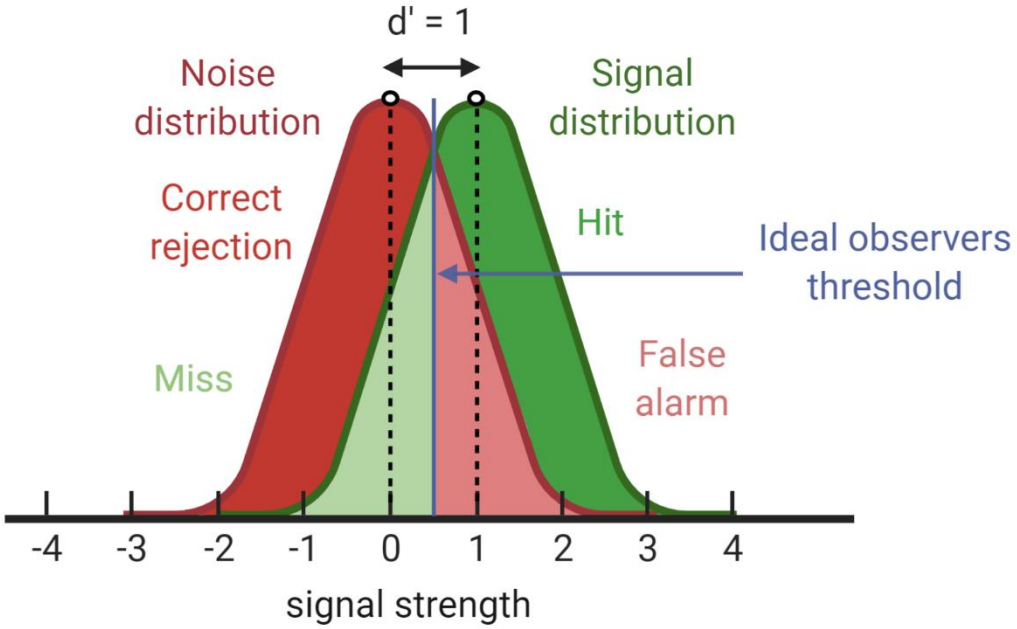

Figure 1.10. The model of signal detection theory. Distance between the mean signal distribution and mean noise (no-signal) distribution is d'. Detection threshold of an ideal observer is located in between noise and signal distribution. Increase in signal strength will result in higher d', increasing the threshold and the probability of a „hit“ outcome. (Adapted from Abdi, 2009)

Two alternative choice task

Another name for this paradigm is the “yes/no task“. It is a modification of the Go/No-go, where the animal chooses between two actions when the stimulus is presented (e.g. “move left“ or “move right“) (Figure 1.11B). In this way, the subject has to engage in every trial so it is not susceptible to false-negative results due to motivation. SDT can be used in this paradigm, to assess the FA rate for each action. This paradigm is still vulnerable to subjects strategy bias (Carandini and Churchland, 2013).

Two alternative forced-choice task

This paradigm consists of presenting two different stimuli during each trial, either in a sequence or simultaneously, where the action associated with the correct stimulus has to be chosen (Figure 1.11C). By forcing the subject to choose between two stimuli, the impact of both motivation as well as strategy bias is eliminated (Carandini and Churchland, 2013).

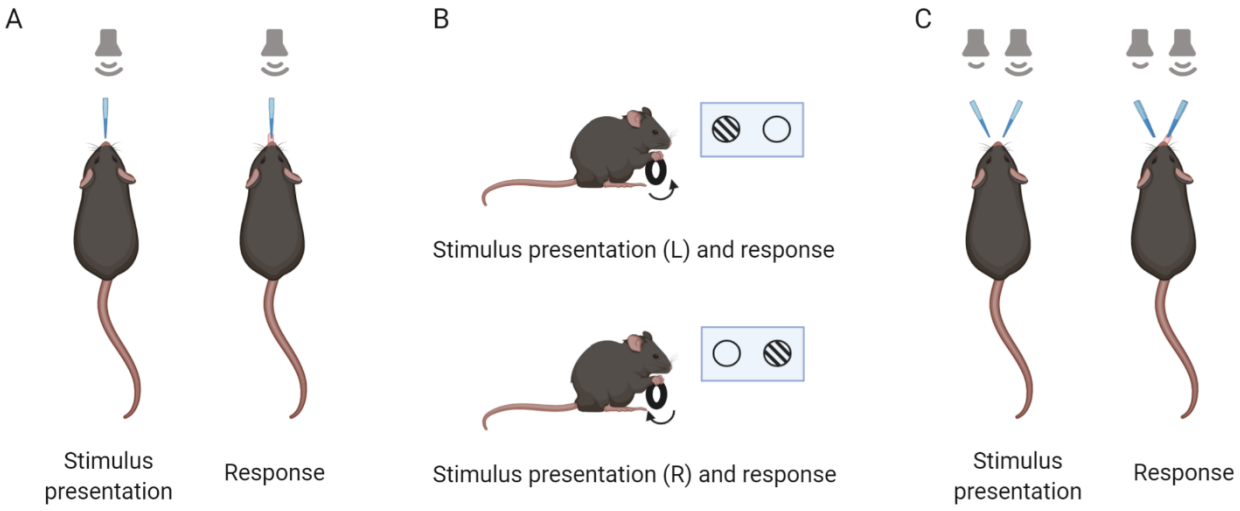

Figure 1.11. Behavioural paradigms for head-fixed conditions. **A**- Go/No-go task. When a stimulus (sound) is presented, the animal has to lick the spout to get a water reward. **B**- Two alternative choice task. Visual stimulus (gratings) are presented. Depending on the location of the gratings, animals have to turn the wheel left or right to get a water reward. **C**- Two alternative forced-choice task. Two different sounds are presented simultaneously. Animals have to lick the spout at the side of the target stimuli, to get a water reward.

To conclude, for the purpose of investigating simple auditory detection in mice while simultaneously recording neural activity, Go/No-Go task in combination with signal detection theory and water/food-restricted head-fixed conditions appears as an optimal choice. In the following subchapter, I will describe the main methods for examining neural activity, and emphasize the ones that could be combined with this behavioural assessment.

1.5. Methods for examining neural activity

In order to understand how and why do behavioural and sensory processing differences emerge in ASD, one should examine neuronal firing dynamics in relevant brain areas. Ideally, this investigation would be done *in vivo*, while the subject is performing a suitable perceptual behavioural paradigm. As mentioned previously, EEG and fMRI studies in ASD patients have indeed found certain abnormalities in neuronal activity during sensory processing assessments.

Techniques for observing and recording neuronal activity have been developed since the 17th century, when Jan Swammerdam and subsequently Luigi Galvani measured contractions of frogs leg muscle caused by stimulating its nerve ends. Later on, Giovanni Aldini in the early 19th century was the first to electrically stimulate the brain itself, a cerebral cortex of a decapitated prisoner, and elicit a physical, facial expression response (Verkhratsky *et al.*, 2006; Meng, 2018).

The field has progressed immensely since then, starting with the recordings of resting and action potentials as well as the development of an early form of EEG in the late 19th century, but especially later, during the 20th century with the development of wire electrodes in the 1950s (Hubel, 1957; Meng, 2018). As microelectronics production grew, microelectrodes and multi-electrode arrays were developed and refined.

Nowadays, the research technology is rapidly improving, with recording devices being smaller and more flexible, as well as yielding a high number of neurons of high quality.

Methods for examining neuronal activity *in vivo* can be grouped into neuroimaging and electrophysiological techniques. Here, I will briefly explain the differences between them and characteristics of main techniques within each group based on their resolution, invasiveness and scale. I will also point out what this project requires in terms of neuronal activity recording, and conclude which method would be ideal for it.

1.5.1. Neuroimaging technology

Imaging techniques are non-invasive or invasive, enabling the monitoring of neural activity through indirect measurements such as changes in blood oxygenation, magnetic field changes or calcium concentration.

Blood Oxygenation Level Dependent functional Magnetic Resonance Imaging (BOLD fMRI)

BOLD fMRI detects changes in deoxyhemoglobin concentration in the brain, caused by neuronal activity. Neuronal firing and signalling processes require the consumption of energy, coming in the form of ATP. When neurons increase their activity, local ATP use is increased, leading to a rise in the rate of glycolytic oxygenation of glucose, a process that produces more ATP. As oxygen is used in this process, blood flow increases to replenish the local tissue with oxygen. Therefore, with a rise in neural activity, there is first a rise in deoxygenated, or deoxyhaemoglobin, followed by an increase in oxygenated haemoglobin and a decrease in deoxyhaemoglobin. BOLD fMRI can detect these changes in the oxygenation of haemoglobin (Glover, 2011).

fMRI has an excellent spatial resolution, allowing the tracking of changes within brain structures with millimetre level precisions. However, its temporal resolution is inferior (peak occurs 5-6 seconds after the stimulus onset), so it cannot track fast changes in neuronal activity, crucial for research of evoked auditory responses. Because of its low temporal resolution, fMRI is often paired with high temporal resolution methods, such as EEG or MEG (Dale and Halgren, 2001). Thus, fMRI is a great technique for observing spatial differences in brain activity, however if temporal and spatial accuracy is required fMRI should be combined with another technique.

Magnetoencephalography (MEG)

MEG is a non-invasive method that measures changes in magnetic fields generated by neuronal electrical activity. Synchronous neuronal activity generates an electric current and consequently a magnetic field perpendicular to its orientation. Since axonal and synaptic magnetic fields cancel out, measured magnetic fields come from

dendritic currents. These magnetic fields are very small, thus observing them requires highly sensitive detectors and magnetically well-isolated space. MEG has a very high temporal, but inferior spatial resolution, so it is beneficial to combine it with MRI (Singh, 2014; Carter and Shieh, 2015). However, both MEG and fMRI require large and very expensive equipment (Carter and Shieh, 2015).

Functional near-infrared spectroscopy (fNIRS)

This non-invasive imaging technique is using near-infrared light for measuring levels of oxygenated and deoxygenated haemoglobin in the brain. Near-infrared light is shined on the scalp of the subject and changes in haemoglobin optical absorption are assessed by the amount of diffused light acquired by a detector. Based on the same biological principles as BOLD fMRI, these changes in deoxyhemoglobin levels can be linked to neural activity.

fNIRS has a medium quality temporal resolution (higher than fMRI, lower than EEG and MEG) and it is significantly cheaper and smaller than MEG or fMRI. Its portability and wireless options enable it to be used for investigating brain development as well as brain activity measurements during motion tasks. However, the major limitations of this method are its poor spatial resolution (1-10 centimetres) and large artefacts produced by movement (Herold *et al.*, 2018; Quaresima and Ferrari, 2019).

Multi-photon calcium imaging

Multi-photon calcium imaging allows real-time monitoring of cell activity *in vivo*, done either through the intact skull (non-invasive) or though thinned skull or a cranial window (minimally invasive). Neural activity is accompanied by an increase in intracellular Ca^{2+} concentration. If we load the neurons with a calcium-sensitive dye or modify them to express genetically encoded calcium indicator (GECI), changes in Ca^{2+} concentrations can cause the cells to emit a fluorescent signal. Therefore, detected fluorescent signals can reflect the activity of labelled neurons (Russell, 2011).

GECI, such as GCaMP, have a high cell specificity, however scanning speed for Ca^{2+} dynamics recording is low, causing a low temporal resolution (Carter and Shieh, 2015; Anderson *et al.*, 2018). Additionally, long-term and high GCaMP epression can lead to abnormalities in cell function (Tian *et al.*, 2009). A fundamental limitation of this technique is its depth penetration. Two-photon calcium imaging allows monitoring activity of mostly superficial neurons (up to ~500 µm), while three-photon microscopy has a better depth reach (~1100 µm) (Svoboda *et al.*, 1997; Kerr and Denk, 2008; Mittmann *et al.*, 2011; Horton *et al.*, 2013).

Thus, calcium imaging has excellent spatial resolution and targeting specificity, allowing us to track the dynamic of specific cell types and investigate their role in certain pathways through genetic or pharmacological manipulations. Additionally, it is possible to track the activity of a large set of cells across time (Huber *et al.*, 2012). However, the main limitations of calcium imaging are temporal resolution and depth penetration.

1.5.2. Electrophysiology

The branch of physiology studying electrical properties of cells is called electrophysiology. In the neuroscientific field, it refers to measuring neuronal electrical activity, either directly from inside a cell (intracellular recording) or from the outside (extracellular recording).

Electroencephalography (EEG)

EEG is a non-invasive electrophysiological method, used widely in human clinical studies, but also animal studies. Neural activity in a cortical tissue aggregates into electrical signals which can be detected externally. Electrical signals in EEG are detected and recorded through electrodes placed on the surface of the subject's scalp. As a result, the method has a poor spatial but good temporal resolution. Another weakness of this method is the reduction in the signal strength caused by its transition through meninges, skull and skin. Nevertheless, this method is very useful for detecting changes in brain waves and it is used in investigating sleep, attention and epilepsy (Srinivasan and Nunez, 2012).

Electrocorticography (ECoG)

ECoG, also called intracranial EEG, is an invasive electrophysiological method, where electrical signals of aggregated neuronal activity from a brain area are recorded directly from the surface of the brain. Compared to EEG, the electrical signals in ECoG are stronger since they are not passing through the dura, skull and scalp. Further, ECoG produces fewer artefacts and it has a higher spatial and temporal resolution than EEG (Worrell *et al.*, 2008; Jeremy Hill *et al.*, 2012).

Patch clamping

This method focuses on single-cell observations. A current is passed through the cell membrane and resulting action potentials are measured using a glass pipette microelectrode sealed to the membrane. Patch clamping is traditionally done on isolated or cultured cells and brain slices, however over the past two decades *in vivo* patch-clamp recordings has also been done in awake and behaving rodents (Furue *et al.*, 2007; Tao *et al.*, 2015). This technique is ideal for studying cell synaptic properties and it can record cell spiking activity with high SNR. Main limitations of *In vivo* patch clamping are its technical difficulty and recording depth, which is mostly reported as less than 500 µm, athough some studies reported imaging at 1000 µm (Tao *et al.*, 2015). This technique also yields a very small number of cells per recording session (Furue *et al.*, 2007; Tao *et al.*, 2015).

Microelectrodes

Electrodes used for extracellular electrophysiological recordings have been developed throughout the late 20th century. They are inserted into the desired brain area, allowing the research of deep cortical layers and deep brain structures. Activity of different neurons can be distinguished based upon their amplitude and waveform shape. If a neuron is further away from the electrode recording site, his measured amplitude is smaller.

Single glass and wire electrodes were first used (Ling and Gerard, 1949; Hubel, 1957; Evarts, 1968). However, distinguishing the activity of a single neuronal unit is impossible with this technique, since recorded neurons surrounding the electrode

are at approximately equal distance from the electrode. Another drawback of this method includes large artefacts and considerable tissue damage. The improvement was made with tetrodes, where 4 wires are tightly bound, leading to 4 electrodes separated in space, thus allowing the distinction of single units (O'Keefe and Recce, 1993; Wilson and McNaughton, 1993). Tetrodes also have low-impedance tips and better mechanical stability (Buzsáki, 2004).

Even though this method allows the recording of deeper brain areas, it can produce only a small amount of neurons per recording session. Further, microelectrodes can record only from a certain depth at a time, so in order to cover the desired depth range, they need to be driven down across multiple recordings (Csicsvari *et al.*, 2003).

High density electrode arrays

Arrays of microelectrodes, or microarrays, offer an improvement in depth coverage as well as spatial resolution, leading to a higher number of isolated single units. Through microfabrication, the recording channels are shaped into a precisely distributed array along the length of a silicon probe (Csicsvari *et al.*, 2003; Buzsáki, 2004). Silicon probes end in a sharp tip, allowing easier insertion into the brain tissue and causing less tissue damage.

Current silicon probes exist with different number of channels, from 4 to 32, allowing for higher or lower coverage of neurons at different depths (Figure 1.12A-B). The number of shanks can also differ, with multi-shank probes allowing for recording across horizontally large brain areas, such as auditory cortex.

To record the activity of regions in large primate brains, three-dimensional microarrays were developed, such as Utah electrode array. These arrays consist of multiple sharp needles arranged on a square grid (Campbell *et al.*, 1991). Utah array contains a single electrode on each shank, with the longest shank length of 1.5mm. These probes have been used for acute as well as chronic recordings in monkeys and humans (Nicolelis *et al.*, 2003; Pinto *et al.*, 2014). Recently, Utah arrays were also developed for rodent research (Cody *et al.*, 2018).

The most recent development in microarrays are Neuropixels probes (Figure 1.12C) (Jun *et al.*, 2017). These probes are very long and have a high number of channels. Neuropixels 1.0 contains 960 electrodes distributed in 2 arrays along 10 mm long shank. The probe is divided into 3 banks, each bank containing an electrode connected to one of the 384 channels (Figure 1.12D). This allows for a depth specific selection of 384 simultaneously recording channels. Recording channels can cover multiple brain areas, including very deep brain structures and produce a high number of single units. The drawback of Neuropixels 1.0 is that it contains only one shank, withholding the possibility to cover a larger surface of horizontally broad brain areas. Recently, Neuropixels 2.0 has been introduced, which has all the advantages of the older version, with a multi-shank option (Steinmetz *et al.*, 2020). Implantation fixtures are also being developed, allowing chronic long-term recordings in freely moving animals, with safer extraction and reusing of the probe (Juavinett *et al.*, 2019; Steinmetz *et al.*, 2020). Since Neuropixels probes are very expensive (~€ 6000 for 5 probes), their preservation and durability are of importance. If maintained properly, these probes can be used for a substantial number of recordings.

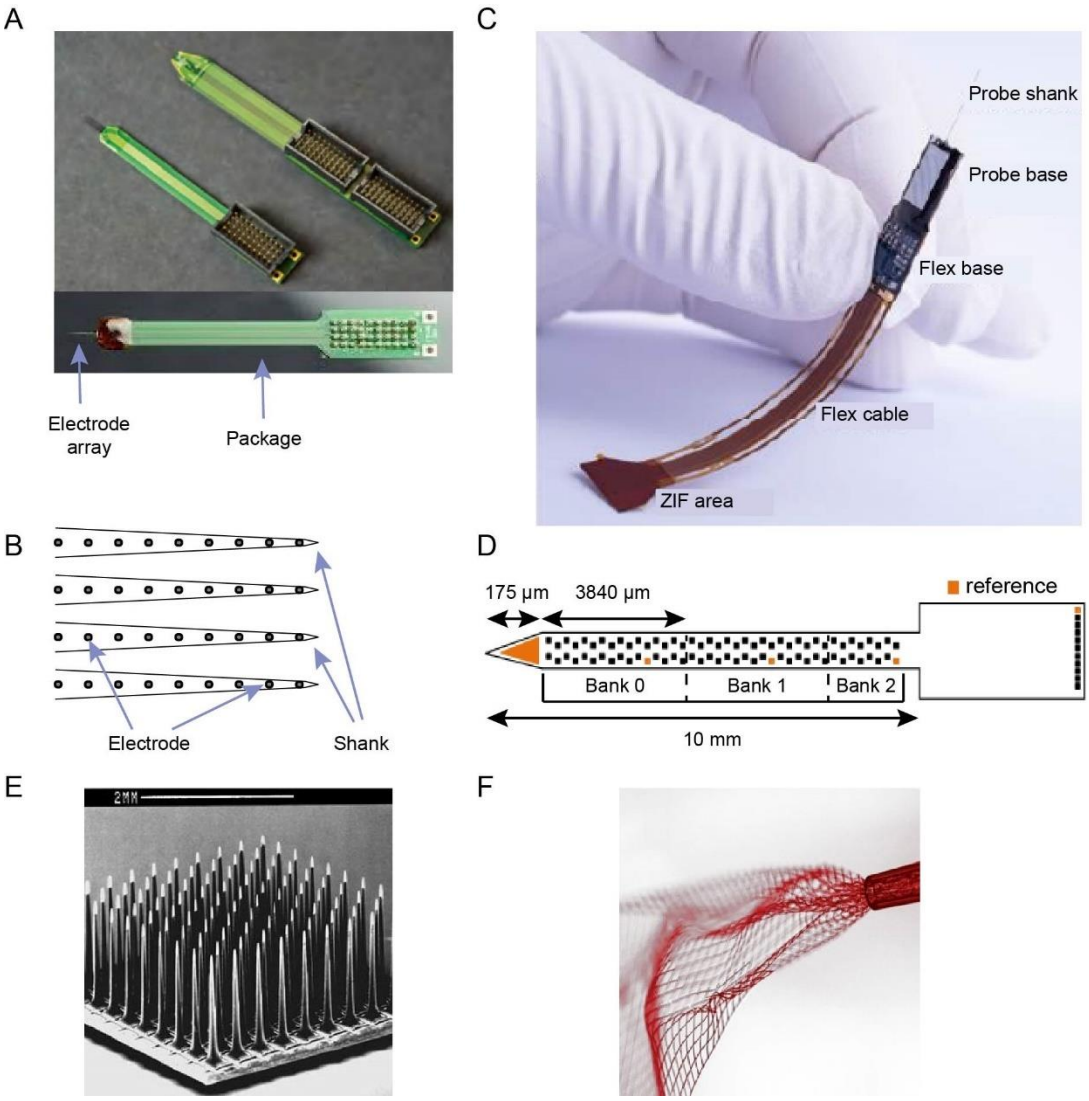

Figure 1.12. Examples of high density electrode arrays. **A**- 32 and 64 channel silicon probes. **B**- schematics of multi-shank microarrays. **C**- Neuropixels probe. **D**- Schematics of electrode arrays on a Neuropixels probe. **E**- Utah array. **F**- Mesh multielectrode polymer probe injected through syringe. (Images adapted from NeuroNexus 2019 design catalog, Neuropixels 1.0 User manual, Mesh Electronics website and (Kim *et al.*, 2006))

Even though high density electrode arrays have many advantages, such as high temporal resolution and the ability to detect spiking activity of single units across depth, their main limitations are invasiveness and tissue damage. In long-term chronic recordings scarring tissue forms around the electrodes, decreasing the transmission of neuronal signals (Turner *et al.*, 1999).

To overcome the rigidness and low biocompatibility of current electrode arrays, thin, flexible multielectrode polymer probes are currently being developed (Hong *et al.*, 2018; Musk, 2019). The drawback of these probes is insertion difficulty. Since they are thin and flexible, they cannot penetrate the tissue, thus injections or stiffeners are used (Fu *et al.*, 2017; Chung *et al.*, 2019).

1.5.3. Project requirements

In this project, we want to investigate neural activity across auditory cortex and auditory thalamus in awake, passive listening and task performing mice. We need a method with a high spatial and temporal resolution, to detect the individual spiking activity of distinct neurons as well as local field potentials during short sound presentation trials, across all cortical layers as well as subcortical structures. We would also ideally record from many neurons, excitatory and inhibitory, to assess changes in population activity caused by the XAV939 treatment.

Because of these requirements, we have decided to use high density electrode arrays. Multi-shank silicon probes are ideal for sampling a high number of single units across width and depth of the auditory cortex. Neuropixels probes are optimal for simultaneous recording across relevant cortical and subcortical structures, also yielding a high number of units. These two types of probes meet all the project demands and they can be used in awake, head-fixed mice.

1.6. Hypothesis and aims

As discussed in the introduction, the size of the cerebral cortex is an important factor in brain function. Alterations in the number of L II/III neurons, the ratio of E and I neurons and their wiring could be the reason behind abnormal sensory processing found in neurodevelopmental disorders, such as autism. However, the exact relationship between these abnormalities in cortical circuitry and sensory perception is still unclear.

We aim to test the hypothesis that a disturbed E-I ratio, caused by an overproduction of superficial cortical E neurons, will result in atypical cortical activity and consequently, abnormalities in sensory processing and auditory perception.

Investigating a specific causality in humans, such as disruptions in the Wnt pathway or overproduction of superficial cortical neurons, is practically impossible. We will take an advantage that XAV939 mouse model was developed exhibiting these exact traits, with macrocephaly and autism-like phenotypes (Fang *et al.*, 2014). Using this mouse model also enables us to apply an invasive electrophysiological method with high spatial and temporal resolution in combination with a behavioural paradigm for assessment of auditory perception. Further, mice are easy to maintain and they have short breeding cycles as well as large litters. All of these factors make them an ideal experimental model for this study.

This project was centred around several specific objectives:

1. Experimental increase in the number of L II/III excitatory neurons in mice using XAV939 and verifying this overproduction histologically.
2. Training mice for performing in an auditory detection task under head-fixed conditions, and assessing the impact of L II/III neuron increase on speed and accuracy of auditory detection.
3. Characterizing differences in spontaneous and evoked auditory cortical activity between XAV939 treated and control animals using microarrays.
4. Assessing mice detection task performance during simultaneous neuronal activity recordings, in order to elucidate the neural basis of sound detection differences.

There are also several key aspects we had to consider when planning XAV939 treatment for manipulating neurodevelopment: dose, treatment time window, frequency of exposure and possible sex differences. Changes in any of these factors could affect the results. In this study, we have tested two treatment volumes, high (0.4 µl) and low (0.15 µl). Embryos were injected only once and always in the same time window (E14), to target the development of L II/III specifically. Finally, we have

looked at electrophysiological and behavioural differences in male mice only, which is in accordance with previous results showing ASD related abnormalities being more prominent in males (the reported approximate ratio is 4:1) (Fombonne, 2002).

Next chapter will summarize the materials and methods used to assess the impact of cortical expansion on auditory processing.

2. Materials and methods

2.1. Mice

All experiments and procedures were performed in accordance with the Animals Scientific Procedures Act of 1986 (PPL 70/8883) and with the consent of the Home Office and the University of Strathclyde's Ethical Committee.

A flowchart of the procedures (Figure 2.1) is showing how the mice were used in this project. Male wild-type (WT) C57BL/6 mice were used for breeding (n=10), behavioural assessment (n=30), electrophysiological recordings (n=20) and simultaneous electrophysiological recording during behavioural assessment (n=7). Female C57BL/6 (n=28) and CBA/Ca (n=1; used during procedure optimization) mice were used for *in utero* microinjections. Some mice were perfused at P2 (n=31) and P21 (n=35) for histological assessment of cortical layers width. Animals that could not learn the auditory detection task were perfused and excluded from the study (n=3).

Male mice used for electrophysiological and behavioural assessments were single housed after headcap surgery in high-roofed cages with ad libitum access to food and water. After a week of recovery from surgery, they were placed into reverse light/dark cycle (dark 10am-10pm). They were water restricted a week after adaptation to the new light/dark cycle (Figure 2.1).

Pregnant female mice were single housed in flat-roof cages with ad libitum access to food and water. They were housed in normal light/dark cycle.

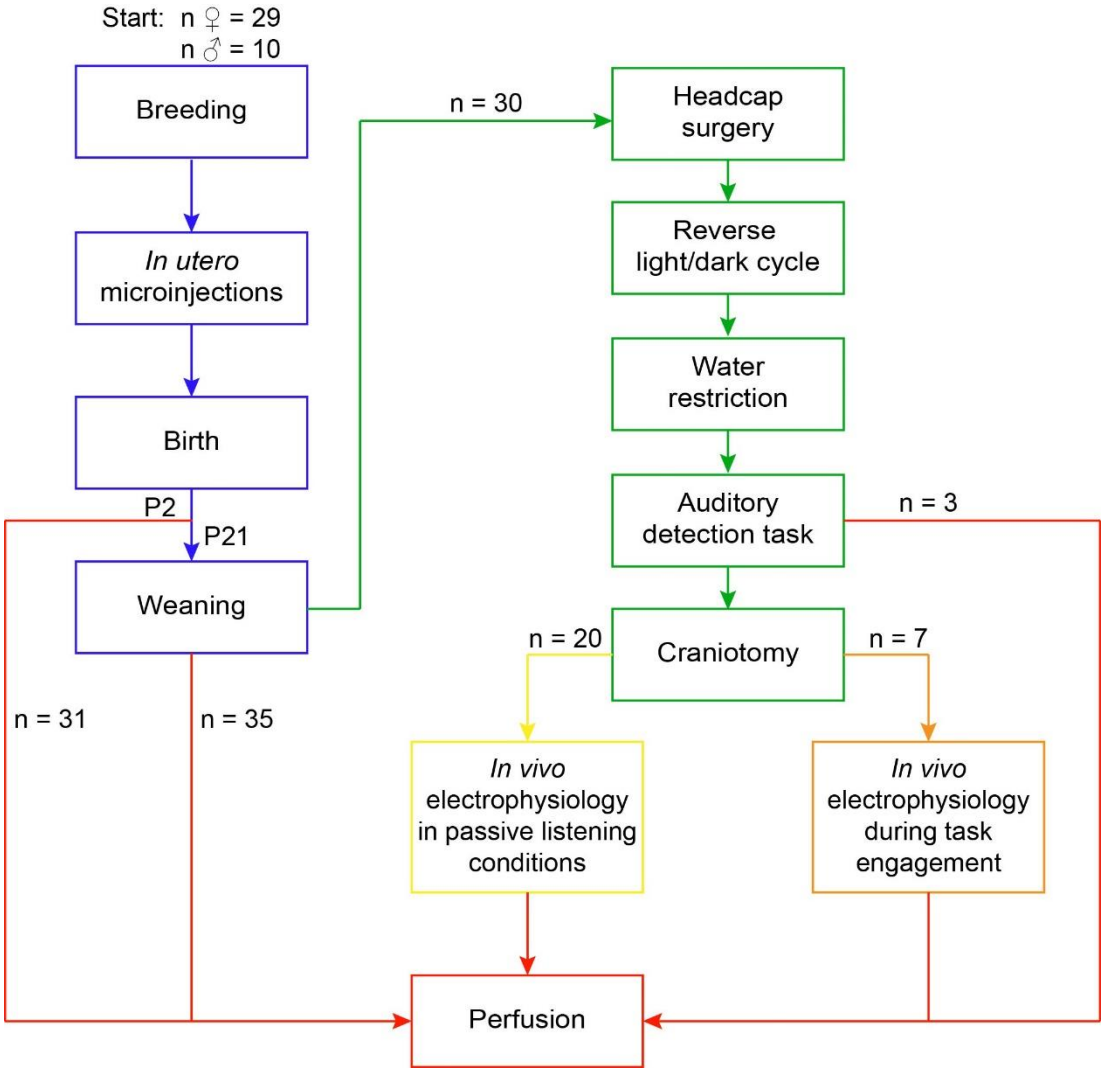

Figure 2.1. Flowchart of the procedures in the project. Each male used for breeding was paired with ~3 females. Male breeders were culled afterwards. All pregnant females went through *in utero* microinjections and were culled after weaning the pups on postnatal day 21 (P21). From each litter, a maximum of 2 male pups was kept for further experiments, and the rest of the litter was perfused on either P2 or P21 and used for histological measurements of cortical layers width. Headcap surgery was done on the male mice when they were ~8 weeks old. After 2 weeks of recovery and adaptation to reverse light/dark cycle, mice were water restricted and habituated for behavioural assessment. Following successful completion of the task, mice were habituated for electrophysiological recordings. Craniotomy was done and we have recorded from the auditory cortex of the mice for 2 days. Mice were perfused afterwards.

2.2. *In utero* microinjections

Female mice were put in the cage with a male mouse for breeding and checked twice a day (early morning and late afternoon) for a vaginal plug. The appearance of a plug was marked as embryonic day 0 (E0) and the female was moved into a separate cage. Females were weighed every couple of days and gain of weight (at least 1.7g before E10) was considered as a confirmation of pregnancy.

Mice embryos were injected with 10µM XAV939 (X3004, Sigma Aldrich) in DMSO solution with 0.05% Fast Green dye (F7258, Sigma Aldrich; treated litter) or DMSO with 0.05% Fast Green dye solution (control litter) on E14.

Glass micropipettes were filled with the mix and placed into the pipette holder of the injector (Pneumatic PicoPump PV820, World Precision Instruments). Volume of injections was either 0.15µl (9 treated and 5 control litters) or 0.4µl (8 treated and 7 control litters).

Aseptic technique was kept during the surgery by using autoclaved instruments, gown and drapes, sterile saline and sterile gloves as well as disinfecting all surfaces before starting the surgery. Female mice were anaesthetized using isofluorane in an anaesthetic chamber and hair was shaved from their abdomen. Subcutaneous injection of a pre-op mix of Vetergesic (3ml/kg, 0.1% diluted in sterile saline), Rimadyl (10ml/kg, 0.01% diluted in water for injection) and sterile saline was administered. The surface of their eyes was covered with artificial tear gel (Lacri-lube, Allergan or Viscotears, Bausch&Lomb) in order to prevent them from drying. Mice were then placed on the heat mat (maintained at 38°C) facing upwards and secured in place, with their head in anaesthesia mask (Figure 2.3.). Their breathing was monitored throughout the surgery and isofluorane and oxygen levels were adjusted accordingly (isofluorane between 1.5-2.5% and oxygen between 1-1.5%). The incision site was cleaned with ethanol (70%) and betadine. A 2cm incision was made 1cm above the vagina, first in the skin and then in the muscle. Before cutting the muscle, blunt dissection was made in order to separate the skin from the muscle. Uterus was found underneath and a part of it was lifted out using ring forceps. Starting from one end

of the uterus and going towards the other end, the embryos were injected with 2-3 injector pulses through the uterus wall into the lateral ventricle (Figure 2.2). When all of the embryos were injected the uterus was positioned back in place and the muscle was sutured, followed by suturing and then stapling the skin. During the whole surgery warm sterile saline (37-38°C) was used to keep the uterus from drying.

Females were closely monitored for the next couple of days and were given post-operative medications and care. They gave birth between E18-E21, which was considered as postnatal day 0 (P0).

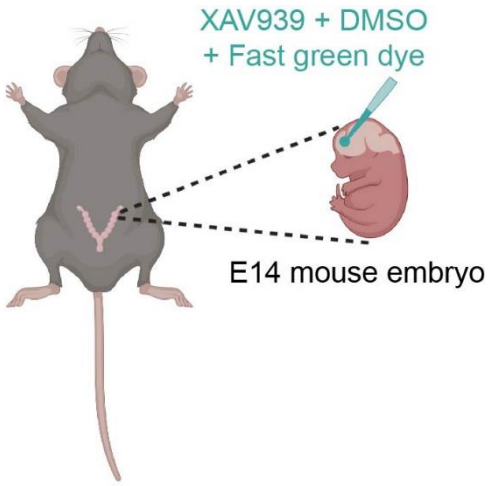

Figure 2.2. Schematics of *in utero* microinjections procedure.

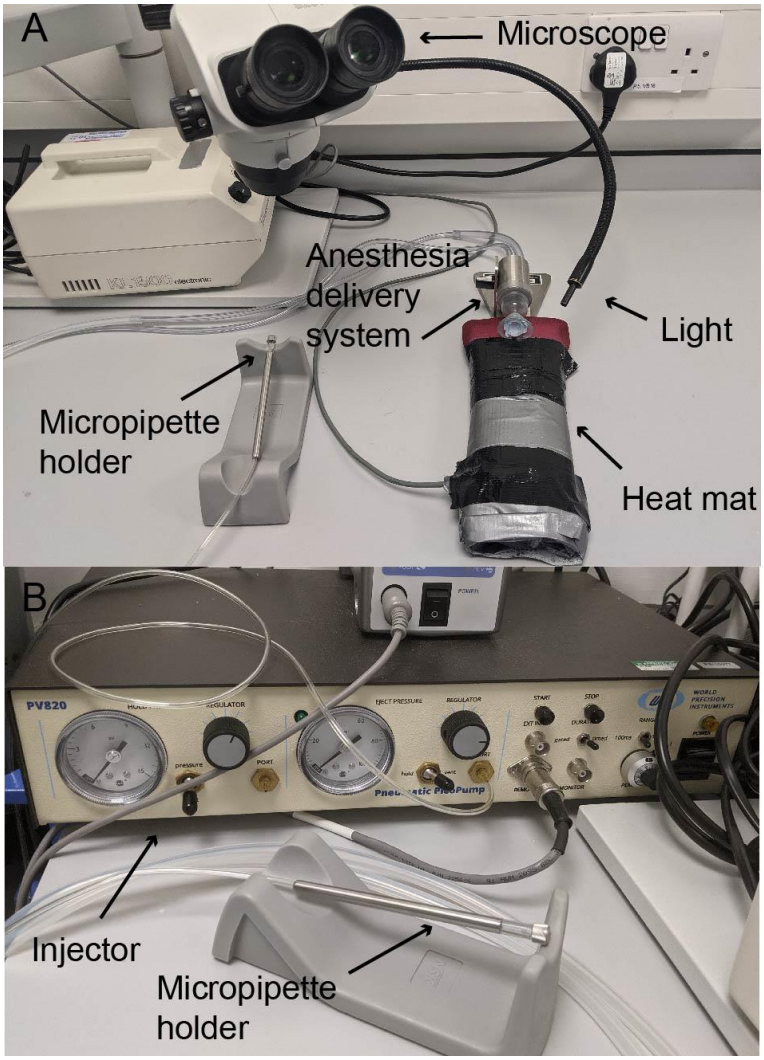

Figure 2.3. Setup for *in utero* microinjections surgery. **A**- The mouse was placed on the heat mat, with its head in the cone of the anaesthesia delivery system. Injections were delivered through a glass micropipette connected to the injector through micropipette holder. **B**- Injector connected to the micropipette holder.

2.3. Headcap surgery for behavioural experiments and in vivo electrophysiology

For the purpose of head-fixed behavioural assessment and electrophysiological recordings, ~8 week old male mice were implanted with head-post and a connector

containing wires for measuring electroencephalography (EEG), electromyography (EMG) and a ground wire (Figure 2.4.).

Aseptic technique was kept during the surgery. Male mice were first anaesthetized using isofluorane in an anaesthetic chamber and hair was shaved from their head. Shaved skin was cleaned with ethanol (70%) and betadine and mice were subcutaneously given Lidocaine (2%, 0.1ml) on the incision site and Rimadyl (10ml/kg, 0.01% diluted in water for injection) in the back. The surface of their eyes was covered with artificial tear gel (Lacri-lube, Allergan or Viscotears, Bausch&Lomb) in order to prevent them from drying. Mice were placed on the heat mat (maintained at 38°C) facing down and head-fixed in the stereotaxic frame (Kopf Instruments) using incisor bar and blunt ear bars (Figure 2.6.). Isofluorane was delivered through a nose cone. Their breathing was monitored throughout the surgery and isofluorane and oxygen levels were adjusted accordingly (isofluorane between 1-2% and oxygen between 0.8-1%). The incision was made on the head along the midline and skin was cut in ~4mm radius circle to expose the skull. Skull was cleaned with ethanol (70%) and hydrogen peroxide, to remove the periosteum membrane. Using microscope (SZ51, Olympus), bregma and midline were identified and measuring distances from them five drill sites were marked, as well as future craniotomy site over the auditory cortex (Figure 2.5.). Burr holes were drilled (Volvere Vmax drill, NSK) and 5 screws (418-7123, RS Components) were implanted (3 anchor screws, EEG and ground). Connector was affixed and EMG wire was inserted into the neck muscles. Skull was cleaned and dried. Dental cement (Simplex rapid liquid and powder mixed together, Kemdent) was applied to the skull, fixing the screws, EMG wire and connector in place. After the first layer of cement dried, head-post was positioned at the front of the skull and sealed with the rest. Hence, the headcap made of dental cement, skull screws, head-post and connector was constructed.

Mice were closely monitored for the next couple of days, weighed and given baby food for recovery.

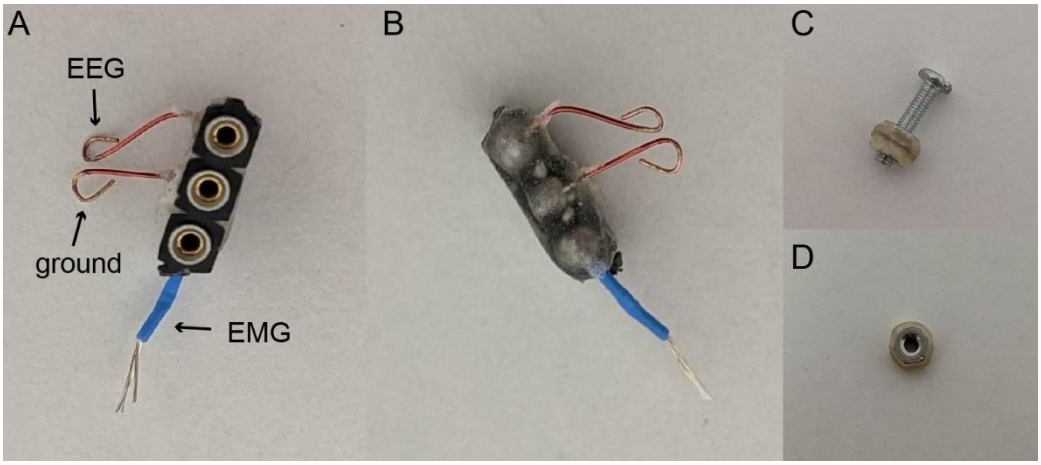

Figure 2.4. Examples of a connector and a head-post. **A**- Connector (top side). **B**- Connector (bottom side). Two copper wires (~1cm) with insulation stripped on both ends were soldered to a connector with 3 pins (1 wire to each pin). A blue, stranded, silver-plated copper wire (~1cm) was also stripped of insulation on both ends and soldered to the third connector pin. The soldered, bottom side of the connector was then covered with dental cement. During the head-post surgery, the top copper wire was coiled around the EEG screw, second copper wire around the ground screw, while the blue EMG wire was inserted into the neck muscle. **C**- Head-post with the screw (lateral view). Head-post was made of 2 nuts (248-4567, RS Components) cemented together. D- Head-post (top view).

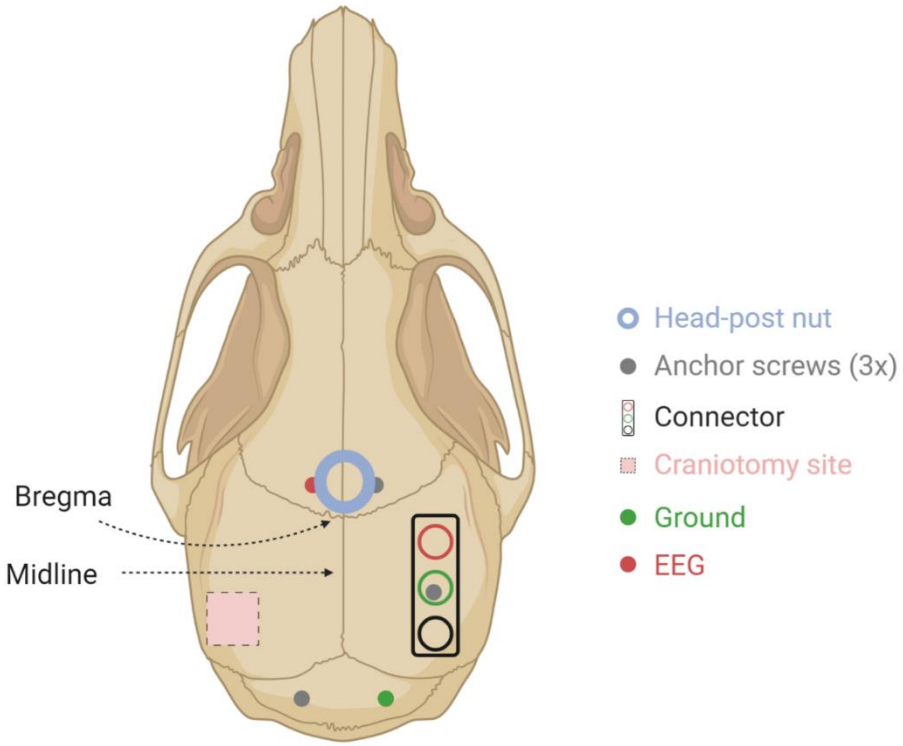

Figure 2.5. Locations of skull screws, head-post, connector and future craniotomy site. EEG connector (first, red) wire is coiled around the left anterior skull screw, ground connector (second, green) wire is coiled around the right posterior skull screw, and EMG connector (third, black) wire is placed onto the neck muscle. Connector is located on top of the lateral skull screw. Head-post is placed on top of the anterior 2 skull screws. A 2x2 craniotomy site was measured starting at -2mm from bregma and 4mm from the midline.

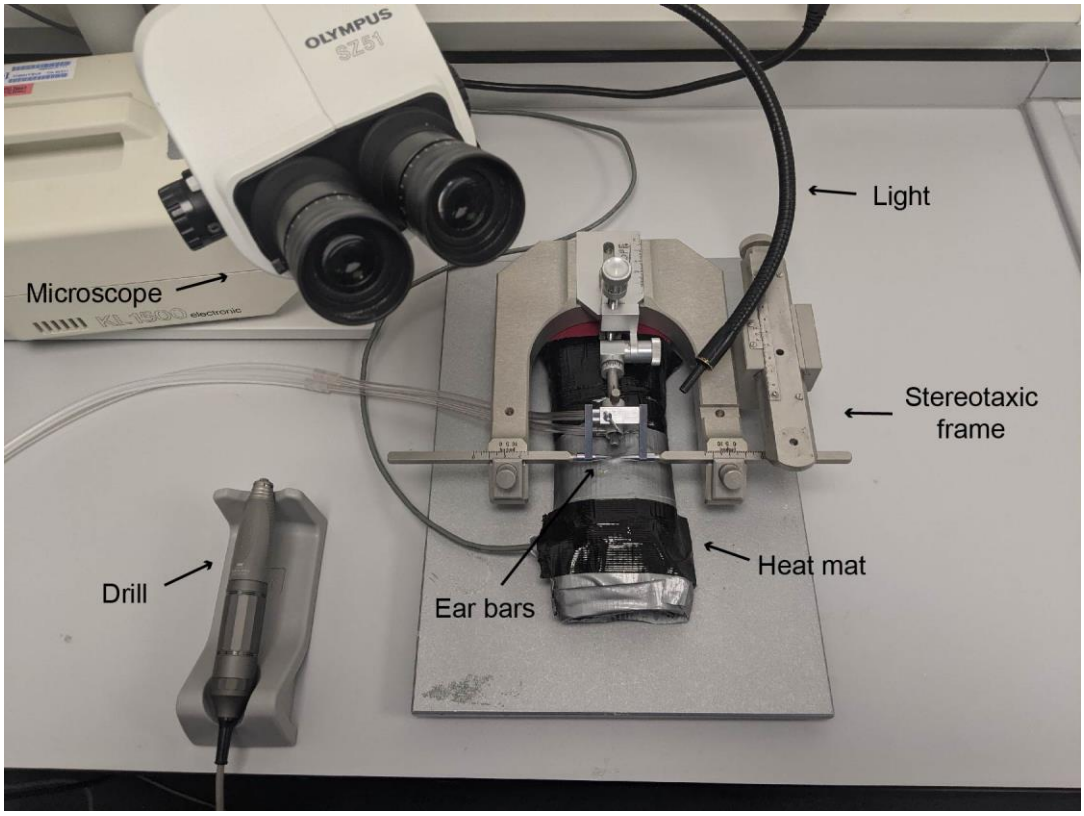

Figure 2.6. Setup for the headcap surgery.

2.4. Training procedures for auditory detection task

A week after headcap surgery, when the mice recovered, they were housed in the reverse light/dark cycle room for a week for adaptation. Since mice are nocturnal animals, this was necessary in order to train and assess them during their most active phase. Mice were trained Monday to Friday between 2 and 6 pm.

After adapting to the reverse lighting cycle, water restriction started. Hydrogel (water in the form of a gel) was first introduced to mice while they still had ad libitum access to water. Then the water bottle was removed and they were given hydrogel in excess amount for the first few days. The amount of hydrogel was gradually reduced until reaching 0.04ml of water per gram of animal per day. Mice were water restricted every day during the behavioural training period, in order to be motivated enough to work for water reward. After a week of adaptation to water restriction, if their weight and overall health state was stable, they started the training for behavioural assessment.

During adaptation to water restriction mice were also habituated to handling and head-fixed conditions. They were scruffed for a couple of minutes every day and were given a reward after that. On the fifth day of water restriction, mice were placed in a restraining tube and head-fixed to a bar through the surgically implanted head-post for 15 minutes. They were given water from the syringe while head-fixed and sunflower seeds as a reward afterwards. Next day the procedure was repeated, but for a longer period of time (45 minutes). They started basic lick training the following day.

Behavioural apparatus was located in a soundproof box (Figure 2.7.). A head-fixed mouse was sitting in a restraining tube, with a spout in front of his mouth (Figure 2.8.). The spout, made from a pipette tip, was connected through tubing to a 10ml syringe located outside of the soundproof box (Med Associates Inc). Syringe was filled with water and fixed into a single-syringe infusion pump (AL-1000, World Precision Instruments). The tip of the spout was aligned with a sensor (PMU24, Panasonic). Finally, a speaker (ES1, Tucker-Davis Technologies) was placed at a distance of 15cm in front of the mouse.

Water delivery, sound presentation and information from the sensor were relayed through NI-DAQ (USB-6343, National Instruments), controlled by a LabView program (2014 and 2017 version, National Instruments) (Figure 2.9.). The sound (broadband

white noise) was generated digitally by NI-DAQ and amplified (System 3 ED1, Tucker-Davis Technologies) before being transmitted to the speaker.

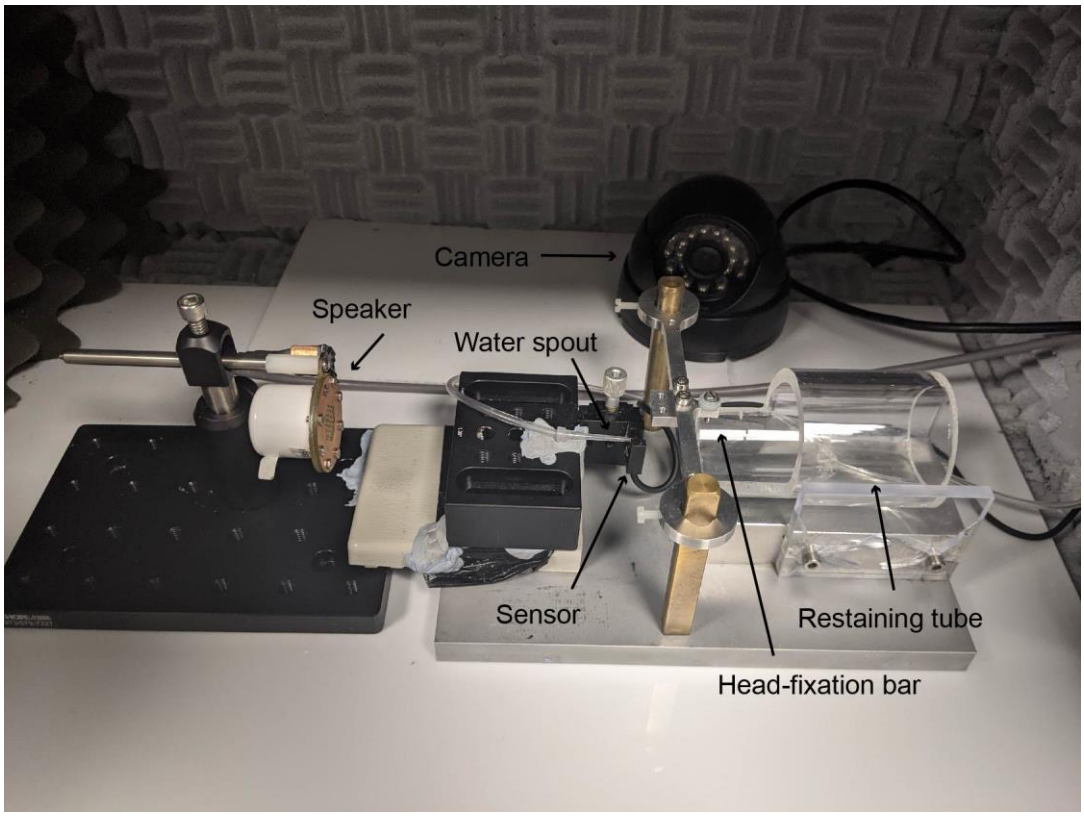

Figure 2.7. Setup for head-fixed behavioural training.

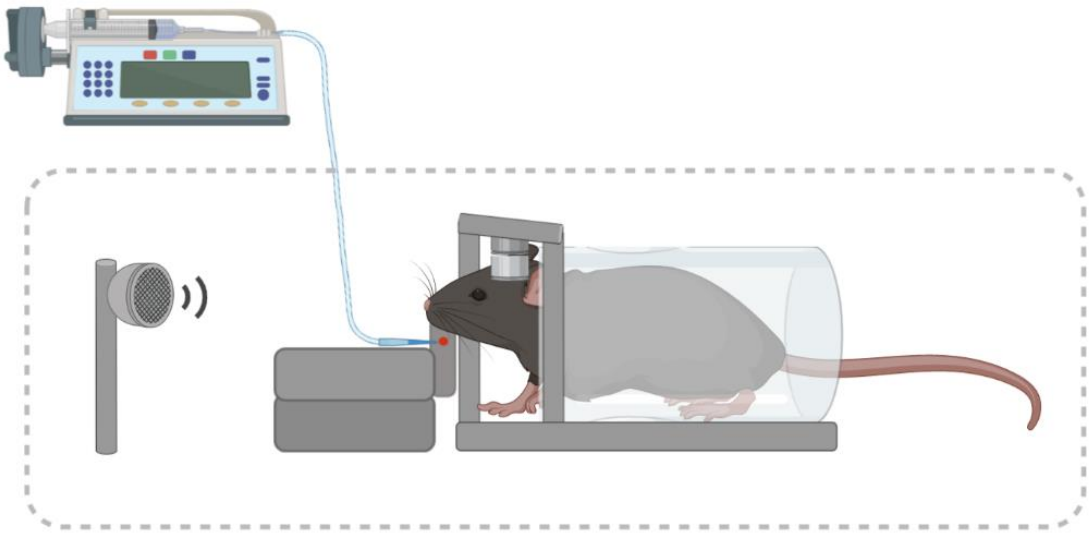

Figure 2.8. Schematics of head-fixed behavioural training. Apparatus located inside a soundproof box is positioned within the dashed box in this figure. The pump is located outside of the box. Soundproof box dimensions were ~40x60x40cm, with a 2cm thick acoustic absorption foam isolation.

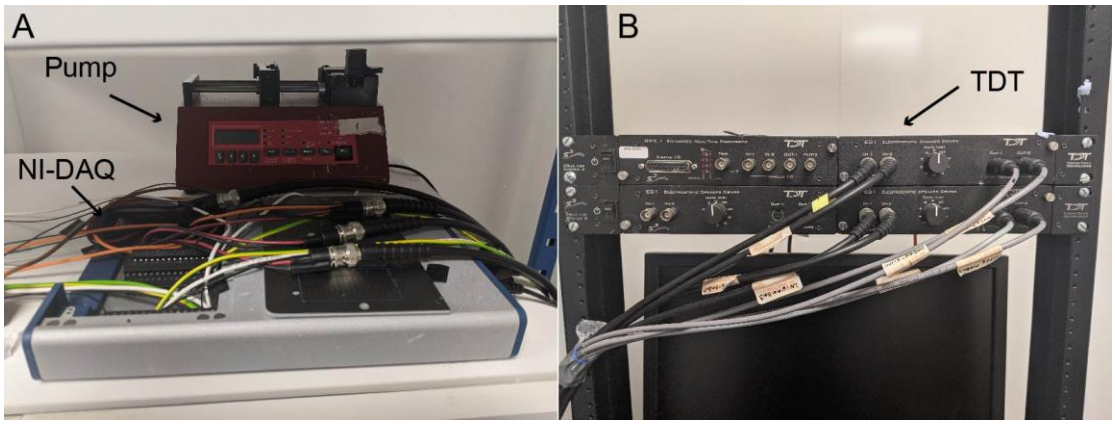

Figure 2.9. Equipment for running the behavioural assessment. **A**- NI-DAQ; a pump connected to the behavioural apparatus inside a box is visible in the background. **B**- System 3 ED1 electrostatic speaker driver, Tucker-Davis Technologies (TDT)

Behavioural assessment consisted of 3 phases: basic lick training, auditory conditioning and auditory detection (Figure 2.10A). In all phases, daily training sessions lasted an hour during which mice received water through a water pump as a reward. Mice were weighed after each session and the amount of water they got during training was calculated. If a mouse did not drink his daily amount of water during training, the rest was given to him after training in the form of hydrogel.

In basic lick training phase, mice were learning how the apparatus works. Whenever the mouse licked the spout, his tongue would cross the beam of the sensor, activating the water pump and 1-3µl drop of water would be delivered to the mouse. When mice made more than 300 licks in a session, they would move on to the next phase.

In auditory conditioning, mice were trained to lick only when a sound was present. A session consisted of sound presentations (trials) and silent periods (intertrial intervals). In the beginning, the sound was presented for 8 seconds, followed by 2

seconds of silence. When mice licked the spout during the sound presentation they would get a water reward. If they licked during silence they would not get a reward. After 50 valid trials, the sound was reduced by 1 second and silence increased by 1 second. This was done until sound presentation lasted only 2 seconds and silence lasted for 4 seconds. When a mouse had at least 150 licks with a 60% total success rate and a reaction time of around 200ms for the sound presentation of 2 seconds in 2 consecutive sessions, it would move on to the final phase.

In auditory detection task, mice were assessed for different sound intensities in order to find their sound detection threshold. Mice were presented with 30-70dB SPL broadband noise with 10dB SPL steps, lasting 1 second. In between the sound presentations was a silent period of 2-4 seconds. Sound intensities and silent period length were randomized across trials. In this phase, mice had to lick the spout when they heard a sound and water was then delivered (Figure 2.6B). Catch trial was introduced in this phase, which is a silent period lasting 1 second put in place of a sound, in order to "catch" how often a mouse licks randomly, when a sound is not present, and discard that percentage of his hit rate (Signal detection theory, explained in 1.4.4.). If the mouse licked during the catch trial, it was counted as a "false alarm", reward was not given and the trial was repeated (Figure 2.10C). When the difference between the false alarm rate and the highest sound intensity hit rate was more than 40% in two consecutive sessions, after at least 10 training sessions, the mouse would finish training. We used this normalized success rate at 70dB to determine the level of animals engagement in the task. A lower normalized success rate for such a high sound intensity would suggest that the animal is not motivated enough to participate in the task or does not understand the task rule. When the animal showed consistently high success for this high sound intensity, we have compared the other behavioural measurements, such as their reaction time. Success rate could be affected by the animal's motivation and thirst, which is high at the beginning of a session and gets lower by the end. Some experimenters use d' as a primary measure of performance, however, this measurement is also affected by thirst, and it differs across the session.

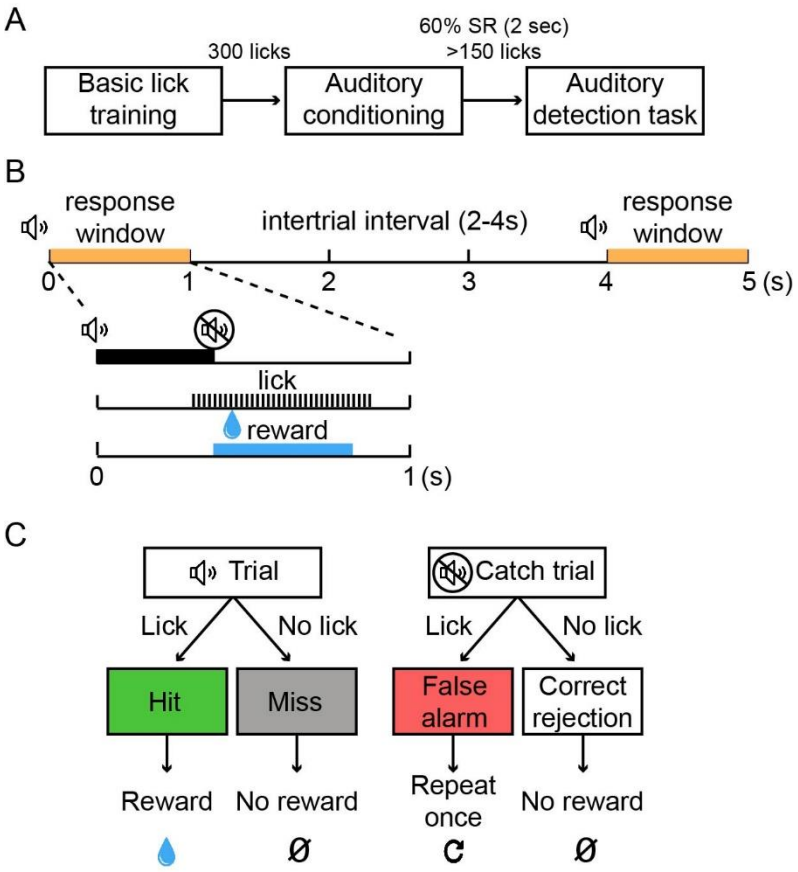

Figure 2.10. Auditory detection task. **A**- Flowchart for auditory detection task training. Conditions for moving to the next phase are specified above the arrows. **B**- Timeline of events in an auditory detection task session. Trial starts with sound onset. If the mouse licks during the response window (lasting 1s), the sound turns off and water reward is delivered. **C**- Diagram of possible events and outcomes during an auditory detection task session. SR – success rate

2.5. Craniotomy and in vivo electrophysiology

After mice finished the behavioural assessment, they were habituated for 5-7 days for *in vivo* electrophysiology recordings. Mice were placed in a restraining tube and head-fixed in a soundproof box. Dummy electrode was positioned next to their head, approximately over the auditory cortex. For habituation to recording in passive listening conditions, broadband noise and pure tones of 0-70dB intensity as well as

60dB natural sounds were played. For habituation to recording during behavioural assessment, mice were engaged in the auditory detection task.

2.5.1. Craniotomy

After habituation, craniotomy was done over the auditory cortex, on the site marked previously during the headcap surgery. Mice were anaesthetized using isofluorane in an anaesthetic chamber and were given Rimadyl (10ml/kg, 0.01% diluted in water for injection) subcutaneously in the back. The surface of their eyes was covered with artificial tear gel (Lacri-lube, Allergan or Viscotears, Bausch&Lomb). Mice were then placed on the heat mat (maintained at 38°C) facing down and head-fixed in the stereotaxic frame (Kopf Instruments) using incisor bar and head-fixation bar (Figure 2.11). Isofluorane was delivered through a nose cone. Their breathing was monitored throughout the surgery and isofluorane and oxygen levels were adjusted accordingly (isofluorane between 1-2% and oxygen between 0.8-1%). Skull and thin layer of dental cement over the craniotomy site were gently drilled off (Volvere Vmax drill, NSK) and removed using craniotomy forceps. Phosphate buffered saline (PBS) was poured over the exposed brain, to clean the site and prevent it from drying. Craniotomy site was covered with Kwik-Sil (World Precision Instruments).

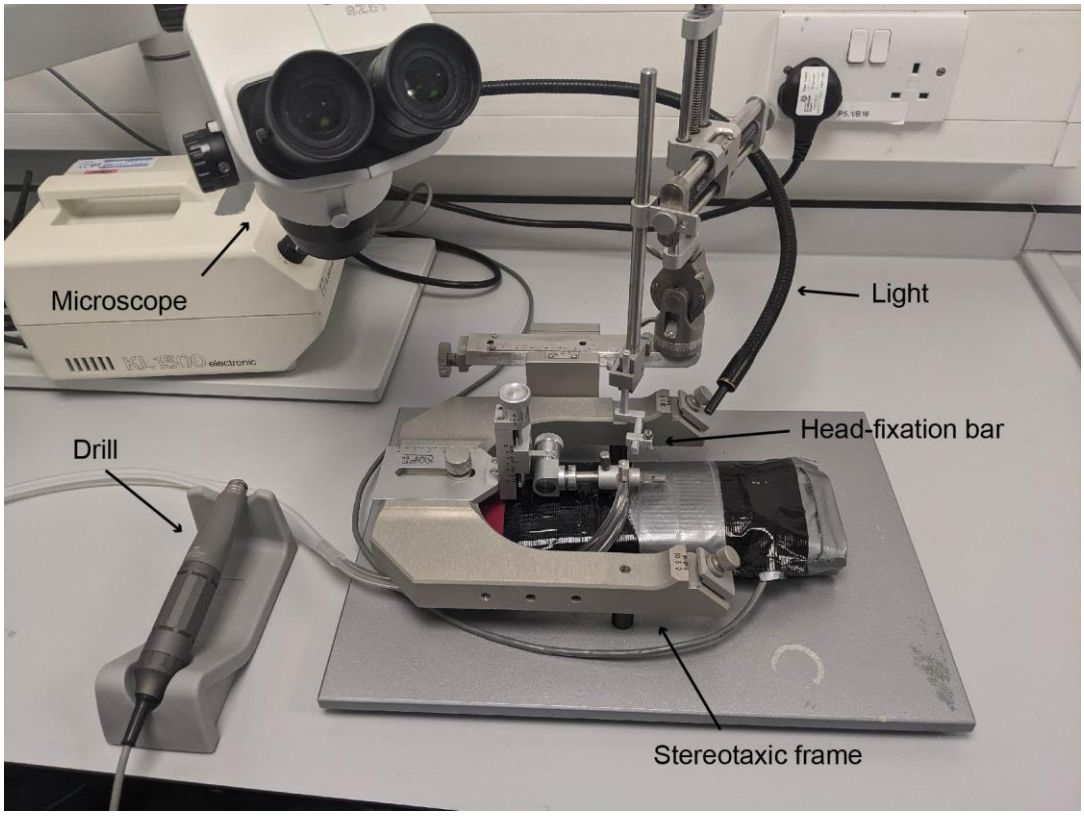

Figure 2.11. Setup for craniotomy.

2.5.2. Silicone probe recording procedure in passive listening conditions

Starting the day after the craniotomy was done, neural population activity was recorded for 1-2 days. In a soundproof box (Industrial Acoustics Company, dimensions ~60x70x65cm, 4cm foam isolation), an awake mouse was sitting in a restraining tube, head-fixed to a bar through the surgically implanted head-post (Figure 2.12.). A speaker (ES1, Tucker-Davis Technologies) was located at a distance of 10cm in front of the mouse and a camera (acA1920-25µm, Basler Ace) with an IR filter (FGL780, Thorlabs) was located at animals right side. Video acquisition for pupil monitoring was controlled using LabView (2017 version, National Instruments).

First, the headcap pins for EEG, EMG and ground were connected to an adaptor and an amplifier (RHD2132, Intan). Then, Kwik-Sil was removed and exposed brain was covered with PBS. While observing under the microscope (SZ51, Olympus), a 64-channel 4 shank silicon probe (A4x16-6mm-50-200-177-A64, NeuroNexus Technologies) was slowly inserted into the brain, targeting auditory cortex (Figure

2.14A). The probe was connected to an adaptor and a micromanipulator (Narishige) and grounded through the mouse and the frame for head-fixation (Narishige). In order to confirm that the probe is located in the auditory cortex before starting the recording, a 60dB broadband noise was played to detect the auditory response of the cells (Figure 2.14B). After waiting ~30 minutes for the brain to settle, recording started. Signals collected through the probe were amplified (RHD2132 amplifier chips and RHD2000 evaluation board, Intan) and recorded using LabView (2017 version, National Instruments) (Figure 2.13.). Probes were labelled with a fluorescent dye DiI (D-282, Invitrogen, 10% diluted in ethanol) before insertion, allowing us to find the probe track later in histology. EEG and EMG signals were also transmitted to the same acquisition system (RHD2000, Intan) and recorded in LabView.

A recording session consisted of 1) 100ms long broadband white noise pulses (1 ms cosine ramps, 0-70dB SPL intensity range with 10 dB SPL steps, 500ms long interstimulus intervals, 200 repetitions), followed by 2) 10s long natural sounds (animal calls, 60dB SPL intensity, 100 repetitions), then 3) 100ms long pure tones (5 ms cosine ramps, 3-48 kHz frequency range with 1/8 octave steps, 0-70dB SPL intensity range with 10 dB SPL steps, 20 repetitions), and finally, 4) a 30 min long silent period (Figure 2.15). Sound presentation was controlled by a LabView programme through NI-DAQ (USB-6211, National Instruments). After receiving the signals from NI-DAQ, sounds were generated digitally (sampling rate 97.7kHz, RZ6 Multi I/O processor, Tucker-Davis Technologies) and transmitted in free-field through the speaker. Sound pulse was relayed from TDT to Intan acquisition system and sync on and off pulse was recorded in LabView recording programme.

The speaker was calibrated before every recording session. A microphone (PS9200KIT-1/4, ACO Pacific Inc) was placed under the head-fixation bar, approximately at the same distance from the speaker as the ears of a mouse. Broadband noise and pure tones were then played at a range of intensities, producing a list of appropriate voltages for each sound frequency and intensity. This information was then used for sound generation in TDT.

In total, recordings contained 68 channels (1 auditory sync and 1 optical sync channel, 64 probe channels, 1 EEG and 1 EMG channel). After every recording, the probe was taken out of the brain and cleaned, and Kwik-Sil was placed over the craniotomy site.

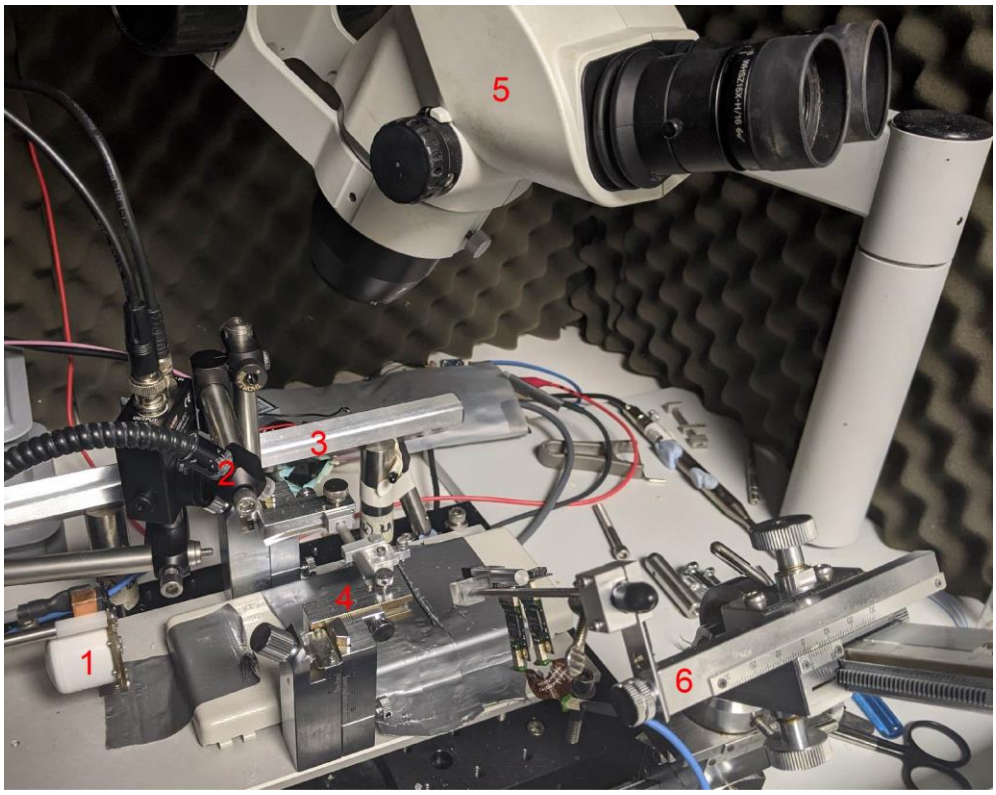

Figure 2.12. Setup for silicon probe recording. 1-speaker, 2-light, 3-camera, 4-head-fixation bar, 5-microscope, 6- probe manipulator with adaptor.

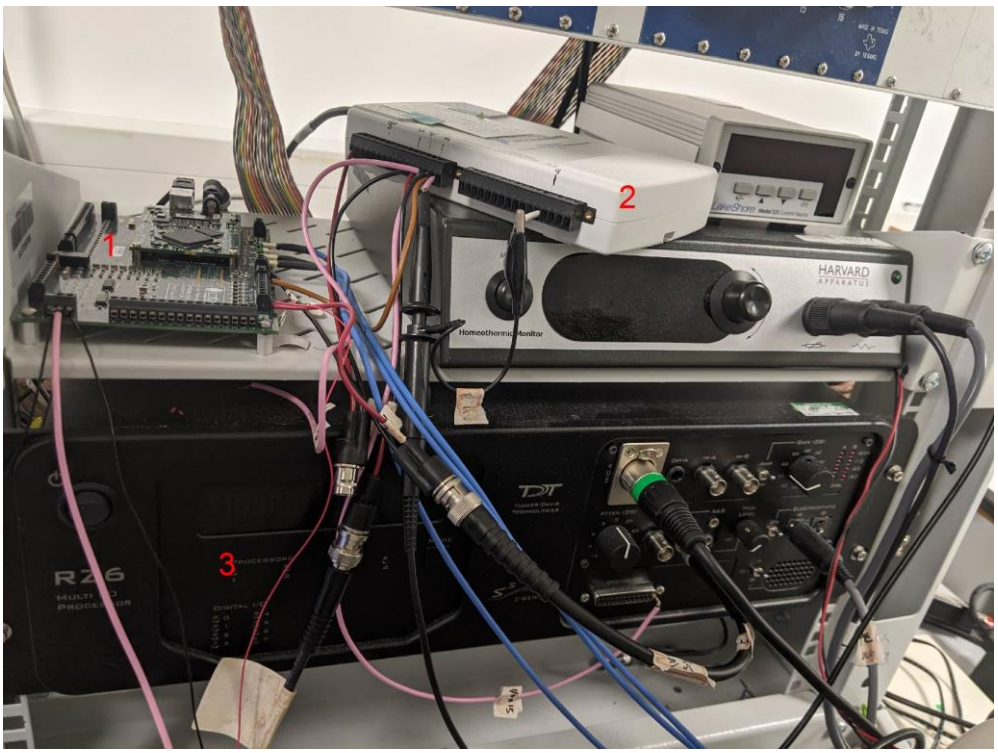

Figure 2.13. Equipment for neural activity recording with silicon probes. 1-Intan board, 2-NI DAQ, 3-TDT RZ6.

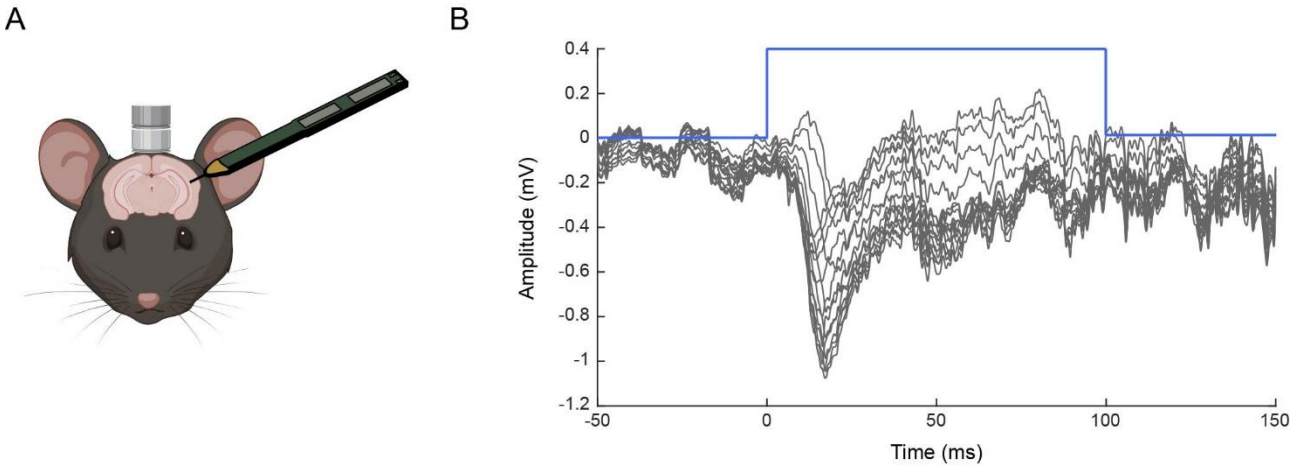

Figure 2.14. Recording of auditory cortical activity. **A**- Schematics of the probe insertion. **B**- Example of an auditory response across 16 channels of one shank of the probe. Sound presentation period is indicated in the top blue channel, lasting 100ms.

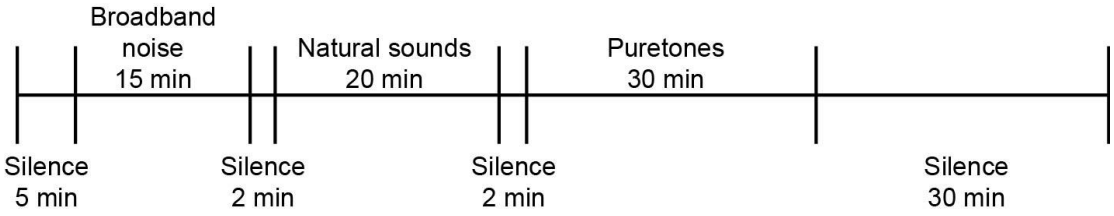

Figure 2.15. Timeline of events during a recording.

2.5.3. Neuropixels probe recording procedure during passive listening conditions

Recording procedure using Neuropixels and silicon probes was similar. Neural population activity was also recorded for 1-2 days, starting a day after the craniotomy. In a soundproof box (Industrial Acoustics Company, dimensions ~70x80x65cm, 4cm foam isolation), an awake mouse was sitting in a restraining tube, head-fixed to a bar through the surgically implanted head-post (Figure 2.16.). A speaker (ES1, Tucker-Davis Technologies) was located at a distance of 10cm in front of the mouse and a camera (acA1920-25µm, Basler Ace) with an IR filter (FGL780, Thorlabs) was located at animals right side. Video acquisition for pupil monitoring was controlled using LabView (2014 version, National Instruments).

Headcap pins for EEG, EMG and ground were connected to an adaptor and an amplifier (Plexon). Then, Kwik-Sil was removed and exposed brain was covered with PBS. While observing under the microscope (SZ51, Olympus), Neuropixels probe was slowly inserted in the brain, targeting auditory cortex and MGB. The probe affixed to a metal pole was inserted into a motorized micromanipulator (Narishige) and connected to a headstage and an interface cable. The probe was grounded through the mouse and the frame for head-fixation (Narishige). Similar to the silicon probe recording procedure, a 60dB broadband noise was first played to detect the auditory response of the cells. After waiting ~30 minutes for the brain to settle, recording started. Signals collected through the probe channels were amplified and digitized in the probes integrated circuit (ASIC), then transferred through the headstage and interface cable to an acquisition module (Neuropixels PXIe, IMEC) located in the PXI chassis (NI PXIe-1071, National Instruments) and recorded using SpikeGLX (Janelia

Research Campus, https://www.janelia.org/open-science/spikeglx-neurophysiology-probe-acquisition-software) (Figure 2.17.). Probes were labelled with a fluorescent dye CM-DiI (C7001, Invitrogen, 0.1% w/v diluted in ethanol) before insertion, allowing us to find the probe track later in histology. EEG and EMG signals were amplified and transmitted to a DAQ module (NI PXI-6254, National Instruments) located in the same PXI chassis as Neuropixels acquisition module, and recorded using SpikeGLX.

Timeline of events during a recording session was similar to silicon probe recordings (Figure 2.15.). It consisted of 100 repetitions of 100ms long broadband white noise pulses (1 ms cosine ramps, 0-70dB SPL intensity range with 10 dB SPL steps), followed by 100 repetitions of 10s long 60dB SPL natural sounds, then 20 repetitions of 100ms long pure tones (5 ms cosine ramps, 3-48 kHz frequency range with 1/8 octave steps, 0-70dB SPL intensity range with 10 dB SPL steps), and finally, a 30 min long silent period. Sounds were generated digitally (sampling rate 97.7kHz, System 3 MA3, RP2.1 and ED1, Tucker-Davis Technologies) and transmitted in free-field through the speaker. Sound presentation was controlled by a LabView programme through NI-DAQ slotted in the computer (NI PCI-6221, National Instruments). The on/off sync pulse was relayed from TDT to the DAQ module in PXI chassis (NI PXI-6254, National Instruments), thus recording the pulse in SpikeGLX.

In total, recordings contained 385 Neuropixels channels (384 probe channels and 1 main sync channel) and additional NI-DAQ channels (auditory sync channel, EEG, EMG and main sync channel). After every recording, the probe was taken out of the brain and cleaned, and Kwik-Sil was placed over the craniotomy site.

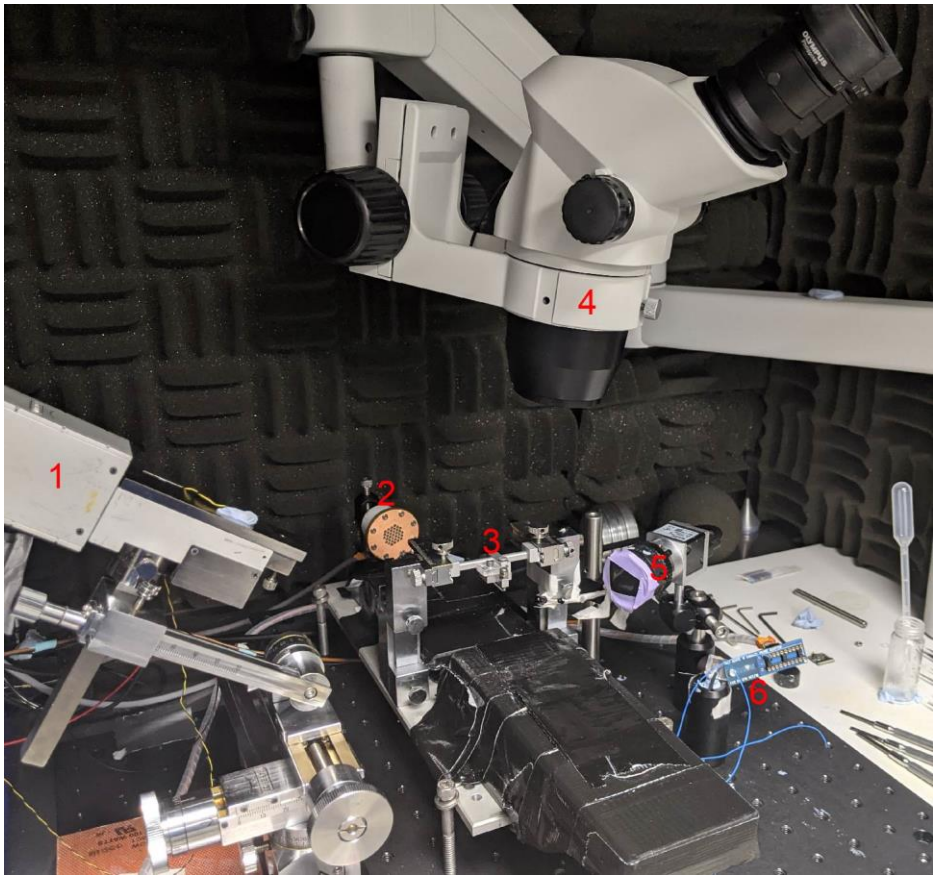

Figure 2.16. Setup for Neuropixels probe recording. 1-probe manipulator, 2-speaker, 3-head-fixation bar, 4-microscope, 5-camera, 6-Plexon adaptor.

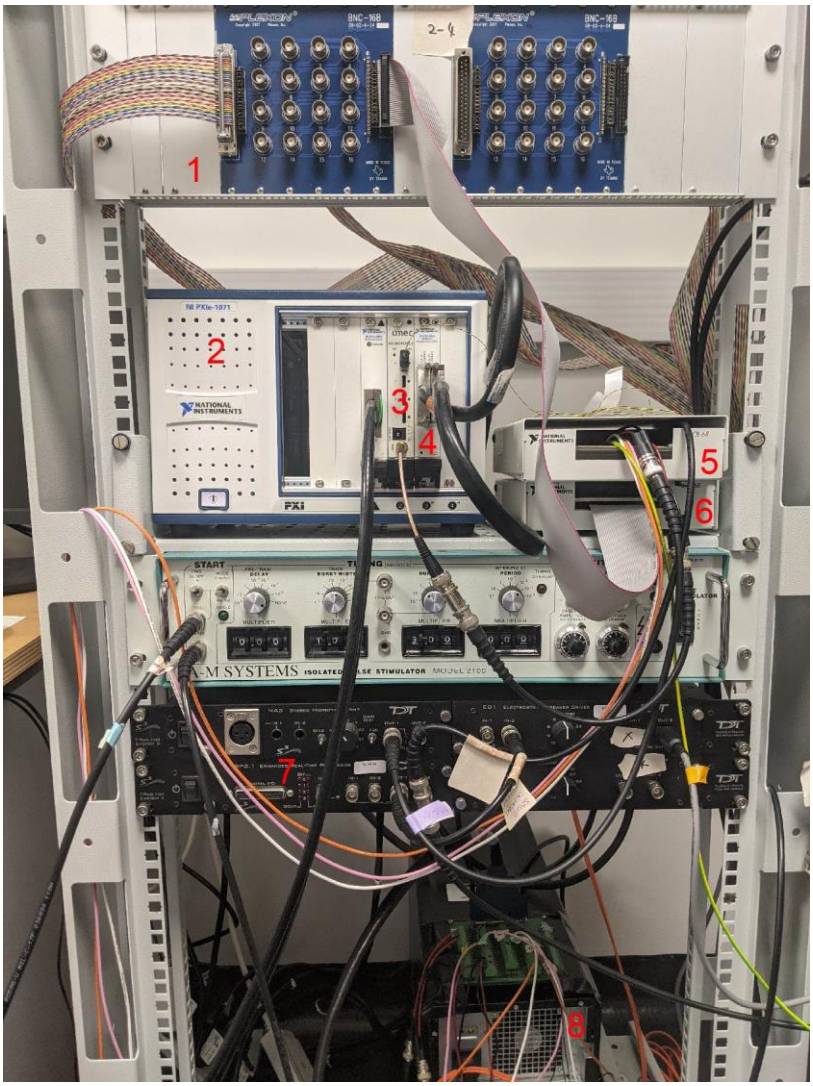

Figure 2.17. Equipment for neural activity recording with Neuropixels probes. 1-Plexon relay board receiving amplified EEG and EMG signals, 2-PXI chassis, 3-Neuropixels PXIe acquisition module, 4-PXI-6254 DAQ module, 5-NI relay module receiving signals from TDT and PCI-6221 and passing them to PXI-6254, 6-NI relay module receiving signals from Plexon relay board and passing them to PXI-6254, 7-TDT System 3, 8-computer containing slotted in DAQ NI PCI-6221

2.5.4. Neuropixels probe recording procedure during behavioural assessment

Starting a day after the craniotomy was done, neural population activity was recorded for 2-3 days. The beginning of the recording procedure was similar to Neuropixels recording in passive listening conditions while the behavioural part of the experiment was similar to the behavioural assessment described in chapter 2.4.

Water pump (AL-1000, World Precision Instruments) activation, sensor (PMU24, Panasonic) information and sound presentation (generated by TDT System 3 and transmitted in free-field through ES1 speaker, Tucker-Davis Technologies) were relayed through NI-DAQ slotted in a computer (NI PCI-6221, National Instruments) and controlled by a LabView programme (2014 version, National Instruments) (Figure 2.17.). Information about the trials and behavioural outcomes was saved through LabView. Sync on and off pulses for pump and sensor were transferred from NI-DAQ in the PC to a DAQ module in the PXI chassis (NI PXI-6254, National Instruments) and recorded in SpikeGLX. Sound sync pulses were transferred from TDT to the same DAQ module in the PXI chassis and recorded in SpikeGLX.

Awake, in this case, water-restricted mouse in a restraining tube was head-fixed in a soundproof box and EEG, EMG and ground were connected (Figure 2.18.). Kwik-Sil was removed and exposed brain was covered with PBS. Neuropixels probe was inserted in the brain, targeting auditory cortex and MGB. Probe was labelled with a CM-DiI before insertion. After confirming the location of the probe was in the auditory areas and waiting ~30 minutes for the brain to settle, water spout and sensor were placed in front of the mouse. A short (~2min) basic lick assessment was carried out, to make sure that the spout was in the right position and animal can easily engage in the task. Then, the recording, pupil monitoring and auditory detection task were initiated. Neural activity was recorded in the same manner as in chapter 2.5.3., using SpikeGLX. Pupillometry was recorded using LabView (2014 version, National Instruments).

Each recording session lasted ~1 hour. In total, recordings contained 385 Neuropixels channels (384 probe channels and 1 main sync channel) and additional NI-DAQ channels (auditory sync channel, licking sensor channel, pump channel, EEG, EMG and main sync channel). After the recording finished, the probe was taken out of the brain and cleaned, and Kwik-Sil was placed over the craniotomy site. The animal was weighed and given the rest of its daily amount of water in the form of hydrogel.

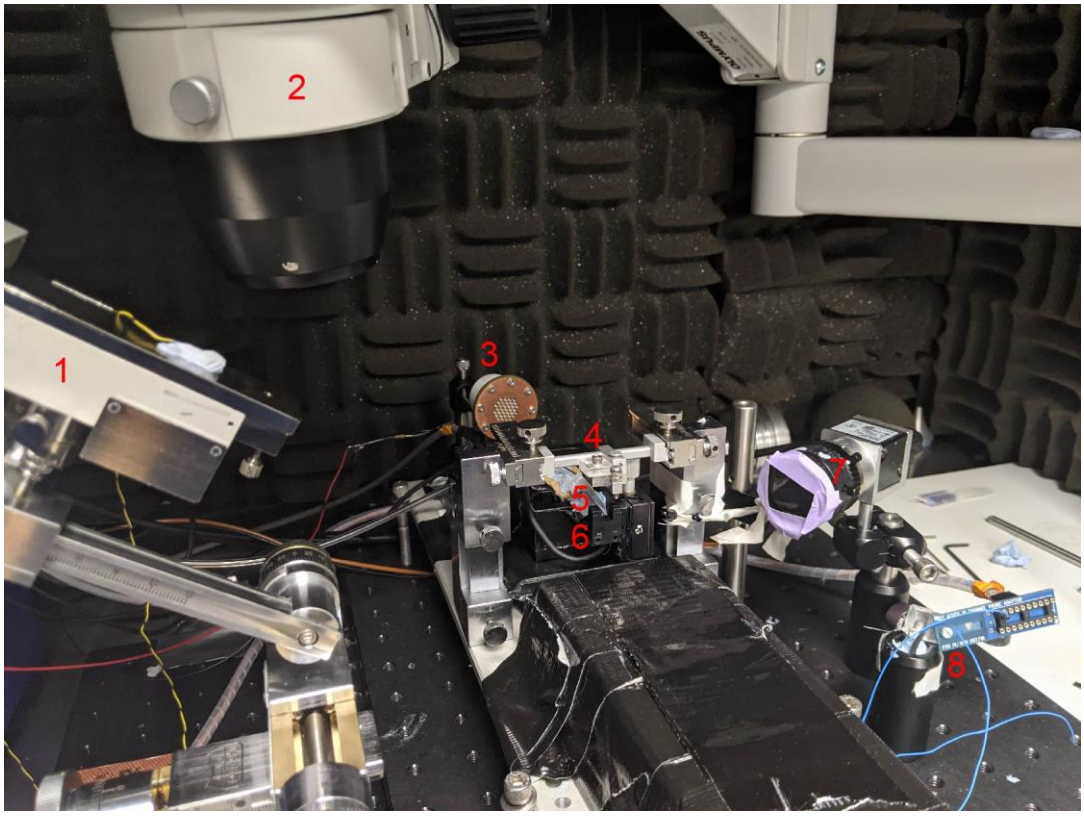

Figure 2.18. Setup for Neuropixels probe recording during behavioural assessment. 1-probe manipulator, 2-microscope, 3-speaker, 4-head-fixation bar, 5-water spout, 6-sensor, 7-camera, 8-Plexon adaptor.

2.6. Perfusion and histology

On postnatal day 2 (P2), P21 or after electrophysiological recording (P ~120), mice were given an intraperitoneal injection of euthatal and lidocaine (0.1ml of each for adult mice; 0.05ml for P2). After they lost all reflex responses, mice were perfused transcardially with 20ml (4ml for P2) of phosphate buffered saline (PBS) following 20ml (4ml for P2) of 4% paraformaldehyde (PFA) in 0.1M PBS. The brain was removed from the skull and placed in PFA solution in the fridge at 4°C. The following day the brain was placed in 30% sucrose solution and stored at 4°C.

The brain was cut in 80µm coronal sections using microtome (SM2010R, Leica) and sections were placed in wells filled with 0.1M PBS. Sections were then stained with DAPI in order to visualize the thickness of cortical layers. Brain sections were first

washed 3 times with 0.3% Triton X-100 in PBS (PBST) and then incubated in 1:5000 DAPI solution in PBST for 30 minutes, covered with foil on a rotating platform. Sections were then washed with PBS 3 times for 10 minutes and mounted on glass slides using gelatine solution. Slides were left to air-dry overnight. The following day, slides were coverslipped with Fluoromount-G (Invitrogen), sealed around the edges and observed under an epifluorescent upright microscope (Eclipse E600, Nikon). In the case of adult mice in which electrophysiology recording was done, red DiI/CM-DiI signals were observed as well.

2.7. Data analysis

2.7.1. Histological evaluation of superficial cortical layers

Width of cortical layers in P2 and P21 mice was measured using Fiji ImageJ on DAPI images taken with 4x magnification. Portion of superficial layers in the cortex was calculated using the formula:

$$\text{ratio} = \text{width(L II-IV)}/\text{width(L II-VI)},$$

where width(L II-IV) and width(L II-VI) were the width of L II-IV and L II-VI, respectively. The approach was taken from previously published work on XAV939 treatment (Fang *et al.*, 2014). Measurements of 3 areas were taken on each brain slice (Figure 2.19.), one brain slice per mouse, and the mean of their ratios was compared to other brain slices. All measurements were done blindly to the treatment and grouped afterwards.

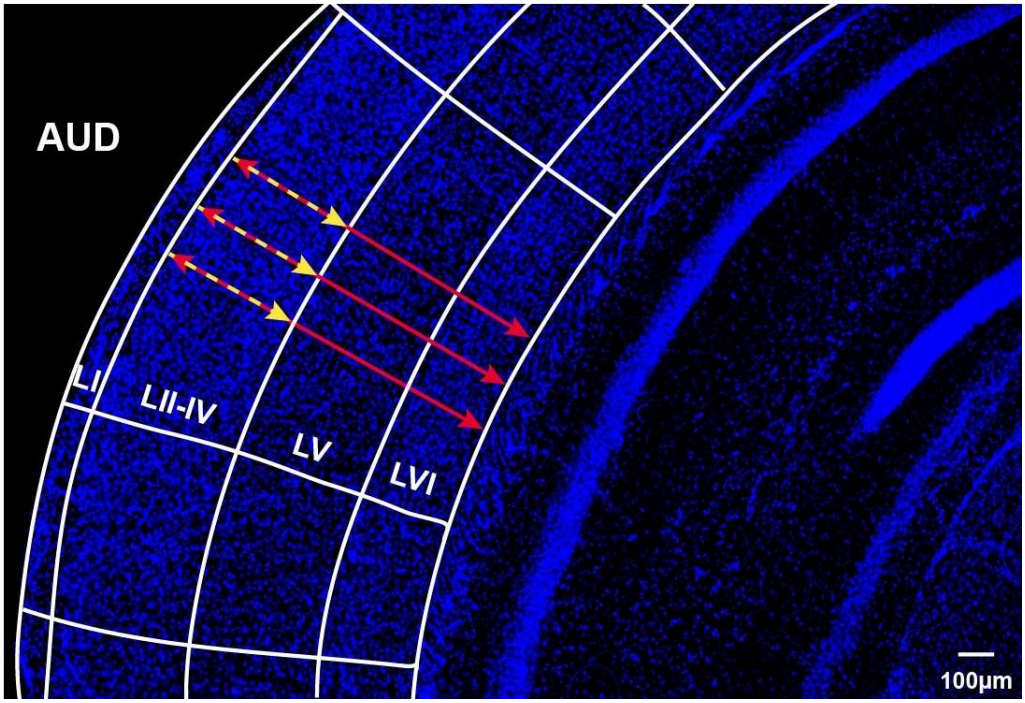

Figure 2.19. Example of cortex width assessment in a P21 mouse brain slice. Measurements of width were made in 3 areas of the auditory cortex. First, the length from the top of L II to the end of L IV was measured (yellow dashed lines), then this line was extended to the end of L VI and its length measured (red lines). Note that the starting point of both lines is the same (start of the yellow line and top of the red arrowhead on the border between L I and L II-IV) and overlapping throughout L II-IV. In this way, the width of L II-IV and L II-VI were taken from the same area, making them comparable for ratio calculations. The mean of the 3 ratios (width(L II-IV)/width(L II-VI)) calculated from measurements on this slice was then compared with the values from other mice.

2.7.2. Behavioural assessment

After the mice were trained for the auditory detection task and passed the threshold in two consecutive sessions (details explained in chapter 2.4.), behavioural assessment ended and data from these two sessions was used for analysis. In each of these sessions individually, hit rate for every sound intensity tested was normalized by subtracting the catch trial false alarm rate ($P_{hit} - P_{FA}$). Detectability index (d') was also calculated for all sound intensities in each session, using the formula:

d' = Z(hit rate) - Z(false alarm rate),

where Z is inverse of the standard normal cumulative distribution function. Finally, median reaction time was calculated for every sound intensity in each of the two sessions.

2.7.3. Electrophysiological data analysis

The pipeline for basic electrophysiological data analysis from silicon probe and Neuropixels probe recordings is shown in Figures 2.20. and 2.21., respectively. In both pipelines, the first step in data analysis was spike sorting. This consisted of automatic processing of recordings with Kilosort or Kilosort2 ((Pachitariu *et al.*, 2016), https://github.com/MouseLand/Kilosort) and manual curation using phy or phy2 template GUI (https://github.com/cortex-lab/phy). Then, basic spike information, such as spike timing and ID of the cluster it belongs to, were extracted. Quality of each spike cluster was assessed and spike waveform metrics were calculated. In silicon probe recordings, this was enough to separate the cortical cells into broad and narrow spiking. In the case of Neuropixels recordings, activity on each probe channel had to be assessed as well, to define which channels belong to which brain regions we recorded from. Additionally, to estimate the location of the Neuropixels recording channels in the brain, a 3D histological evaluation of the probe's trajectory had to be done. This was done using SHARP-Track (https://github.com/cortex-lab/allenCCF/tree/master/SHARP-Track). By combining the electrophysiological channel activity information and histological probe location across brain regions, we could extract the cortical cells and separate them into broad and narrow spiking.

Finally, in both silicon probe and Neuropixels probe recordings, event files were made, containing the information about sound presentation time and intensity. This information was extracted from the auditory sync channel and sound presentation files. All these steps in the pipeline were necessary to assess the cell-type-specific activity during different sound presentations and the silent period.

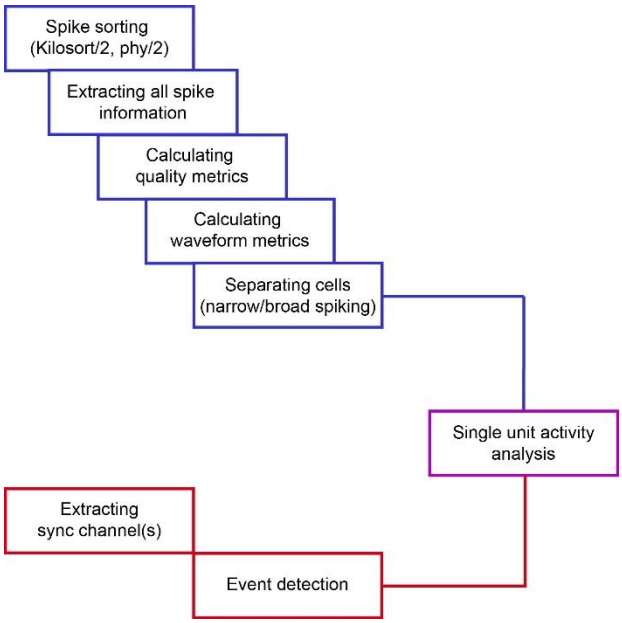

Figure 2.20. Silicon probe data analysis pipeline.

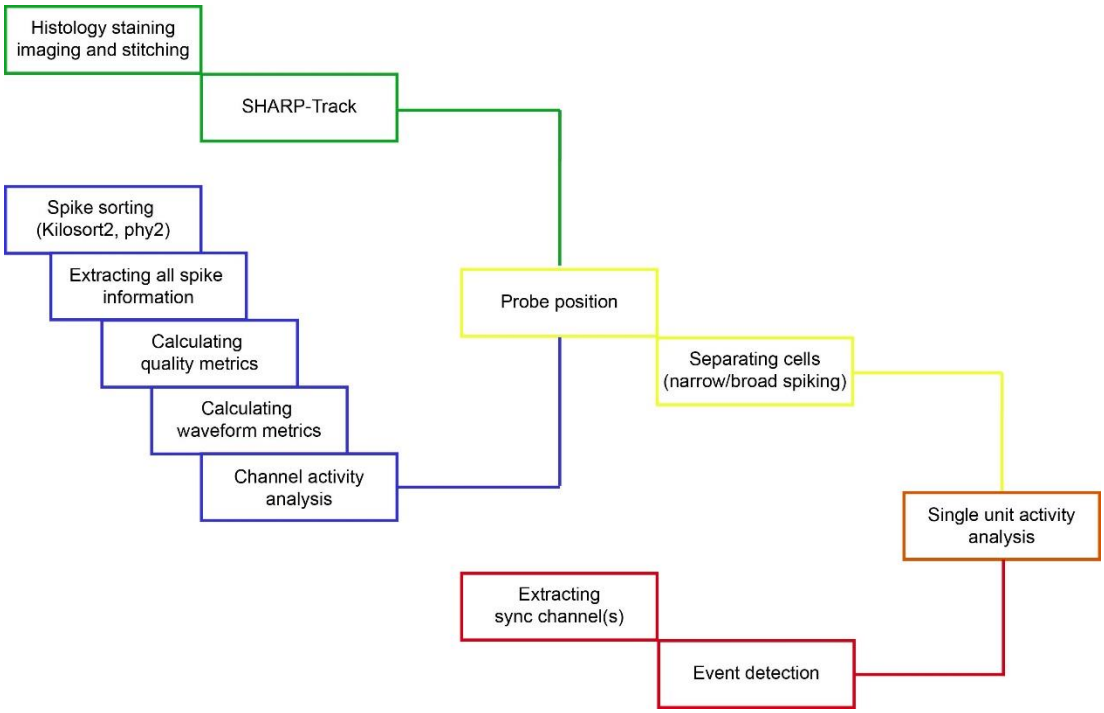

Figure 2.21. Neuropixels data analysis pipeline.

Spike sorting

As mentioned earlier, spike sorting was done in 2 steps: automatic processing with Kilosort/2 and manual curation with phy/2. Spike clusters identified and grouped by automated sorter were manually sorted into three groups: single units (labelled as "good"), multi-units (labelled as "MUA") and noise. Good, single units were considered as clusters showing a well-defined waveform (with a larger amplitude on one channel and decreasing across several neighbouring channels), a clear refractory period in the autocorrelogram and one clear cluster separated from the others in the principal component space (PCs) (Figure 2.22A, D and E).

Noise was defined as clusters with unclear waveforms, without a decrease in amplitude (non-neural activity) spread across channels (Figure 2.22B). Additionally, noise clusters were not well clustered in PCs or have a clear refractory period in autocorrelogram.

If the activity was neural but not coming from one cluster, it was labelled as MUA. This was often visible as multiple waveforms on a channel, unclear refractory period or multiple clusters in the PCs (Figure 2.22C and F).

In silicon probe recordings, all detected clusters were manually curated after automatic processing. In Neuropixels recordings, all cluster labelled as "noise" by Kilosort2 automated sorter were removed while only the clusters labelled as "good" were further looked into and accepted as good or rejected as "MUA".

Quality of each cluster was assessed by their Mahalanobis (isolation) distance (Schmitzer-Torbert *et al.*, 2005), calculated as the distance of spikes to the cluster mean (code from Cortexlab, UCL, https://github.com/cortex-lab/sortingQuality).

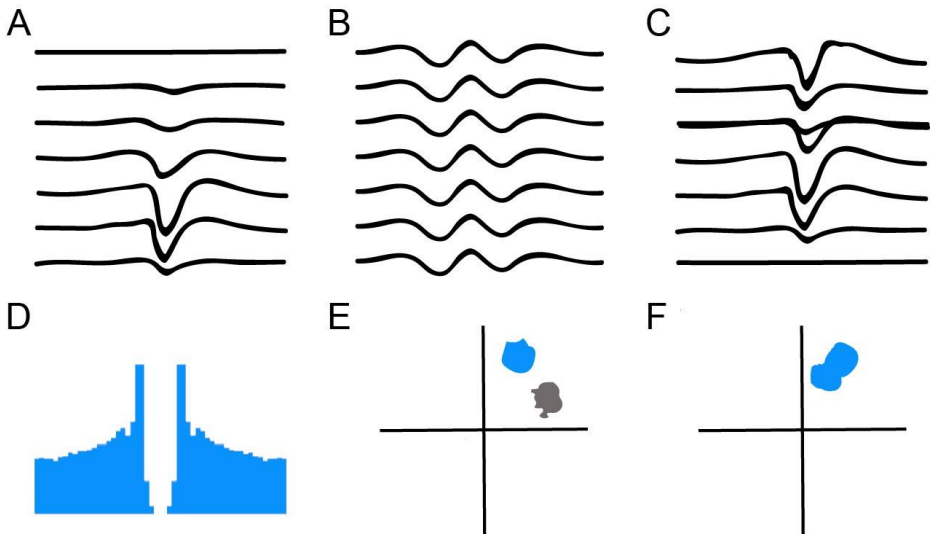

Figure 2.22. Spike sorting. Example of waveform across channels for **A**- "good unit", **B**- noise, **C**- "MUA". MUA in this example shows two different waveforms in the third channel, indicating that the waveforms on the top three channels belong to one cluster, while the bigger waveform on the third channel and lower channels belong to a second cluster. **D**- Autocorrelogram example for a "good unit", with a clear refractory period. **E**- Example of a well-separated unit in the PCs. **F**- Example of an "MUA" cluster in the PCs.

Evaluation of Neuropixels probe location

Since Neuropixels probe extends through several brain areas, a 3D histological evaluation of the probe's trajectory had to be done in order to estimate its location in the brain. Brain slices were cut and stained with DAPI, as described in chapter 2.6. Images of all brain slices with a visible red CM-DiI track were taken under the microscope, followed by stitching and pseudo-colouring in Fiji ImageJ. Then, all images belonging to the same brain were processed together using SHARP-Track (https://github.com/cortex-lab/allenCCF/tree/master/SHARP-Track). In SHARP-Track, all slices were registered into the 3D interactive Allen Mouse Brain Atlas and probe track was labelled across the slices. Probe trajectory was then estimated and visualized (Figure 2.23.).

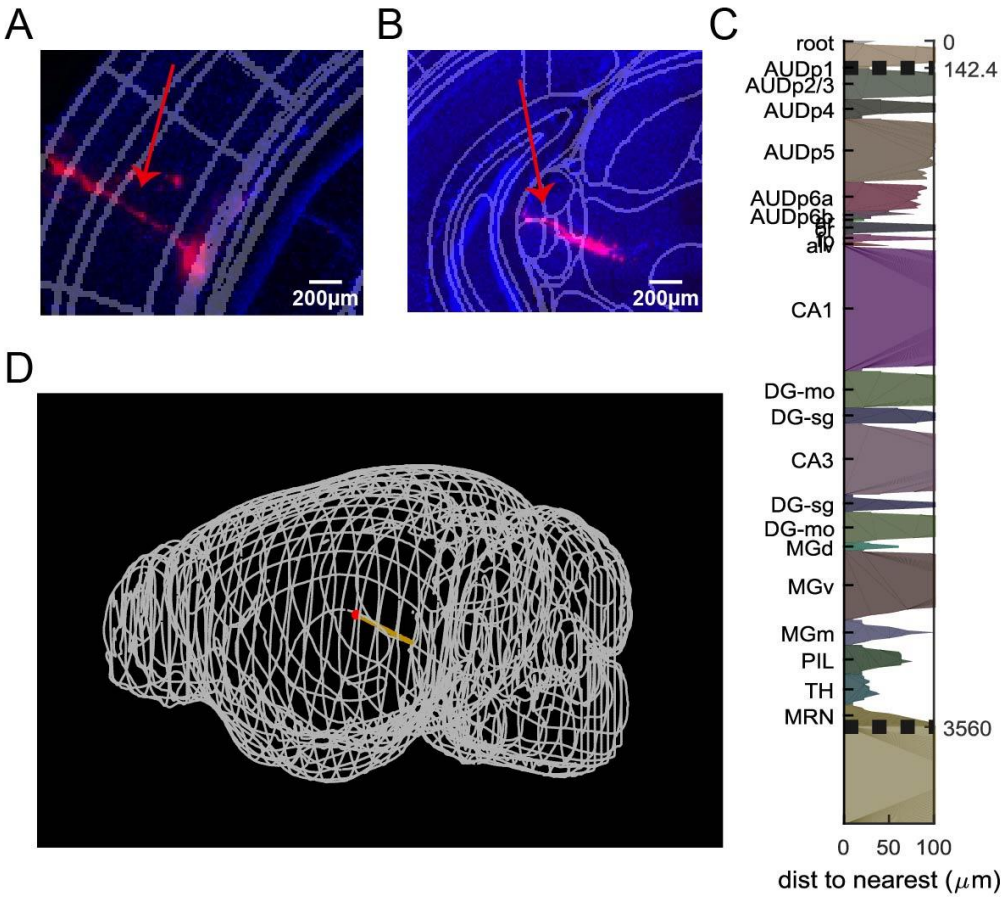

Figure 2.23. Examples of SHARP-Track processing steps. **A**- Brain slice registered in the 3D atlas, with a probe track going through the auditory cortex (red arrow pointing to the track). **B**- Same as A, but located in MGB. **C**- An output profile with a list of brain areas caught by the probe. X-axis shows the certainty for each brain area. **D**- 3D mesh brain with the probe track location (yellow line; red dot indicates the brain surface).

The next step in Neuropixels analysis pipeline was to combine histological probe location and electrophysiological channel activity, to identify which channels are in which brain area. For that reason, we first had to extract spike waveforms from raw recordings and find a main channel for each cluster (channel with the largest waveform amplitude). This was done in parallel with waveform metrics calculations, using the mean waveforms module of ecephys spike sorting (https://github.com/AllenInstitute/ecephys_spike_sorting).

Then, MUA activity across the whole recording was estimated for each channel, as well as the activity during broadband noise presentation (Figure 2.24.). Combining the knowledge from SHARP-Track with known brain-area specific activity allowed us to determine which recording channels were located in the auditory cortex and which were in the thalamus (MGB identification within thalamic channels is explained later in this chapter).

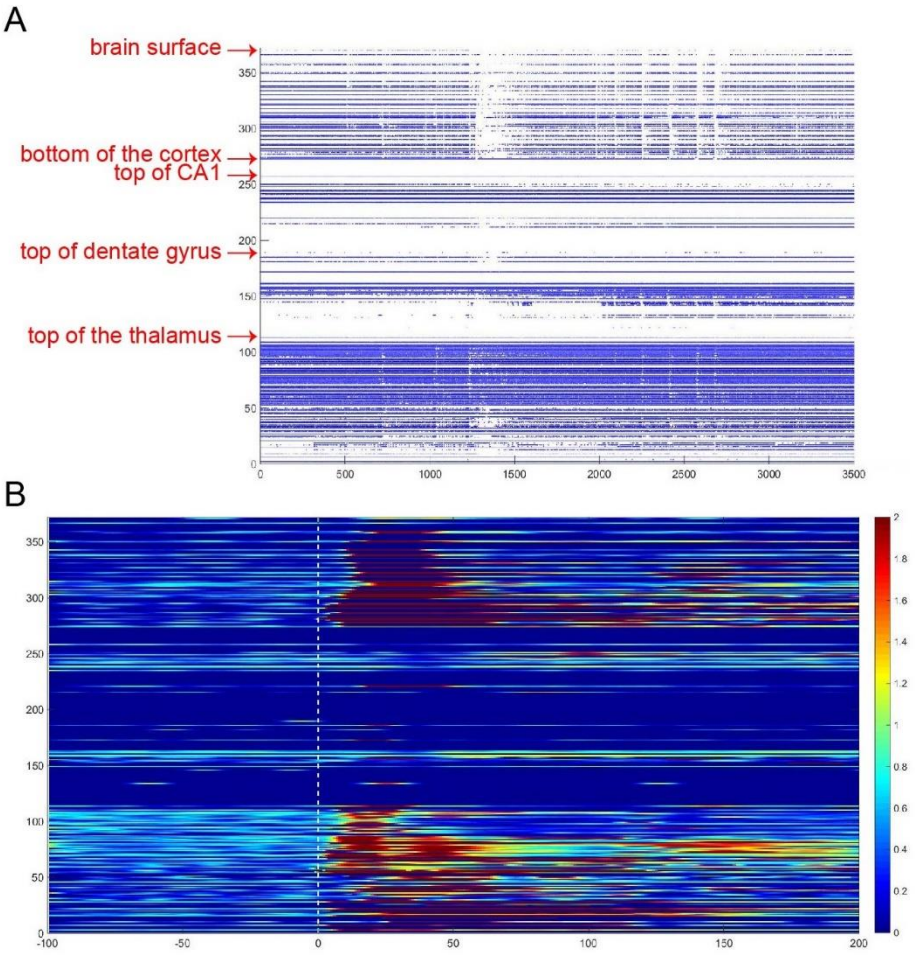

Figure 2.24. Neuronal activity across Neuropixels probe channels. **A**- Raster plot of activity across channels (y-axis) in time (x-axis, in ms). In each recording, five borders could be recognized through histological, anatomical and electrophysiological information. **B**- Colourmap of normalized activity across channels during 100ms broadband white noise presentation (sound onset marked with a vertical white line). Evoked auditory responses, defined as activity higher than 2.8 standard deviations above mean, are visible in the cortex and thalamus (colours higher than 1 on the colour bar).

Cortical cell type classification

Spike waveforms were extracted from the raw recordings and a mean waveform was calculated for each cluster. In silicon probe recordings, up to 2000 spikes were used to make the mean representative waveform, and from it, trough to peak duration was measured using MATLAB (custom code, Sakata lab) (Figure 2.25A).

In Neuropixels recordings, mean waveform was made from 500 waveforms and waveform metrics were assessed in Python, using the mean waveforms module of ecephys spike sorting (https://github.com/AllenInstitute/ecephys_spike_sorting).

Cortical cells were divided into broad-spiking and narrow-spiking depending on their trough to peak duration ((Barthó *et al.*, 2004), Figure 2.25B).

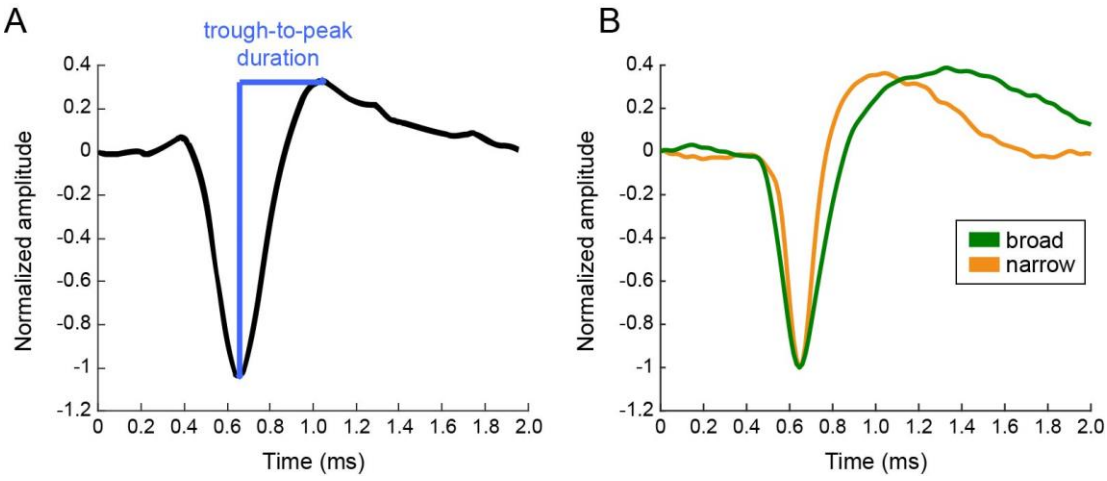

Figure 2.25. Cell type classification. **A**- An example of a waveform with its trough to peak duration. **B**- Depending on their trough to peak duration, cells can be split into narrow-spiking, with a short duration, and broad-spiking, with long duration. In this example, the cut-off between broad and narrow spiking cells was made at 0.5 ms.

Cortical single-unit activity analysis

In the analysis of neuronal activity we have included only the cells that have been classified as "good" in spike sorting, had an isolation distance higher or equal to 20 and a spontaneous spike rate higher than 0.1 Hz. Spontaneous activity of a cell was calculated during a 30min silent period, as the number of spikes divided by the time.

Activity during broadband noise presentation of different intensities (0-70dB) was calculated across 100 (Neuropixels) or 200 (silicon probes) trials lasting 100ms. For each cell and each intensity, spike trains during 100ms time window before the sound onset, 100ms of sound presentation and 200ms after the sound presentation were binned into 1ms bins. Cell activity was filtered using 5ms Gaussian kernel and then normalized by its maximum activity.

For statistical analysis, raw cell activity during 50ms time window from the sound onset was used. Latency to peak activity was calculated as the time from the sound onset to the highest spike rate of evoked cells. Evoked response was considered as non-normalized activity higher than 2.8 standard deviations from baseline mean (taken from 100ms before the sound onset across trials).

Current source density

In order to examine layer-specific cell activity, we first needed to identify the borders of cortical layers in electrophysiological recordings. For this purpose, current source density analysis (CSD) was used. Current source density is the analysis of extracellular field potentials, used to determine the location and strength of neuronal inputs (current sink) and outputs (current source) (Freeman and Nicholson, 1975; Nicholson and Freeman, 1975).

Using MATLAB, local field potential (LFP) signals were extracted from the silicon probe recordings with a lowpass filter (800 Hz) and downsampled to 1kHz. With Neuropixels, LFP is extracted and saved separately during recordings.

From LFP, event-related potentials (ERP) were calculated, filtered and smoothed. CSD was then calculated for each probe channel using the formula:

$$CSD = ((V_a+V_b)-2V_o)/(d^2),$$

where V_o is the observed channel, while V_a and V_b are the neighbouring channels of V_o. d is the distance between channels in millimetres. Uppermost and lowermost

channels were doubled for this purpose. Resulting CSD colourmap shows the locations of sink and source relative to the probe channels (Figure 2.26.).

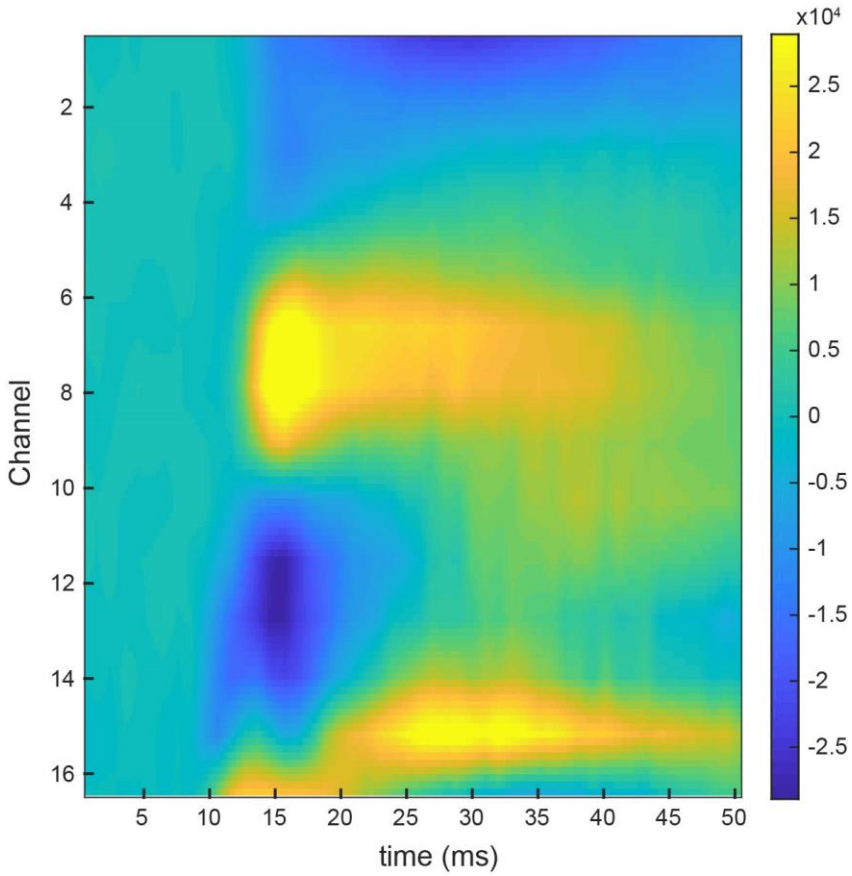

Figure 2.26. Current source density example for one shank (16 channels) of a silicon probe recording. Current sinks are visible in yellow, current sources are dark blue. Top sink (channel 8) is at the border of L II/III and L IV. This channel will be set as zero and cell depths relative to this channel will be used for layer-specific analysis.

Medial geniculate body identification and activity analysis

To analyse the cell activity in medial geniculate body, we utilised the information obtained from SHARP-Track and electrophysiological channel activity. For every recording, SHARP-Track provided the length of MGB sampled by Neuropixels probe, which could be translated into the number of channels located in the MGB. Additionally, from cell activity in channels, we could determine thalamic borders in our recordings, as shown in Figure 2.24A. Taking into account that MGB is an auditory

region, and medial and ventral MGB cells have a short (median <20ms) latency to auditory response (Anderson and Linden, 2011), we have looked into the activity of thalamic channels and calculated the latency to first evoked response during broadband noise presentation (defined as activity higher than 2.8 standard deviations from baseline mean), for each channel. Then, we determined MGB as the channels with short latency corresponding to the number given by SHARP-Track (Figure 2.27.). In example shown in Figure 2.27, SHARP-Track provided an estimate of 59 MGB channels (output was in the form of a MATLAB matrix, as the length in μm). If we look at the latency and activity in this colourmap, the 59 channels would correspond to channels 114-55, with channel 55 being the deepest.

SHARP-Track borders are not exact, as they are affected by tissue distortion and tearing during slice fixation. On average, the median absolute deviation between our electrophysiological borders and histological borders was 76μm. Because of this, we cannot define precise borders between different parts of MGB. However, according to SHARP-Track, in the passive listening recordings we were mostly in MGBv (53% of treated MGB channels and 75% of control MGB channels), followed by MGBm (24% of treated MGB channels and 19% of control MGB channels) and MGBd (23% treated MGB channels and 6% of control MGB channels). In the behavioural recordings, we were mostly in the MGBv in controls (46% of the MGB channels), but in the treated mice the most targeted area was MGBm (74% of treated MGB channels vs. 16% in controls), followed by MGBd (26% in treated vs. 38% in controls). Taking these results into account, we can presume that most of the MGB neurons we have recorded in passive listening conditions came from MGBv. In behaving mice on the other hand, most of the treated group neurons probably came from MGBm, while in controls they most likely came from MGBv.

For all further analysis of MGB neuronal activity, we have included only the cells from MGB channels that were classified as “good“ in spike sorting, had an isolation distance higher or equal to 20 and a spontaneous spike rate higher than 0.1 Hz.

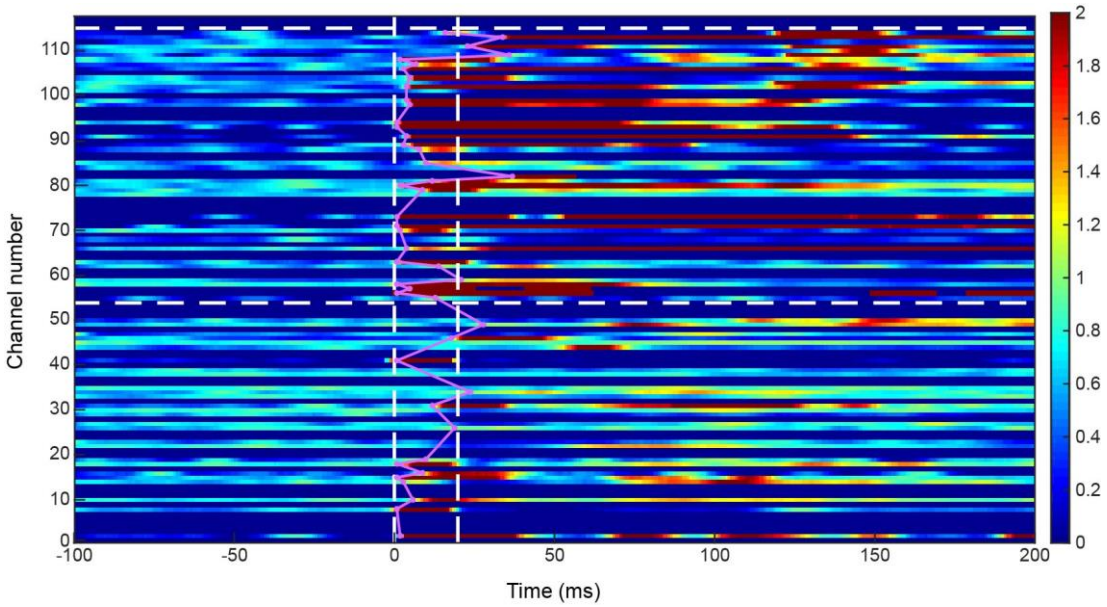

Figure 2.27. Determining the borders of medial geniculate body in electrophysiological recordings. Cell activity in thalamic channels during 100ms long broadband noise presentation is shown as a colourmap, where the sound onset is at 0ms. Activity across 100 trials was binned into 1ms bins, filtered using 5ms Gaussian kernel and normalized by evoked response threshold (2.8 standard deviations from baseline mean). Therefore, activity higher than 1 is considered evoked. Latency to the first evoked response was determined for each channel (purple). We then searched for the channels with latency within 0-20ms time window (vertical white dashed lines). The total MGB channel number was obtained from histological SHARP-Track information, and borders were drawn accordingly (horizontal dashed white lines).

Monosynaptic interactions assessment

In order to assess the cortical neuronal connectivity, we determined the monosynaptic connections probability from cell activity obtained through electrophysiological recordings. The method was adjusted from Fujisawa *et al.* (Fujisawa *et al.*, 2008).

For each cell in one recording, every spike was randomly "jittered" either +3ms or -3ms. This was done 1000 times, resulting in 1000 different, surrogate data sets. From these surrogate and the original data sets, cross-correlograms (CCGs) of activity within a 15ms time window were constructed for each cell pair in the recording (Figure 2.28). Upper and lower bound of confidence limit (1%; p=0.01) was computed

based on jittered CCGs. If the values in original CCG passed the upper confidence limit within the [-3:0ms, 0:3ms] time window, the interaction between cells was considered significant ($p<0.01$), and interaction was labelled as excitatory (Figure 2.28A). If the values in the original CCG were less than the lower confidence limit, the interaction was labelled as inhibitory (Figure 2.28B). Finally, if the values were within the limits, it was considered that there was no connection between the observed cells (Figure 2.28C).

In this analysis, we used only cortical cells with isolation distance higher or equal to 20, spike rate higher than 0.1Hz and classified as “good“ in spike sorting.

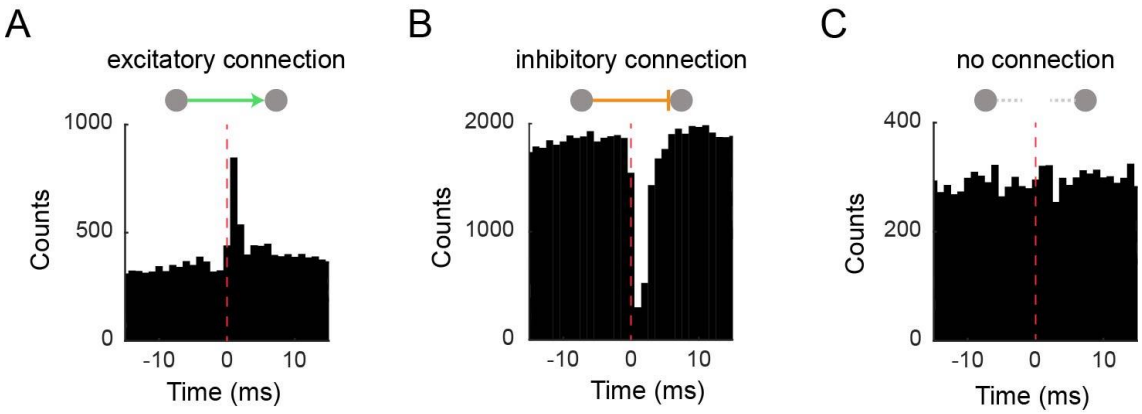

Figure 2.28. Cross-correlograms of activity between neuron pairs. **A**- Excitatory connection, **B**- Inhibitory connection, **C**- No connection.

Neural activity analysis during behavioural task performance

To examine the cell-type and brain region specific activity in mice performing the auditory detection task, we have first extracted the information from auditory sync channel. In combination with LabView behavioural output file that contained basic information about each trial (such as sound intensity and outcome), we were able to make event files. Then, we assessed the activity of cortical broad and narrow-spiking cells as well as MGB cells during behavioural trials where 30-70dB broadband noise was presented, with “hit“ outcomes.

In this analysis, we have included the cells from either cortical or MGB channels that were classified as “good“ or “MUA“ in spike sorting, had an isolation distance higher

or equal to 20 and a spontaneous spike rate higher than 0.1 Hz. Spontaneous spike rate was calculated as a mean “baseline“ activity during the 50ms time window before the sound onset, across all intensities and trials regardless of the outcome. Broad and narrow spiking cells were determined depending on their trough-to-peak duration.

2.7.4. Statistical analysis

All statistical analysis was done using MATLAB. The effect was considered significant at $p<0.05$.

Group comparisons for *in utero* microinjections survival and weight were done using a Wilcoxon rank-sum test, while the comparisons of the width of cortical layers were done with a two-sample t-test. Group comparisons of neuronal spike rate and latency as well as monosynaptic connection probabilities were done using the Wilcoxon rank-sum test with post-hoc Bonferroni corrections. Group comparisons in the behavioural assessment were done using two-way ANOVA with post-hoc Tukey-Kramer multicomparisons test.

Figures in this thesis were created using Adobe Illustrator and BioRender.

3. Effects of XAV939 treatment on embryonic survival and cortical lamination

3.1. Overview

One of the objectives in this project was to experimentally increase the number of L II/III excitatory neurons in mice using XAV939 and histologically verify the overproduction. In this chapter, I will present the results of XAV939 *in utero* microinjections.

Since this treatment is invasive and occurring during embryonic development, there is a possibility of it affecting the health status of the animals. Chapter 3.2. will therefore overview the effect of XAV939 microinjections on the survival and weight of the mice, as well as its dose dependency.

Given that XAV939 treatment is expected to increase the amount of superficial cortical excitatory neurons, and with it the width of superficial cortical layers, we have quantified the cortical layer width in young (P2) and adult (P21) mice. Results from the histological evaluation of the cortical layer width will be shown in chapter 3.3.

3.2. Survival and weight of the mice

To manipulate the thickness of cortical layer II/III in mice, *in utero* microinjections of XAV939 were performed in their lateral ventricle at E14 (XAV939 treatment litter number: n = 17; vehicle control litter number: n = 12). Because the drug injections were done during embryonic development, we began with assessing how XAV939 affects mice survival and other health conditions, before assessing their postnatal cortical laminae. A total of 143 mouse embryos were injected with XAV939 and 95 embryos were injected with the control vehicle. Percentage of total mice born did not differ significantly between the two groups (control 0.70 ± 0.04, treated 0.74 ±

0.07, mean ± SEM; p = 0.144; Figure 3.1A), nor did the percentage of stillborn mice (control 0.15 ± 0.05, treated 0.20 ± 0.04, mean ± SEM; p = 0.5210; Figure 3.1B). The groups also had a similar litter size (control 5.18 ± 0.60, treated 5.47 ± 0.62, mean ± SEM; p = 0.7528; Figure 3.1C).

Out of 29 pregnant females that underwent surgery, 26 gave birth in the expected time period between E18 and E21, and there were no significant differences in the birth day between groups (control 19.18 ± 0.12, treated 19.20 ± 0.14, mean ± SEM; p = 0.8932; Figure 3.1D). From the other three, the first mouse pulled her abdominal sutures out which resulted in protocol optimisation and use of staples on top of sutures in the next surgeries. The second female did not give birth by E22, so a Schedule 1 was performed. This animal was more than 7 months old, which was likely the cause of the issue. The third female died while giving birth, which was suspected to be a consequence of her age and large litter size.

Weight (in grams) of the mice sacrificed for histology on P2 (control 1.78 ± 0.11, treated 1.88 ± 0.14, mean ± SEM; p = 0.5714; Figure 3.1E) and P21 (control 9.19 ± 0.39, treated 9.42 ± 0.52, mean ± SEM; p = 0.9340; Figure 3.1F) was not significantly different between the XAV939 treated and control groups.

When comparing low volume (0.15µL; n embryos injected = 71) and high volume (0.4µL; n embryos injected = 72) of XAV939 injections, no significant differences were found in the percentage of pups born (low 0.71 ± 0.13, high 0.76 ± 0.07, mean ± SEM; p = 0.9340; Figure 3.2A), percentage of stillborn (low 0.17 ± 0.06, high 0.22 ± 0.07, mean ± SEM; p = 0.6076; Figure 3.2B), litter size (low 5.86 ± 1.22, high 5.13 ± 0.52, mean ± SEM; p = 0.7574; Figure 3.2C) or day of birth (low 19.29 ± 0.29, high 19.13 ± 0.13, mean ± SEM; p = 0.4615; Figure 3.2D). Mice weight did not differ significantly between the groups injected with low and high volume on P2 (low 1.50 ± 0.29, high 2.06 ± 0.13, mean ± SEM; p = 0.1287; Figure 3.2E) or P21 (low 9.23 ± 0.53, high 9.63 ± 0.98, mean ± SEM; p = 0.3513; Figure 3.2F).

Thus, XAV939 injections during embryonic development did not significantly affect the health and survival of mice. Further, increasing the volume of injected drug did not significantly change the health conditions and survival of mice.

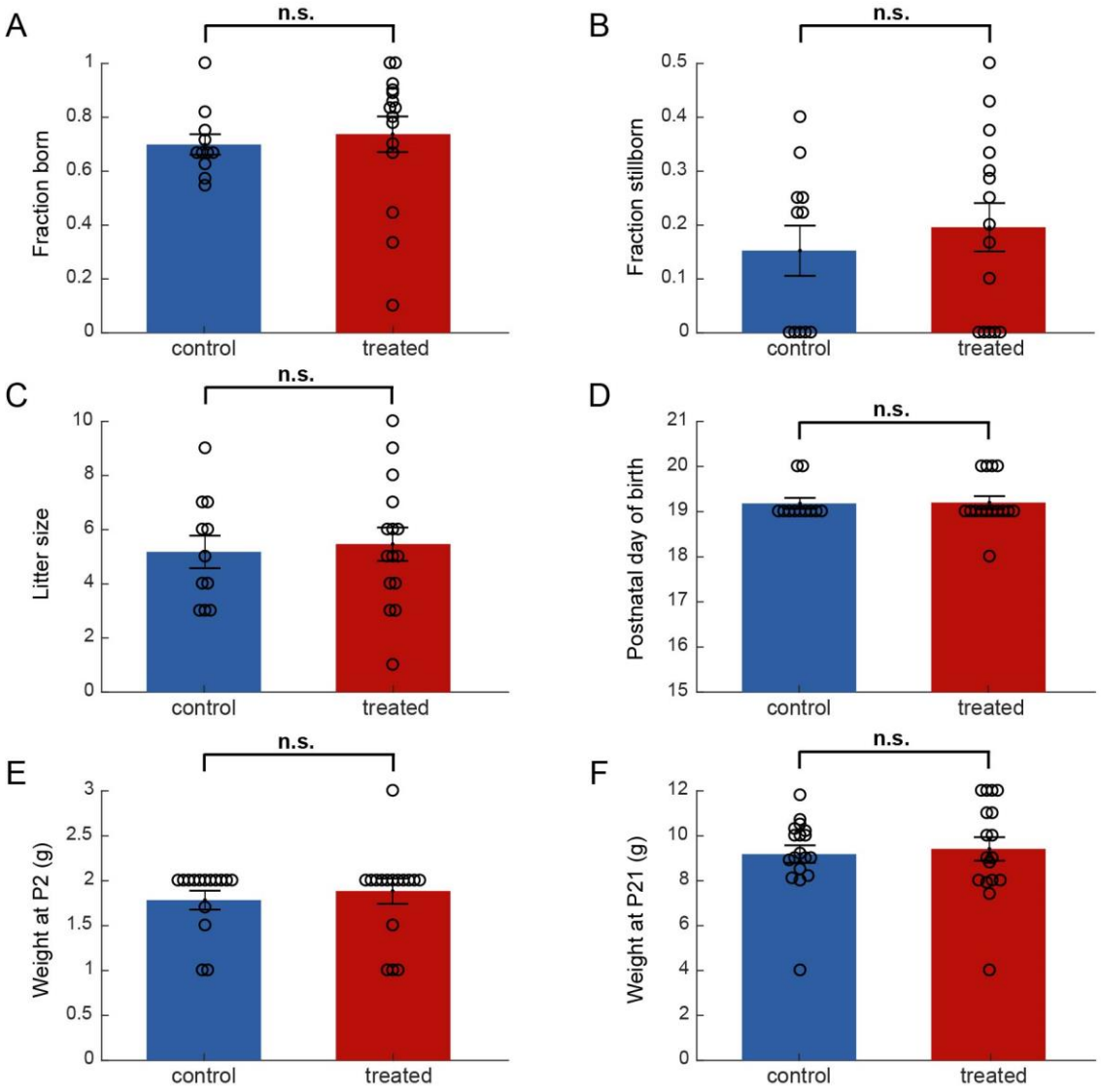

Figure 3.1. Comparison of survival and weight between XAV939 treated mice and controls. **A-** Percentage of pups born out of total number injected per litter (n control = 11, n treated = 15; p = 0.6556) **B-** Percentage of stillborn pups in total number born per litter (n control = 11, n treated = 15; p = 0.5158) **C-** Litter size (n control = 11, n treated = 15; p = 0.7504) **D-** Postnatal day of birth (n control = 11, n treated = 15; p = 0.9280) **E-** Weight of mice at 2nd postnatal day (n control = 15, n treated = 16; p = 0.5745) **F-** Weight of mice at 21st postnatal day (n control = 18, n treated = 17; p = 0.7262). All group comparisons were done using a Wilcoxon rank-sum test.

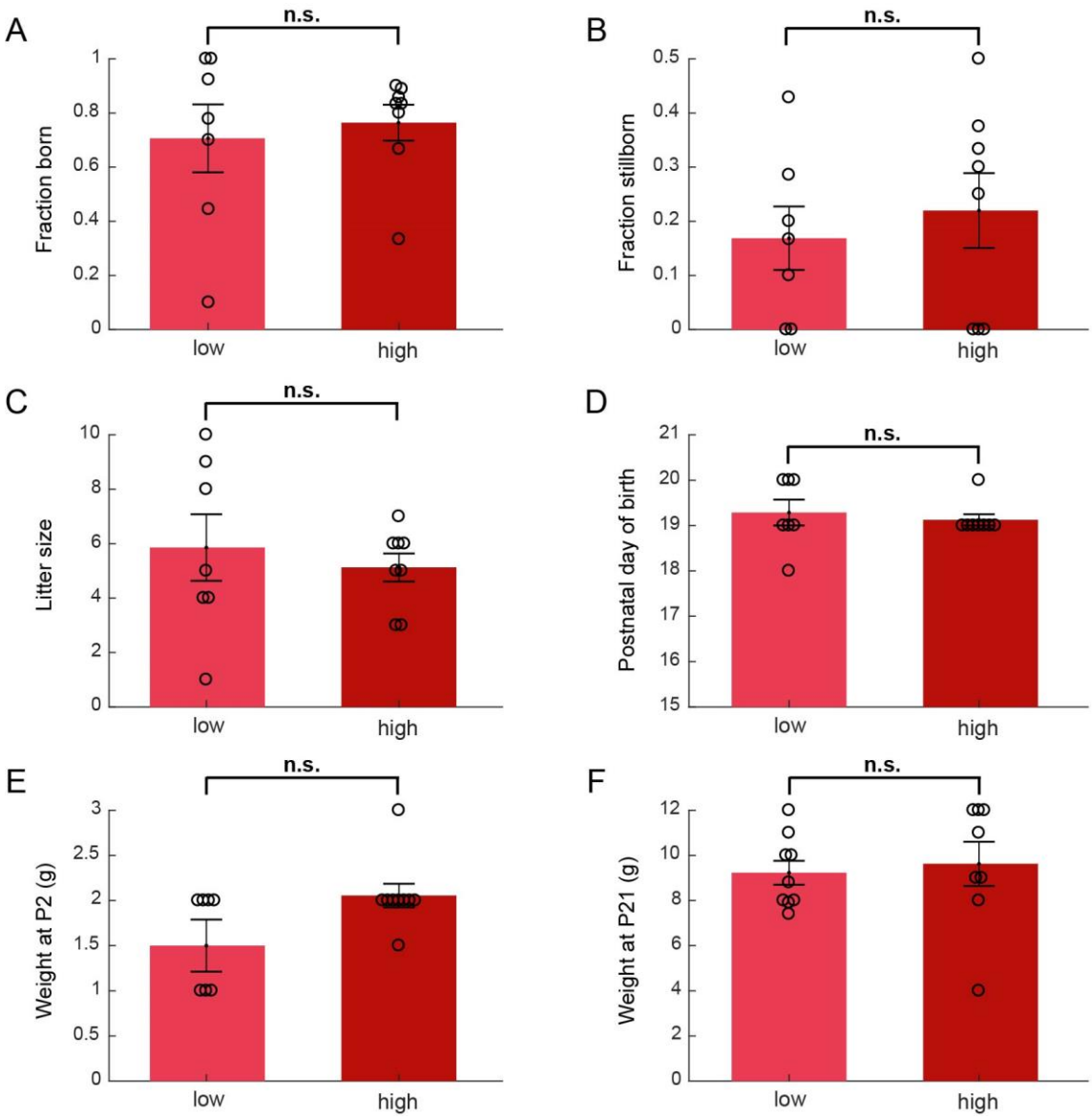

Figure 3.2. Comparison of survival and weight between low volume (0.15µL) and high volume (0.4µL) injected XAV939 treated mice. **A-** Percentage of pups born out of total number injected per litter (n low volume = 7, n high volume = 8; p = 0.6807) **B-** Percentage of stillborn pups in total number born per litter (n low volume = 7, n high volume = 8; p = 0.5885) **C-** Litter size (n low volume = 7, n high volume = 8; p = 0.5728) **D-** Postnatal day of birth (n low volume = 7, n high volume = 8; p = 0.5985) **E-** Weight of mice at 2nd postnatal day (n low volume = 7, n high volume = 9; p =0.0642) **F-** Weight of mice at 21st postnatal day (n low volume = 9, n high volume = 8; p = 0.7221). All group comparisons were done using a Wilcoxon rank-sum test.

3.3. Histological evaluation of cortical layers

To confirm whether the treatment can overproduce superificial cortical neurons, some mice were sacrificed on either P2 (n control = 15, n treated = 16) or P21 (n control = 18, n treated = 17) for the purpose of histological evaluation of cortical layers. A few of the P21 mice brains (n control = 5, n treated = 4) were used during histology procedure training and optimisation, and were not of good quality. These brains were therefore not used in analysis of cortical layers width and the sample size for P21 layer analysis was: n control = 13, n treated = 13.

Figure 3.3 shows the comparisons between the cortex of a control mouse brain and an XAV939 treated mouse brain at P2 (Figure 3.3A) and P21 (Figure 3.3B). The width of superficial cortical layers (L II-IV) is visibly larger in treated mice.

Comparison of superficial layers width between control and treated mice indicates that XAV939 treated mice exhibit a significant increase in superficial layer width at P2 (control 0.33 ± 0.005, treated 0.35 ± 0.006, mean ± SEM; $p < 0.05$; Figure 3.3C) and P21 (control 0.34 ± 0.005, treated 0.37 ± 0.005, mean ± SEM; $p < 0.001$; Figure 3.3D).

Since our quantification method can be affected by determining the border between L IV and L V, potentially giving false results as a consequence of including a part of L V into the superficial layer's width, we have also compared the width of LV-LVI between the 2 groups as a control measurement. In this way, if the superficial layer's width has wrongly included a part of L V in treated mice, there would be a significantly lower width of deep layers in the treated group compared to controls.

The width of deep cortical layers between control and treated mice was not significantly different at P2 (control 235.71 ± 13.78, treated 233.54 ± 11.74, mean ± SEM; $p = 0.9050$; Figure 3.3E) nor P21 (control 457.29 ± 5.97, treated 431.90 ± 12.49, mean ± SEM; $p = 0.0791$; Figure 3.3F).

Thus, our results suggest that *in utero* XAV939 microinjections at E14 caused an overproduction of neurons in superficial cortical layers in mice, visible through an increase in the width of superifical cortical layers.

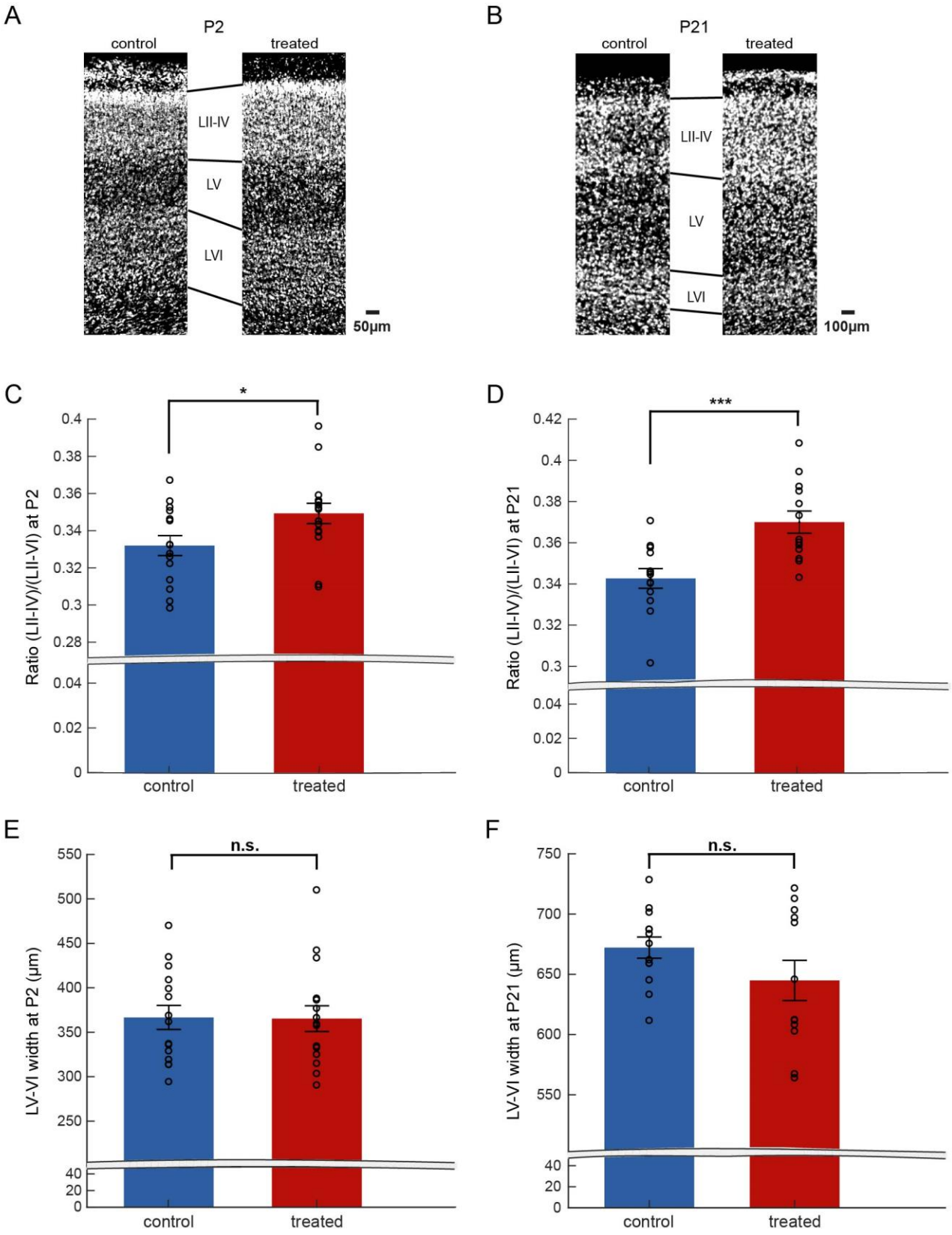

Figure 3.3. Histological evaluation of cortical layers width in XAV939 treated and control mice. Examples of DAPI stained cortical layers measured at P2 in the area of the frontal cortex

(**A**) and P21 in the area of auditory cortex (**B**). Cortical superficial layers of XAV939 treated mice were significantly wider than controls at **C-** P2 (n control = 15, n treated = 16; $p < 0.05$) and **D-** P21 (n control = 13, n treated = 13; $p < 0.001$). Width of deep cortical layers was not significantly different between groups on **E-** P2 (n control = 15, n treated = 16; $p = 0.9050$) or **F-** P21 (n control = 13, n treated = 13; $p = 0.0791$). All group comparisons were done using a two-sample t-test.

3.4. Summary

This chapter shows that XAV939 treatment did not have a significant effect on the survival or weight of the mice (Figure 3.1.), and neither did an increase of injected volume (Figure 3.2.). The procedure itself also did not seem to have significant adverse effects. According to Jacksons Laboratory information (The Jackson Laboratory, 2021), the weight of C57BL/6J mice in the third postnatal week is around 10g, which is consistent with our results in treated and control groups (Figure 3.1F and 3.2F). The litter size of our mice (Figure 3.1C and 3.2C) is also comparable with that of wild-type C57BL/6J mice (mean litter size = 5.6, (The Jackson Laboratory, 2009)). In Fang *et al.* from 2014 (Fang *et al.*, 2014), it was reported that XAV939 does not affect body weight, measured in P60 mice. Here, we have confirmed their results in P2 and P21 mice, and we showed that the treatment does not affect their survival, which wasn't shown previously. We have also looked at the effect of injected volume, which hasn't been done before.

Nevertheless, XAV939 injections at E14 caused a significant increase in the width of superficial cortical layers in mice (Figure 3.3C-D). This change in superficial layer width was present in young (P2) and adult (P21) mice, suggesting that XAV939 treatment causes long-term cortical abnormalities. Significant changes in the width were not observed in deep cortical layers (Figure 3.3E-F), indicating that XAV939 injections at E14 affected only the production of neurons in superficial cortical layers. These results are consistent with previous studies on XAV939 (Fang *et al.*, 2013, 2014; Fang and Yuste, 2017), where they also reported an increase in the superficial layer

width. It was previously shown that this treatment affects the production of pyramidal neurons specifically, and it does not affect the production of interneurons, microglia or astrocytes (Fang *et al.*, 2014). Therefore, we can assume that the change in superficial cortical layers width we observed is due to the overproduction of pyramidal neurons.

4. Spontaneous and auditory evoked activity in the auditory cortex of XAV939 model

4.1. Overview

Since XAV939 treatment overproduced only the excitatory neurons in the cortex, we wanted to see how the change in excitatory-inhibitory ratio affected the cortical neuronal activity. Therefore, another objective in this project was to characterize the differences in spontaneous and evoked auditory cortical activity between XAV939 treated and control animals using silicon and Neuropixels probes. In this chapter, cortical neuronal activity during passive listening conditions will be examined in-depth, and compared between treated and control mice.

To examine the potential treatment-related changes in activity of putative excitatory and inhibitory neurons, we first had to split the recorded neurons into these two groups. Chapter 4.2. contains the cell type classification results, demonstrating how cells were split into groups depending on their spike waveforms. The activity of these cell groups is then compared between control and treated mice in chapter 4.3.

Seeing that histological evaluation showed XAV939 treatment affected cortical superficial layers specifically, we also examined changes in activity for each cortical layer. Results from layer-specific comparisons in treatment groups are covered in chapter 4.4.

XAV939-induced overproduction of excitatory cortical neurons could also potentially cause alterations in neuronal connections. For this reason, we have assessed monosynaptic interactions between cells in our recordings. Differences in connectivity between treatment groups are assessed in chapter 4.5.

4.2. Cell type classification

We recorded neuronal activity from a total of 27 mice, out of which 14 (n control = 7, n treated = 7) were recorded with silicon probe while passively listening to sounds, 6 (n control = 1, n treated = 5) were recorded with Neuropixels while passively listening to sounds and 7 (n control = 3, n treated = 4) were recorded with Neuropixels while performing the auditory detection task. From these mice, we have obtained 22 (n control = 13, n treated = 9) silicon probe recordings, 10 (n control = 2, n treated = 8) Neuropixels passive listening and 15 (n control = 7, n treated = 8) Neuropixels task-engaging recordings. We had to dismiss some of the task-engaging recordings because of the poor behavioural performance of mice (explained in details in chapter 6), which brought us to a total of 8 (n control = 4, n treated = 4) recordings analysed in task-engaging mice.

We obtained 323 (n control = 203, n treated = 120) well-isolated (isolation distance ≥20) single units from auditory cortex using silicon probes, and 157 (n control = 57, n treated = 100) well-isolated auditory cortical single units with Neuropixels.

In order to assess the effect of excitatory neuronal overproduction on inhibitory and excitatory neuronal activity in the auditory cortex, we needed to identify cell-types from our recordings. Since we cannot define with certainty which cells are excitatory and which are inhibitory from extracellular recordings, in this thesis, we will be comparing broad-spiking and narrow-spiking populations. Cells were divided into the 2 groups based on the trough to peak duration of their average spike waveform (method described in chapter 2.7.4). In both silicon probe and Neuropixels recordings the two cell clusters were clearly separated (Figure 4.1A and C), with the border around 0.5ms. From the silicon probe recordings, 73% of neurons were broad-spiking and 27% narrow-spiking (Figure 4.1B). In the Neuropixels recordings, 72% of neurons were broad-spiking and 28% narrow-spiking (Figure 4.1D). Anatomically, around 20-30% of cortical neurons are GABAergic interneurons (Xu *et al.*, 2004), and ~40% of those are PV+ (Rudy *et al.*, 2011). Since excitatory neurons most likely make up a majority of broad-spiking cells and most of the narrow-spiking cells should be fast-

spiking inhibitory neurons (Barthó *et al.*, 2004), one would expect that in electrophysiological recordings 8-12% of recorded cells would be narrow-spiking. However, we obtained a higher number of narrow-spiking cells than this anatomical estimation. The reason for this could be the difference in their electrophysiological activity. While PV+ interneurons are highly active, excitatory neurons especially in superficial layers fire sparsely, and a lot of cortical neurons fire only in specific conditions (Shoham *et al.*, 2006; Sakata and Harris, 2009). Thus, the percentage of narrow and broad-spiking neurons in extracellular electrophysiological recordings could mirror their activity rather than anatomical prevalence, resulting in a higher percentage of narrow spiking neurons.

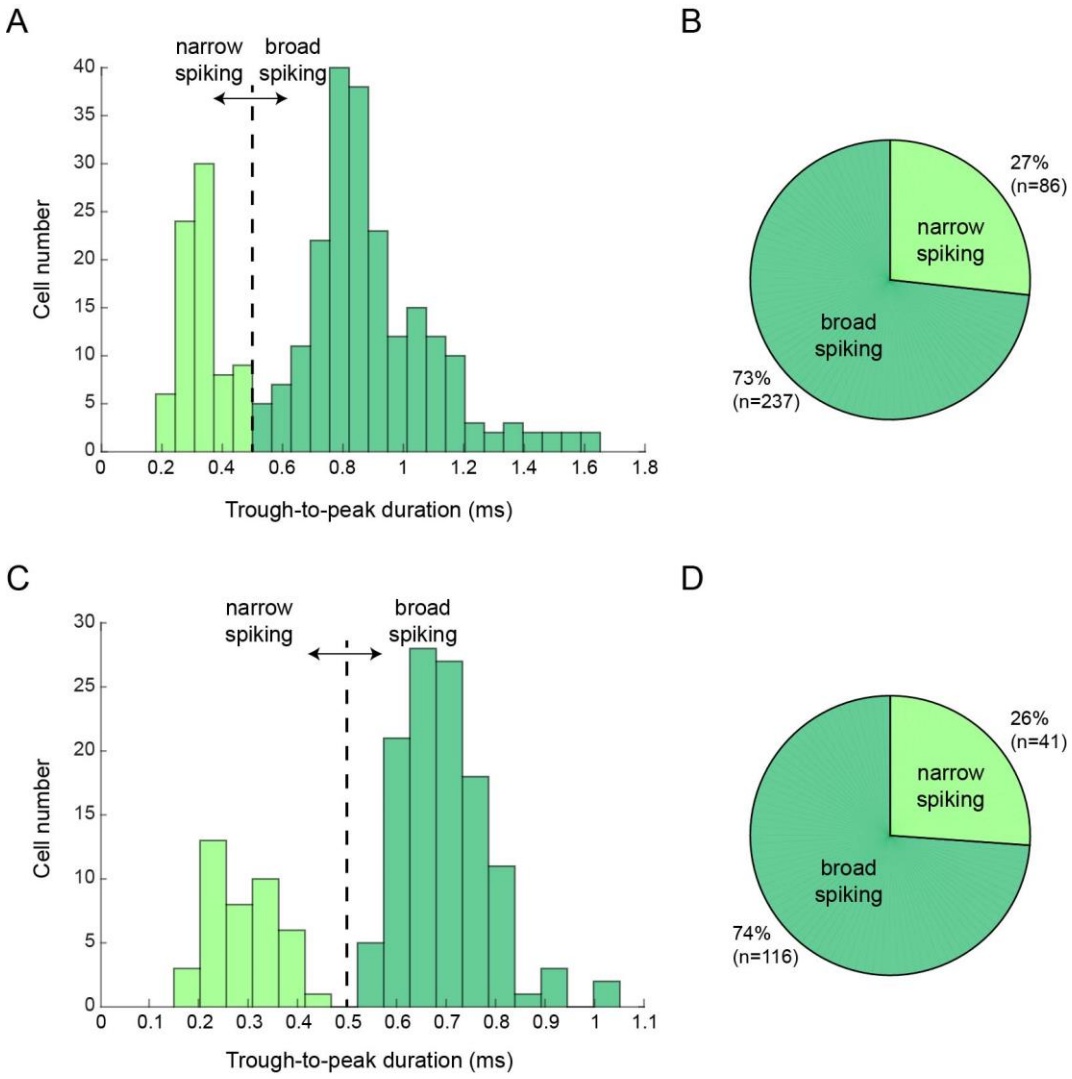

Figure 4.1. Splitting the cells into narrow and broad-spiking clusters. Depending on their trough to peak duration, cells were split into two clusters, narrow-spiking (duration <0.5ms)

and broad-spiking (duration ≥0.5ms). For analysis of silicon probe (**A**) and Neuropixels (**C**) electrophysiological recordings, the cut-off between clusters was set at 0.5 ms. In both groups of recordings, there were more broad-spiking cells (73% vs 27% in silicon probe recordings (**B**) and 74% vs 26% in Neuropixels recordings (**D**)).

4.3. Comparison of auditory cortical activity in treated and control mice

To assess if increasing the number of superficial cortical excitatory neurons affects cortical neuronal population activity, we have looked at spontaneous, non-evoked activity in the auditory cortex as well as evoked cell activity during passive sound presentations in adult control (n = 8) and treated mice (n = 12). A total of 32 (n control = 15, n treated = 17) recordings were done with silicon probes and Neuropixels, and analysed. In these recordings, we looked for well isolated (isolation distance ≥20) cortical single units with activity >0.1Hz during the long silent period, for assessing the spontaneous activity, and well isolated cortical single units with activity >0.1Hz during the 50ms time window before broadband noise onset, across broadband noise presentation trials. For the spontaneous activity analysis, we have obtained 171 neurons from control mice (n broad-spiking = 111, n narrow-spiking = 60), and 167 neurons from treated mice (n broad-spiking = 127, n narrow-spiking = 40). For the auditory evoked activity analysis, we have obtained 183 neurons in control mice (n broad-spiking = 127, n narrow-spiking = 56), and 163 neurons in treated (n broad-spiking = 116, n narrow-spiking = 39) (Figure 4.5A).

Looking into cell activity during the sound presentation, there was a consistent increase in activity with an increase in sound intensity in both cell groups of treated and control mice. Figure 4.2. shows colourmaps of activity across sound intensities comparing broad-spiking cells in treated and control mice. Figure 4.3. compares the activity of narrow-spiking cells in treated and control mice. Peristimulus time histogram (PSTH) of cell activities (Figure 4.4.) indicates that there are differences between cell groups and treatment groups. As expected, narrow-spiking neurons in treated and control groups seem to have a higher spike rate compared to broad-

spiking cells. However, we noticed at least two qualitative differences: first, broad-spiking neurons in the treated group seem to have a lower activity compared to the control group. Additionally, both narrow and broad-spiking cells in the treated group seem to have a longer peak response latency compared to controls.

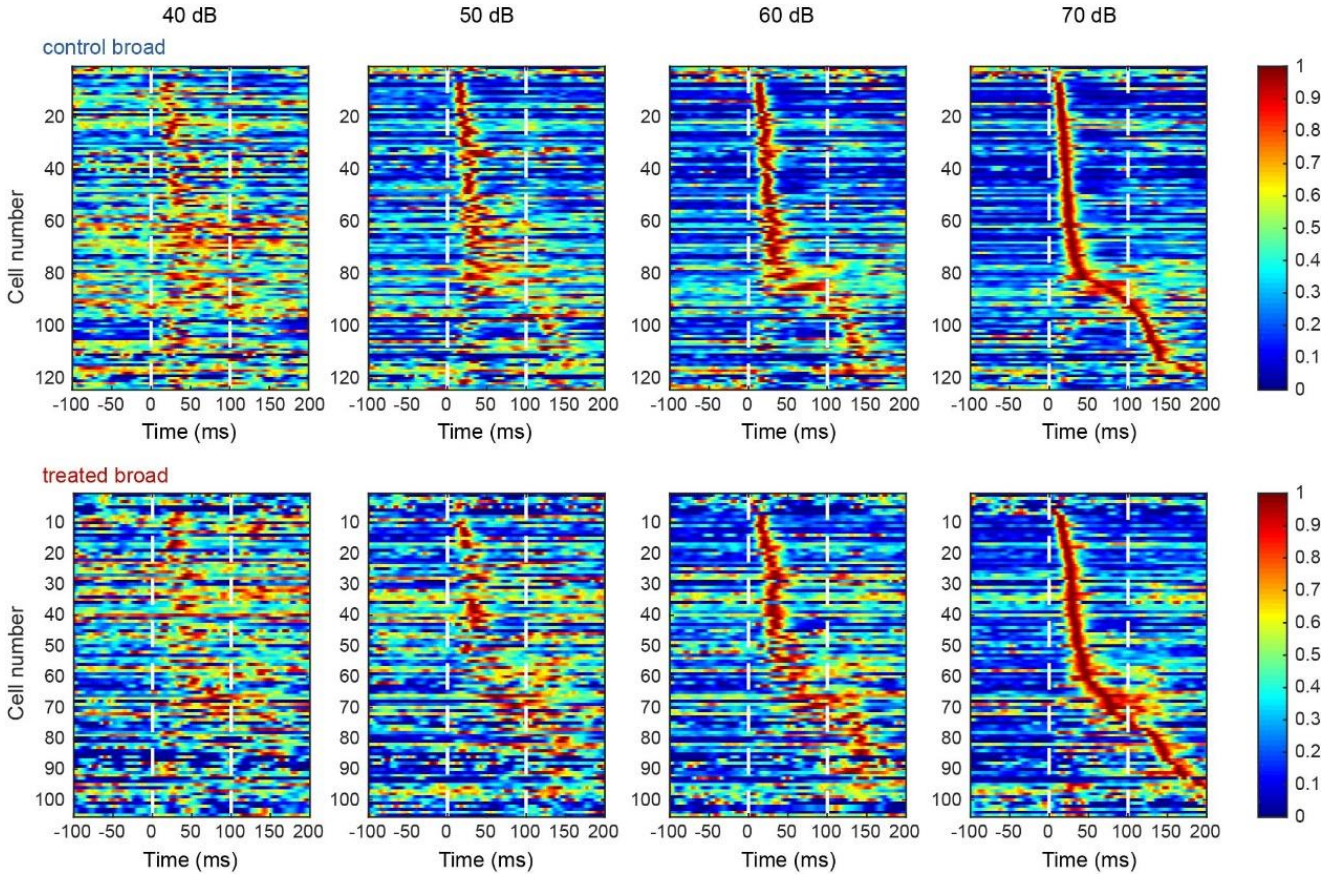

Figure 4.2. Colourmaps of evoked broad-spiking cell activity across sound intensities (here shown 40-70dB). The activity of each cell was filtered using 5ms Gaussian kernel and then normalized by its maximum activity. Evoked response was considered as non-normalized activity higher than 2.8 standard deviations from baseline mean (taken from 100ms before the sound onset across trials). Cells were ordered (top to bottom) depending on the timing of their maximum activity during 70dB sound presentation. The activity of control cells (top row) and treated cells (bottom row) increases with sound intensity. White dashed lines mark the sound onset and offset (duration 100ms).

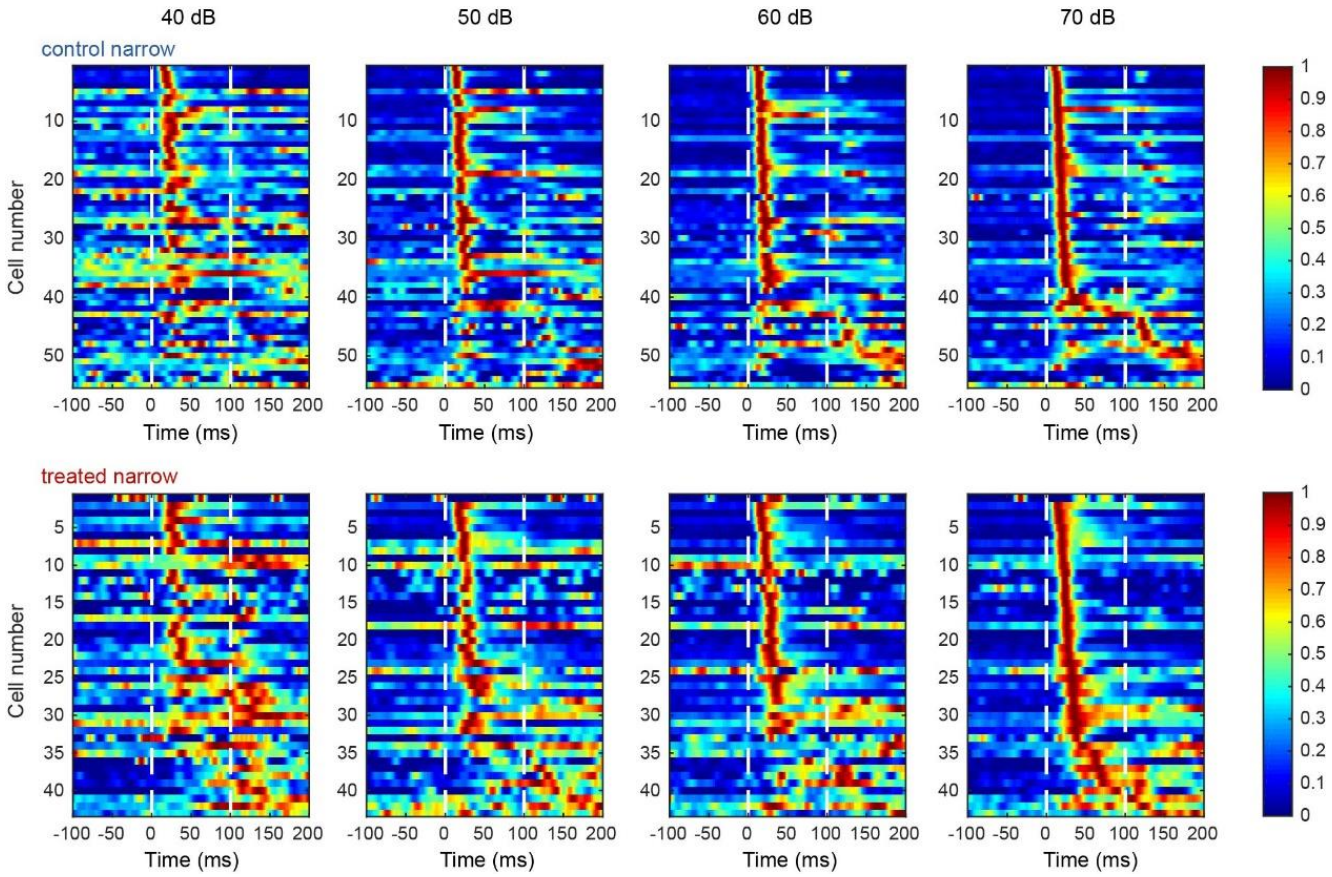

Figure 4.3. Colourmaps of evoked narrow-spiking cell activity across sound intensities (shown 40-70dB). The activity was calculated and cells were ordered in the same manner as in Figure 4.2. Similar to broad-spiking cells, the activity of both control (top row) and treated cells (bottom row) increases with sound intensity. White dashed lines mark the sound onset and offset (duration 100ms).

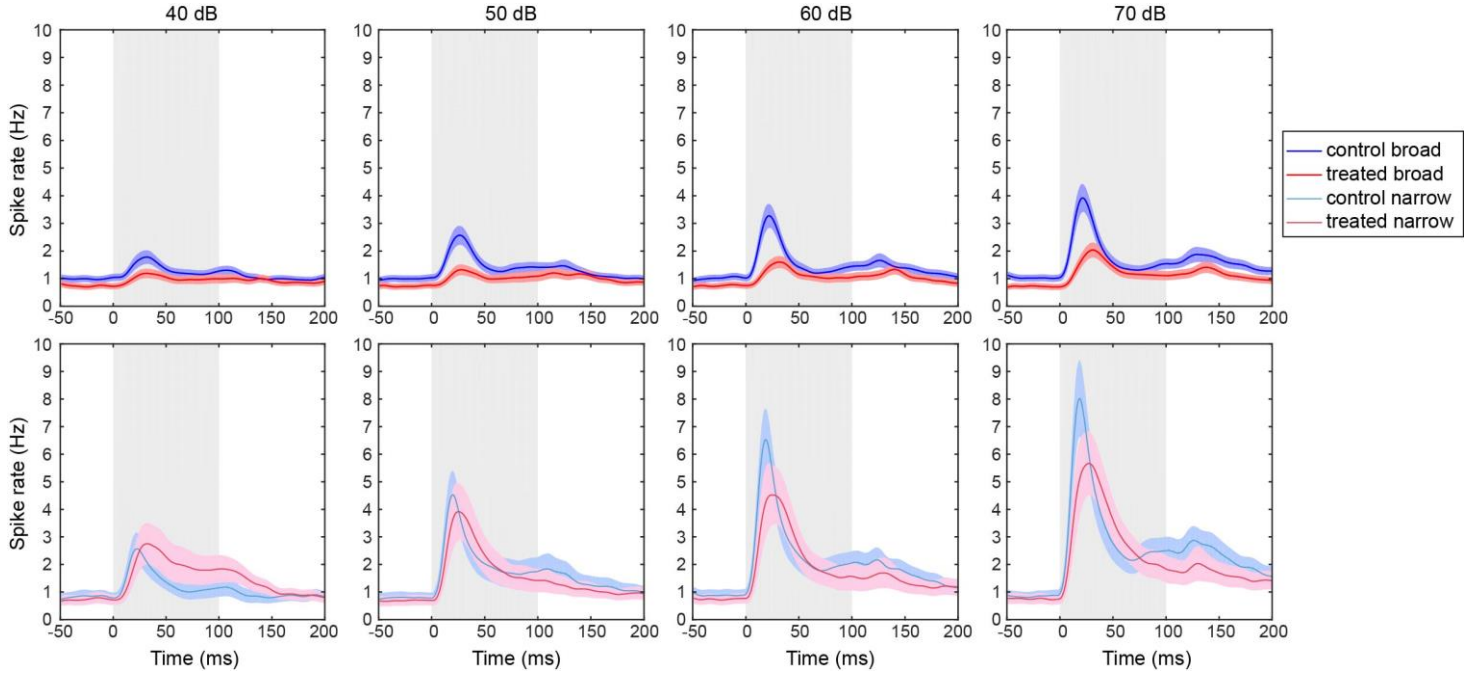

Figure 4.4. Peristimulus time histogram (PSTH) of cell activity (mean ± SEM) during the sound presentation (shown 40-70dB). Sound presentation period is labelled as a gray background (lasting 100ms). Top row: broad-spiking neurons, bottow row: narrow-spiking neurons.

Quantification of activity in cell groups across sound intensities confirmed the differences seen in PSTH. We have calculated the spike rate of cells by taking the cell activity across trials in the 50ms time window from the sound onset. The 50ms time window was taken due to PSTH showing that evoked response occured in this time window for all cell types. Spike rate of broad-spiking cells (Figure 4.5C) in treated mice was significantly lower for 50dB ($p < 0.01$) and 60dB ($p < 0.05$) sounds, compared to controls. On the other hand, the spike rate of narrow-spiking cells (Figure 4.5D) was not affected by the treatment.

We have also looked at the latency to peak evoked response, calculated as the time from the sound onset to the highest spike rate of evoked cells. Peak response latency of both broad and narrow-spiking cells was affected by the treatment. Broad-spiking cells (Figure 4.5E) in treated mice demonstrated a significantly longer latency to peak evoked response during 50dB ($p < 0.05$), 60dB ($p < 0.05$) and 70dB ($p < 0.01$) sound presentations. Narrow-spiking cells (Figure 4.5F) in treated mice also showed longer

peak response latency for 40dB ($p < 0.001$), 50dB ($p < 0.05$), 60 ($p < 0.001$) and 70dB ($p < 0.001$) sounds.

Spontaneous activity of neurons, calculated during a 30min silent period as the number of spikes divided by the time, was also affected by the treatment (Figure 4.5B). Treated mice showed significantly lower spontaneous activity of narrow-spiking neurons compared to controls ($p < 0.01$). Further, narrow-spiking neurons were significantly more active than broad-spiking neurons in control mice ($p < 0.05$), while in treated mice this difference between cell groups was not present ($p = 0.9996$).

Altogether, these results indicate that the XAV939-induced overproduction of excitatory neurons resulted in significant changes of neuronal activity in the auditory cortex. Spontaneous activity of narrow-spiking neurons was significantly lower in treated mice. Further, during sound presentation, broad-spiking cells demonstrated a significantly lower auditory evoked activity for 50 and 60dB sounds. Finally, both cell types had a longer latency to peak evoked response, with a significant difference in broad-spiking neurons for 50-70dB sounds and in narrow-spiking for 40-70dB sounds.

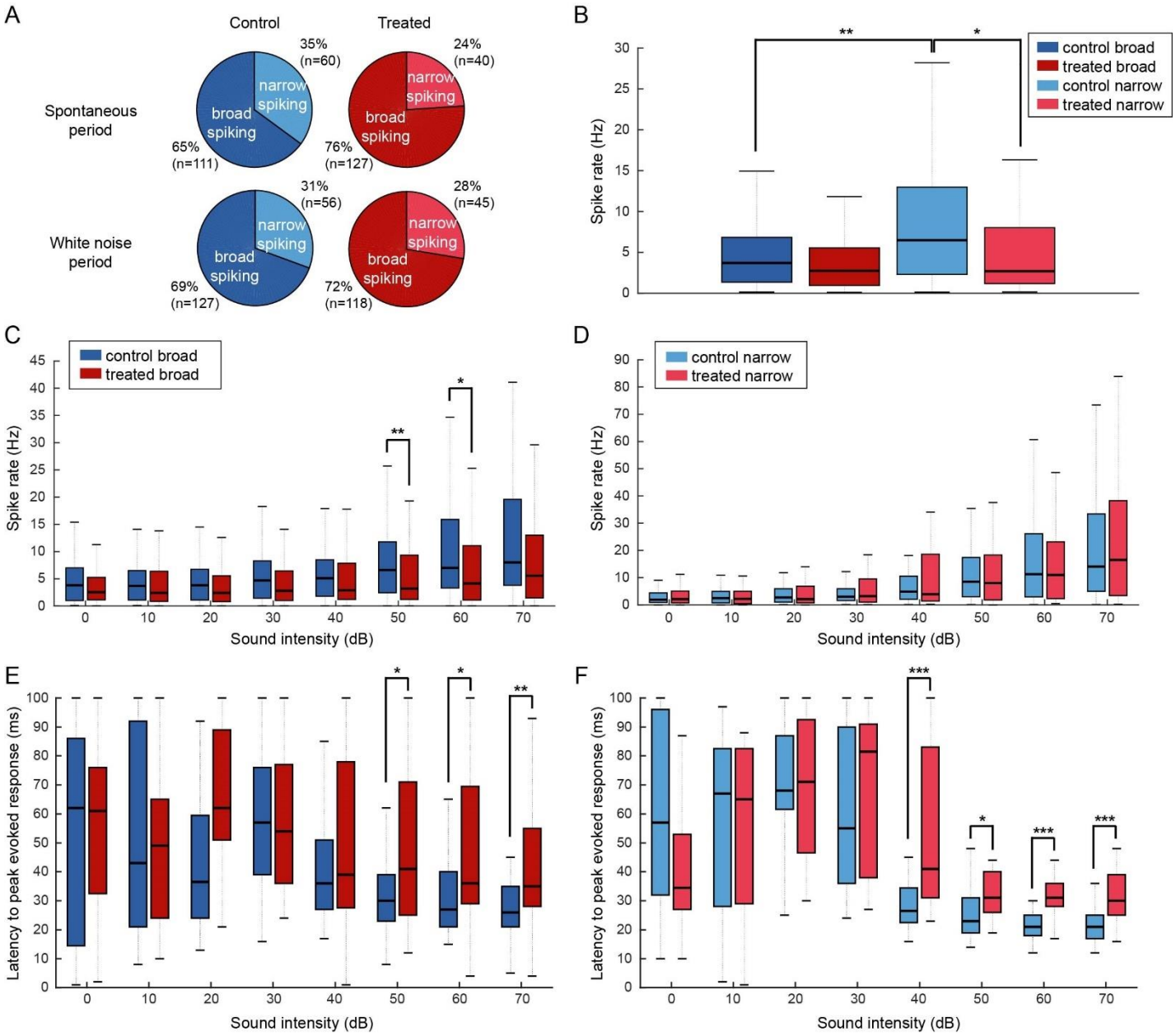

Figure 4.5. Quantification of broad and narrow-spiking cell activity during passive listening conditions. **A-** Percentage of cells in recordings of control and treated mice. In both groups of mice, there were more broad-spiking cells recorded during spontaneous and white noise period. **B-** Spontaneous activity of neurons recorded during a long silent period (30min). In control animals, narrow-spiking neurons had significantly higher spontaneous activity than broad-spiking neurons ($p < 0.05$). However, in treated mice, this difference between cell groups was not present ($p = 0.9996$). Additionally, narrow-spiking neurons of treated mice had significantly lower spontaneous activity compared to controls ($p < 0.01$). **C-** During sound presentation, treated mice showed lower activity of broad-spiking neurons, significant for 50dB ($p < 0.01$) and 60dB ($p < 0.05$). This difference was not present in narrow-spiking

neurons (**D**). Latency to peak evoked response was significantly longer in treated mice for broad-spiking (50-60dB $p<0.05$; 70dB $p<0.01$; **E**) and narrow-spiking (40,60,70dB $p<0.001$; 50dB $p<0.05$; **F**) neurons. Group comparisons for spontaneous activity were done using the Wilcoxon rank-sum test. All statistical comparisons for spike rate and latency during sound presentation were done using the Wilcoxon rank-sum test with post-hoc Bonferroni corrections.

4.4. Layer-specific differences in auditory cortical activity between treated and control mice

Since our treatment causes an overproduction of superifical cortical neurons, we wanted to determine if the observed changes in cortical activity are layer-specific. For that purpose, we have first determined the depth of recorded cells using CSD analysis (method explained in chapter 2.7.4). Cells recoded during the long silent period were split into cortical layers according to the CSD results and literature (Figure 4.6A). The proportion and number of neurons we obtained per layer for each cell type and treatment group is shown in Figure 4.6B.

Spontaneous activity (Figure 4.6C) of narrow-spiking cells in L V was significantly lower in treated compared to control group ($p < 0.05$). This tendency of lower activity was also visible in L I-III as well as L VI. However, the differences in these cortical layers were not significant.

Cells recorded during the sound presentation period were split into cortical layers in the same manner as neurons from Figure 4.6. The scatter plot of neurons across depth and proportion of neurons per layer is shown in Figures 4.7A and 4.7B. During the sound presentation, broad-spiking cells in treated mice mostly showed lower activity in L V and L VI, however, the differences were not significant (Figure 4.7C, left). Narrow-spiking neurons of L I-III in treated mice showed a tendency of increased activity compared to controls, while L VI cells showed a decreased activity (Figure

4.7C, right). Yet, none of the observed layer-specific differences in activity were significant.

Both broad and narrow-spiking neurons in treated mice showed a tendency of longer peak response latency compared to controls across cortical layers, but the differences were not significant in any of the layers (Figure 4.7D).

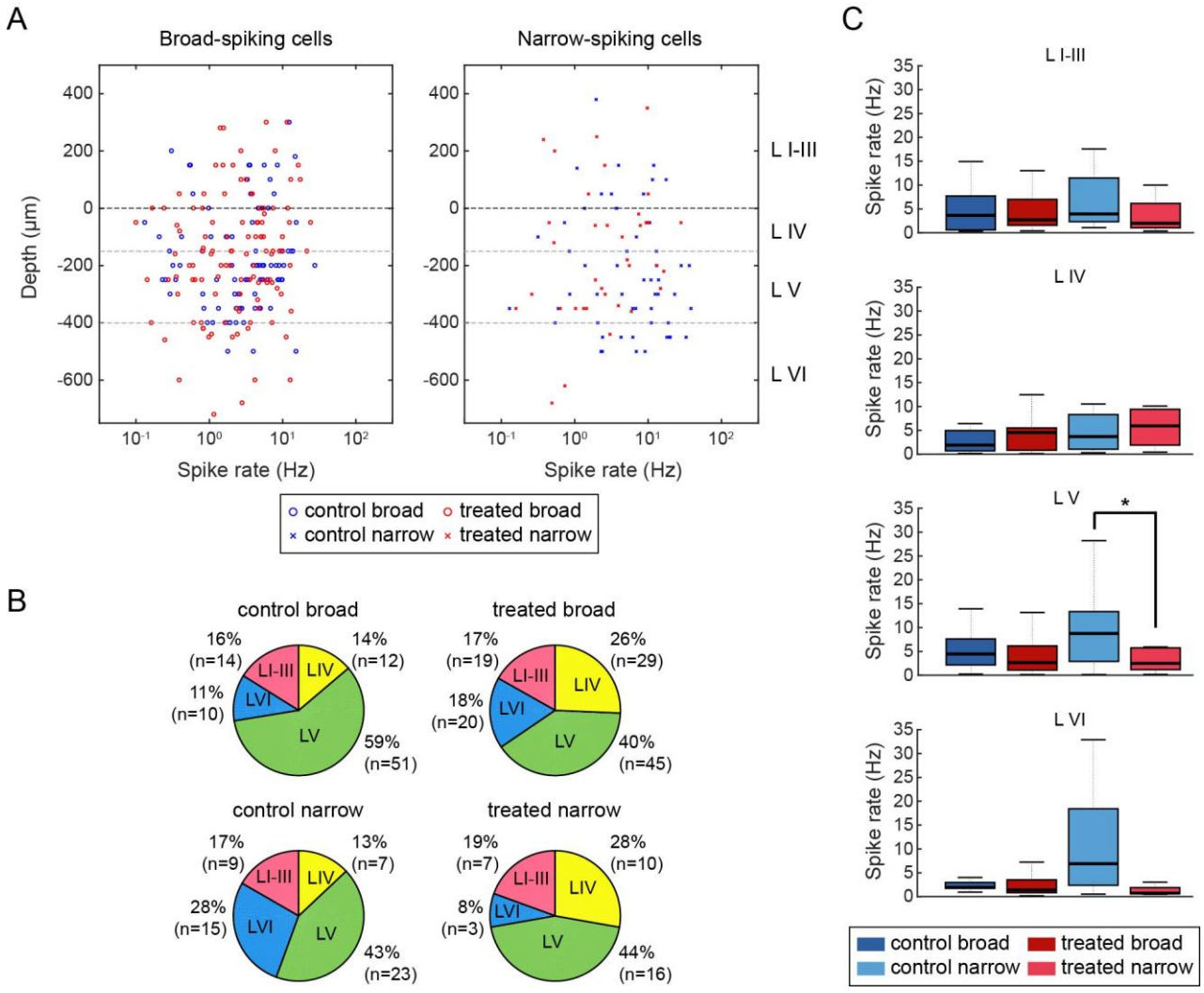

Figure 4.6. Layer-specific spontaneous activity. Cell depth was determined using CSD analysis. **A-** Scatter plots showing the depth positions of broad-spiking and narrow-spiking cells used in the analysis. The top border of L IV was determined through CSD, while the borders of L V and L VI were determined according to literature (Ji *et al.*, 2016; Cooke *et al.*, 2018). **B-** Percentage of cells recorded from each layer across cell groups. **C-** Spontaneous activity of cells across cortical layers. Narrow-spiking treated cells show a tendency of lower activity

across L I-III, L V and L VI compared to control, with a significant difference in L V ($p < 0.05$). Group comparisons were made using the Wilcoxon rank-sum test.

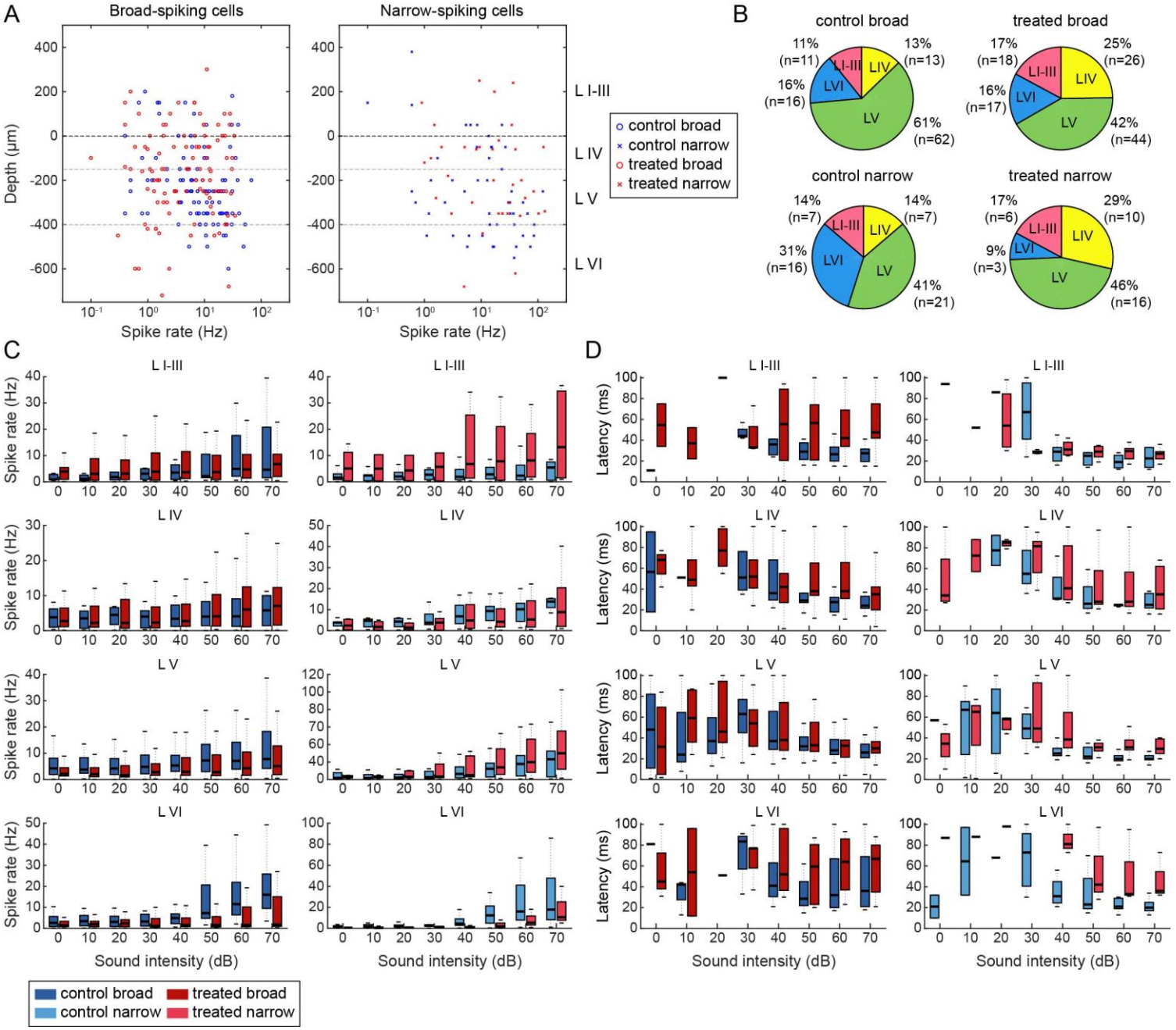

Figure 4.7. Layer-specific evoked activity. **A-** Scatter plot of cells across cortical layers, showing activity during 70dB sound presentation. Layers were determined in the same manner as Figure 4.6A. **B-** Percentage of cells recorded from each layer across cell groups. **C-** Layer-specific activity of treated and control broad-spiking (left column) and narrow-spiking neurons (right column) across sound intensities. **D-** Latency to peak evoked response for treated and control broad-spiking (left column) and narrow-spiking neurons (right column)

across sound intensities. Group comparisons were made using the Wilcoxon rank-sum test with post-hoc Bonferroni corrections.

All in all, except for the difference in spontaneous activity of narrow-spiking neurons in L V, we have not found any other significant layer-specific differences between treated and control group.

4.5. XAV939 impact on monosynaptic connectivity

Considering that we have overproduced only the excitatory cortical neurons with our treatment, we wanted to investigate if this overproduction resulted in changes in neuronal connectivity. Changes in connectivity might also explain the abnormalities observed in neuronal activity.

For that purpose, we have analysed putative monosynaptic interactions of simultaneously recorded neurons in our recordings (method explained in chapter 2.7.4). Cross-correlograms between neuron pairs were analysed and if an interaction was detected, it was classified as either an excitatory or inhibitory connection. Examples of connectivity matrices for one control and one treated mouse recording are shown in Figure 4.8A. Each matrix shows all the connections and their types, going from the origin cell to the target cell.

Results indicate that narrow-spiking neurons in treated mice form significantly fewer connections compared to controls. There was a significantly lower probability of an inhibitory connection from narrow to broad-spiking neuron ($p < 0.05$) as well as narrow-to-narrow-spiking neuron ($p < 0.01$) in treated mice (Figure 4.8B). Additionally, broad-spiking neurons also had a significantly lower probability to form excitatory connections towards narrow-spiking neurons in treated mice ($p < 0.001$; Figure 4.8C). Broad-to-broad spiking neuron excitatory connections did not seem to be significantly affected by the treatment. Further, through this analysis we found that the connections from narrow-spiking neurons were predominantly inhibitory, supporting the assumption that narrow-spiking neurons are mostly inhibitory PV+

cells (probabilities for excitatory connections coming from narrow-spiking neurons were significantly lower compared to inhibitory connections; $p < 0.001$, Wilcoxon rank-sum test). Broad-spiking neurons, presumably comprised of excitatory neurons and other types of inhibitory neurons, did not have a significant difference in the probability to form excitatory and inhibitory connections ($p = 0.7758$). The excitatory and inhibitory connectivity results observed for the broad-spiking neurons might also be affected by several factors, such as low firing rate.

We have also looked into neuronal connectivity across cortical layers. Figure 4.9. shows the probability of connections coming from neurons in L I-III, L IV and L VI towards neurons across cortical layers. Connection probabilities in most cases seem to be the highest within the origin layer or nearby layers, and decreasing with the distance. When comparing layer-specific treated and control groups of neurons, no significant differences were observed in any of the layers.

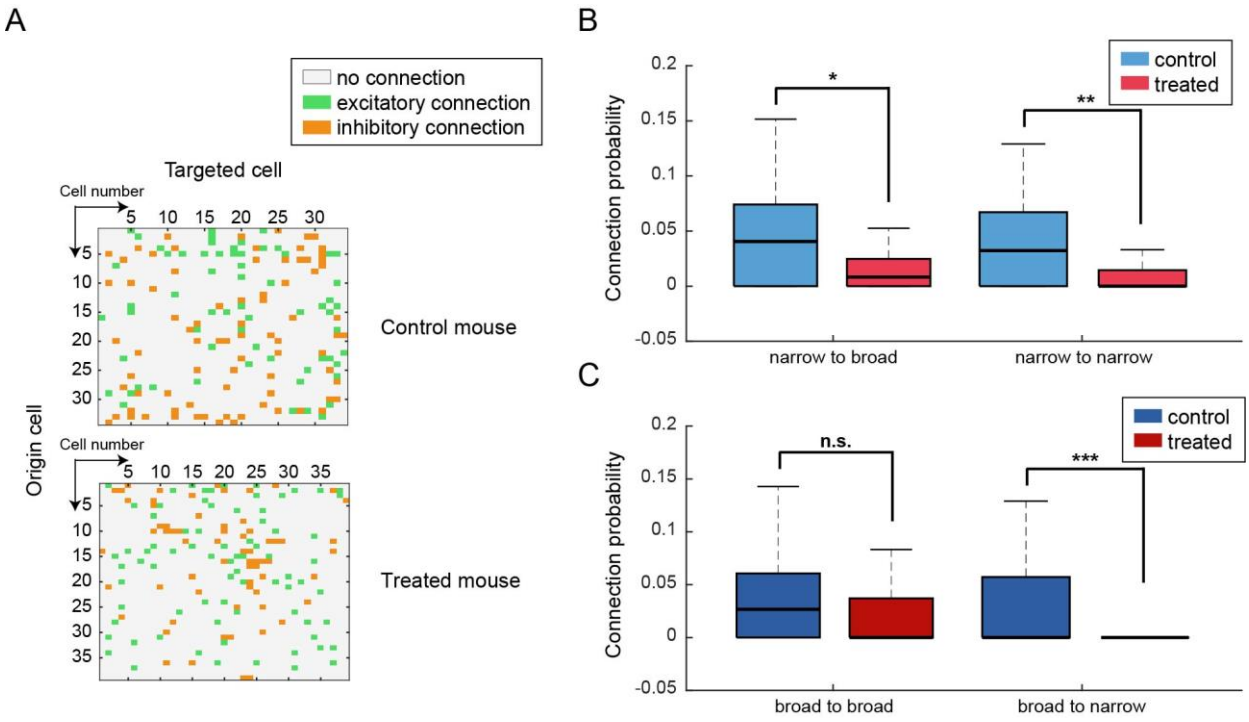

Figure 4.8. Monosynaptic interactions analysis. **A-** Example CCG matrices from one control and one treated mouse recording showing simultaneously recorded neuron pairs. Orange squares represent an inhibitory connection coming from the origin cell towards the targeted

cell, while green squares depict excitatory connections. **B-** Probability of an inhibitory connection occurring from narrow-spiking neurons to broad-spiking and narrow-spiking neurons was significantly lower in treated mice. **C-** Probability of an excitatory connection occurring from broad-spiking neurons to broad-spiking and narrow-spiking neurons. Connection probability from broad-spiking to narrow-spiking is significantly lower in treated mice.

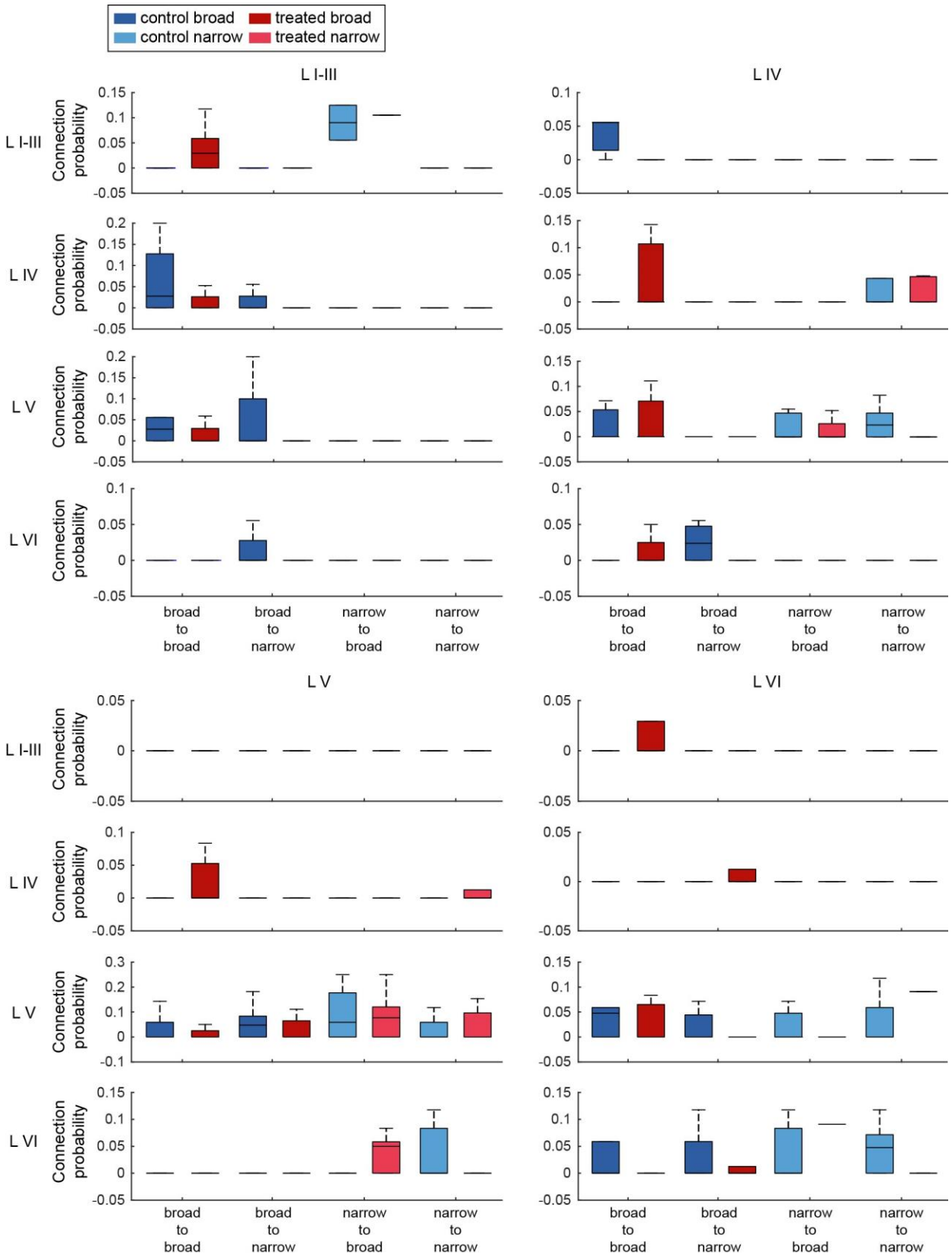
control broad
treated broad
control narrow
treated narrow
L I-III
L IV
L V
L VI
Connection probability
broad to broad
broad to narrow
narrow to broad
narrow to narrow

Figure 4.9. Layer-specific monosynaptic interactions. Probabilities of connections coming from neurons in L I-III, L IV, L V and L VI (columns) towards neurons across cortical layers (rows). In most cases, the connection probability between layers was low to zero.

4.6. Summary

Results from electrophysiological recordings during passive listening conditions suggest that the XAV939 treatment affected cortical neuronal population activity in multiple ways. Treated mice exhibit a significantly lower spontaneous activity of narrow-spiking cells (Figure 4.5B), lower evoked activity of broad-spiking cells during 50dB and 60dB sounds (Figure 4.5C), as well as longer peak response latency in broad (50-70dB; Figure 4.5E) and narrow-spiking cells (40-70dB; Figure 4.5F).

Layer-specific activity analysis suggests that the observed abnormalities in the activity of treated broad and narrow-spiking cells are present across cortical layers. The significant differences in spontaneous activity, evoked activity and peak response latency observed at a group cortical level were confirmed only in L V spontaneous activity (Figure 4.6C), however, there are visible tendencies towards these group results across almost all layers (Figures 4.6. and 4.7.). Small cell numbers could be the reason behind these results. Figures 4.6B and 4.7B show the total number of neurons recorded per each layer, suggesting that on average, there were 18 cells recorded per group in a layer, with as little as 3 narrow-spiking treated cells in L VI.

Overproduction of superficial cortical excitatory neurons has also affected the connectivity of narrow-spiking neurons. In treated mice, these neurons formed significantly fewer connections compared to controls (Figure 4.8B-C). But, when looking into layer-specific connectivity, no significant differences were observed between treatment groups (Figure 4.9.). This could, however, be caused by the small sample size.

5. Effect of treatment on auditory detection

5.1. Overview

In the previous chapter, we found changes in auditory evoked responses in the auditory cortex of the treated animals. This finding raised a question - how do changes in auditory evoked responses affect auditory perceptual detection? For this purpose, we trained both treated and control mice to perform an auditory detection task and assessed their speed and accuracy in the task by measuring their success rate, d' and reaction time.

Chapter 5.2. contains the information on age and success of the mice trained and their training progress. Individual and group results from the task are covered in chapter 5.3.

5.2. Training progress

A total of 30 mice (17 treated and 13 controls) were trained for auditory detection task in head-fixed conditions. Out of these 30, 1 treated mouse and 2 controls could not pass the training threshold, most likely due to their eardrums being broken during head cap surgery (changes in hearing acuity after tympanic membrane perforations have been described in several studies (Bordley and Hardy, 1937; Pannu *et al.*, 2011; Littlefield and Brungart, 2020)).

Since C57BL/6J mice tend to lose hearing early with age (Bowl and Dawson, 2015), we have compared the age of our treated and control mice groups in Figure 5.1A, to verify that age-related hearing loss did not affect our results. Age of the animals in the control and treated group was similar at the beginning of the training (73.4 ± 1.0 days for control vs 73.9 ± 1.5 for treated; mean ± SEM; $p = 0.8100$) as well as at the end of the training (106.7 ± 3.7 days for control vs 103.2 ± 2.8 for treated; mean ± SEM; $p = 0.4559$).

Training time for each phase (Figure 5.1B) was also not significantly different between groups (basic lick training 1.9 ± 0.2 days for control vs 1.7 ± 0.2 for treated, mean ± SEM, p = 0.6355; auditory conditioning 8.3 ± 1.3 days for control vs 6.5 ± 0.6 for treated, mean ± SEM, p = 0.1761; auditory detection task 12.7 ± 1.0 days for control vs 12.4 ± 0.7 for treated, mean ± SEM, p = 0.7663). As the task difficulty increased (e.g. from basic lick training to auditory conditioning) both groups took longer time to become proficient. An example of the learning curve from each phase of training is shown in Figures 5.2., 5.3. and 5.4. In basic lick training (Figure 5.2.) the threshold was passed very quickly, on average in 2 training sessions. Auditory conditioning (Figure 5.3.) required longer learning time and parameter adjustments on a daily basis. The final phase, auditory detection (Figure 5.4.), lasted for a minimum of 10 days in order for the animals to become proficient in the task. In the auditory detection task, 30dB sound intensity was not properly presented due to hardware limitations, and was therefore excluded from all further analysis.

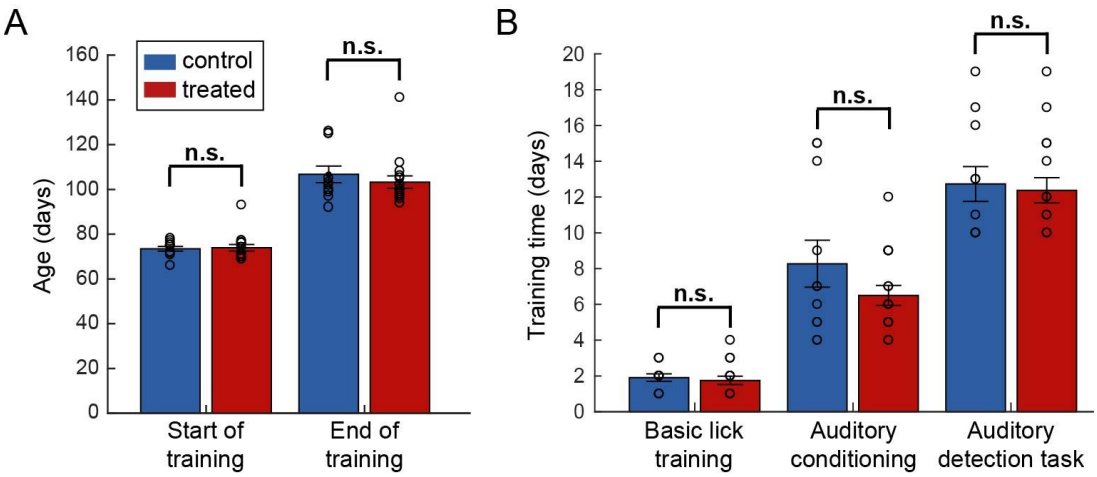

Figure 5.1. Age and traning time of treated and control mice in the behavioural assessment. **A-** Age of treated and control mice at the start and the end of behavioural assessment training. There were no significant differences between groups (start of training p = 0.8100; end of training p = 0.4559). **B-** Comparison of training time the mice needed in order to pass each of the 3 phases in the behavioural assessment. Learning time was not significantly different between groups across assessment phases (basic lick training p = 0.6355; auditory conditioning p = 0.1761; auditory detection task p = 0.7663).

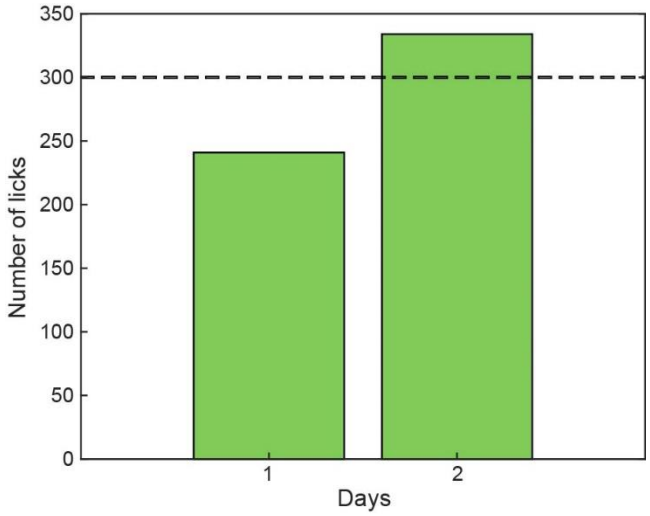

Figure 5.2. Basic lick training. As shown in Figure 5.1B, mice have, on average, learned this task in 2 sessions. In this example, the mouse passed our threshold of 300 licks (labelled as black dashed line) on the second training day.

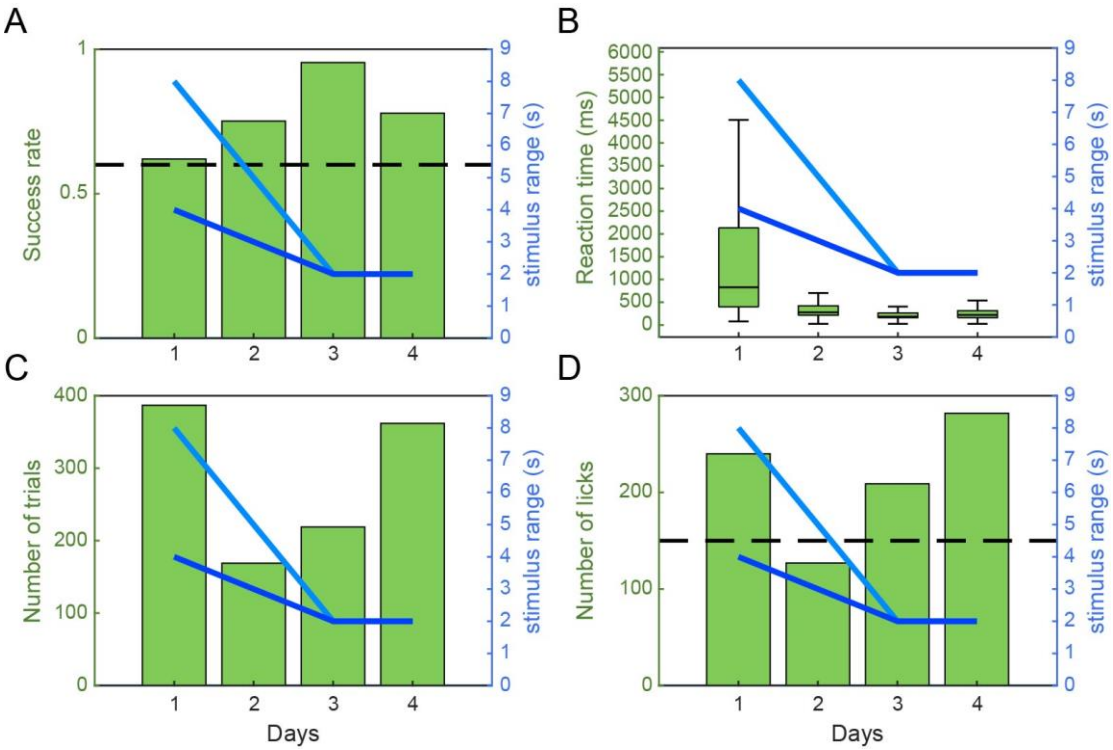

Figure 5.3. Auditory conditioning. In this task, the length of stimulus presentation was reduced as the mouse successfully reacted to the sound, until reaching 2 second time window. Light blue line indicates the starting stimulus duration in every session, while dark blue line indicates the stimulus duration at the end of a session (values are on the right y-axis

on all 4 figures). In one session, trial length would decrease by 1 second after every 50 correct trials (e.g. during the first session in this example, stimulus duration reduced from 8s to 4s, meaning that the mouse engaged in at least 200 trials). For this mouse, the stimulus length in the first session ranged 8 - 4 seconds, decreasing in each session until reaching continuous 2 second window on sessions 3 and 4. Success rate (**A**), reaction time (**B**), number of trials (**C**) and number of licks (**D**) were calculated after every session during the training period, in order to adjust the parameters in time for the next session and encourage learning. This animal had a success rate over 60%, quick reaction times and more than 150 licks in 2 consecutive sessions, therefore passing the thresholds (labelled with black dashed line) after 4 training days.

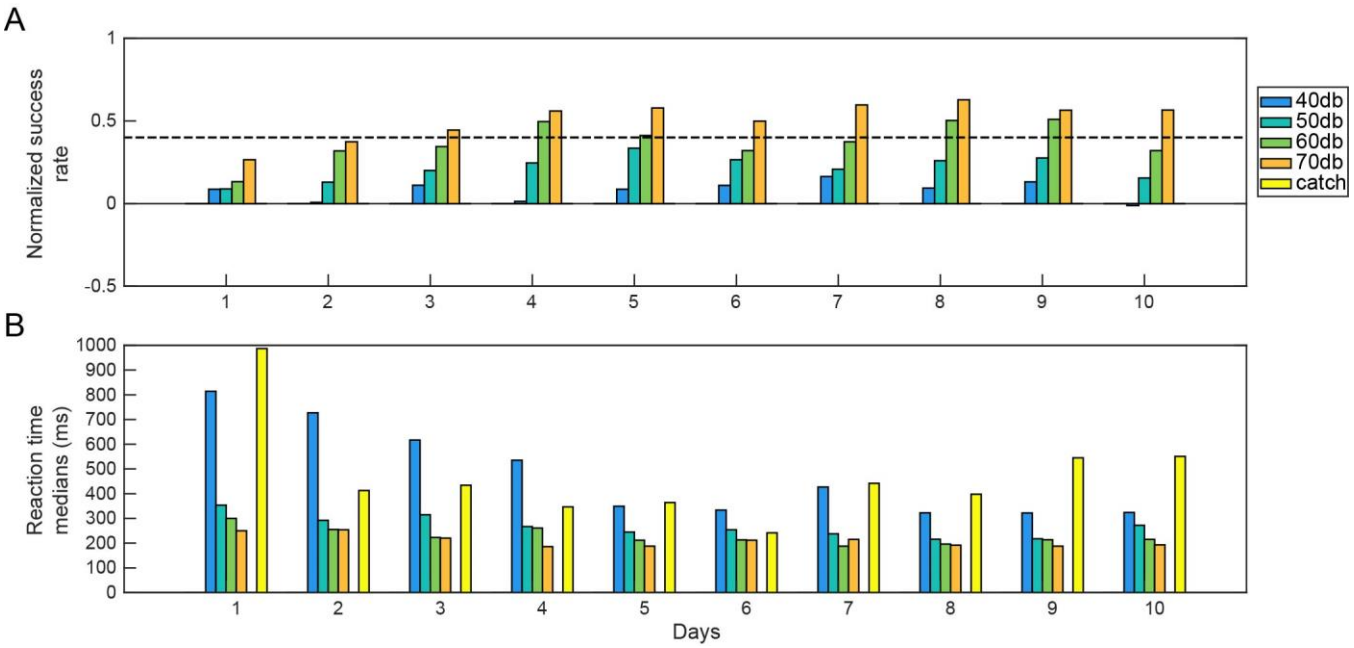

Figure 5.4. Auditory detection. In the final phase of assessment, mice were trained for a minimum of 10 days. Normalized success rate (**A**) and reaction time medians (**B**) were calculated for each session. Here, the difference between catch trial false alarm rate and 70dB hit rate (also labelled as normalized success rate) was higher than 40% in sessions 9 and 10, thus passing the threshold (black dashed line). Results from these 2 consecutive sessions were taken into group analysis.

5.3. Individual and group comparisons of auditory detection task performance

We measured and compared the normalized success rate, discriminability index and reaction time from the last 2 auditory detection task sessions of mice that passed all the thresholds.

Comparing the final sessions from one treated and one control mouse, the results show that both mice had a higher success rate and d' as well as faster response time as the sound intensity increased (Figure 5.5). However, the treated mouse seems to have a lower success rate for lower sound intensities and longer reaction time for 40dB sound intensities compared to the control mouse.

These differences are present in group comparisons as well (Figure 5.6). Two-way ANOVA showed that the treatment had a significant effect on reaction time ($F = 9.48$, $p < 0.01$). More precisely, treated mice had a higher reaction time at 40dB sound intensity level compared to controls (post-hoc Tukey-Kramer multicomparisons test $p < 0.05$; Figure 5.6C). On the other hand, treatment did not have a significant effect on the success rate ($F = 2.67$, $p = 0.1037$; Figure 5.6A) or on d' ($F = 3.73$, $p = 0.0547$; Figure 5.6B).

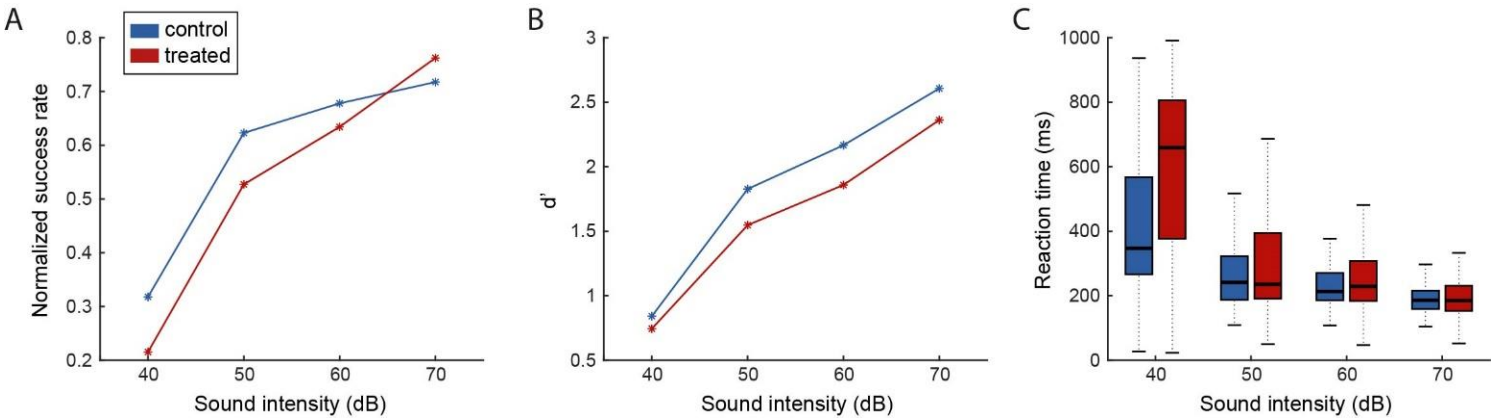

Figure 5.5. Behavioural performance comparison between 1 control and 1 treated mouse in 1 session. Normalized success rate (**A**), detectability index (d') (**B**) and boxplots of reaction time (**C**) across sound intensities are shown depending on the treatment. Both mice exhibit

an increase in success rate and d' with an increase in the sound intensity. Additionally, both mice show a faster response time with an increase in sound intensity.

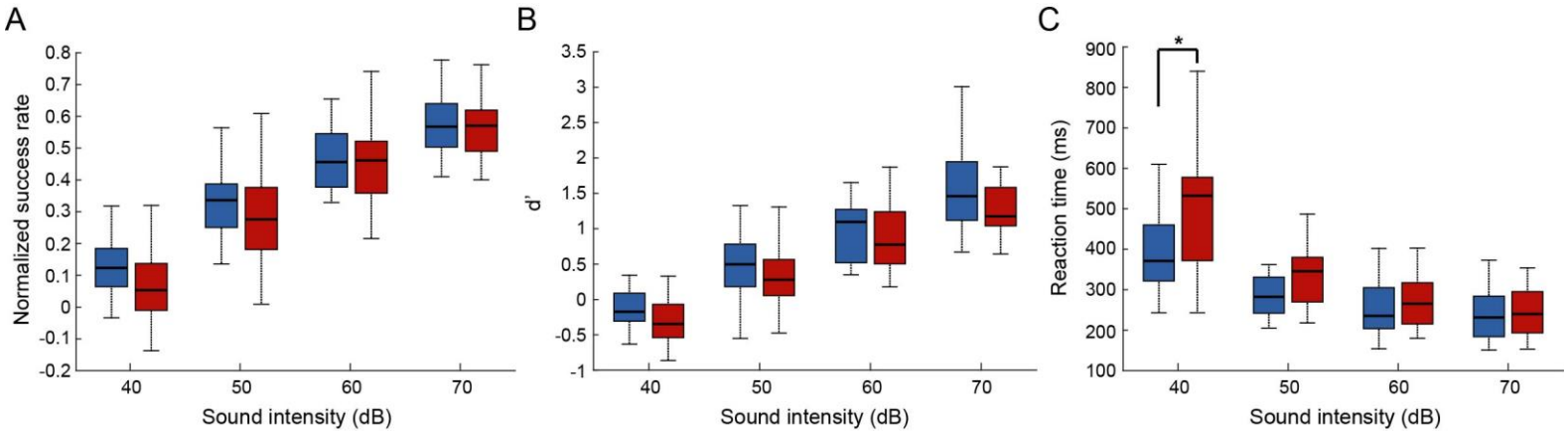

Figure 5.6. Behavioural performance comparison between control and treated mice groups. Boxplots are showing normalized success rate (**A**), detectability index (d') (**B**) and median reaction time per session (**C**) across sound intensities depending on the treatment. The reaction time of treated mice was significantly longer for 40dB sound intensity ($p < 0.05$). Group comparisons were done using two-way ANOVA with post-hoc Tukey-Kramer multicomparisons test.

5.4. Summary

Results presented in this chapter suggest that the overproduction of L II/III excitatory neurons had a significant effect on auditory detection. Treated mice showed hyposensitivity to near-threshold auditory stimuli during behavioural auditory detection assessment. Reaction time of treated mice was significantly longer at 40dB compared to controls (Figure 5.6C), however, the success rate (Figure 5.6A) and d' (Figure 5.6B) were not significantly affected by the treatment.

In control mice, hit rate for 40dB was on average 0.44, while FA rate was lower, at 0.32. Additionally, average reaction time of control mice at 40dB was quicker than for false alarms (405.8ms vs. 427.8ms). Average 40dB hit rate for treated mice was 0.35, while false alarm rate was at 0.28. FA reaction time for treated mice was

442.7ms while reaction time at 40dB was 493ms. Since in both mice groups the hit rate was higher during 40dB trials than during catch trials, meaning that mice engaged more often during 40dB trials, we can assume that their engagement is indeed a response to the stimulus. While control group on average reacts a bit faster to 40dB sounds, treated mice, which also have a lower hit rate difference (0.12 vs 0.07), have a longer reaction time at 40dB compared to FA. This longer reaction time in treated mice on top of the small difference between FA and 40dB hit rate suggests that their licking at 40dB could be random, while control mice seem to hear the 40dB sounds.

Our results were not affected by the age of the trained animals. Mice in control and treated groups were of similar age at the beginning and the end of the training (Figure 5.1A). Additionally, the treatment did not seem to have an effect on task learning. Both groups of mice required a similar amount of time to become proficient in all 3 phases of our assessment (Figure 5.1B), with a very high percentage of mice successfully finishing it (94% of treated and 84% of control mice).

6. Estimation of treatment impact on cortical neuronal activity in task performing mice

6.1. Overview

Results from chapter 5 indicate that the XAV939 treatment has an effect on auditory detection in mice, and we have also seen differences in neuronal activity in treated mice during passive listening conditions in chapter 4. In order to further investigate the neural basis of this behavioural auditory hyposensitivity, we have recorded neuronal activity in the auditory cortex of mice performing the auditory detection task.

Chapter 6.2. will cover the success and performance of mice in the auditory detection task during electrophysiological recordings.

Neuronal activity during behavioural trials with "hit" outcomes is shown and compared between cell and treatment groups in chapter 6.3.

6.2. Behavioural performance results

Out of 3 control and 4 treated mice initially trained for this purpose, 1 mouse from each group had to be dismissed from analysis because of their poor performance in the behavioural task during electrophysiological recording ($P_{hit} - P_{FA}$ for 70dB trials was lower than 40%). From the remaining mice, a total of 8 good recordings were obtained (4 from control and 4 from treated group).

The behavioural performance of the mice is shown in Figure 6.1. The treated group seems to have a lower success rate (Figure 6.1A) and d' (Figure 6.1B) compared to controls across sound intensities. Their reaction time (Figure 6.1C) also seems more variable at 30dB, higher at 40dB and then lower at 50-70dB compared to controls. When comparing the groups using two-way ANOVA with post-hoc Tukey-Kramer multicomparisons test, the differences in success rate and reaction time were not

significant (success rate: F = 2.91, p = 0.0981; reaction time: F = 0.86, p = 0.3619) but the effect of treatment was significant in d' (F = 12.38, p < 0.01). Multicomparisons test, however, did not reveal a significant difference for a specific sound intensity in d'. Repeated measures ANOVA also resulted in a non-significant treatment effect on reaction time (F = 0.48, p = 0.7499), success rate (F = 0.49, p = 0.7411) and d' (F = 0.66, p = 0.6282).

The lack of significant difference for reaction time and specific sound intensity for d' might be due to a low number of sessions compared, considering that we are comparing only 4 recorded sessions per group.

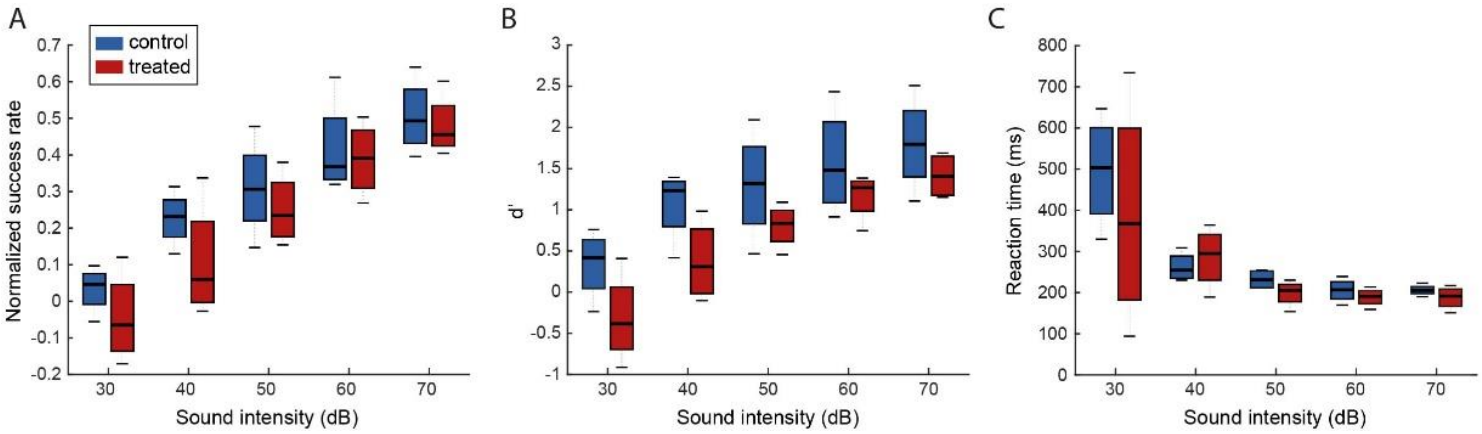

Figure 6.1. Comparison of behavioural performance during electrophysiological recordings between control and treated mice groups. Boxplots are showing normalized success rate (**A**), detectability index (d') (**B**) and median reaction time per session (**C**) across sound intensities depending on the treatment. Treated mice tend to have a lower success rate and d' across sound intensities, with treatment having a significant effect on d' (p<0.01), however, none of the differences for sound intensities were significant. The reaction time of treated mice seems to be longer for 40dB and shorter for 50-70dB intensities, but not significantly. Group comparisons were done using two-way ANOVA with post-hoc Tukey-Kramer multicomparisons test.

6.3. Neuronal activity in "hit" trials

Since we were mostly interested in the neural basis of the reaction time differences, here we have looked into the neuronal activity in trials with "hit" outcomes. In the 8 electrophysiological recordings (4 control, 4 treated) acquired during good behavioural sessions ($P_{hit} - P_{FA}$ for 70dB trials >40%), we have examined well isolated (isolation distance ≥ 20) cortical units, labelled as single or multi units during spike sorting. Additionally, the activity of observed cells had to be >0.1Hz during the 50ms time window before sound onset (method explained in details in chapter 2.7.3.). We have obtained 50 neurons from control mice (n broad-spiking = 42, n narrow-spiking = 8) and 42 neurons from treated mice (n broad-spiking = 31, n narrow-spiking = 11) (Figure 6.5A).

Colourmaps are comparing the activity of broad-spiking (Figure 6.2.) and narrow-spiking cells (Figure 6.3.) in treated and control mice across sound intensities. As seen in passive listening conditions, cell activity during task engagement increases with sound intensity. Additionally, cell activity also becomes less variable with the increase in sound intensity.

The difference between treated and control groups seems to be present at 40 and 50dB for broad-spiking cells; controls show a clear evoked response across multiple broad-spiking cells for both sound intensities, while treated group shows an evoked response in only a few cells. In comparison, at 70dB both groups demonstrate clear evoked responses across nearly all broad-spiking cells.

PSTH of cell activities (Figure 6.4.) also indicates that there are differences between cell groups and treatment groups. As expected, narrow-spiking neurons show a higher spike rate compared to broad-spiking neurons in treated and control groups. However, broad-spiking neurons in the treated group exhibit a much lower spike rate during 40dB sound intensity and slightly lower at 50dB, compared to controls.

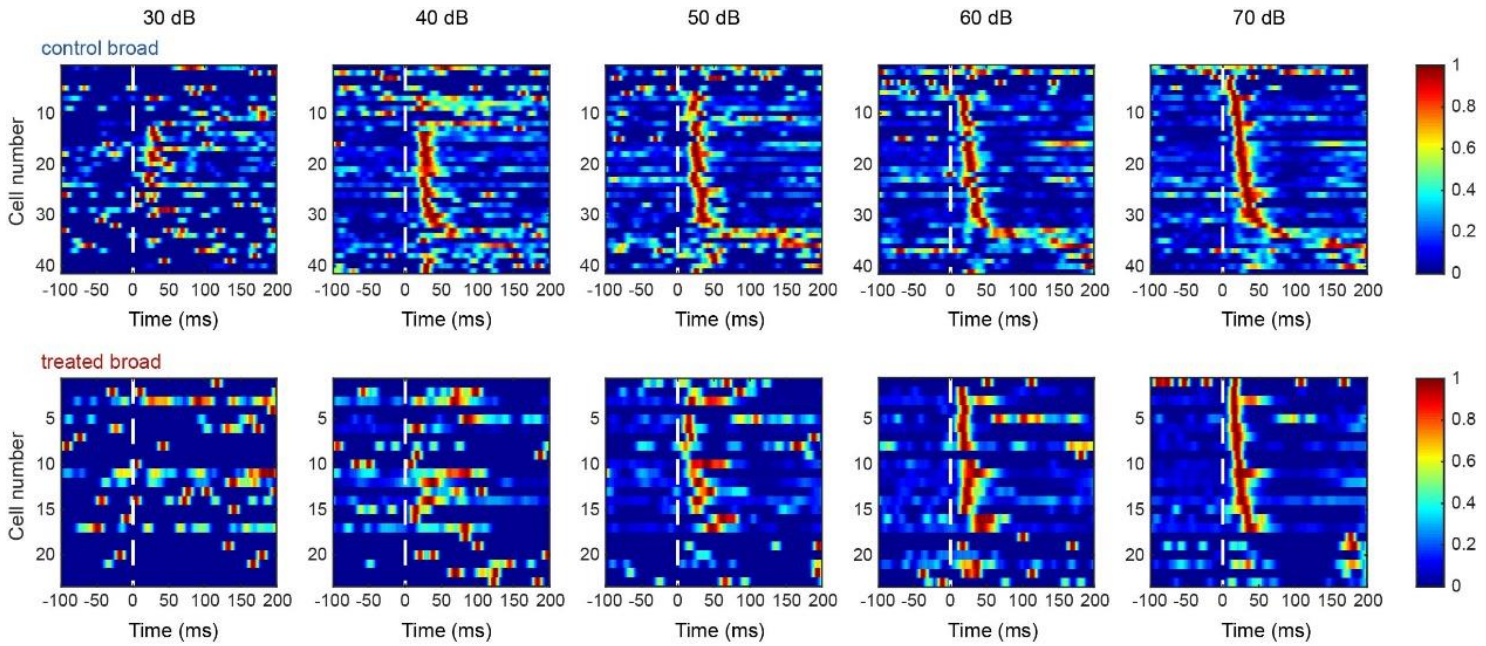

Figure 6.2. Colourmaps of broad-spiking cell activity during trials with "hit" outcomes in behavioural assessment across sound intensities (30-70dB). The activity of each cell was filtered using 5ms Gaussian kernel and then normalized by its maximum activity. Evoked response was considered as non-normalized activity higher than 2.8 standard deviations from baseline mean (taken from 100ms before the sound onset across trials). The activity of control cells (top row) and treated cells (bottom row) increases and becomes less variable with sound intensity. There seems to be a difference in activity between control and treated cells at 40-50dB. The white dashed line marks the sound onset (offset occurred after animals reacted to the sound, or after 1sec).

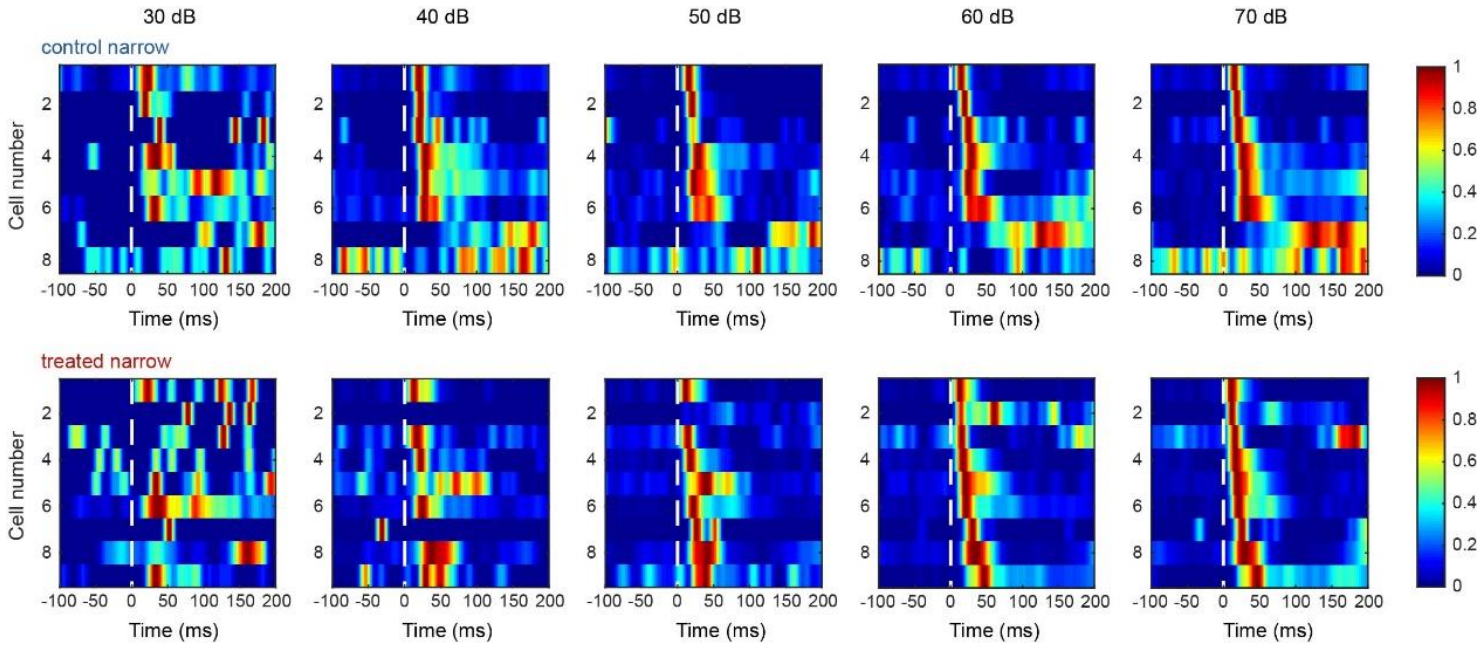

Figure 6.3. Colourmaps of narrow-spiking cell activity during trials with "hit" outcomes in behavioural assessment across sound intensities (30-70dB). The activity was calculated in the same manner as in Figure 6.2. As seen in broad-spiking cells, the activity of control (top row) and treated cells (bottom row) increases and becomes less variable with sound intensity. The white dashed line marks the sound onset.

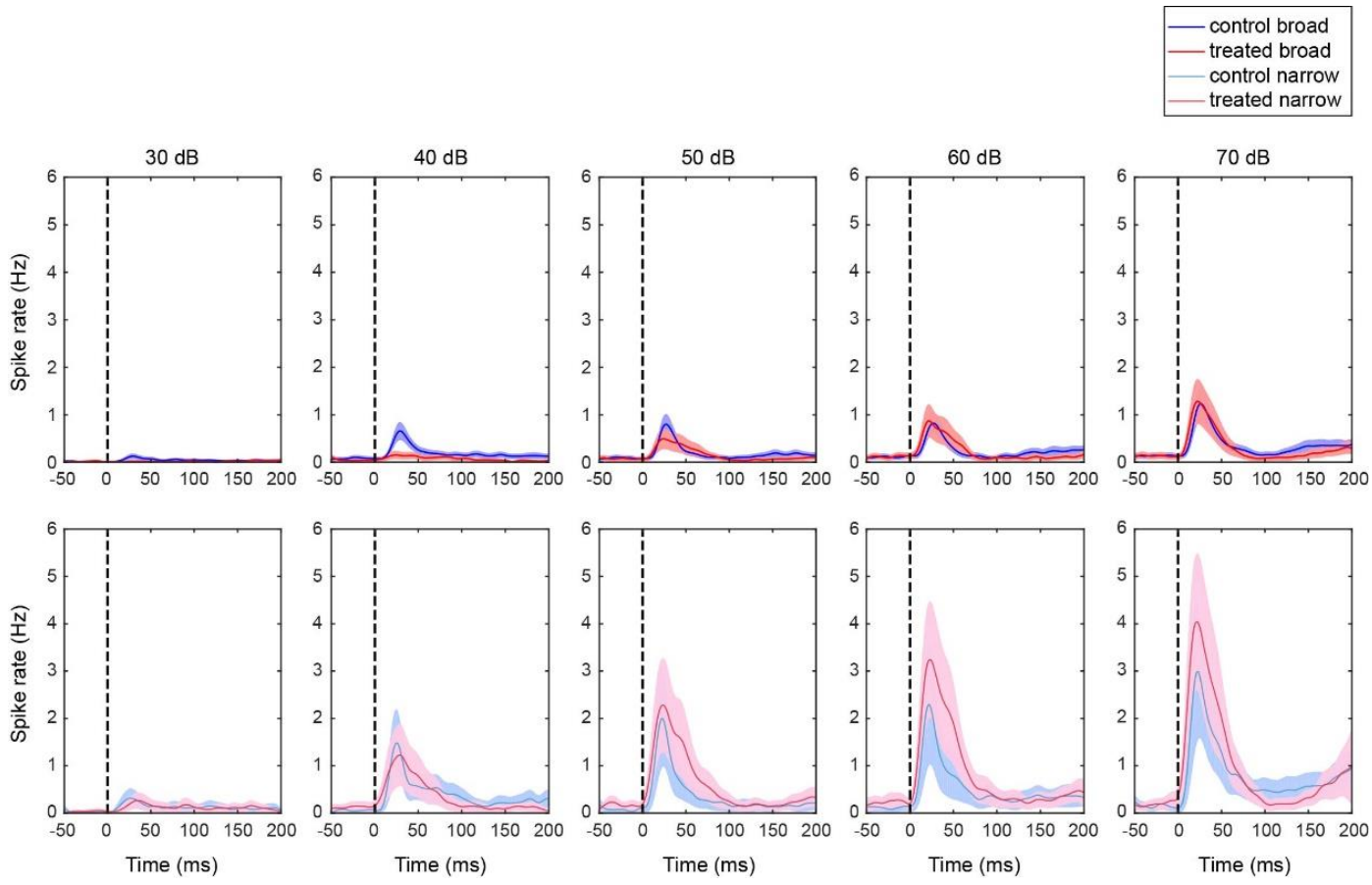

Figure 6.4. Peristimulus time histogram (PSTH) of cell activity (mean ± SEM) during trials with "hit" outcomes in behavioural assessment across sound intensities (30-70dB). Sound onset is labelled as a black dashed line. Top row: broad-spiking neurons, bottow row: narrow-spiking neurons. Broad-spiking cells of treated mice seem to have a lower spike rate at 40dB and 50dB compared to broad-spiking neurons in controls.

Quantification of cell activity further confirmed the observed differences. Treated mice had a significantly lower activity of broad-spiking neurons (Figure 6.5C) during 40dB ($p < 0.01$) and 50dB sound trials ($p < 0.05$), compared to controls. The activity of narrow-spiking neurons during "hit" trials did not seem to be affected by the treatment (Figure 6.5D).

Latency to peak evoked activity was not significantly different between control and treated mice in either of the cell groups (Figure 6.5E and F), however, there seem to be some tendencies of longer latency in treated groups during low sound intensities. These could potentially be false-negative results, caused by the low number of cells. More specifically, since we are comparing only the latency of cells that showed evoked activity for specific sound intensity, in some cases we did not even have 1 cell (e.g. treated broad-spiking group at 30dB had zero evoked responses, therefore it is missing from Figure 6.5E).

We have also assessed the baseline, spontaneous activity of cells occurring during 400ms before the trial onset. The activity was assessed across the recording, regardless of the trial outcome. Baseline activity of broad-spiking cells was significantly lower in treated compared to control mice ($p < 0.05$; Figure 6.5B). On the other hand, narrow-spiking cells did not show a significant difference in baseline activity depending on the treatment. These results are different from what we observed in passive listening mice (Figure 4.5B). This discrepancy will be addressed in the discussion chapter 8.2.

Altogether, these results indicate that the XAV939 treatment resulted in significant changes of neuronal activity in the auditory cortex during auditory detection. Spontaneous activity of broad-spiking neurons was significantly lower in treated

mice. Broad-spiking neurons also demonstrated a significantly lower auditory evoked activity for sounds of 40 and 50dB intensity.

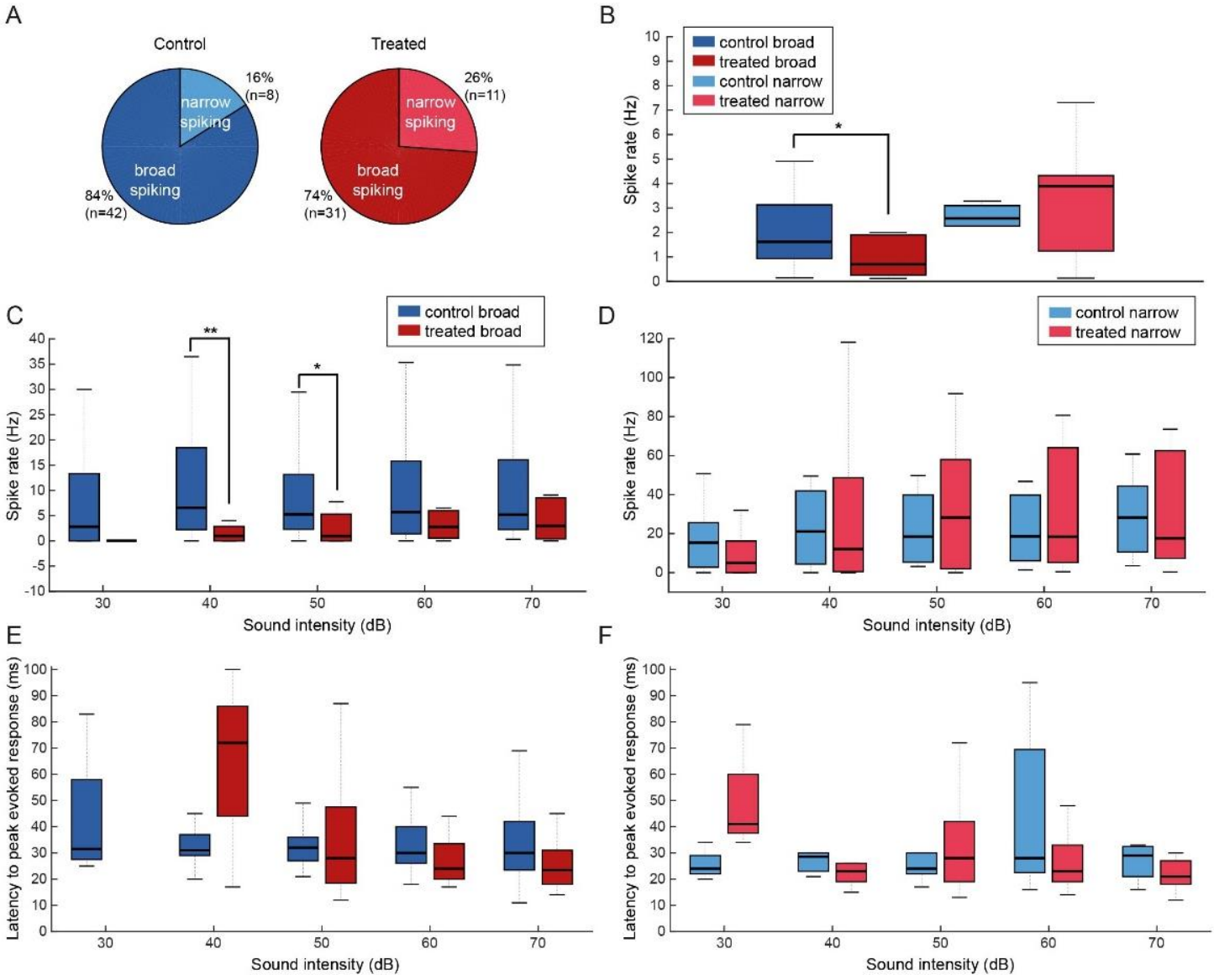

Figure 6.5. Quantification of broad and narrow-spiking cell activity during trials with "hit" outcomes in task engaging animals. **A-** Percentage of cells recorded in control and treated mice. **B-** Spontaneous activity of neurons recorded during interstimulus intertrials (400ms time window before the trial onset). In treated animals, broad-spiking neurons had significantly lower baseline activity compared to controls. **C-** During behavioural trials with "hit" outcomes, treated mice showed a lower activity of broad-spiking neurons compared to controls, significant for 40 and 50dB. This difference was not present in narrow-spiking neurons (**D**). Latency to peak evoked response tends to be longer for broad-spiking (**E**) and

narrow-spiking (**F**) neurons in treated mice during lower sound intensities (30dB in narrow-spiking and 40dB in broad-spiking neurons), however, none of the differences across sound intensities were significant.

6.4. Summary

Overproduction of superficial cortical excitatory neurons had a significant effect on the activity of broad-spiking neurons during auditory detection. Broad-spiking neurons demonstrated a significantly lower baseline activity (Figure 6.5B) as well as a lower activity during 40dB and 50dB trials with “hit“ outcomes (Figure 6.5C).

Unlike passive listening conditions, latency to peak evoked response during task engagement was not significantly different between treatment groups (Figure 6.5E-F). This could, however, be a result of a low cell number. We got a total of 50 neurons from control and 42 neurons from treated mice (Figure 6.5A), out of which only cells showing evoked response were compared in peak response latency analysis.

Behaviourally, treatment had a significant effect on d' in these recording sessions, but there were no significant differences for specific sound intensities (Figure 6.1B). Small sample size (4 vs 4) could be the reason why we have not observed any treatment-dependent specific differences in d' or in reaction time of these mice.

7. Medial geniculate body activity in XAV939 treated mice

7.1. Overview

As reviewed in chapter 1.3.3., the auditory cortex has a lot of input and output connections. To make sure that the observed auditory abnormalities in treated mice are caused by the overproduction of auditory cortical excitatory neurons and not inherited from upstream changes in the auditory pathway, we have also looked into MGB activity in passive listening and task engaging mice.

Results from these experiments as well as details about recordings are presented in chapter 7.2.

7.2. MGB activity in passive listening and task engaging mice

We got a total of 8 MGB recordings (2 from control and 6 from treated mice) during passive listening conditions and 7 MGB recordings (4 from control and 3 from treated mice) during the behavioural assessment, all with Neuropixels probe. Inclusion criteria for neurons was the same as in cortical analysis: for passive listening recordings, cells from MGB channels had to be well isolated (isolation distance ≥ 20) single units, with a spontaneous spike rate >0.1 Hz. For spontaneous activity analysis, cells activity had to be >0.1Hz during the long silent period , while for auditory evoked analysis, cell activity had to be >0.1Hz during the 50ms time window before broadband noise onset, across trials. For task-engaging recordings, cells from MGB channels had to be well isolated single or multi units, with a spike rate >0.1 Hz during the 50ms time window before sound onset, across all trials.

We obtained 94 neurons from the passive listening recordings (n control = 13, n treated = 81) and 106 neurons from task-engaging recordings (n control = 41, n treated = 65).

Colourmaps comparing MGB cell activity between treated and control mice during passive listening conditions and task engagement are shown in Figure 7.1. and 7.2.,

respectively. Although a lot less MGB cells were recorded in the control group during passive listening conditions, the auditory response is visible in both groups across sound intensities shown. There are also no apparent differences between groups for any sound intensity.

During the behavioural assessment, a similar number of MGB cells was recorded in the treated and control group. Both groups also exhibit a clear auditory evoked response and an increase in activity with sound intensity. Still, in this case, there are also no visible differences between groups for any sound intensity.

PSTHs of MGB cell activities indicate that there might be some differences between control and treated groups. During passive listening conditions, activity of treated and control MGB neurons seems similar (Figure 7.3A). On the other hand, during task engagement activity levels seem similar between groups, but the peak evoked latency seems shorter in the treated group for 60 and 70dB (Figure 7.3B). Additionally, there seems to be a prolonged stimulus-evoked activity of control neurons. Since PSTH shows a mean and SEM of grouped cell activity, this could be a result of a few cells with strong sustained activity, visible in Figure 7.2 (e.g. cells 19 and 20), skewing the activity mean and SEM of control group upwards.

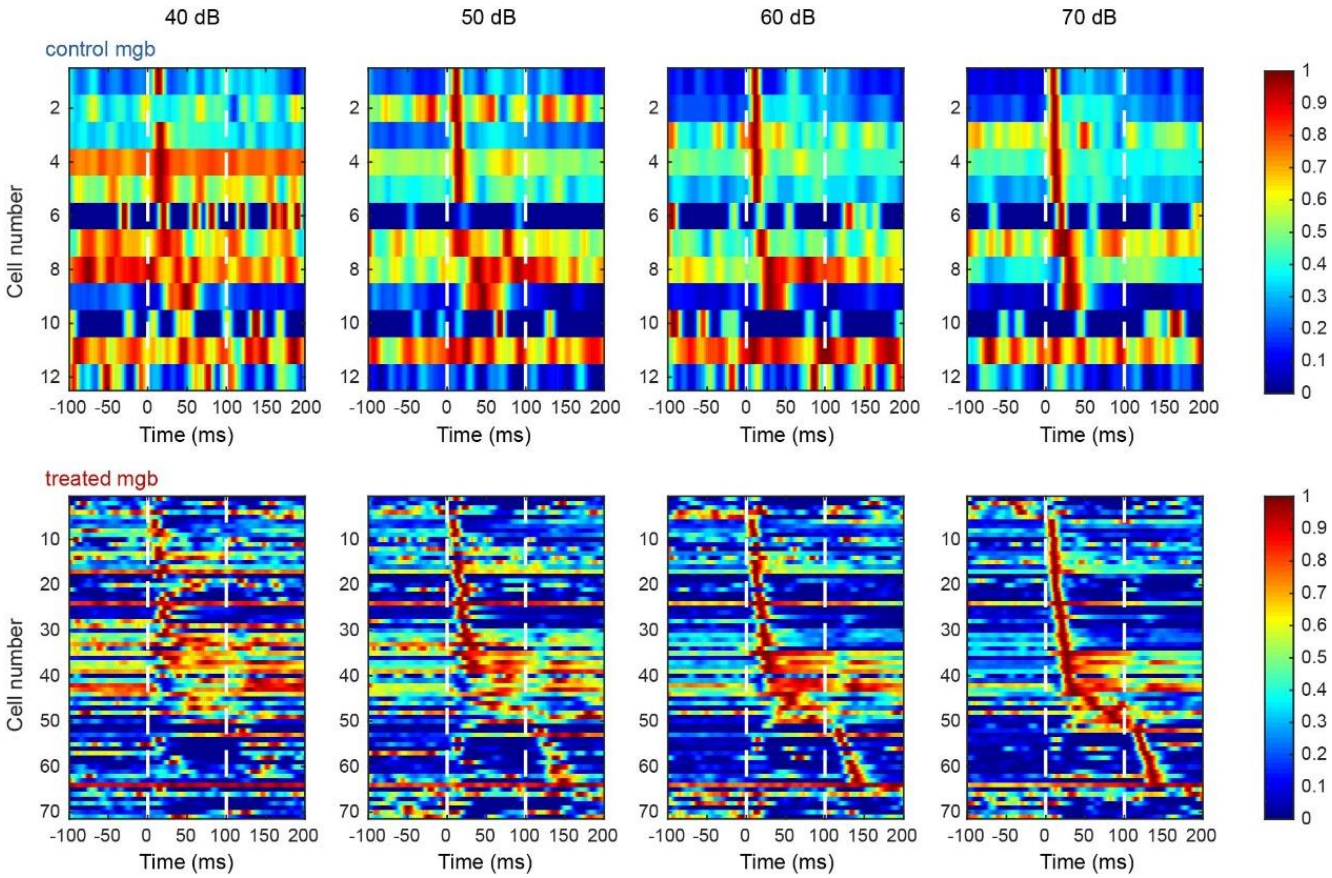

Figure 7.1. Colourmaps of cell activity in MGB across sound intensities during passive listening conditions (here shown 40-70dB). The activity of each cell was filtered using 5ms Gaussian kernel and then normalized by its maximum activity. Evoked response was considered as non-normalized activity higher than 2.8 standard deviations from baseline mean (taken from 100ms before the sound onset across trials). The activity of control cells (top row) and treated cells (bottom row) increases with sound intensity. White dashed lines mark the sound onset and offset (duration 100ms).

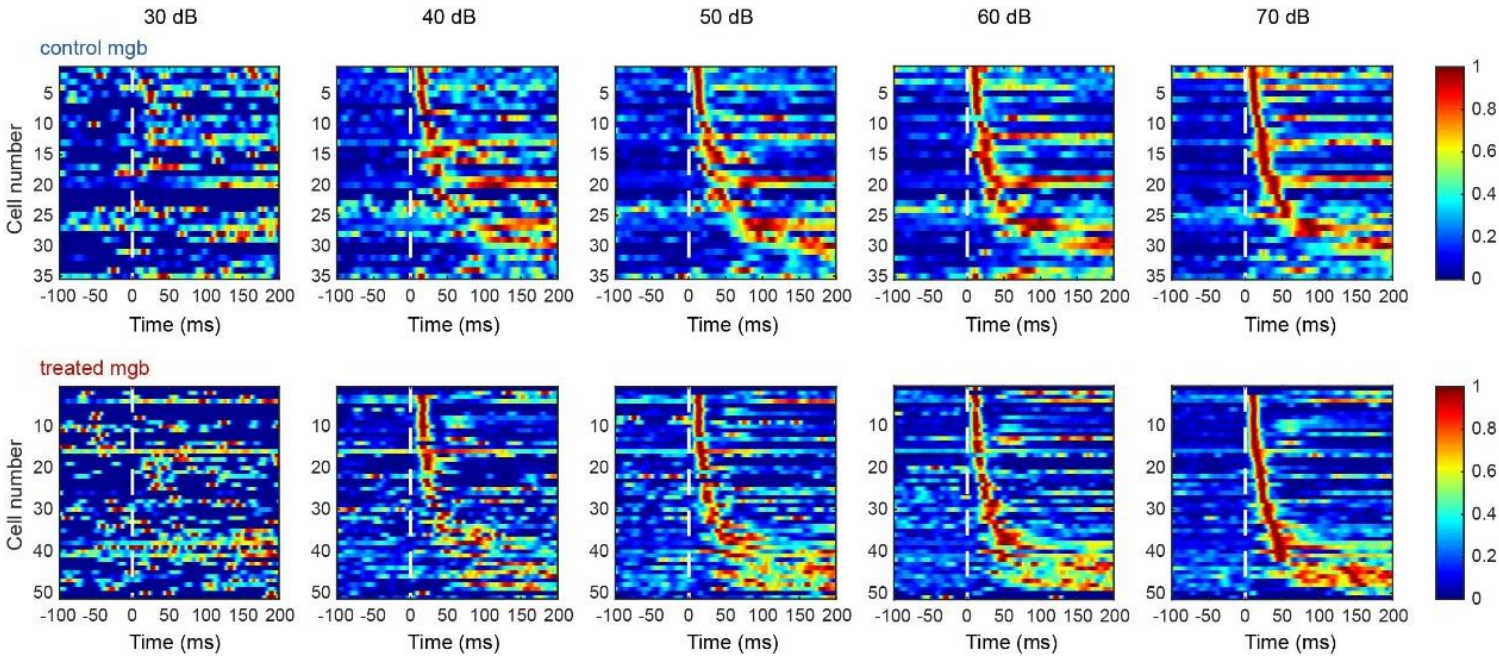

Figure 7.2. Colourmaps of cell activity in MGB during “hit“ outcomes in task-engaging mice across sound intensities (30-70dB). The activity was calculated in the same manner as in Figure 7.1. The activity of control (top row) and treated cells (bottom row) increases with sound intensity. The white dashed line marks the sound onset (offset occurred after animals reacted to the sound).

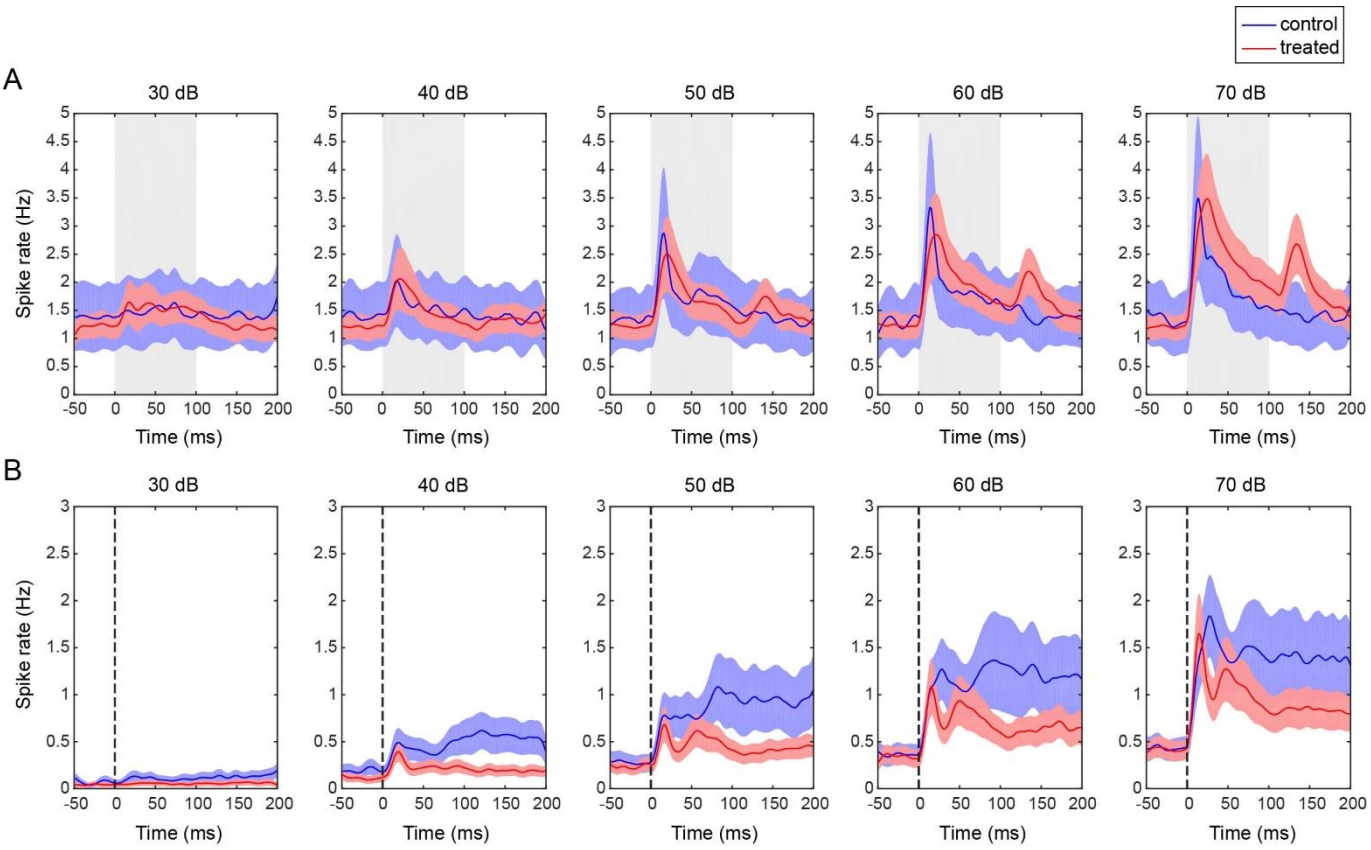

Figure 7.3. Peristimulus time histogram (PSTH) of MGB cell activity (mean ± SEM) during passive listening conditions (**A**) and in behavioural trials with "hit" outcomes (**B**) across sound intensities (here shown 30-70dB). Sound duration in passive listening conditions is labelled as a gray background, while sound onset in behavioural assessment is labelled as a black dashed line.

Further quantification of the activity of these cells indicates that there are no significant differences in MGB activity between treated and control group. Spontaneous activity of treated and control MGB cells was not significantly different during passive listening conditions (Figure 7.4A) nor the behavioural assessment (Figure 7.4B). Activity across sound intensities was also not significantly different between the groups during passive listening conditions (Figure 7.4C) nor behavioural trials with "hit" outcomes (Figure 7.4D). Finally, peak evoked latency across sound intensities was not significantly different between groups during passive listening conditions (Figure 7.4E) or during behavioural trials with "hit" outcomes (Figure 7.4F).

Taken together, these results indicate that there were no significant differences in MGB activity between control and XAV939-treated mice.

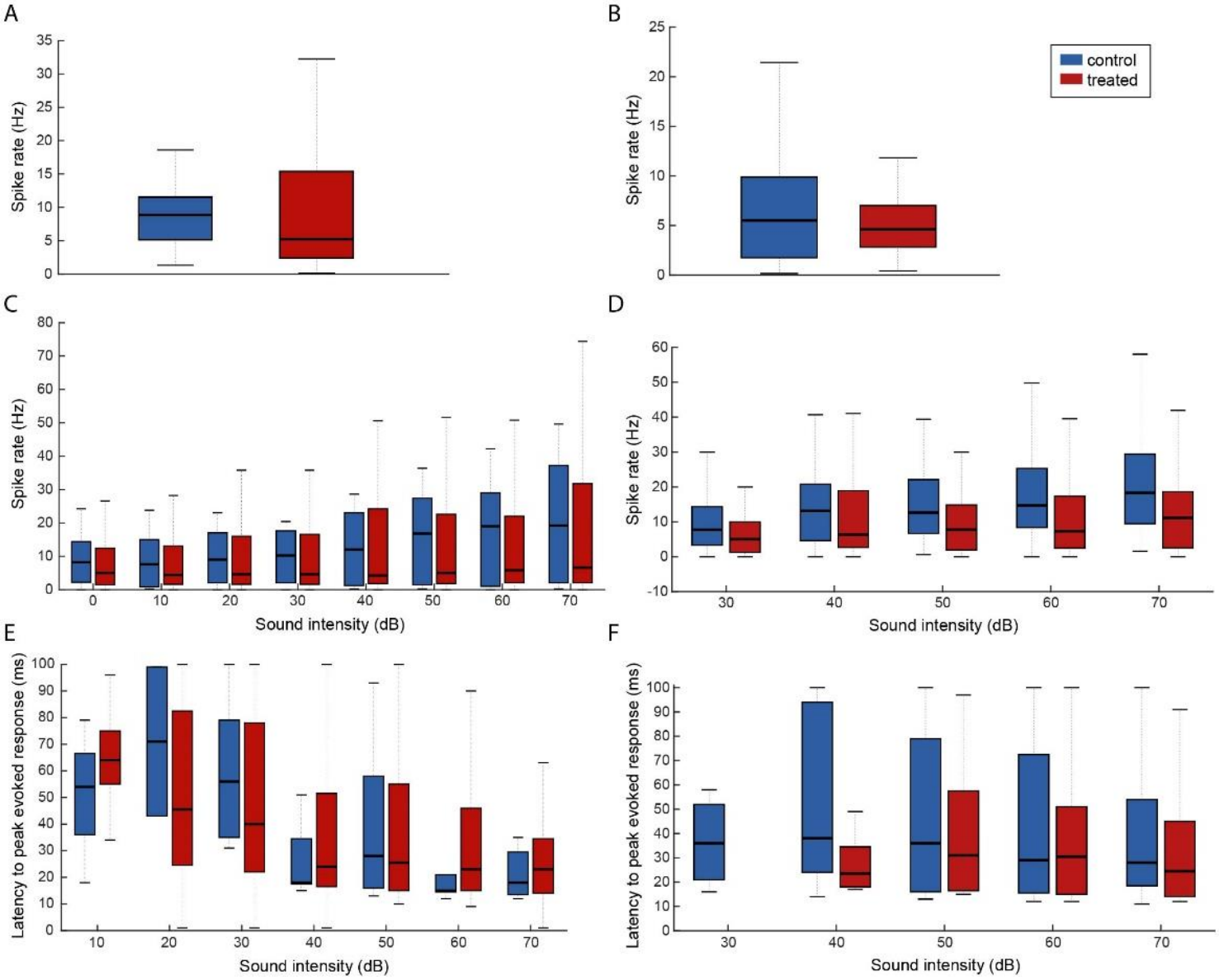

Figure 7.4. Quantification of cell activity in MGB. **A-** Spontaneous activity of neurons recorded during 30min silent period in passive listening conditions. Difference between groups was not significant. **B-** Spontaneous activity of neurons recorded during interstimulus intertrials in task behaving animals. Difference between groups was not significant. There were also no significant differences in neuronal activity between mice groups across sound intensities in passive listening conditions (**C**) or during behavioural trials with "hit" outcomes (**D**). Finally,

latency to peak evoked response was not significantly different between mice groups across sound intensities in passive listening conditions (**E**) or during behavioural trials with “hit“ outcomes (**F**).

7.3. Summary

Albeit it looks like some small differences between groups might be present, neuronal activity in MGB during passive listening conditions and task engagement was not significantly different between control and XAV939-treated mice.

These results are further suggesting that the auditory abnormalities in treated mice observed through auditory cortical activity and behavioural auditory detection were not inherited from upstream changes in the auditory pathway, but caused by the overproduction of excitatory neurons in the cortex.

8. Discussion

8.1. Summary of the results

The overall aim of this project was to investigate the relationship between abnormal expansion of the cerebral cortex and atypical sensory perception. We hypothesized that an overproduction of L II/III excitatory neurons during corticogenesis can lead to atypical cortical activity, ultimately causing abnormalities in sensory processing.

To test this hypothesis, we utilized the XAV939 mouse model, in which the number of L II/III excitatory neurons was increased pharmacologically through *in utero* microinjections of XAV939, a known inhibitor of axin degradation. Further, we have evaluated the auditory perception of this mouse model through a behavioural assessment. Finally, we have also examined neuronal population activity in the auditory cortex and medial geniculate body of these mice during passive listening conditions as well as task engagement.

Main results from the neurophysiological and behavioural assessments in this project can be found summarized in Table 3.1. Firstly, we have confirmed histologically that XAV939 injections at E14 caused a significant increase in the width of superficial cortical layers in mice, which was present in young (P2) and adult (P21) mice.

This cortical expansion significantly affected neuronal activity in the auditory cortex of passive listening mice. Treated mice showed lower spontaneous activity of narrow-spiking neurons, as well as lower evoked activity of broad-spiking neurons during 50dB and 60dB sounds. Furthermore, their broad-spiking cells exhibited longer latency to peak evoked response for 50-70dB sounds while narrow-spiking cells had longer latency for 40-70dB sounds.

Monosynaptic connectivity was also affected by the treatment. Narrow-spiking neurons in treated mice formed significantly fewer connections with both broad-spiking and narrow-spiking neurons compared to controls.

Cortical expansion had a significant effect on auditory perception as well. In the auditory detection task, treated mice displayed a significantly longer reaction time for 40dB sounds, compared to control mice.

Additionally, during the task engagement, broad-spiking neurons in treated mice exhibited a lower spontaneous activity along with lower activity during 40dB and 50dB trials with “hit“ outcomes.

Finally, we did not find any significant alterations in the MGB caused by the treatment.

Table 8.1. Summary of the results. For each sound intensity (columns) significant differences observed in treated mice are colour-coded as either low (blue) or high (red) in comparison to controls. Differences non-related to sound presentation are listed at the bottom of the table.

low	high	Sound intensity (dB)				
		30	40	50	60	70
behavioural performance	success rate					
	d'					
	reaction time					
cortical activity during passive listening	broad spiking activity					
	narrow spiking activity					
	broad spiking latency					
	narrow spiking latency					
cortical activity	broad spiking activity					

during task engagement	narrow spiking activity					
	broad spiking latency					
	narrow spiking latency					
medial geniculate body	passive listening activity					
	passive listening latency					
	task engaging activity					
	task engaging latency					

spontaneous activity	broad spiking activity	
	narrow spiking activity	
baseline activity during task engagement	broad spiking activity	
	narrow spiking activity	
connectivity	broad to broad	
	broad to narrow	
	narrow to broad	
	narrow to narrow	

8.2. Interpretation of the results

Our results persistently indicate that adult XAV939 treated mice have a lower evoked activity of broad-spiking neurons in the auditory cortex. This is consistent with previous reports on cortical activity in brain slices of adult XAV939 mice (Fang *et al.*, 2014), showing that excitatory neurons have a lower evoked activity.

This lower activity could be a consequence of certain compensatory mechanisms shifting the E-I balance towards inhibition, since young XAV939 mice exhibit higher spontaneous and evoked activity of excitatory neurons (Fang *et al.*, 2014).

Some other ASD models also report this age-related shift in activity, such as *in utero* valproic acid (VPA) rats. These animals demonstrate a decreased excitability of pyramidal neurons at a young age (Rinaldi *et al.*, 2007, 2008), but the abnormalities are diminished in adults (Walcott *et al.*, 2011).

Spontaneous activity between passive listening and task engaging treated mice is very different in our study. In the passive listening conditions, the activity of narrow-spiking neurons in treated mice is significantly lower compared to controls, while in task engaging mice the activity of broad-spiking neurons is affected. These changes could potentially be explained by the difference in the observed time window of activity (one period of 30 minutes vs. ~300 periods of 400ms) or by differences in brain states of the mice. In the passive listening conditions, a lot of the mice might fall asleep during the silent period, while during task performance mice were alert and focused. Since pupil dilation reflects changes in brain states (Reimer *et al.*, 2014), examining potential differences through pupillometry might elucidate the origin of these neuronal activity inconsistencies.

Observed changes in activity could be a consequence of perturbations in neuronal connectivity. In young XAV939 mice, a higher number of excitatory synapses was reported, while in contrast, adult mice had more inhibitory connections (Fang *et al.*, 2014). Our results suggest that adult XAV939 mice have less inhibitory connections, compared to controls. This discrepancy could be due to the method used in our study for assessing the connection probability, which relies on the activity of neurons for connectivity evaluation. The limitations of this method are addressed further in chapter 8.3.

Finally, we have found that broad and narrow-spiking neurons in XAV939 mice have a significantly longer latency to peak evoked response. Previous studies in ASD

patients and ASD mouse models have also reported delayed auditory evoked responses (Oram Cardy *et al.*, 2008; Gandal *et al.*, 2010; Roberts *et al.*, 2010, 2011; Edgar *et al.*, 2015). It has been hypothesized that these delays in cell responses to sounds could cause speech processing difficulties. In our study, these delays could be the cause of slower reaction time of XAV939 mice to 40dB sounds, observed during auditory detection task.

Genetic alterations in LII/III excitatory neurons were recently found in ASD patients (Velmeshev *et al.*, 2019). These alterations were correlated with ASD severity, implying the involvement of upper-layer neurons in behavioural and perceptual abnormalities in ASD. Our mouse model with perturbations in LII/III excitatory neuron development shows perceptual abnormalities, thus supporting these findings.

In conclusion, XAV939-induced overproduction of L II/III excitatory neurons during embryonic development leads to hypoactivity of excitatory neurons and delayed auditory evoked responses in adulthood, resulting in slower behavioural reaction to near-threshold auditory stimuli.

8.3. Limitations in the project

There were several limiting factors in this project, with time being the most constricting one. Since we were working with neurodevelopmental changes, the timeline of experiments had to be carefully planned. For instance, it took on average around 16 weeks from setting up breeding pairs for embryo injections to obtaining electrophysiological recordings from matured mice. Since this was a 3-year project, the number of mice litters we could get through this timeline was very limited.

Further, we lost a certain number of mice during this timeline. A percentage of embryos typically dies *in utero* and gets reabsorbed, and females often eat the pups in the early postnatal days. Thus, if we would inject around 10 embryos, it would very often leave us with 3-5 live mice on P2. Additionally, some of the mature mice had

behavioural and potential hearing problems, while others had head cap issues, so they had to be removed from the project.

The number of recordings and well-isolated neurons we have acquired was relatively low. In a lot of cases, especially for layer-specific analysis, we were lacking the numbers for comparisons. Increasing the numbers of mice would have improved the quality of the analysis.

There were some limitations in the types of analysis as well. For example, monosynaptic connectivity was calculated through the activity of neurons during passive listening conditions. Yet, we have shown that narrow-spiking neurons have a significantly lower spontaneous activity as well as longer latency to peak auditory-evoked responses in treated mice. The smaller number of spikes can lead to the lower statistical power to detect putative monosynaptic connections. The temporal slowing of auditory-evoked responses might also link to more false negatives although the exact quantitative relationship has to be assessed by taking a computational approach in the future. Therefore, it is possible that the altered activity of narrow-spiking neurons is the reason why our results indicate that there are lower connection probabilities in these neurons. Although taking different window sizes could be an option, longer time window could lead to the ambiguity in truly monosynaptic connections, resulting in more false positives instead. Thus, the current approach can be considered as a conservative one.

Analysis of the medial geniculate nucleus implies that the treatment did not have a significant effect on this brain region. However, the lack of significant differences found between mice groups does not indisputably mean that MGB activity was not changed. Our results could have been affected by the small sample size (especially in the passive listening conditions) or by the way we have defined the MGB channels in our recordings. In the passive listening group, we have only 2 recordings from 1 control mouse for assessment of treatment effect on MGB.

Additionally, ventral, medial and dorsal MGB are very different in terms of latency to evoked activity. Getting different ratios of cells from these 3 MGB parts in control and treated groups could potentially mask the treatment-related differences in latency. Unfortunately, with the current recording technique, it is not possible to confidently split the MGB.

Another caveat of this project is the animal model. Our mice had an increased amount of excitatory neurons in layer II/III of the whole cortex. If we expanded neuronal numbers only in the auditory cortex, the interpretation of our results, especially behavioural, would be more straightforward. Since other cortical areas most likely also contribute to detection task performance (such as associative areas, prefrontal and motor cortex), making a clear connection between auditory cortical activity and behavioural outcome is more challenging.

Our electrophysiological recordings are constricted to auditory cortex and MGB. If we were able to record neuronal activity across the whole cortex, especially in behaving animals, we would have been able to examine the signal flow and engagement of different cortical areas in treated mice. We would also be able to investigate if the functional connectivity between brain areas in these treated mice has been affected with the abnormal cortical expansion.

Finally, since we are injecting our drug in the lateral ventricle, it is possible that some of it could get to upstream auditory regions through CSF, causing an acceleration of age-related hearing loss. An accelerated hearing loss could result in the hearing deficits that we observed in the treated mice. This potential issue could be evaluated by testing and comparing auditory brainstem responses in treated and control mice, where a significant difference would suggest that the treatment affected the early auditory pathway.

8.4. Future work

There are several potential smaller and larger bodies of work that could be done building on this project.

First, we have noticed that the latency to peak evoked response of broad-spiking neurons in task engaging mice looks very similar to their behavioural reaction time. Thus, it might be worth investigating the correlation coefficients between behavioural reaction time and latency of broad-spiking neurons, as well as between the activity of broad-spiking neurons and behavioural success rate. This could potentially be the basis of behavioural abnormalities we have observed in the treated mice.

Second, we have recorded neuronal activity throughout the auditory detection task performance but analysed only the trials with “hit“ outcomes. Comparison of neuronal activity in “miss“ and “hit“ trials could be done, in order to investigate why animals occasionally fail to react, even during loud sounds. Additionally, examining the activity during “false alarm“ compared to “correct rejection“ trials could potentially give some insights into why animals react at times when there is no sound present.

Further, as reviewed in chapter 1.2.1, previous studies in ASD patients have reported abnormalities in gamma frequency oscillations, which is important for perceptual and cognitive functions. Since PV+ interneuronal activity is important for generating gamma (Traub *et al.*, 1996; Cardin *et al.*, 2009; Fries, 2009; Sohal *et al.*, 2009), E-I disbalance could cause gamma abnormalities. XAV939 mouse model has an abnormal E-I ratio, therefore, it would be worth looking into gamma oscillations in relation to sensory perception deficits in this mouse model.

In this thesis, we have demonstrated how abnormal cortical expansion affects the detection of sound intensities. However, we have not researched how it affects other sound components, such as frequency discrimination. These mice with neuronal

overproduction may show superior results in frequency discrimination, as they have in visual orientation discrimination (Fang and Yuste, 2017).

Since studies in ASD patients have reported communication difficulties and electrophysiological abnormalities during speech stimuli (Gervais *et al.*, 2004; Mody *et al.*, 2013), it would also be interesting to explore these changes in our mouse model, to examine the influence of cortical expansion on social function and communication development. This could be done by examining neuronal responses to ultrasonic vocalizations during interactions with littermates or unfamiliar mice, across different developmental stages.

Finally, we should think about potential therapies. At young age, the XAV939 mouse model exhibits higher excitatory activity, which becomes more suppressed with age, as a compensatory mechanism. Increasing suppression in young mice through optogenetics or chemogenetics might recover the connectivity balance and normalize their neuronal activity in adulthood. This could provide insights into compensatory mechanisms in the cortex and help in devising future treatments of E-I disbalance.

Altogether, this PhD project has provided some new findings about the relationship between abnormal cortical expansion and auditory processing, thus giving contribution in elucidating perceptual deficits in ASD. Further research on neural underpinnings of perception needs to be done, as well as studies on developmental signaling pathways, to understand the origins of abnormal stimulus sensitivities in ASD.

9. References

Abdi, H. (2009) 'Signal Detection Theory', *Encyclopedia of Education (3rd Ed)*. doi: 10.1016/B978-0-08-097086-8.43090-4.

Abrams, D. A. *et al.* (2013) 'Underconnectivity between voice-selective cortex and reward circuitry in children with autism', *Proceedings of the National Academy of Sciences of the United States of America*, 110(29), pp. 12060–12065. doi: 10.1073/pnas.1302982110.

Adab, N. *et al.* (2004) 'The longer term outcome of children born to mothers with epilepsy', *Journal of Neurology, Neurosurgery and Psychiatry*, 75(11), pp. 1575–1583. doi: 10.1136/jnnp.2003.029132.

Adhya, D. *et al.* (2021) 'Atypical Neurogenesis in Induced Pluripotent Stem Cells From Autistic Individuals', *Biological Psychiatry*, 89(5), pp. 486–496. doi: 10.1016/j.biopsych.2020.06.014.

Adviento, B. *et al.* (2014) 'Autism traits in the RASopathies', *Journal of Medical Genetics*, 51(1), pp. 10–20. doi: 10.1136/jmedgenet-2013-101951.

Aitkin, L. M. *et al.* (1975) 'Inferior colliculus. I. Comparison of response properties of neurons in central, pericentral, and external nuclei of adult cat', *Journal of Neurophysiology*, 38(5), pp. 1196–1207. doi: 10.1152/jn.1975.38.5.1196.

Aitkin, L. M., Kenyon, C. E. and Philpott, P. (1981) 'The representation of the auditory and somatosensory systems in the external nucleus of the cat inferior colliculus', *Journal of Comparative Neurology*, 196(1), pp. 25–40. doi: 10.1002/cne.901960104.

Aitkin, L., Tran, L. and Syka, J. (1994) 'The responses of neurons in subdivisions of the inferior colliculus of cats to tonal, noise and vocal stimuli', *Experimental Brain Research*, 98(1), pp. 53–64. doi: 10.1007/BF00229109.

Aizenberg, M. *et al.* (2015) 'Bidirectional Regulation of Innate and Learned Behaviors That Rely on Frequency Discrimination by Cortical Inhibitory Neurons', *PLOS Biology*. Edited by R. C. Froemke, 13(12), p. e1002308. doi: 10.1371/journal.pbio.1002308.

Al-Ayadhi, L. Y. (2012) 'Relationship between sonic hedgehog protein, brain-derived neurotrophic factor and oxidative stress in autism spectrum Disorders', *Neurochemical Research*, 37(2), pp. 394–400. doi: 10.1007/s11064-011-0624-x.

Alcántara, J. I. *et al.* (2004) 'Speech-in-noise perception in high-functioning individuals with autism or Asperger's syndrome', *Journal of Child Psychology and Psychiatry and Allied Disciplines*, 45(6), pp. 1107–1114. doi: 10.1111/j.1469-

7610.2004.t01-1-00303.x.

Allen, W. E. *et al.* (2019) 'Thirst regulates motivated behavior through modulation of brainwide neural population dynamics', *Science*, 364(6437), pp. 0–10. doi: 10.1126/science.aav3932.

Alvarez-Buylla, A., García-Verdugo, J. M. and Tramontin, A. D. (2001) 'A unified hypothesis on the lineage of neural stem cells', *Nature Reviews Neuroscience*, 2(4), pp. 287–293. doi: 10.1038/35067582.

American Psychiatric Association (2013) *Diagnostic and Statistical Manual of Mental Disorders (DSM-5)*. 5th Ed.

Anderson, L. A. and Linden, J. F. (2011) 'Physiological differences between histologically defined subdivisions in the mouse auditory thalamus', *Hearing Research*, 274(1–2), pp. 48–60. doi: 10.1016/j.heares.2010.12.016.

Anderson, M., Zheng, Q. and Dong, X. (2018) 'Investigation of Pain Mechanisms by Calcium Imaging Approaches', *Neuroscience Bulletin*, 34(1), pp. 194–199. doi: 10.1007/s12264-017-0139-9.

Anderson, S. A. *et al.* (1997) 'Interneuron Migration from Basal Forebrain to Neocortex: Dependence on Dlx Genes', *Science*, 278, pp. 474–476.

Antoine, M. W. *et al.* (2019) 'Increased Excitation-Inhibition Ratio Stabilizes Synapse and Circuit Excitability in Four Autism Mouse Models', *Neuron*, 101(4), pp. 648-661.e4. doi: 10.1016/j.neuron.2018.12.026.

Antonelli, F., Casciati, A. and Pazzaglia, S. (2019) 'Sonic hedgehog signaling controls dentate gyrus patterning and adult neurogenesis in the hippocampus', *Neural Regeneration Research*, 14(1), p. 59. doi: 10.4103/1673-5374.243703.

Ashburner, J., Ziviani, J. and Rodger, S. (2008) 'Sensory processing and classroom emotional, behavioral, and educational outcomes in children with autism spectrum disorder', *American Journal of Occupational Therapy*, 62(5), pp. 564–573. doi: 10.5014/ajot.62.5.564.

Asperger, H. (1944) 'Die "Autistischen Psychopathen" im Kindesalter', *Archiv für Psychiatrie und Nervenkrankheiten*, 117(1), pp. 76–136. doi: 10.1007/BF01837709.

Atladóttir, H. Ó. *et al.* (2010a) 'Association of hospitalization for infection in childhood with diagnosis of autism spectrum disorders: A danish cohort study', *Archives of Pediatrics and Adolescent Medicine*, 164(5), pp. 470–477. doi: 10.1001/archpediatrics.2010.9.

Atladóttir, H. Ó. *et al.* (2010b) 'Maternal infection requiring hospitalization during pregnancy and autism spectrum disorders', *Journal of Autism and Developmental Disorders*, 40(12), pp. 1423–1430. doi: 10.1007/s10803-010-1006-y.

Avillac, M. *et al.* (2005) 'Reference frames for representing visual and tactile locations in parietal cortex', *Nature Neuroscience*, 8(7), pp. 941–949. doi: 10.1038/nn1480.

Aylward, E. H. *et al.* (2002) 'Effects of age on brain volume and head circumference in autism', *Neurology*, 59(2), pp. 175–183. doi: 10.1212/WNL.59.2.175.

Bailey, A. *et al.* (1995) 'Autism as a strongly genetic disorder evidence from a british twin Study', *Psychological Medicine*, 25(1), pp. 63–77. doi: 10.1017/S0033291700028099.

Bailey, A. *et al.* (1998) 'A clinicopathological study of autism', *Brain*, 121(5), pp. 889–905. doi: 10.1093/brain/121.5.889.

Bajo, V. M. *et al.* (2007) 'The ferret auditory cortex: Descending projections to the inferior colliculus', *Cerebral Cortex*, 17(2), pp. 475–491. doi: 10.1093/cercor/bhj164.

Baldassi, S. *et al.* (2009) 'Search superiority in autism within, but not outside the crowding regime', *Vision Research*, 49(16), pp. 2151–2156. doi: 10.1016/j.visres.2009.06.007.

Ball, G. *et al.* (2014) 'Rich-club organization of the newborn human brain', *Proceedings of the National Academy of Sciences of the United States of America*, 111(20), pp. 7456–7461. doi: 10.1073/pnas.1324118111.

Baranek, G. T. *et al.* (2013) 'Hyporesponsiveness to social and nonsocial sensory stimuli in children with autism, children with developmental delays, and typically developing children', *Development and Psychopathology*, 25(2), pp. 307–320. doi: 10.1017/S0954579412001071.

Baranova, J. *et al.* (2020) 'Autism Spectrum Disorder: Signaling Pathways and Prospective Therapeutic Targets', *Cellular and molecular neurobiology*, p. published online May 2020. doi: 10.1007/s10571-020-00882-7.

Barnea-Goraly, N. *et al.* (2004) 'White matter structure in autism: Preliminary evidence from diffusion tensor imaging', *Biological Psychiatry*, 55(3), pp. 323–326. doi: 10.1016/j.biopsych.2003.10.022.

Baron-Cohen, S., Leslie, A. M. and Frith, U. (1985) 'Does the autistic child have a "theory of mind" ?', *Cognition*, 21(1), pp. 37–46. doi: 10.1016/0010-0277(85)90022-8.

Barrett, L. and Henzi, P. (2005) 'The social nature of primate cognition', *Proceedings of the Royal Society B*, 272, pp. 1865–1875. doi: 10.1098/rspb.2005.3200.

Barthó, P. *et al.* (2004) 'Characterization of Neocortical Principal Cells and Interneurons by Network Interactions and Extracellular Features', *J Neurophysiol*, 92(1), pp. 600–608. doi: 10.1152/jn.01170.2003.

Bartholomeusz, H. H., Courchesne, E. and Karns, C. M. (2002) 'Relationship between head circumference and brain volume in healthy normal toddlers, children, and adults', *Neuropediatrics*, 33(5), pp. 239–241. doi: 10.1055/s-2002-36735.

Bashir, S. *et al.* (2014) 'Role of hedgehog protein family members in autistic children', *Neurology Psychiatry and Brain Research*, 20(3), pp. 63–67. doi: 10.1016/j.npbr.2014.06.002.

von Bekesy, G. (1960) *Experiments in hearing.* New York: McGraw-Hill.

Belgacem, Y. H. *et al.* (2016) 'The many hats of Sonic hedgehog signaling in nervous system development and disease', *Journal of Developmental Biology*, 4(35), pp. 1–18. doi: 10.3390/jdb4040035.

Le Belle, J. E. *et al.* (2014) 'Maternal inflammation contributes to brain overgrowth and autism-associated behaviors through altered redox signaling in stem and progenitor cells', *Stem Cell Reports*, 3(5), pp. 725–734. doi: 10.1016/j.stemcr.2014.09.004.

Belmonte, M. K. *et al.* (2004a) 'Autism and abnormal development of brain connectivity', *Journal of Neuroscience*, 24(42), pp. 9228–9231. doi: 10.1523/JNEUROSCI.3340-04.2004.

Belmonte, M. K. *et al.* (2004b) 'Autism as a disorder of neural information processing: directions for research and targets for therapy', *Molecular Psychiatry*, 9(7), pp. 646–663.

Ben-Sasson, A. *et al.* (2007) 'Extreme sensory modulation behaviors in toddlers with autism spectrum disorders', *American Journal of Occupational Therapy*, 61(5), pp. 584–592. doi: 10.5014/ajot.61.5.584.

Ben-Sasson, A. *et al.* (2009) 'A meta-analysis of sensory modulation symptoms in individuals with autism spectrum disorders', *Journal of Autism and Developmental Disorders*, 39(1), pp. 1–11. doi: 10.1007/s10803-008-0593-3.

Benson, T. E. and Brown, M. C. (2004) 'Postsynaptic targets of type II auditory nerve fibers in the cochlear nucleus', *Journal of the Association for Research in Otolaryngology*, 5(2), pp. 111–125. doi: 10.1007/s10162-003-4012-3.

Bertone, A. *et al.* (2005a) 'Enhanced and diminished visuo-spatial information processing in autism depends on stimulus complexity', *Brain*, 128(10), pp. 2430–2441. doi: 10.1093/brain/awh561.

Bertone, A. *et al.* (2005b) 'Enhanced and diminished visuo-spatial information processing in autism depends on stimulus complexity', *Brain*, 128, pp. 2430–2441. doi: 10.1093/brain/awh561.

Binns, K. E. *et al.* (1992) 'A topographic representation of auditory space in the

external nucleus of the inferior colliculus of the guinea-pig', *Brain Research*, 589(2), pp. 231–242. doi: 10.1016/0006-8993(92)91282-J.

Blackstock, E. G. (1978) 'Cerebral Asymmetry and the Development of Early Infantile Autism', *Journal of Autism and Childhood Schizophrenia*, 8(3), pp. 339–353.

Blake, R. *et al.* (2003) 'Visual recognition of biological motion is impaired in children with autism', *Psychological Science*, 14(2), pp. 151–157. doi: 10.1111/1467-9280.01434.

Blakemore, S. J. *et al.* (2006) 'Tactile sensitivity in Asperger syndrome', *Brain and Cognition*, 61(1), pp. 5–13. doi: 10.1016/j.bandc.2005.12.013.

de Boer-Schellekens, L., Eussen, M. and Vroomen, J. (2013) 'Diminished sensitivity of audiovisual temporal order in autism spectrum disorder', *Frontiers in Integrative Neuroscience*, 7(8), pp. 1–8. doi: 10.3389/fnint.2013.00008.

Bonnel, A. *et al.* (2003) 'Enhanced pitch sensitivity in individuals with autism: A signal detection analysis', *Journal of Cognitive Neuroscience*, 15(2), pp. 226–235. doi: 10.1162/089892903321208169.

Bonnel, A. *et al.* (2010) 'Enhanced pure-tone pitch discrimination among persons with autism but not Asperger syndrome', *Neuropsychologia*, 48(9), pp. 2465–2475. doi: 10.1016/j.neuropsychologia.2010.04.020.

Bordi, F. and LeDoux, J. E. (1994) 'Response properties of single units in areas of rat auditory thalamus that project to the amygdala - I. Acoustic discharge patterns and frequency receptive fields', *Experimental Brain Research*, 98(2), pp. 261–274. doi: 10.1007/BF00228414.

Bordley, J. E. and Hardy, M. (1937) 'Effect of lesions of the tympanic membrane on the hearing acuity: observations on experimental animals and on man', *Archives of Otolaryngology - Head and Neck Surgery*, 26(6), pp. 649–657. doi: 10.1001/archotol.1937.00650020721001.

Bouvet, L. *et al.* (2014) 'Auditory local bias and reduced global interference in autism', *Cognition*, 131(3), pp. 367–372. doi: 10.1016/j.cognition.2014.02.006.

Bowl, M. R. and Dawson, S. J. (2015) 'The mouse as a model for age-related hearing loss - A mini-review', *Gerontology*, 61(2), pp. 149–157. doi: 10.1159/000368399.

Brandwein, A. B. *et al.* (2013) 'The development of multisensory integration in high-functioning autism: High-density electrical mapping and psychophysical measures reveal impairments in the processing of audiovisual inputs', *Cerebral Cortex*, 23(6), pp. 1329–1341. doi: 10.1093/cercor/bhs109.

Brandwein, A. B. *et al.* (2015) 'Neurophysiological Indices of Atypical Auditory Processing and Multisensory Integration are Associated with Symptom Severity in

Autism', *Journal of Autism and Developmental Disorders*, 45(1), pp. 230–244. doi: 10.1007/s10803-014-2212-9.

Briggs (2010) 'Organizing principles of cortical layer 6', *Frontiers in Neural Circuits*, 4(3), pp. 1–8.

Briscoe, S. D. and Ragsdale, C. W. (2018) 'Homology, neocortex, and the evolution of developmental mechanisms', *Science*, 362, pp. 190–193. doi: 10.1126/science.aau3711.

Brock, J. *et al.* (2002) 'The temporal binding deficit hypothesis of autism', *Development and Psychopathology*, 14(2), pp. 209–224. doi: 10.1017/s0954579402002018.

Brown, A. S. *et al.* (2014) 'Elevated maternal C-reactive protein and autism in a national birth cohort', *Molecular Psychiatry*, 19(2), pp. 259–264. doi: 10.1038/mp.2012.197.

Bruneau, N. *et al.* (2003) 'Cortical auditory processing and communication in children with autism: Electrophysiological/behavioral relations', *International Journal of Psychophysiology*, 51(1), pp. 17–25. doi: 10.1016/S0167-8760(03)00149-1.

Brunetti-Pierri, N. *et al.* (2008) 'Recurrent reciprocal 1q21.1 deletions and duplications associated with microcephaly or macrocephaly and developmental and behavioral abnormalities', *Nature Genetics*, 40(12), pp. 1466–1471.

Buchwald, J. S. *et al.* (1992) 'Midlatency auditory evoked responses: P1 abnormalities in adult autistic subjects', *Electroencephalography and Clinical Neurophysiology/ Evoked Potentials*, 84(2), pp. 164–171. doi: 10.1016/0168-5597(92)90021-3.

Budday, S., Steinmann, P. and Kuhl, E. (2015) 'Physical biology of human brain development', *Frontiers in Cellular Neuroscience*, 9(257), pp. 1–17. doi: 10.3389/fncel.2015.00257.

Burton, A. *et al.* (2020) 'Wireless, battery-free subdermally implantable photometry systems for chronic recording of neural dynamics', *Proceedings of the National Academy of Sciences of the United States of America*, 117(6), pp. 2835–2845. doi: 10.1073/pnas.1920073117.

Busse, L. *et al.* (2011) 'The detection of visual contrast in the behaving mouse', *Journal of Neuroscience*, 31(31), pp. 11351–11361. doi: 10.1523/JNEUROSCI.6689-10.2011.

Buxbaum, J. D. *et al.* (2007) 'Mutation screening of the PTEN gene in patients with autism spectrum disorders and macrocephaly', *American Journal of Medical*

Genetics, Part B: Neuropsychiatric Genetics, 144(4), pp. 484–491. doi: 10.1002/ajmg.b.30493.

Buzsáki, G. (2004) 'Large-scale recording of neuronal ensembles', *Nature Neuroscience*, pp. 446–451. doi: 10.1038/nn1233.

Cain, K. and Oakhill, J. (eds) (2007) *Children's Comprehension Problems in Oral and Written Language: A Cognitive Perspective*. The Guilford Press.

Calvert, G. A. and Thesen, T. (2004) 'Multisensory integration: methodological approaches and emerging principles in the human brain', *Journal of Physiology Paris*, 98, pp. 191–205. doi: 10.1016/j.jphysparis.2004.03.018.

Campbell, P. K. *et al.* (1991) 'A Silicon-Based, Three-Dimensional Neural Interface: Manufacturing Processes for an Intracortical Electrode Array', *IEEE Transactions on Biomedical Engineering*, 38(8), pp. 758–768. doi: 10.1109/10.83588.

Canitano, R. (2007) 'Epilepsy in autism spectrum disorders', *European Child and Adolescent Psychiatry*, 16(1), pp. 61–66. doi: 10.1007/s00787-006-0563-2.

Carandini, M. and Churchland, A. K. (2013) 'Probing perceptual decisions in rodents', *Nature Neuroscience*, 16(7), pp. 824–831. doi: 10.1038/nn.3410.

Carcea, I., Insanally, M. N. and Froemke, R. C. (2017) 'Dynamics of auditory cortical activity during behavioural engagement and auditory perception', *Nature Communications*, 8(14412), pp. 1–12. doi: 10.1038/ncomms14412.

Cardin, J. A. *et al.* (2009) 'Driving fast-spiking cells induces gamma rhythm and controls sensory responses', *Nature*, 459(7247), pp. 663–667. doi: 10.1038/nature08002.

Carper, R. A. *et al.* (2002) 'Cerebral lobes in autism: early hyperplasia and abnormal age effects.', *NeuroImage*, 16(4), pp. 1038–51. doi: 10.1006/nimg.2002.1099.

Carper, R. A. and Courchesne, E. (2005) 'Localized enlargement of the frontal cortex in early autism', *Biological Psychiatry*, 57(2), pp. 126–133. doi: 10.1016/j.biopsych.2004.11.005.

Carter, M. and Shieh, J. (2015) *Guide to Research Techniques in Neuroscience*. Elsevier.

Casanova, M. F. *et al.* (2006) 'Minicolumnar abnormalities in autism', *Acta Neuropathologica*, 112(3), pp. 287–303.

Cascio, C. *et al.* (2008) 'Tactile perception in adults with autism: A multidimensional psychophysical study', *Journal of Autism and Developmental Disorders*, 38(1), pp. 127–137. doi: 10.1007/s10803-007-0370-8.

Cascio, C. J., Lorenzi, J. and Baranek, G. T. (2016) 'Self-reported Pleasantness Ratings and Examiner-Coded Defensiveness in Response to Touch in Children with ASD: Effects of Stimulus Material and Bodily Location', *Journal of Autism and Developmental Disorders*, 46(5), pp. 1528–1537. doi: 10.1007/s10803-013-1961-1.

Caviness, V. S. *et al.* (2003) 'Cell output, cell cycle duration and neuronal specification: A model of integrated mechanisms of the neocortical proliferative process', *Cerebral Cortex*, 13(6), pp. 592–598. doi: 10.1093/cercor/13.6.592.

Caviness, V. S., Takahashi, T. and Nowakowski, R. S. (1995) 'Numbers, time and neocortical neuronogenesis: a general developmental and evolutionary model', *Trends in Neurosciences*, 18(9), pp. 379–383. doi: 10.1016/0166-2236(95)93933-O.

Chang, Y. S. *et al.* (2014) 'Autism and sensory processing disorders: Shared white matter disruption in sensory pathways but divergent connectivity in social-emotional pathways', *PLoS ONE*, 9(7). doi: 10.1371/journal.pone.0103038.

Chao, H. T. *et al.* (2010) 'Dysfunction in GABA signalling mediates autism-like stereotypies and Rett syndrome phenotypes', *Nature*, 468(7321), pp. 263–269. doi: 10.1038/nature09582.

Charbonneau, G. *et al.* (2013) 'Multilevel alterations in the processing of audio-visual emotion expressions in autism spectrum disorders', *Neuropsychologia*, 51(5), pp. 1002–1010. doi: 10.1016/j.neuropsychologia.2013.02.009.

Chatterjee, S. and Sil, P. C. (2019) 'Targeting the crosstalks of Wnt pathway with Hedgehog and Notch for cancer therapy', *Pharmacological Research*, 142, pp. 251–261. doi: 10.1016/j.phrs.2019.02.027.

Chen, C. H. *et al.* (2014) 'Genetic analysis of GABRB3 as a candidate gene of autism spectrum disorders', *Molecular Autism*, 5(1), p. 36. doi: 10.1186/2040-2392-5-36.

Chen, X. Y. *et al.* (2015) 'Pten Mutations Alter Brain Growth Trajectory and Allocation of Cell Types through Elevated-Catenin Signaling', *Journal of Neuroscience*, 35(28), pp. 10252–10267. doi: 10.1523/JNEUROSCI.5272-14.2015.

Chen, Y. *et al.* (2012) 'Enhanced local processing of dynamic visual information in autism: Evidence from speed discrimination', *Neuropsychologia*, 50(5), pp. 733–739. doi: 10.1016/j.neuropsychologia.2012.01.007.

Cheng, Y. *et al.* (2010) 'Atypical development of white matter microstructure in adolescents with autism spectrum disorders', *NeuroImage*, 50(3), pp. 873–882. doi: 10.1016/j.neuroimage.2010.01.011.

Chenn, A. and Walsh, C. A. (2002) 'Regulation of cerebral cortical size by control of cell cycle exit in neural precursors', *Science*, 297(5580), pp. 365–369. doi: 10.1126/science.1074192.

Chi, T., Ru, P. and Shamma, S. A. (2005) 'Multiresolution spectrotemporal analysis of complex sounds', *The Journal of the Acoustical Society of America*, 118(2), pp. 887–906. doi: 10.1121/1.1945807.

Christensen, J. *et al.* (2013) 'Prenatal valproate exposure and risk of autism spectrum disorders and childhood autism', *Journal of the American Medical Association*, 309(16), pp. 1696–1703. doi: 10.1001/jama.2013.2270.

Chung, J. E. *et al.* (2019) 'High-Density, Long-Lasting, and Multi-region Electrophysiological Recordings Using Polymer Electrode Arrays', *Neuron*, 101(1), pp. 21-31.e5. doi: 10.1016/j.neuron.2018.11.002.

Ciesielski, K. T., Courchesne, E. and Elmasian, R. (1990) 'Effects of focused selective attention tasks on event-related potentials in autistic and normal individuals', *Electroencephalography and Clinical Neurophysiology*, 75(3), pp. 207–220. doi: 10.1016/0013-4694(90)90174-I.

Ciuman, R. R. (2010) 'The efferent system or olivocochlear function bundle - fine regulator and protector of hearing perception', *International Journal of Biomedical Science*, 6(4), pp. 276–288.

Cody, P. A. *et al.* (2018) 'Unique electrophysiological and impedance signatures between encapsulation types: An analysis of biological Utah array failure and benefit of a biomimetic coating in a rat model', *Biomaterials*, 161, pp. 117–128. doi: 10.1016/j.biomaterials.2018.01.025.

Cohen, Y. E. and Andersen, R. A. (2002) 'A common reference frame for movement plans in the posterior parietal cortex', *Nature Reviews Neuroscience*. Nature Publishing Group, pp. 553–562. doi: 10.1038/nrn873.

Collignon, O. *et al.* (2013) 'Reduced multisensory facilitation in persons with autism', *Cortex*, 49(6), pp. 1704–1710. doi: 10.1016/j.cortex.2012.06.001.

Collins, C. E. *et al.* (2010) 'Neuron densities vary across and within cortical areas in primates', *Proceedings of the National Academy of Sciences*, 107(36), pp. 15927–15932. doi: 10.1073/pnas.1010356107.

Cooke, J. E. *et al.* (2018) 'Contrast gain control in mouse auditory cortex', *J Neurophysiol*, 120, pp. 1872–1884. doi: 10.1152/jn.00847.2017.

Coskun, M. A. *et al.* (2009) 'How somatic cortical maps differ in autistic and typical brains', *NeuroReport*, 20(2), pp. 175–179. doi: 10.1097/WNR.0b013e32831f47d1.

Coskun, M. A. *et al.* (2013) 'Functional Assays of Local Connectivity in the Somatosensory Cortex of Individuals with Autism', *Autism Research*, 6(3), pp. 190–200. doi: 10.1002/aur.1276.

Courchesne, E. *et al.* (1985) 'Event-related brain potential correlates of the

processing of novel visual and auditory information in autism', *Journal of Autism and Developmental Disorders*, 15(1), pp. 55–76. doi: 10.1007/BF01837899.

Courchesne, E. *et al.* (1989) 'Pathophysiologic findings in nonretarded autism and receptive developmental language disorder', *Journal of Autism and Developmental Disorders*, 19(1), pp. 1–17. doi: 10.1007/BF02212714.

Courchesne, E. *et al.* (2001) 'Unusual brain growth patterns in early life in patients with autistic disorder: An MRI study', *Neurology*, 57(2), pp. 245–254. doi: 10.1212/WNL.57.2.245.

Courchesne, E. *et al.* (2005) 'Autism at the beginning: Microstructural and growth abnormalities underlying the cognitive and behavioral phenotype of autism', *Development and Psychopathology*, 17(3), pp. 577–597. doi: 10.1017/S0954579405050285.

Courchesne, E. *et al.* (2011) 'Neuron number and size in prefrontal cortex of children with autism', *JAMA - Journal of the American Medical Association*, 306(18), pp. 2001–2010.

Courchesne, E. *et al.* (2019) 'The ASD Living Biology: from cell proliferation to clinical phenotype', *Molecular Psychiatry*, 24(1), pp. 88–107. doi: 10.1038/s41380-018-0056-y.

Courchesne, E., Carper, R. and Akshoomoff, N. (2003) 'Evidence of Brain Overgrowth in the First Year of Life in Autism', *Journal of the American Medical Association*, 290(3), pp. 337–344. doi: 10.1001/jama.290.3.337.

Courchesne, E., Gazestani, V. H. and Lewis, N. E. (2020) 'Prenatal Origins of ASD : The When , What , and How of ASD Development', *Trends in Neurosciences*, 43(5), pp. 326–342. doi: 10.1016/j.tins.2020.03.005.

Courchesne, E. and Pierce, K. (2005) 'Brain overgrowth in autism during a critical time in development: Implications for frontal pyramidal neuron and interneuron development and connectivity', *International Journal of Developmental Neuroscience*, 23(2–3), pp. 153–170. doi: 10.1016/j.ijdevneu.2005.01.003.

Crane, L., Goddard, L. and Pring, L. (2009) 'Sensory processing in adults with autism spectrum disorders', *Autism : the international journal of research and practice*, 13(3), pp. 215–228. doi: 10.1177/1362361309103794.

Csicsvari, J. *et al.* (2003) 'Massively Parallel Recording of Unit and Local Field Potentials With Silicon-Based Electrodes', *J Neurophysiol*, 90(2), pp. 1314–23. doi: 10.1152/jn.00116.2003.

Dakin, S. and Frith, U. (2005) 'Vagaries of visual perception in autism', *Neuron*, 48(3), pp. 497–507. doi: 10.1016/j.neuron.2005.10.018.

Dale, A. M. and Halgren, E. (2001) 'Spatiotemporal mapping of brain activity by integration of multiple imaging modalities', *Curr Opin Neurobiol.*, 11(2), pp. 202–8.

Dalton, K. M. *et al.* (2005) 'Gaze fixation and the neural circuitry of face processing in autism', *Nature Neuroscience*, 8(4), pp. 519–526. doi: 10.1038/nn1421.

Damarla, S. R. *et al.* (2010) 'Cortical underconnectivity coupled with preserved visuospatial cognition in autism: Evidence from an fMRI study of an embedded figures task', *Autism Research*, 3(5), pp. 273–279. doi: 10.1002/aur.153.

Dani, V. S. *et al.* (2005) 'Reduced cortical activity due to a shift in the balance between excitation and inhibition in a mouse model of Rett Syndrome', *Proceedings of the National Academy of Sciences of the United States of America*, 102(35), pp. 12560–12565. doi: 10.1073/pnas.0506071102.

Dani, V. S. and Nelson, S. B. (2009) 'Intact long-term potentiation but reduced connectivity between neocortical layer 5 pyramidal neurons in a mouse model of Rett syndrome', *Journal of Neuroscience*, 29(36), pp. 11263–11270. doi: 10.1523/JNEUROSCI.1019-09.2009.

Dawson, G. *et al.* (1998) 'Children with autism fail to orient to naturally occurring social stimuli', *Journal of Autism and Developmental Disorders*, 28(6), pp. 479–485. doi: 10.1023/A:1026043926488.

Dawson, G. *et al.* (2002) 'Neural correlates of face and object recognition in young children with autism spectrum disorder, developmental delay, and typical development', *Child Development*, 73(3), pp. 700–717. doi: 10.1111/1467-8624.00433.

Dawson, G. *et al.* (2004) 'Early Social Attention Impairments in Autism: Social Orienting, Joint Attention, and Attention to Distress', *Developmental Psychology*, 40(2), pp. 271–283. doi: 10.1037/0012-1649.40.2.271.

Dawson, G., Webb, S. J. and McPartland, J. (2005) 'Understanding the nature of face processing impairment in autism: Insights from behavioral and electrophysiological studies', *Developmental Neuropsychology*, 27(3), pp. 403–424. doi: 10.1207/s15326942dn2703_6.

Dehay, C. and Kennedy, H. (2007) 'Cell-cycle control and cortical development', *Nature Reviews Neuroscience*, 8(6), pp. 438–450. doi: 10.1038/nrn2097.

Dehay, C., Kennedy, H. and Kosik, K. S. (2015) 'The Outer Subventricular Zone and Primate-Specific Cortical Complexification', *Neuron*, 85(4), pp. 683–694. doi: 10.1016/j.neuron.2014.12.060.

Delattre, V. *et al.* (2013) 'Nlgn4 knockout induces network hypo-excitability in juvenile mouse somatosensory cortex in vitro', *Scientific Reports*, 3(1), pp. 1–6. doi:

10.1038/srep02897.

DeLorey, T. M. *et al.* (1998) 'Mice lacking the β3 subunit of the GABA(A) receptor have the epilepsy phenotype and many of the behavioral characteristics of Angelman syndrome', *Journal of Neuroscience*, 18(20), pp. 8505–8514. doi: 10.1523/jneurosci.18-20-08505.1998.

Derosa, B. A. *et al.* (2018) 'Convergent Pathways in Idiopathic Autism Revealed by Time Course Transcriptomic Analysis of Patient-Derived Neurons', *Scientific Reports*, 8(1), pp. 1–15. doi: 10.1038/s41598-018-26495-1.

Dicke, U. and Roth, G. (2016) 'Neuronal factors determining high intelligence', *Philosophical Transactions of the Royal Society B: Biological Sciences*, 371(1685).

Diederich, A. and Colonius, H. (2004) 'Bimodal and trimodal multisensory enhancement: Effects of stimulus onset and intensity on reaction time', *Perception and Psychophysics*, 66(8), pp. 1388–1404. doi: 10.3758/BF03195006.

Dinstein, I. *et al.* (2012) 'Unreliable Evoked Responses in Autism', *Neuron*, 75(6), pp. 981–991. doi: 10.1016/j.neuron.2012.07.026.

Dinstein, I., Heeger, D. J. and Behrmann, M. (2015) 'Neural variability: friend or foe?', *Trends in Cognitive Sciences*, 19, pp. 322–328.

Divenyi, P. L. and Hirsh, I. J. (1974) 'Identification of temporal order in three-tone sequences', *Journal of the Acoustical Society of America*, 56(1), pp. 144–151. doi: 10.1121/1.1903245.

Donaldson, C. K., Stauder, J. E. A. and Donkers, F. C. L. (2017) 'Increased Sensory Processing Atypicalities in Parents of Multiplex ASD Families Versus Typically Developing and Simplex ASD Families', *Journal of Autism and Developmental Disorders*, 47(3), pp. 535–548. doi: 10.1007/s10803-016-2888-0.

Dong, F. *et al.* (2016) 'Deletion of CTNNB1 in inhibitory circuitry contributes to autism-associated behavioral defects', *Human Molecular Genetics*, 25(13), pp. 2738–2751. doi: 10.1093/hmg/ddw131.

Donohue, S. E., Darling, E. F. and Mitroff, S. R. (2012) 'Links between multisensory processing and autism', *Experimental Brain Research*, 222(4), pp. 377–387. doi: 10.1007/s00221-012-3223-4.

Doucet, J. R., Molavi, D. L. and Ryugo, D. K. (2003) 'The source of corticocollicular and corticobulbar projections in area Te1 of the rat', *Experimental Brain Research*, 153(4), pp. 461–466. doi: 10.1007/s00221-003-1604-4.

Doyle-Thomas, K. A. R. *et al.* (2013) 'Neurofunctional Underpinnings of Audiovisual Emotion Processing in Teens with Autism Spectrum Disorders', *Frontiers in Psychiatry*, 4. doi: 10.3389/fpsyt.2013.00048.

Edgar, J. C. *et al.* (2015) 'Neuromagnetic Oscillations Predict Evoked-Response Latency Delays and Core Language Deficits in Autism Spectrum Disorders', *Journal of Autism and Developmental Disorders*, 45(2), pp. 395–405. doi: 10.1007/s10803-013-1904-x.

Ehret, G. *et al.* (2003) 'Spatial map of frequency tuning-curve shapes in the mouse inferior colliculus', *NeuroReport*, 14(10), pp. 1365–1369. doi: 10.1097/01.wnr.0000078545.07662.85.

Emerson, R. W. *et al.* (2017) 'Functional neuroimaging of high-risk 6-month-old infants predicts a diagnosis of autism at 24 months of age', *Science Translational Medicine*, 9(393). doi: 10.1126/scitranslmed.aag2882.

Esbensen, A. J. *et al.* (2009) 'Age-Related Differences in Restricted Repetitive Behaviors in Autism Spectrum Disorders', *J Autism Dev Disord*, 39, pp. 57–66. doi: 10.1007/s10803-008-0599-x.

Van Essen, D. C., Donahue, C. J. and Glasser, M. F. (2018) 'Development and Evolution of Cerebral and Cerebellar Cortex', *Brain, Behavior and Evolution*, 91, pp. 158–169. doi: 10.1159/000489943.

Estes, A. *et al.* (2015) 'Behavioral, cognitive, and adaptive development in infants with autism spectrum disorder in the first 2 years of life', *Journal of Neurodevelopmental Disorders*, 7(1), p. 24. doi: 10.1186/s11689-015-9117-6.

Estes, M. L. and McAllister, A. K. (2016) 'Maternal immune activation: Implications for neuropsychiatric disorders', *Science*, 353(6301), pp. 772–777. doi: 10.1126/science.aag3194.

Etherton, M. R. *et al.* (2009) 'Mouse neurexin-1α deletion causes correlated electrophysiological and behavioral changes consistent with cognitive impairments', *Proceedings of the National Academy of Sciences of the United States of America*, 106(42), pp. 17998–18003. doi: 10.1073/pnas.0910297106.

Evarts, E. V. (1968) 'A technique for recording activity of subcortical neurons in moving animals', *Electroencephalography and Clinical Neurophysiology*, 24(1), pp. 83–86. doi: 10.1016/0013-4694(68)90070-9.

Falk, D. and Gibson, K. (2001) *Evolutionary Anatomy of the Primate Cerebral Cortex*. Cambridge University Press.

Fame, R. M., MacDonald, J. L. and Macklis, J. D. (2011) 'Development, specification, and diversity of callosal projection neurons', *Trends Neurosci.*, 34(1), pp. 41–50. doi: 10.1016/j.tins.2010.10.002.

Fang, W. Q. *et al.* (2011) 'Cdk5-Mediated Phosphorylation of Axin Directs Axon Formation during Cerebral Cortex Development', *Journal of Neuroscience*, 31(38),

pp. 13613–13624.

Fang, W. Q. *et al.* (2013) 'Axin directs the amplification and differentiation of intermediate progenitors in the developing cerebral cortex', *Neuron*, 79, pp. 665–679.

Fang, W. Q. *et al.* (2014) 'Overproduction of Upper-Layer Neurons in the Neocortex Leads to Autism-like Features in Mice', *Cell Reports*, 9, pp. 1635–1643.

Fang, W. Q. and Yuste, R. (2017) 'Overproduction of Neurons Is Correlated with Enhanced Cortical Ensembles and Increased Perceptual Discrimination', *Cell Reports*, 21, pp. 381–392.

Fatemi, S. H. *et al.* (2002) 'Prenatal viral infection leads to pyramidal cell atrophy and macrocephaly in adulthood: implications for genesis of autism and schizophrenia.', *Cellular and molecular neurobiology*, 22(1), pp. 25–33.

Fatemi, S. H. *et al.* (2009) 'GABAA receptor downregulation in brains of subjects with autism', *Journal of Autism and Developmental Disorders*, 39(2), pp. 223–230. doi: 10.1007/s10803-008-0646-7.

Faye-Lund, H. (1986) 'Projection from the inferior colliculus to the superior olivary complex in the albino rat', *Anatomy and Embryology*, 175(1), pp. 35–52. doi: 10.1007/BF00315454.

Feigenson, K. *et al.* (2011) 'Canonical Wnt signalling requires the BMP pathway to inhibit oligodendrocyte maturation', *ASN Neuro*, 3(3), pp. 147–158. doi: 10.1042/AN20110004.

Fein, D. (ed.) (2011) *The Neuropsychology of Autism*. Oxford University Press.

Fekete, D. M. *et al.* (1984) 'The central projections of intracellularly labeled auditory nerve fibers in cats', *Journal of Comparative Neurology*, 229(3), pp. 432–450. doi: 10.1002/cne.902290311.

Feliciano, M., Saldana, E. and Mugnaini, E. (1995) *Direct Projections from the Rat Primary Auditory Neocortex to Nucleus Sagulum, Paralemniscal Regions, Superior Olivary Complex and Cochlear Nuclei*, *Auditory Neuroscience*.

Felsen, G. and Mainen, Z. F. (2012) 'Midbrain contributions to sensorimotor decision making', *Journal of Neurophysiology*, 108(1), pp. 135–147. doi: 10.1152/jn.01181.2011.

Ferezou, I. *et al.* (2007) 'Spatiotemporal Dynamics of Cortical Sensorimotor Integration in Behaving Mice', *Neuron*, 56(5), pp. 907–923. doi: 10.1016/j.neuron.2007.10.007.

Ferrara, N. C. *et al.* (2017) 'Input from the medial geniculate nucleus modulates

amygdala encoding of fear memory discrimination', *Learning and Memory*, 24(9), pp. 414–421. doi: 10.1101/lm.044131.116.

Ferri, R. *et al.* (2003) 'The mismatch negativity and the P3a components of the auditory event-related potentials in autistic low-functioning subjects', *Clinical Neurophysiology*, 114(9), pp. 1671–1680. doi: 10.1016/S1388-2457(03)00153-6.

Finlay, B. L. and Darlington, R. B. (1995) 'Linked Regularities in the Development and Evolution of Mammalian Brains', *Science*, 268(5217), pp. 1578–1584.

Fitzpatrick, D. (2004) 'The Auditory System', in Purves, D. et al. (eds) *Neuroscience*. 3rd edn. Sinauer Associates, Inc.

Flore, G. *et al.* (2016) 'Cortical Development Requires Mesodermal Expression of Tbx1 , a Gene Haploinsufficient in 22q11.2 Deletion Syndrome', *Cerebral Cortex*, 27(3), pp. 2210–2225.

Fombonne, E. *et al.* (1999) 'Microcephaly and macrocephaly in autism.', *Journal of autism and developmental disorders*, 29(2), pp. 113–9.

Fombonne, E. (2002) 'Epidemiological trends in rates of autism', *Molecular Psychiatry*, 7, pp. 4–6. doi: 10.1038/sj.mp.4001162.

Forrest, C. M. *et al.* (2012) 'Prenatal activation of Toll-like receptors-3 by administration of the viral mimetic poly(I:C) changes synaptic proteins, N-methyl-D-aspartate receptors and neurogenesis markers in offspring', *Molecular Brain*, 5(1). doi: 10.1186/1756-6606-5-22.

Forrest, M. P. *et al.* (2018) 'The psychiatric risk gene transcription factor 4 (TCF4) regulates neurodevelopmental pathways associated with schizophrenia, Autism, and intellectual disability', *Schizophrenia Bulletin*, 44(5), pp. 1100–1110. doi: 10.1093/schbul/sbx164.

Foss-Feig, J. H. *et al.* (2010) 'An extended multisensory temporal binding window in autism spectrum disorders', *Experimental Brain Research*, 203(2), pp. 381–389. doi: 10.1007/s00221-010-2240-4.

Foss-Feig, J. H. *et al.* (2013) 'A substantial and unexpected enhancement of motion perception in autism', *Journal of Neuroscience*, 33(19), pp. 8243–8249. doi: 10.1523/JNEUROSCI.1608-12.2013.

Foss-Feig, J. H., Heacock, J. L. and Cascio, C. J. (2012) 'Tactile responsiveness patterns and their association with core features in autism spectrum disorders', *Research in Autism Spectrum Disorders*, 6(1), pp. 337–344. doi: 10.1016/j.rasd.2011.06.007.

Foxe, J. J. *et al.* (2015) 'Severe Multisensory Speech Integration Deficits in High-Functioning School-Aged Children with Autism Spectrum Disorder (ASD) and Their

Resolution During Early Adolescence', *Cerebral Cortex*, 25(2), pp. 298–312. doi: 10.1093/cercor/bht213.

Freeman, J. A. and Nicholson, C. (1975) 'Experimental Optimization of Current Source-Density Technique for Anuran Cerebellum', *J Neurophysiol*, 38(2), pp. 369–82.

Freyberg, J., Robertson, C. E. and Baron-Cohen, S. (2016) 'Typical magnitude and spatial extent of crowding in autism', *Journal of Vision*, 16(5). doi: 10.1167/16.5.17.

Friederici, A. D. (2011) 'The brain basis of language processing: From structure to function', *Physiological Reviews*, 91(4), pp. 1357–1392. doi: 10.1152/physrev.00006.2011.

Fries, P. (2009) 'Neuronal gamma-band synchronization as a fundamental process in cortical computation', *Annual Review of Neuroscience*, 32, pp. 209–224. doi: 10.1146/annurev.neuro.051508.135603.

Frith, U. (1989) *Autism: Explaining the Enigma.*, *British Journal of Psychiatry*. Oxford: Basil Blackwell.

Frye, R. E. *et al.* (2016) 'Neuropathological mechanisms of seizures in autism spectrum disorder', *Frontiers in Neuroscience*, 10(192), pp. 1–9. doi: 10.3389/fnins.2016.00192.

Fu, T.-M. *et al.* (2017) 'Highly scalable multichannel mesh electronics for stable chronic brain electrophysiology', *Proceedings of the National Academy of Sciences*, p. 201717695. doi: 10.1073/pnas.1717695114.

Fujimura, K. *et al.* (2016) 'In utero exposure to valproic acid induces neocortical dysgenesis via dysregulation of neural progenitor cell proliferation/differentiation', *Journal of Neuroscience*, 36(42), pp. 10908–10919. doi: 10.1523/JNEUROSCI.0229-16.2016.

Fujisawa, S. *et al.* (2008) 'Behavior-dependent short-term assembly dynamics in the medial prefrontal cortex', *Nat Neurosci*, 11(7), pp. 823–833. doi: 10.1038/nn.2134.

Furue, H., Katafuchi, T. and Yoshimura, M. (2007) 'In Vivo Patch-Clamp Technique', in Waltz, W. (ed.) *Patch Clamp Analysis*. Humana Press, pp. 229–251. doi: 10.1007/978-1-59745-492-6_7.

Gage, N. M. *et al.* (2009) 'Rightward hemispheric asymmetries in auditory language cortex in children with autistic disorder: an MRI investigation', *Journal of Neurodevelopmental Disorders*, 1(3), pp. 205–214. doi: 10.1007/s11689-009-9010-2.

Gallero-Salas, Y. *et al.* (2021) 'Sensory and Behavioral Components of Neocortical Signal Flow in Discrimination Tasks with Short-Term Memory', *Neuron*, 109(1), pp.

135-148.e6. doi: 10.1016/j.neuron.2020.10.017.

Gandal, M. J. *et al.* (2010) 'Validating gamma oscillations and delayed auditory responses as translational biomarkers of autism', *Biological Psychiatry*, 68(12), pp. 1100–1106. doi: 10.1016/j.biopsych.2010.09.031.

Garg, S. *et al.* (2017) 'Autism spectrum disorder and other neurobehavioural comorbidities in rare disorders of the Ras/MAPK pathway', *Developmental Medicine and Child Neurology*, 59(5), pp. 544–549. doi: 10.1111/dmcn.13394.

Gazestani, V. H. *et al.* (2019) 'A perturbed gene network containing PI3K–AKT, RAS–ERK and WNT–β-catenin pathways in leukocytes is linked to ASD genetics and symptom severity', *Nature Neuroscience*, 22(10), pp. 1624–1634. doi: 10.1038/s41593-019-0489-x.

Georgala, P. A., Manuel, M. and Price, D. J. (2011) 'The generation of superficial cortical layers is regulated by levels of the transcription factor Pax6', *Cerebral Cortex*, 21(1), pp. 81–94. doi: 10.1093/cercor/bhq061.

Gervais, H. *et al.* (2004) 'Abnormal cortical voice processing in autism', *Nature Neuroscience*, 7(8), pp. 801–802. doi: 10.1038/nn1291.

Gillmeister, H. and Eimer, M. (2007) 'Tactile enhancement of auditory detection and perceived loudness', *Brain Research*, 1160(1), pp. 58–68. doi: 10.1016/j.brainres.2007.03.041.

Gilmore, E. C. and Walsh, C. A. (2013) 'Genetic causes of microcephaly and lessons for neuronal development', *Wiley Interdisciplinary Reviews: Developmental Biology*, 2(4), pp. 461–478.

Gilmore, J. H., Knickmeyer, R. C. and Gao, W. (2018) 'Imaging structural and functional brain development in early childhood', *Nature Reviews Neuroscience*. Nature Publishing Group, pp. 123–137. doi: 10.1038/nrn.2018.1.

Glad Mihai, P. *et al.* (2019) 'Modulation of tonotopic ventral medial geniculate body is behaviorally relevant for speech recognition', *eLife*, 8. doi: 10.7554/eLife.44837.

Glover, G. H. (2011) 'Overview of functional magnetic resonance imaging', *Neurosurgery Clinics of North America*, 22(2), pp. 133–139. doi: 10.1016/j.nec.2010.11.001.

Go, H. S. *et al.* (2011) 'Valproic acid inhibits neural progenitor cell death by activation of NF-B signaling pathway and up-regulation of Bcl-XL', *Journal of Biomedical Science*, 18(1). doi: 10.1186/1423-0127-18-48.

Goffinet, A. M. and Rakic, P. (2000) *Mouse Brain Development. Results and Problems in Cell Differentiation*, *Springer*.

Goines, P. E. *et al.* (2011) 'Increased midgestational IFN-γ, IL-4 and IL-5 in women bearing a child with autism: A case-control study', *Molecular Autism*, 2(1). doi: 10.1186/2040-2392-2-13.

González Hernández, T. H., Meyer, G. and Ferres-Torres, R. (1986) 'The commissural interconnections of the inferior colliculus in the albino mouse', *Brain Research*, 368(2), pp. 268–276. doi: 10.1016/0006-8993(86)90571-8.

Göttlicher, M. *et al.* (2001) 'Valproic acid defines a novel class of HDAC inhibitors inducing differentiation of transformed cells', *EMBO Journal*, 20(24), pp. 6969–6978. doi: 10.1093/emboj/20.24.6969.

Gould, E. and McEwen, B. S. (1993) 'Neuronal birth and death', *Current Opinion in Neurobiology*, 3(5), pp. 676–682. doi: 10.1016/0959-4388(93)90138-O.

Green, D. M. and Swets, J. A. (1966) *Signal detection theory and psychophysics*. J. Wiley, New York.

Greig, L. C. *et al.* (2013) 'Molecular logic of neocortical projection neuron specification, development and diversity', *Nature Reviews Neuroscience*, 14, pp. 755–769. doi: 10.1038/nrn3586.

Grice, S. J. *et al.* (2001) 'Disordered visual processing and oscillatory brain activity in autism and Williams syndrome', *NeuroReport*, 12(12), pp. 2697–2700. doi: 10.1097/00001756-200108280-00021.

Griswold, A. J. *et al.* (2012) 'Evaluation of copy number variations reveals novel candidate genes in autism spectrum disorder-associated pathways', *Human Molecular Genetics*, 21(15), pp. 3513–3523. doi: 10.1093/hmg/dds164.

Groen, W. B. *et al.* (2009) 'Intact spectral but abnormal temporal processing of auditory stimuli in autism', *Journal of Autism and Developmental Disorders*, 39(5), pp. 742–750. doi: 10.1007/s10803-008-0682-3.

Grossmann, T. N. *et al.* (2012) 'Inhibition of oncogenic Wnt signaling through direct targeting of β-catenin', *Proceedings of the National Academy of Sciences of the United States of America*, 109(44), pp. 17942–17947. doi: 10.1073/pnas.1208396109.

Groszer, M. *et al.* (2001) 'Negative regulation of neural stem/progenitor cell proliferation by the Pten tumor suppressor gene in vivo', *Science*, 294(5549), pp. 2186–2189. doi: 10.1126/science.1065518.

Grubb, M. A. *et al.* (2013) 'Endogenous Spatial Attention: Evidence for Intact Functioning in Adults With Autism', *Autism Research*, 6(2), pp. 108–118. doi: 10.1002/aur.1269.

Güçlü, B. *et al.* (2007) 'Tactile sensitivity of normal and autistic children',

Somatosensory and Motor Research, 24(1–2), pp. 21–33. doi: 10.1080/08990220601179418.

Gulino, A. *et al.* (2007) 'Hedgehog signaling pathway in neural development and disease', *Psychoneuroendocrinology*, 32(1), pp. 52–6. doi: 10.1016/j.psyneuen.2007.03.017.

Guo, X. *et al.* (2008) 'Axin and GSK3-β control Smad3 protein stability and modulate TGF-β signaling', *Genes and Development*, 22(1), pp. 106–120. doi: 10.1101/gad.1590908.

Guo, Z. V. *et al.* (2014a) 'Flow of cortical activity underlying a tactile decision in mice', *Neuron*, 81(1), pp. 179–194. doi: 10.1016/j.neuron.2013.10.020.

Guo, Z. V. *et al.* (2014b) 'Procedures for behavioral experiments in head-fixed mice', *PLoS ONE*, 9(2), pp. 1–16. doi: 10.1371/journal.pone.0088678.

Gurney, A. *et al.* (2012) 'Wnt pathway inhibition via the targeting of Frizzled receptors results in decreased growth and tumorigenicity of human tumors', *Proceedings of the National Academy of Sciences of the United States of America*, 109(29), pp. 11717–11722. doi: 10.1073/pnas.1120068109.

Hahne, G. and Grossmann, T. N. (2013) 'Direct targeting of β-catenin: Inhibition of protein-protein interactions for the inactivation of Wnt signaling', *Bioorganic and Medicinal Chemistry*, 21(14), pp. 4020–4026. doi: 10.1016/j.bmc.2013.02.050.

Haigh, S. M. *et al.* (2015) 'Cortical Variability in the Sensory-Evoked Response in Autism', *Journal of Autism and Developmental Disorders*, 45(5), pp. 1176–1190. doi: 10.1007/s10803-014-2276-6.

Halepoto, D. M. *et al.* (2015) 'Correlation Between Hedgehog (Hh) Protein Family and Brain-Derived Neurotrophic Factor (BDNF) in Autism Spectrum Disorder (ASD)', *Journal of the College of Physicians and Surgeons Pakistan*, 25(12), pp. 882–885. doi: 12.2015/JCPSP.882885.

Hallmayer, J. *et al.* (2011) 'Genetic heritability and shared environmental factors among twin pairs with autism', *Archives of General Psychiatry*, 68(11), pp. 1095–1102. doi: 10.1001/archgenpsychiatry.2011.76.

Hand, R. A. *et al.* (2015) 'Axon Dynamics during Neocortical Laminar Innervation', *Cell Reports*, 12(2), pp. 172–182. doi: 10.1016/j.celrep.2015.06.026.

Handel, S. (1995) 'Timbre Perception and Auditory Object Identification', in *Hearing*. Elsevier, pp. 425–461. doi: 10.1016/b978-012505626-7/50014-5.

Happé, F. (1999) 'Autism: cognitive deficit or cognitive style?', *Trends in Cognitive Sciences*, 3(6), pp. 216–222. doi: 10.1016/S1364-6613(99)01318-2.

Happé, F. and Frith, U. (2006) 'The weak coherence account: Detail-focused cognitive style in autism spectrum disorders', *Journal of Autism and Developmental Disorders*, 36(1), pp. 5–25. doi: 10.1007/s10803-005-0039-0.

Harris, K. D. and Shepherd, G. M. G. (2015) 'The neocortical circuit: themes and variations', *Nature Neuroscience*, 18(2), pp. 170–181.

Hashimoto, T., Tayama, M. and Miyao, M. (1986) 'Short latency somatosensory evoked potentials in children with autism', *Brain and Development*, 8(4), pp. 428–432. doi: 10.1016/S0387-7604(86)80065-1.

Hazlett, H. C. *et al.* (2017) 'Early brain development in infants at high risk for autism spectrum disorder', *Nature*, 542(7641), pp. 348–351. doi: 10.1038/nature21369.

Heaton, P. (2003) 'Pitch memory, labelling and disembedding in autism', *Journal of Child Psychology and Psychiatry and Allied Disciplines*, 44(4), pp. 543–551. doi: 10.1111/1469-7610.00143.

Heaton, P. *et al.* (2008) 'Autism and pitch processing splinter skills: A group and subgroup analysis', *Autism*, 12(2), pp. 203–219. doi: 10.1177/1362361307085270.

Heaton, P., Hermelin, B. and Pring, L. (1998) 'Autism and pitch processing: A precursor for savant musical ability?', *Music Perception*, 15(3), pp. 291–305. doi: 10.2307/40285769.

Heaton, P., Pring, L. and Hermelin, B. (1999) 'A pseudo-savant: A case of exceptional musical splinter skills', *Psychology*, 5(6), pp. 503–509. doi: 10.1080/13554799908402745.

Heeger, D. J., Behrmann, M. and Dinstein, I. (2017) 'Vision as a Beachhead', *Biological Psychiatry*, 81(10), pp. 832–837. doi: 10.1016/j.biopsych.2016.09.019.

Heisenberg, C. P. *et al.* (2001) 'A mutation in the Gsk3-binding domain of zebrafish masterblind/Axin1 leads to a fate transformation of telencephalon and eyes to diencephalon', *Genes and Development*, 15(11), pp. 1427–1434. doi: 10.1101/gad.194301.

Henderson, W. R. *et al.* (2010) 'Inhibition of Wnt/β-catenin/CREB binding protein (CBP) signaling reverses pulmonary fibrosis', *Proceedings of the National Academy of Sciences of the United States of America*, 107(32), pp. 14309–14314. doi: 10.1073/pnas.1001520107.

Hendry, S. H. C. and Jones, E. G. (1991) 'GABA neuronal subpopulations in cat primary auditory cortex: co-localization with calcium binding proteins', *Brain Research*, 543(1), pp. 45–55. doi: 10.1016/0006-8993(91)91046-4.

Hensch, T. K. and Fagiolini, M. (2005) 'Excitatory-inhibitory balance and critical period plasticity in developing visual cortex', *Progress in Brain Research*, 147, pp.

115–124.

Herbert, M. R. *et al.* (2003) ‘Dissociations of cerebral cortex, subcortical and cerebral white matter volumes in autistic boys’, *Brain*, 126(5), pp. 1182–1192. doi: 10.1093/brain/awg110.

Herbert, M. R. *et al.* (2004) ‘Localization of White Matter Volume Increase in Autism and Developmental Language Disorder’, *Annals of Neurology*, 55(4), pp. 530–540. doi: 10.1002/ana.20032.

Herculano-Houzel, S. *et al.* (2007) ‘Cellular scaling rules for primate brains’, *Proceedings of the National Academy of Sciences of the United States of America*, 104(9), pp. 3562–3567.

Herculano-Houzel, S. (2009) ‘The human brain in numbers: A linearly scaled-up primate brain’, *Frontiers in Human Neuroscience*, 3(31), pp. 1–11.

Herculano-Houzel, S. (2017) ‘Numbers of neurons as biological correlates of cognitive capability’, *Current Opinion in Behavioral Sciences*, 16, pp. 1–7.

Herculano-Houzel, S., Manger, P. R. and Kaas, J. H. (2014) ‘Brain scaling in mammalian evolution as a consequence of concerted and mosaic changes in numbers of neurons and average neuronal cell size’, *Frontiers in Neuroanatomy*, 8(77), pp. 1–28.

Herold, F. *et al.* (2018) ‘Applications of Functional Near-Infrared Spectroscopy (fNIRS) Neuroimaging in Exercise–Cognition Science: A Systematic, Methodology-Focused Review’, *Journal of Clinical Medicine*, 7(12), p. 466. doi: 10.3390/jcm7120466.

Herrnberger, B., Kempf, S. and Ehret, G. (2002) ‘Basic maps in the auditory midbrain’, *Biological Cybernetics*, 87(4), pp. 231–240. doi: 10.1007/s00422-002-0337-y.

van den Heuvel, M. P. *et al.* (2015) ‘The Neonatal Connectome During Preterm Brain Development’, *Cerebral Cortex*, 25(9), pp. 3000–3013. doi: 10.1093/cercor/bhu095.

Hidalgo, A. and Ffrench-Constant, C. (2003) ‘The control of cell number during central nervous system development in flies and mice’, *Mechanisms of Development*, 120(11), pp. 1311–1325.

Hirabayashi, Y. *et al.* (2004) ‘The Wnt/β-catenin pathway directs neuronal differentation of cortical neural precursor cells’, *Development*, 131, pp. 2791–2801.

Hodges, S. L. *et al.* (2018) ‘Neuronal subset-specific deletion of Pten results in aberrant Wnt signaling and memory impairments’, *Brain Research*, 1699, pp. 100–106. doi: 10.1016/j.brainres.2018.08.007.

Hong, G. *et al.* (2018) 'Mesh electronics: a new paradigm for tissue-like brain probes', *Current Opinion in Neurobiology*. Elsevier Ltd, pp. 33–41. doi: 10.1016/j.conb.2017.11.007.

Hornig, M. *et al.* (2018) 'Prenatal fever and autism risk', *Molecular Psychiatry*, 23(3), pp. 759–766. doi: 10.1038/mp.2017.119.

Horton, N. G. *et al.* (2013) 'In vivo three-photon microscopy of subcortical structures within an intact mouse brain', *Nature Photonics*, 7(3), pp. 205–209. doi: 10.1038/nphoton.2012.336.

Huang, C. L. and Winer, J. A. (2000) 'Auditory thalamocortical projections in the cat: Laminar and areal patterns of input', *Journal of Comparative Neurology*, 427(2), pp. 302–331. doi: 10.1002/1096-9861(20001113)427:2.

Huang, S.-M. A. *et al.* (2009) 'Tankyrase inhibition stabilizes axin and antagonizes Wnt signalling', *Nature*, 461, pp. 614–620.

Hubel, D. H. (1957) 'Tungsten microelectrode for recording from single units', *Science*, 125(3247), pp. 549–550. doi: 10.1126/science.125.3247.549.

Huber, D. *et al.* (2012) 'Multiple dynamic representations in the motor cortex during sensorimotor learning', *Nature*, 484(7395), pp. 473–478. doi: 10.1038/nature11039.

Hubl, D. *et al.* (2003) 'Functional imbalance of visual pathways indicates alternative face processing strategies in autism', *Neurology*, 61(9), pp. 1232–1237. doi: 10.1212/01.WNL.0000091862.22033.1A.

Huffman, L. C. *et al.* (2011) 'Management of Symptoms in Children With Autism Spectrum Disorders: A Comprehensive Review of Pharmacologic and Complementary-Alternative Medicine Treatments', *Journal of Developmental & Behavioral Pediatrics*, 32(1), pp. 56–68. doi: 10.1097/DBP.0b013e3182040acf.

Hutsler, J. J. and Zhang, H. (2010) 'Increased dendritic spine densities on cortical projection neurons in autism spectrum disorders', *Brain Research*, 1309, pp. 83–94. doi: 10.1016/j.brainres.2009.09.120.

Huttenlocher, P. R. (1990) 'Morphometric study of human cerebral cortex development', *Neuropsychologia*, 28(6), pp. 517–527. doi: 10.1016/0028-3932(90)90031-I.

Huttenlocher, P. R. and Dabholkar, A. S. (1997) 'Regional differences in synaptogenesis in human cerebral cortex', *Journal of Comparative Neurology*, 387(2), pp. 167–178. doi: 10.1002/(SICI)1096-9861(19971020)387:2<167::AID-CNE1>3.0.CO;2-Z.

Hyde, K. L. *et al.* (2010) 'Neuroanatomical differences in brain areas implicated in perceptual and other core features of autism revealed by cortical thickness analysis

and voxel-based morphometry', *Human Brain Mapping*, 31(4), pp. 556–566. doi: 10.1002/hbm.20887.

Imig, T. J. and Brugge, J. F. (1978) 'Sources and terminations of callosal axons related to binaural and frequency maps in primary auditory cortex of the cat', *The Journal of Comparative Neurology*, 182(4), pp. 637–660. doi: 10.1002/cne.901820406.

Imig, T. J. and Morel, A. (1985) 'Tonotopic organization in ventral nucleus of medial geniculate body in the cat', *Journal of Neurophysiology*, 53(1), pp. 309–340. doi: 10.1152/jn.1985.53.1.309.

Inagaki, S. *et al.* (2019) 'Imaging local brain activity of multiple freely moving mice sharing the same environment', *Scientific Reports*, 9(1), pp. 1–9. doi: 10.1038/s41598-019-43897-x.

Inamura, N. *et al.* (2012) 'Intrinsic and extrinsic mechanisms control the termination of cortical interneuron migration', *Journal of Neuroscience*, 32(17), pp. 6032–6042. doi: 10.1523/jneurosci.3446-11.2012.

Jaramillo, S. and Zador, A. M. (2011) 'The auditory cortex mediates the perceptual effects of acoustic temporal expectation', *Nature Neuroscience*, 14(2), pp. 246–253. doi: 10.1038/nn.2688.

Järvinen-Pasley, A. *et al.* (2008a) 'Enhanced perceptual processing of speech in autism', *Developmental Science*, 11(1), pp. 109–121. doi: 10.1111/j.1467-7687.2007.00644.x.

Järvinen-Pasley, A. and Heaton, P. (2007) 'Evidence for reduced domain-specificity in auditory processing in autism', *Developmental Science*, 10(6), pp. 786–793. doi: 10.1111/j.1467-7687.2007.00637.x.

Järvinen-Pasley, A., Pasley, J. and Heaton, P. (2008b) 'Is the linguistic content of speech less salient than its perceptual features in autism?', *Journal of Autism and Developmental Disorders*, 38(2), pp. 239–248. doi: 10.1007/s10803-007-0386-0.

Jeremy Hill, N. *et al.* (2012) 'Recording human electrocorticographic (ECoG) signals for neuroscientific research and real-time functional cortical mapping', *Journal of Visualized Experiments*, (64), p. 3993. doi: 10.3791/3993.

Ji, X. Y. *et al.* (2016) 'Thalamocortical Innervation Pattern in Mouse Auditory and Visual Cortex: Laminar and Cell-Type Specificity', *Cerebral Cortex*, 26(6), pp. 2612–2625. doi: 10.1093/cercor/bhv099.

Jiang, X. and Nardelli, J. (2016) 'Cellular and molecular introduction to brain development', *Neurobiol Dis.*, 92, pp. 3–17.

Johnson, C. P. *et al.* (2007) 'Identification and evaluation of children with autism

spectrum disorders', *Pediatrics*, 120(5), pp. 1183–1215. doi: 10.1542/peds.2007-2361.

Jolliffe, T. and Baron-Cohen, S. (1997) 'Are people with autism and Asperger syndrome faster than normal on the Embedded Figures Test?', *Journal of Child Psychology and Psychiatry and Allied Disciplines*, 38(5), pp. 527–534. doi: 10.1111/j.1469-7610.1997.tb01539.x.

Jones, C. R. G. *et al.* (2009) 'Auditory discrimination and auditory sensory behaviours in autism spectrum disorders', *Neuropsychologia*, 47(13), pp. 2850–2858. doi: 10.1016/j.neuropsychologia.2009.06.015.

De Jonge, M. V. *et al.* (2007) 'Visual information processing in high-functioning individuals with autism spectrum disorders and their parents', *Neuropsychology*, 21(1), pp. 65–73. doi: 10.1037/0894-4105.21.1.65.

Ju, A. *et al.* (2014) 'Juvenile manifestation of ultrasound communication deficits in the neuroligin-4 null mutant mouse model of autism', *Behavioural Brain Research*, 270, pp. 159–164. doi: 10.1016/j.bbr.2014.05.019.

Juavinett, A. L., Bekheet, G. and Churchland, A. K. (2019) 'Chronically implanted Neuropixels probes enable high-yield recordings in freely moving mice', *eLife*, 8, pp. 1–17. doi: 10.7554/elife.47188.

Jun, J. J. *et al.* (2017) 'Fully integrated silicon probes for high-density recording of neural activity', *Nature*, 551(7679), pp. 232–236. doi: 10.1038/nature24636.

Just, M. A. *et al.* (2004) 'Cortical activation and synchronization during sentence comprehension in high-functioning autism: Evidence of underconnectivity', *Brain*, 127(8), pp. 1811–1821. doi: 10.1093/brain/awh199.

Just, M. A. *et al.* (2007) 'Functional and anatomical cortical underconnectivity in autism: Evidence from an fmri study of an executive function task and corpus callosum morphometry', *Cerebral Cortex*, 17(4), pp. 951–961. doi: 10.1093/cercor/bhl006.

Kaas, J. H. and Hackett, T. A. (1998) 'Subdivisions of auditory cortex and levels of processing in primates', *Audiology and Neuro-Otology*, 3(2–3), pp. 73–85. doi: 10.1159/000013783.

Kaas, J. H. and Hackett, T. A. (2000) 'Subdivisions of auditory cortex and processing streams in primates', *Proceedings of the National Academy of Sciences of the United States of America*, 97(22), pp. 11793–11799. doi: 10.1073/pnas.97.22.11793.

Kadunce, D. C. *et al.* (2001) 'The influence of visual and auditory receptive field organization on multisensory integration in the superior colliculus', *Experimental Brain Research*, 139(3), pp. 303–310. doi: 10.1007/s002210100772.

Kanner, L. (1943) ‘Autistic disturbances of affective contract’, *Nervous Child*, 2, pp. 217–250.

Kataoka, S. *et al.* (2013) ‘Autism-like behaviours with transient histone hyperacetylation in mice treated prenatally with valproic acid’, *International Journal of Neuropsychopharmacology*, 16(1), pp. 91–103. doi: 10.1017/S1461145711001714.

Kato, H. K., Gillet, S. N. and Isaacson, J. S. (2015) ‘Flexible Sensory Representations in Auditory Cortex Driven by Behavioral Relevance’, *Neuron*, 88, pp. 1027–1039. doi: 10.1016/j.neuron.2015.10.024.

Kéïta, L., Mottron, L. and Bertone, A. (2010) ‘Far visual acuity is unremarkable in autism: Do we need to focus on crowding?’, *Autism Research*, 3(6), pp. 333–341. doi: 10.1002/aur.164.

Kennedy, D. P., Redcay, E. and Courchesne, E. (2006) ‘Failing to deactivate: Resting functional abnormalities in autism’, *Proceedings of the National Academy of Sciences of the United States of America*, 103(21), pp. 8275–8280. doi: 10.1073/pnas.0600674103.

Kennedy, H., Wianny, F. and Dehay, C. (2021) ‘Determinants of primate neurogenesis and the deployment of top-down generative networks in the cortical hierarchy’, *Current Opinion in Neurobiology*, 66. doi: 10.1016/j.conb.2020.09.012ï.

Kern, J. K. *et al.* (2006) ‘The pattern of sensory processing abnormalities in autism’, *Autism*, 10(5), pp. 480–494. doi: 10.1177/1362361306066564.

Kerr, J. N. D. and Denk, W. (2008) ‘Imaging in vivo: Watching the brain in action’, *Nature Reviews Neuroscience*, 9(3), pp. 195–205. doi: 10.1038/nrn2338.

Khalfa, S. *et al.* (2004) ‘Increased perception of loudness in autism’, *Hearing Research*, 198(1–2), pp. 87–92. doi: 10.1016/j.heares.2004.07.006.

Kim, E. J. *et al.* (2015) ‘Three Types of Cortical Layer 5 Neurons That Differ in Brain-wide Connectivity and Function’, *Neuron*, 88(6), pp. 1253–1267.

Kim, K. C. *et al.* (2011) ‘The critical period of valproate exposure to induce autistic symptoms in Sprague-Dawley rats’, *Toxicology Letters*, 201(2), pp. 137–142. doi: 10.1016/j.toxlet.2010.12.018.

Kim, S. J. *et al.* (2006) ‘Electrophysiological mapping of cat primary auditory cortex with multielectrode arrays’, *Annals of Biomedical Engineering*, 34(2), pp. 300–309. doi: 10.1007/s10439-005-9037-9.

Klaus, A. and Birchmeier, W. (2008) ‘Wnt signalling and its impact on development and cancer’, *Nature Reviews Cancer*, 8(5), pp. 387–398. doi: 10.1038/nrc2389.

Klin, A. (1993) 'Auditory brainstem responses in autism: Brainstem dysfunction or peripheral hearing loss?', *Journal of Autism and Developmental Disorders*, 23(1), pp. 15–35. doi: 10.1007/BF01066416.

Koh, H. C., Milne, E. and Dobkins, K. (2010a) 'Contrast sensitivity for motion detection and direction discrimination in adolescents with autism spectrum disorders and their siblings', *Neuropsychologia*, 48(14), pp. 4046–4056. doi: 10.1016/j.neuropsychologia.2010.10.008.

Koh, H. C., Milne, E. and Dobkins, K. (2010b) 'Spatial contrast sensitivity in adolescents with autism spectrum disorders', *Journal of Autism and Developmental Disorders*, 40(8), pp. 978–987. doi: 10.1007/s10803-010-0953-7.

Komiyama, T. *et al.* (2010) 'Learning-related fine-scale specificity imaged in motor cortex circuits of behaving mice', *Nature*, 464, pp. 1182–1186. doi: 10.1038/nature08897.

von Kriegstein, K., Patterson, R. D. and Griffiths, T. D. (2008) 'Task-Dependent Modulation of Medial Geniculate Body Is Behaviorally Relevant for Speech Recognition', *Current Biology*, 18(23), pp. 1855–1859. doi: 10.1016/j.cub.2008.10.052.

Kuida, K. *et al.* (1998) 'Reduced apoptosis and cytochrome C-mediated caspase activation in mice lacking Caspase 9', *Cell*, 94(3), pp. 325–337. doi: 10.1016/S0092-8674(00)81476-2.

Kumar, S. *et al.* (2019) 'Impaired neurodevelopmental pathways in autism spectrum disorder: A review of signaling mechanisms and crosstalk', *Journal of Neurodevelopmental Disorders*, 11(1), pp. 1–14. doi: 10.1186/s11689-019-9268-y.

Kwakye, L. D. *et al.* (2011) 'Altered auditory and multisensory temporal processing in autism spectrum disorders', *Frontiers in Integrative Neuroscience*, 4(129), pp. 1–11. doi: 10.3389/fnint.2010.00129.

Kwon, S. *et al.* (2007) 'Electrophysiologic assessment of central auditory processing by auditory brainstem responses in children with autism spectrum disorders', *Journal of Korean Medical Science*, 22(4), pp. 656–659. doi: 10.3346/jkms.2007.22.4.656.

Labouesse, M. A. *et al.* (2015) 'Maternal immune activation induces GAD1 and GAD2 promoter remodeling in the offspring prefrontal cortex', *Epigenetics*, 10(12), pp. 1143–1155. doi: 10.1080/15592294.2015.1114202.

Lai, X. *et al.* (2018) 'Vitamin A Deficiency Induces Autistic-Like Behaviors in Rats by Regulating the RARβ-CD38-Oxytocin Axis in the Hypothalamus', *Molecular Nutrition and Food Research*, 62(5). doi: 10.1002/mnfr.201700754.

Lainhart, J. E. *et al.* (2006) 'Head circumference and height in autism: A study by the collaborative program of excellence in autism', *American Journal of Medical Genetics, Part A*, 140(21), pp. 2257–2274. doi: 10.1002/ajmg.a.31465.

Lange, N. *et al.* (2010) 'Atypical diffusion tensor hemispheric asymmetry in autism', *Autism Research*, 3(6), pp. 350–358. doi: 10.1002/aur.162.

Larkum, M. E. (2013) 'The yin and yang of cortical layer 1', *Nature Neuroscience*, 16, pp. 114–115.

Lee, B. K. *et al.* (2015) 'Maternal hospitalization with infection during pregnancy and risk of autism spectrum disorders', *Brain, Behavior, and Immunity*, 44, pp. 100–105. doi: 10.1016/j.bbi.2014.09.001.

Lee, C. C. *et al.* (2004) 'Concurrent Tonotopic Processing Streams in Auditory Cortex', *Cerebral Cortex*, 14(4), pp. 441–451. doi: 10.1093/cercor/bhh006.

Lee, C. C. (2013) 'Thalamic and cortical pathways supporting auditory processing.', *Brain and language*, 126(1), pp. 22–28. doi: 10.1016/j.bandl.2012.05.004.

Lee, C. C. and Sherman, S. M. (2010) 'Drivers and modulators in the central auditory pathways', *Frontiers in Neuroscience*, 4(1), pp. 79–86. doi: 10.3389/neuro.01.014.2010.

Lee, C. C. and Winer, J. A. (2008) 'Connections of cat auditory cortex: II. Commissural system', *Journal of Comparative Neurology*, 507(6), pp. 1901–1919. doi: 10.1002/cne.21614.

Lee, J. E. *et al.* (2007a) 'Diffusion tensor imaging of white matter in the superior temporal gyrus and temporal stem in autism', *Neuroscience Letters*, 424(2), pp. 127–132. doi: 10.1016/j.neulet.2007.07.042.

Lee, P. S. *et al.* (2007b) 'Atypical neural substrates of Embedded Figures Task performance in children with Autism Spectrum Disorder', *NeuroImage*, 38(1), pp. 184–193. doi: 10.1016/j.neuroimage.2007.07.013.

Leekam, S. R. *et al.* (2007) 'Describing the sensory abnormalities of children and adults with autism', *Journal of Autism and Developmental Disorders*, 37(5), pp. 894–910. doi: 10.1007/s10803-006-0218-7.

Letzkus, J. J. *et al.* (2011) 'A disinhibitory microcircuit for associative fear learning in the auditory cortex', *Nature*, 480(7377), pp. 331–335. doi: 10.1038/nature10674.

Lichtenstein, P. *et al.* (2010) 'The genetics of autism spectrum disorders and related neuropsychiatric disorders in childhood', *American Journal of Psychiatry*, 167(11), pp. 1357–1363. doi: 10.1176/appi.ajp.2010.10020223.

Lim, L. *et al.* (2018) 'Development and Functional Diversification of Cortical

Interneurons', *Neuron*, 100, pp. 294–313. doi: 10.1016/j.neuron.2018.10.009.

Lincoln, A. J. *et al.* (1993) 'Contextual probability evaluation in autistic, receptive developmental language disorder, and control children: Event-related brain potential evidence', *Journal of Autism and Developmental Disorders*, 23(1), pp. 37–58. doi: 10.1007/BF01066417.

Linden, J. F. (2003) 'Columnar Transformations in Auditory Cortex? A Comparison to Visual and Somatosensory Cortices', *Cerebral Cortex*, 13(1), pp. 83–89. doi: 10.1093/cercor/13.1.83.

Lindholm, E. and Koriath, J. J. (1985) 'Analysis of multiple event related potential components in a tone discrimination task', *International Journal of Psychophysiology*, 3(2), pp. 121–129. doi: 10.1016/0167-8760(85)90032-7.

Ling, G. and Gerard, R. W. (1949) 'The normal membrane potential of frog sartorius fibers', *Journal of cellular physiology*, 34(3), pp. 383–396. doi: 10.1002/jcp.1030340304.

Linke, A. C. *et al.* (2018) 'Children with ASD show links between aberrant sound processing, social symptoms, and atypical auditory interhemispheric and thalamocortical functional connectivity', *Developmental Cognitive Neuroscience*, 29, pp. 117–126. doi: 10.1016/j.dcn.2017.01.007.

Littlefield, P. D. and Brungart, D. S. (2020) 'Long-Term Sensorineural Hearing Loss in Patients With Blast-Induced Tympanic Membrane Perforations', *Ear & Hearing*, 41(1), pp. 165–172. doi: 10.1097/AUD.0000000000000751.

Liu, C. *et al.* (2002) 'Control of β-catenin phosphorylation/degradation by a dual-kinase mechanism', *Cell*, 108(6), pp. 837–847. doi: 10.1016/S0092-8674(02)00685-2.

Lombardo, M. V. *et al.* (2018) 'Maternal immune activation dysregulation of the fetal brain transcriptome and relevance to the pathophysiology of autism spectrum disorder', *Molecular Psychiatry*, 23(4), pp. 1001–1013. doi: 10.1038/mp.2017.15.

Lotspeich, L. J. *et al.* (2004) 'Investigation of Neuroanatomical Differences between Autism and Asperger Syndrome', *Archives of General Psychiatry*, 61(3), pp. 291–298. doi: 10.1001/archpsyc.61.3.291.

Lovelace, C. T., Stein, B. E. and Wallace, M. T. (2003) 'An irrelevant light enhances auditory detection in humans: A psychophysical analysis of multisensory integration in stimulus detection', *Cognitive Brain Research*, 17(2), pp. 447–453. doi: 10.1016/S0926-6410(03)00160-5.

Loveland, K. A. *et al.* (2008) 'Judgments of auditory-visual affective congruence in adolescents with and without autism: A pilot study of a new task using fMRI',

Perceptual and Motor Skills, 107(2), pp. 557–575. doi: 10.2466/PMS.107.2.557-575.

Lu, J., Wang, D. and Shen, J. (2017) 'Hedgehog signalling is required for cell survival in Drosophila wing pouch cells', *Scientific Reports*, 7(1), pp. 1–10. doi: 10.1038/s41598-017-10550-4.

Lui, J. H., Hansen, D. V and Kriegstein, A. R. (2011) 'Development and Evolution of the Human Neocortex', *Cell*, 146, pp. 18–36. doi: 10.1016/j.cell.2011.06.030.

Lukaszewicz, A. *et al.* (2005) 'G1 phase regulation, area-specific cell cycle control, and cytoarchitectonics in the primate cortex', *Neuron*, 47(3), pp. 353–364. doi: 10.1016/j.neuron.2005.06.032.

Luo, W. and Lin, S. C. (2004) 'Axin: A master scaffold for multiple signaling pathways', *NeuroSignals*, 13, pp. 99–113.

Ma, B. and Hottiger, M. O. (2016) 'Crosstalk between wnt/β-catenin and NF-κB signaling pathway during inflammation', *Frontiers in Immunology*, 7(387), pp. 1–14. doi: 10.3389/fimmu.2016.00378.

Ma, D. Q. *et al.* (2005) 'Identification of significant association and gene-gene interaction of GABA receptor subunit genes in autism', *American Journal of Human Genetics*, 77(3), pp. 377–388. doi: 10.1086/433195.

Machold, R. *et al.* (2003) 'Sonic hedgehog is required for progenitor cell maintenance in telencephalic stem cell niches', *Neuron*, 39(6), pp. 937–950. doi: 10.1016/S0896-6273(03)00561-0.

Malkova, N. V. *et al.* (2012) 'Maternal immune activation yields offspring displaying mouse versions of the three core symptoms of autism', *Brain, Behavior, and Immunity*, 26(4), pp. 607–616. doi: 10.1016/j.bbi.2012.01.011.

Malmierca, M. S., Le Beau, F. E. N. and Rees, A. (1996) 'The topographical organization of descending projections from the central nucleus of the inferior colliculus in guinea pig', *Hearing Research*, 93(1–2), pp. 167–180. doi: 10.1016/0378-5955(95)00227-8.

Malmierca, M. S. and Ryugo, D. K. (2012) 'Auditory system', in Watson, C., Paxinos, G., and Puelles, L. (eds) *The Mouse Nervous System*. Elsevier, pp. 607–638.

Manjaly, Z. M. *et al.* (2007) 'Neurophysiological correlates of relatively enhanced local visual search in autistic adolescents', *NeuroImage*, 35(1), pp. 283–291. doi: 10.1016/j.neuroimage.2006.11.036.

Manning, C. *et al.* (2015) 'Enhanced integration of motion information in children with autism', *Journal of Neuroscience*, 35(18), pp. 6979–6986. doi: 10.1523/JNEUROSCI.4645-14.2015.

Marchetto, M. C. *et al.* (2017) 'Altered proliferation and networks in neural cells derived from idiopathic autistic individuals', *Mol Psychiatry*, 22(6), pp. 820–835. doi: 10.1038/mp.2016.95.

Marchetto, M. C. N. *et al.* (2010) 'A model for neural development and treatment of rett syndrome using human induced pluripotent stem cells', *Cell*, 143(4), pp. 527–539. doi: 10.1016/j.cell.2010.10.016.

Marco, E. J. *et al.* (2011) 'Sensory Processing in Autism: A Review of Neurophysiologic Findings', *Pediatr Res*, 69(5 Pt 2), pp. 48R-54R.

Marco, E. J. *et al.* (2012) 'Children With Autism Show Reduced Somatosensory Response: An MEG Study', *Autism Research*, 5(5), pp. 340–351. doi: 10.1002/aur.1247.

Mariani, J. *et al.* (2015) 'FOXG1-Dependent Dysregulation of GABA/Glutamate Neuron Differentiation in Autism Spectrum Disorders', *Cell*, 162(2), pp. 375–390. doi: 10.1016/j.cell.2015.06.034.

Marín, O. and Rubenstein, J. L. R. (2001) 'A long, remarkable journey: Tangential migration in the telencephalon', *Nature Reviews Neuroscience*, 2(11), pp. 780–790. doi: 10.1038/35097509.

Markram, H. *et al.* (2008a) 'The origin and specification of cortical interneurons', *Nature Reviews Neuroscience*, 7(july), pp. 687–696. doi: 10.1038/nrn1954.

Markram, K. *et al.* (2008b) 'Abnormal fear conditioning and amygdala processing in an animal model of autism', *Neuropsychopharmacology*, 33(4), pp. 901–912. doi: 10.1038/sj.npp.1301453.

Martin, P. M. *et al.* (2013) 'A rare WNT1 missense variant overrepresented in ASD leads to increased Wnt signal pathway activation.', *Translational psychiatry*, 3(9), p. 301. doi: 10.1038/tp.2013.75.

Martineau, J. *et al.* (1984) 'Evoked Potentials and P 300 during Sensory Conditioning in Autistic Children', *Annals of the New York Academy of Sciences*, 425, pp. 362–369. doi: 10.1111/j.1749-6632.1984.tb23557.x.

Marx, M. *et al.* (2015) 'Neocortical Layer 6B as a Remnant of the Subplate - A Morphological Comparison', *Cerebral Cortex*, 27(2), p. bhv279. doi: 10.1093/cercor/bhv279.

Matsuzaki, J. *et al.* (2012) 'Differential responses of primary auditory cortex in autistic spectrum disorder with auditory hypersensitivity', *NeuroReport*, 23(2), pp. 113–118. doi: 10.1097/WNR.0b013e32834ebf44.

Mayer, C. *et al.* (2018) 'Developmental diversification of cortical inhibitory interneurons', *Nature Publishing Group*, 555. doi: 10.1038/nature25999.

McBride, K. L. *et al.* (2010) 'Confirmation study of PTEN mutations among individuals with autism or developmental delays/mental retardation and macrocephaly', *Autism Research*, 3(3), pp. 137–141. doi: 10.1002/aur.132.

McCaffery, P. and Deutsch, C. K. (2005) 'Macrocephaly and the control of brain growth in autistic disorders', *Progress in Neurobiology*, 77(1–2), pp. 38–56.

McPartland, J. *et al.* (2004) 'Event-related brain potentials reveal anomalies in temporal processing of faces in autism spectrum disorder', *Journal of Child Psychology and Psychiatry and Allied Disciplines*, 45(7), pp. 1235–1245. doi: 10.1111/j.1469-7610.2004.00318.x.

Meador, K. J. (2008) 'Effects of in Utero Antiepileptic Drug Exposure', *Epilepsy Currents*, 8(6), pp. 143–147. doi: 10.1111/j.1535-7511.2008.00273.x.

Meador, K. J. *et al.* (2009) 'Cognitive function at 3 years of age after fetal exposure to antiepileptic drugs', *New England Journal of Medicine*, 360(16), pp. 1597–1605. doi: 10.1056/NEJMoa0803531.

Meador, K. J. *et al.* (2011) 'Foetal antiepileptic drug exposure and verbal versus non-verbal abilities at three years of age', *Brain*, 134(2), pp. 396–404. doi: 10.1093/brain/awq352.

Medzhitov, R. (2001) 'Toll-like receptors and innate immunity', *Nature Reviews Immunology*, 1(2), pp. 135–145. doi: 10.1038/35100529.

Meininger, V., Pol, D. and Derer, P. (1986) 'The inferior colliculus of the mouse. A Nissl and Golgi study', *Neuroscience*, 17(4), pp. 1159–1171. doi: 10.1016/0306-4522(86)90085-0.

Meltzer, A. and Van De Water, J. (2017) 'The Role of the Immune System in Autism Spectrum Disorder', *Neuropsychopharmacology*, 42(1), pp. 284–298. doi: 10.1038/npp.2016.158.

Meltzer, N. E. and Ryugo, D. K. (2006) 'Projections from auditory cortex to cochlear nucleus: A comparative analysis of rat and mouse', *Anatomical Record - Part A Discoveries in Molecular, Cellular, and Evolutionary Biology*. Anat Rec A Discov Mol Cell Evol Biol, pp. 397–408. doi: 10.1002/ar.a.20300.

Meng, E. (2018) 'Technologies to Interface with the Brain for Recording and Modulation', in *National Academy of Engineering. Frontiers of Engineering: Reports on Leading-Edge Engineering from the 2017 Symposium.* National Academies Press. doi: 10.17226/24906.

Meredith, M. A. and Stein, B. E. (1986) 'Visual, auditory, and somatosensory convergence on cells in superior colliculus results in multisensory integration', *Journal of Neurophysiology*, 56(3), pp. 640–662. doi: 10.1152/jn.1986.56.3.640.

Meyer, A. C. *et al.* (2009) 'Tuning of synapse number, structure and function in the cochlea', *Nature Neuroscience*, 12(4), pp. 444–453. doi: 10.1038/nn.2293.

Meyer, A. F. *et al.* (2018) 'A Head-Mounted Camera System Integrates Detailed Behavioral Monitoring with Multichannel Electrophysiology in Freely Moving Mice', *Neuron*, 100(1), pp. 46-60.e7. doi: 10.1016/j.neuron.2018.09.020.

Meyer, U. *et al.* (2008) 'Adult brain and behavioral pathological markers of prenatal immune challenge during early/middle and late fetal development in mice', *Brain, Behavior, and Immunity*, 22(4), pp. 469–486. doi: 10.1016/j.bbi.2007.09.012.

Meyer, U. (2014) 'Prenatal Poly(I:C) exposure and other developmental immune activation models in rodent systems', *Biological Psychiatry*, 75(4), pp. 307–315. doi: 10.1016/j.biopsych.2013.07.011.

Meyer, U. and Feldon, J. (2012) 'To poly(I:C) or not to poly(I:C): Advancing preclinical schizophrenia research through the use of prenatal immune activation models', *Neuropharmacology*, 62(3), pp. 1308–1321. doi: 10.1016/j.neuropharm.2011.01.009.

Mihrshahi, R. (2006) 'The corpus callosum as an evolutionary innovation', *Journal of Experimental Zoology Part B: Molecular and Developmental Evolution*, 306(1), pp. 8–17. doi: 10.1002/jez.b.21067.

Mikkelsen, M. *et al.* (2018) 'Autism spectrum disorder in the scope of tactile processing', *Developmental Cognitive Neuroscience*, 29, pp. 140–150. doi: 10.1016/j.dcn.2016.12.005.

Miles, J. H. (2011) 'Autism spectrum disorders-A genetics review', *Genetics in Medicine*, 13(4), pp. 278–294. doi: 10.1097/GIM.0b013e3181ff67ba.

Milne, E. *et al.* (2002) 'High motion coherence thresholds in children with autism', *Journal of Child Psychology and Psychiatry and Allied Disciplines*, 43(2), pp. 255–263. doi: 10.1111/1469-7610.00018.

Mines, M. A. *et al.* (2010) 'GSK3 Influences Social Preference and Anxiety-Related Behaviors during Social Interaction in a Mouse Model of Fragile X Syndrome and Autism', *PLoS ONE*. Edited by M. A. Smith, 5(3), p. e9706. doi: 10.1371/journal.pone.0009706.

Mirzaa, G. M. and Dobyns, W. B. (2017) 'Disorders of brain size', in *Swaiman's Pediatric Neurology: Principles and Practice: Sixth Edition*. Elsevier Inc., pp. 208–217.

Mittmann, W. *et al.* (2011) 'Two-photon calcium imaging of evoked activity from L5 somatosensory neurons in vivo', *Nature Neuroscience*, 14(8), pp. 1089–1093. doi: 10.1038/nn.2879.

Miyazaki, M. *et al.* (2007) 'Short-latency somatosensory evoked potentials in

infantile autism: Evidence of hyperactivity in the right primary somatosensory area', *Developmental Medicine and Child Neurology*, 49(1), pp. 13–17. doi: 10.1017/S0012162207000059.x.

Mody, M. *et al.* (2013) 'Speech and language in autism spectrum disorder: a view through the lens of behavior and brain imaging', *Neuropsychiatry*, 3(2), pp. 223–232. doi: 10.2217/NPY.13.19.

Moessner, R. *et al.* (2007) 'Contribution of SHANK3 mutations to autism spectrum disorder', *American Journal of Human Genetics*, 81(6), pp. 1289–1297. doi: 10.1086/522590.

Molnár, Z. *et al.* (2006) 'Comparative aspects of cerebral cortical development', *European Journal of Neuroscience*, 23(4), pp. 921–934. doi: 10.1111/j.1460-9568.2006.04611.x.

Molnár, Z. (2011) 'Evolution of Cerebral Cortical Development', *Brain, Behavior and Evolution*, 78, pp. 94–107. doi: 10.1159/000327325.

Molyneaux, B. J. *et al.* (2007) 'Neuronal subtype specification in the cerebral cortex', *Nature Reviews Neuroscience*, 8, pp. 427–437.

Mongillo, E. A. *et al.* (2008) 'Audiovisual processing in children with and without autism spectrum disorders', *Journal of Autism and Developmental Disorders*, 38(7), pp. 1349–1358. doi: 10.1007/s10803-007-0521-y.

Moore, A. K. and Wehr, M. (2013) 'Parvalbumin-expressing inhibitory interneurons in auditory cortex are well-tuned for frequency', *Journal of Neuroscience*, 33(34), pp. 13713–13723. doi: 10.1523/JNEUROSCI.0663-13.2013.

Moore, J. K. *et al.* (1996) 'gamma-Aminobutyric acid and glycine in the baboon cochlear nuclei: an immunocytochemical colocalization study with reference to interspecies differences in inhibitory systems', *J Comp Neurol*, 369(4), pp. 497–519.

Moore, J. K. and Osen, K. K. (1979) 'The cochlear nuclei in man', *American Journal of Anatomy*, 154(3), pp. 393–417. doi: 10.1002/aja.1001540306.

Moran, J. M. *et al.* (2011) 'Impaired theory of mind for moral judgment in high-functioning autism', *Proceedings of the National Academy of Sciences of the United States of America*, 108(7), pp. 2688–2692. doi: 10.1073/pnas.1011734108.

Mottron, L. *et al.* (2006) 'Enhanced Perceptual Functioning in Autism: An Update, and Eight Principles of Autistic Perception', *Journal of Autism and Developmental Disorders*, 36(1), pp. 27–43. doi: 10.1007/s10803-005-0040-7.

Mottron, L. and Belleville, S. (1993) 'A study of perceptual analysis in a high-level autistic subject with exceptional graphic abilities', *Brain and Cognitiion*, 23, pp. 279–309.

Mottron, L. and Burack, J. (2001) 'Enchanced Perceptual Functioning in the Development of Autism', in Burack, J. et al. (eds) *The development of Autism: Perspectives from Theory and Research*, pp. 131–148.

Mottron, L., Peretz, I. and Menard, E. (2000) 'Local and Global Processing of Music in High-functioning Persons with Autism: Beyond Central Coherence?', *Journal of Child Psychology and Psychiatry*, 41(8), pp. 1057–1065. doi: 10.1111/1469-7610.00693.

Müller, R. A. *et al.* (1999) 'Brain mapping of language and auditory perception in high-functioning autistic adults: A PET study', *Journal of Autism and Developmental Disorders*, 29(1), pp. 19–31. doi: 10.1023/A:1025914515203.

Mulligan, K. A. and Cheyette, B. N. R. (2016) 'Neurodevelopmental Perspectives on Wnt Signaling in Psychiatry', *Molecular Neuropsychiatry*, 2(4), pp. 219–246. doi: 10.1159/000453266.

Munji, R. N. *et al.* (2011) 'Wnt Signaling Regulates Neuronal Differentiation of Cortical Intermediate Progenitors', *Journal of Neuroscience*, 31(5), pp. 1676–1687. doi: 10.1523/JNEUROSCI.5404-10.2011.

Musk, E. (2019) 'An integrated brain-machine interface platform with thousands of channels', *Journal of Medical Internet Research*, 21(10), p. e16194. doi: 10.2196/16194.

Myers, S. M. *et al.* (2007) 'Management of children with autism spectrum disorders', *Pediatrics*, 120(5), pp. 1162–1182. doi: 10.1542/peds.2007-2362.

Nadebaum, C. *et al.* (2011a) 'Language skills of school-aged children prenatally exposed to antiepileptic drugs', *Neurology*, 76(8), pp. 719–726. doi: 10.1212/WNL.0b013e31820d62c7.

Nadebaum, C. *et al.* (2011b) 'The australian brain and cognition and antiepileptic drugs study: IQ in school-aged children exposed to sodium valproate and polytherapy', *Journal of the International Neuropsychological Society*, 17(1), pp. 133–142. doi: 10.1017/S1355617710001359.

Nelson, E. D., Kavalali, E. T. and Monteggia, L. M. (2006) 'MeCP2-Dependent Transcriptional Repression Regulates Excitatory Neurotransmission', *Current Biology*, 16(7), pp. 710–716. doi: 10.1016/j.cub.2006.02.062.

Nelson, S. B. and Valakh, V. (2015) 'Excitatory/Inhibitory balance and circuit homeostasis in Autism Spectrum Disorders', *Neuron*, 87(4), pp. 684–698. doi: 10.1016/j.neuron.2015.07.033.

Neumann, N. *et al.* (2011) 'Electromagnetic evidence of altered visual processing in autism', *Neuropsychologia*, 49(11), pp. 3011–3017. doi:

10.1016/j.neuropsychologia.2011.06.028.

Nguyen, A. *et al.* (2010) ' Global methylation profiling of lymphoblastoid cell lines reveals epigenetic contributions to autism spectrum disorders and a novel autism candidate gene, RORA , whose protein product is reduced in autistic brain ', *The FASEB Journal*, 24(8), pp. 3036–3051. doi: 10.1096/fj.10-154484.

NHS (2012) *Estimating the Prevalence of Autism Spectrum Conditions in Adults - Extending the 2007 Adult Psychiatric Morbidity Survey*. Available at: https://digital.nhs.uk/data-and-information/publications/statistical/estimating-the-prevalence-of-autism-spectrum-conditions-in-adults/estimating-the-prevalence-of-autism-spectrum-conditions-in-adults-extending-the-2007-adult-psychiatric-morbidity-survey (Accessed: 14 September 2020).

Nicholson, C. and Freeman, J. A. (1975) 'Theory of Current Source-Density Analysis and Determination of Conductivity Tensor for Anuran Cerebellum', *J Neurophysiol*, 38(2), pp. 356–68.

Nicolelis, M. A. L. *et al.* (2003) 'Chronic, multisite, multielectrode recordings in macaque monkeys', *Proceedings of the National Academy of Sciences of the United States of America*, 100(19), pp. 11041–11046. doi: 10.1073/pnas.1934665100.

Nicolini, C. and Fahnestock, M. (2018) 'The valproic acid-induced rodent model of autism', *Experimental Neurology*, 299, pp. 217–227. doi: 10.1016/j.expneurol.2017.04.017.

Novick, B. *et al.* (1980) 'An electrophysiologic indication of auditory processing defects in autism', *Psychiatry Research*, 3(1), pp. 107–114. doi: 10.1016/0165-1781(80)90052-9.

O'Connor, D. H. *et al.* (2010) 'Vibrissa-based object localization in head-fixed mice', *Journal of Neuroscience*, 30(5), pp. 1947–1967. doi: 10.1523/JNEUROSCI.3762-09.2010.

O'Connor, K. (2012) 'Auditory processing in autism spectrum disorder: A review', *Neuroscience and Biobehavioral Reviews*, 36(2), pp. 836–854. doi: 10.1016/j.neubiorev.2011.11.008.

O'Keefe, J. and Recce, M. L. (1993) 'Phase relationship between hippocampal place units and the EEG theta rhythm', *Hippocampus*, 3(3), pp. 317–330. doi: 10.1002/hipo.450030307.

O'Rahilly, R. and Müller, F. (2008) 'Significant features in the early prenatal development of the human brain', *Annals of Anatomy*, 190(2), pp. 105–118. doi: 10.1016/j.aanat.2008.01.001.

O'Riordan, M. A. *et al.* (2001) 'Superior visual search in autism.', *Journal of*

Experimental Psychology: Human Perception and Performance, 27(3), pp. 719–730. doi: 10.1037//0096-1523.27.3.719.

O'Riordan, M. and Plaisted, K. (2001) 'Enhanced discrimination in autism', *Quarterly Journal of Experimental Psychology Section A: Human Experimental Psychology*, 54(4), pp. 961–979. doi: 10.1080/713756000.

O'Roak, B. J. *et al.* (2012) 'Multiplex targeted sequencing identifies recurrently mutated genes in autism spectrum disorders', *Science*, 338(6114), pp. 1619–1622. doi: 10.1126/science.1227764.

Oades, R. D. *et al.* (1988) 'Event-related potentials in autistic and healthy children on an auditory choice reaction time task', *International Journal of Psychophysiology*, 6(1), pp. 25–37. doi: 10.1016/0167-8760(88)90032-3.

Oblak, A. L. *et al.* (2011) 'Altered posterior cingulate cortical cyctoarchitecture, but normal density of neurons and interneurons in the posterior cingulate cortex and fusiform gyrus in autism', *Autism Research*, 4(3), pp. 200–211. doi: 10.1002/aur.188.

Okamoto, H. *et al.* (2010) 'Wnt2 expression and signaling is increased by different classes of antidepressant treatments', *Biological Psychiatry*, 68(6), pp. 521–527. doi: 10.1016/j.biopsych.2010.04.023.

Okerlund, N. D. and Cheyette, B. N. R. (2011) 'Synaptic Wnt signaling-a contributor to major psychiatric disorders?', *Journal of Neurodevelopmental Disorders*, 3(2), pp. 162–174. doi: 10.1007/s11689-011-9083-6.

Oliver, D. L. (1987) 'Projections to the inferior colliculus from the anteroventral cochlear nucleus in the cat: Possible substrates for binaural interaction', *Journal of Comparative Neurology*, 264(1), pp. 24–46. doi: 10.1002/cne.902640104.

Olkowicz, S. *et al.* (2016) 'Birds have primate-like numbers of neurons in the forebrain', *Proceedings of the National Academy of Sciences*, 113(26), pp. 7255–7260.

Oram Cardy, J. E. *et al.* (2008) 'Auditory evoked fields predict language ability and impairment in children', *International Journal of Psychophysiology*, 68(2), pp. 170–175. doi: 10.1016/j.ijpsycho.2007.10.015.

Osei-Sarfo, K. and Gudas, L. J. (2014) 'Retinoic acid suppresses the canonical Wnt signaling pathway in embryonic stem cells and activates the noncanonical Wnt signaling pathway', *Stem Cells*, 32(8), pp. 2061–2071. doi: 10.1002/stem.1706.

Osen, K. K. *et al.* (1984) 'Histochemical localization of acetylcholinesterase in the cochlear and superior olivary nuclei. A reappraisal with emphasis on the cochlear granule cell system - PubMed', *Arch Ital Biol*, 122(3), pp. 169–212.

Oskvig, D. B. *et al.* (2012) 'Maternal immune activation by LPS selectively alters

specific gene expression profiles of interneuron migration and oxidative stress in the fetus without triggering a fetal immune response', *Brain, Behavior, and Immunity*, 26(4), pp. 623–634. doi: 10.1016/j.bbi.2012.01.015.

Otero, J. J. *et al.* (2004) 'β-catenin signaling is required for neural diffrerentiation of embryonic stem cells', *Development*, 131(15), pp. 3545–3557.

Ouellet, L. and de Villers-Sidani, E. (2014) 'Trajectory of the main GABAergic interneuron populations from early development to old age in the rat primary auditory cortex', *Frontiers in Neuroanatomy*, 8(40), pp. 1–15. doi: 10.3389/fnana.2014.00040.

Pachitariu, M. *et al.* (2016) 'Kilosort: realtime spike-sorting for extracellular electrophysiology with hundreds of channels', *bioRxiv*. doi: 10.1101/061481.

Pai, S. *et al.* (2011) 'Minimal Impairment in a Rat Model of Duration Discrimination Following Excitotoxic Lesions of Primary Auditory and Prefrontal Cortices', *Frontiers in Systems Neuroscience*, 5(74), pp. 1–13. doi: 10.3389/fnsys.2011.00074.

Panizzon, M. S. *et al.* (2009) 'Distinct genetic influences on cortical surface area and cortical thickness', *Cerebral Cortex*, 19(11), pp. 2728–2735. doi: 10.1093/cercor/bhp026.

Pannu, K. K. *et al.* (2011) 'Evaluation of Hearing Loss in Tympanic Membrane Perforation', *Indian Journal of Otolaryngology and Head and Neck Surgery*, 63(3), pp. 208–213. doi: 10.1007/s12070-011-0129-6.

Patterson, P. H. (2009) 'Immune involvement in schizophrenia and autism: Etiology, pathology and animal models', *Behavioural Brain Research*, 204(2), pp. 313–321. doi: 10.1016/j.bbr.2008.12.016.

Patterson, P. H. (2011) 'Maternal infection and immune involvement in autism', *Trends in Molecular Medicine*, 17(7), pp. 389–394. doi: 10.1016/j.molmed.2011.03.001.

Pavăl, D. *et al.* (2017) 'Low retinal dehydrogenase 1 (RALDH1) level in prepubertal boys with autism spectrum disorder: A possible link to dopamine dysfunction?', *Clinical Psychopharmacology and Neuroscience*, 15(3), pp. 229–236. doi: 10.9758/cpn.2017.15.3.229.

Peça, J. *et al.* (2011) 'Shank3 mutant mice display autistic-like behaviours and striatal dysfunction', *Nature*, 472(7344), pp. 437–442. doi: 10.1038/nature09965.

Pei, F. *et al.* (2009) 'Neural correlates of texture and contour integration in children with autism spectrum disorders', *Vision Research*, 49(16), pp. 2140–2150. doi: 10.1016/j.visres.2009.06.006.

Pellicano, E. *et al.* (2005) 'Abnormal global processing along the dorsal visual

pathway in autism: A possible mechanism for weak visuospatial coherence?', *Neuropsychologia*, 43(7), pp. 1044–1053. doi: 10.1016/j.neuropsychologia.2004.10.003.

Pelullo, M. *et al.* (2019) 'Wnt, Notch, and TGF-β pathways impinge on hedgehog signaling complexity: An open window on cancer', *Frontiers in Genetics*, 10(711), pp. 1–16. doi: 10.3389/fgene.2019.00711.

Phiel, C. J. *et al.* (2001) 'Histone Deacetylase is a Direct Target of Valproic Acid, a Potent Anticonvulsant, Mood Stabilizer, and Teratogen', *Journal of Biological Chemistry*, 276(39), pp. 36734–36741. doi: 10.1074/jbc.M101287200.

Pierce, K. *et al.* (2011) 'Detecting, studying, and treating autism early: The one-year well-baby check-up approach', *Journal of Pediatrics*, 159(3). doi: 10.1016/j.jpeds.2011.02.036.

Pierce, K. *et al.* (2019) 'Evaluation of the Diagnostic Stability of the Early Autism Spectrum Disorder Phenotype in the General Population Starting at 12 Months', *JAMA Pediatrics*, 173(6), pp. 578–587. doi: 10.1001/jamapediatrics.2019.0624.

Pilaz, L. J. *et al.* (2009) 'Forced G1-phase reduction alters mode of division, neuron number, and laminar phenotype in the cerebral cortex', *Proceedings of the National Academy of Sciences of the United States of America*, 106(51), pp. 21924–21929. doi: 10.1073/pnas.0909894106.

Pinto, D. *et al.* (2014) 'Convergence of genes and cellular pathways dysregulated in autism spectrum disorders', *American Journal of Human Genetics*, 94(5), pp. 677–694. doi: 10.1016/j.ajhg.2014.03.018.

Piton, A. *et al.* (2013) 'Analysis of the effects of rare variants on splicing identifies alterations in GABA A receptor genes in autism spectrum disorder individuals', *European Journal of Human Genetics*, 21(7), pp. 749–756. doi: 10.1038/ejhg.2012.243.

Piven, J. *et al.* (1995) 'An MRI study of brain size in autism', *American Journal of Psychiatry*, 152(8), pp. 1145–1149. doi: 10.1176/ajp.152.8.1145.

Piven, J. *et al.* (1996) 'Regional Brain Enlargement in Autism: A Magnetic Resonance Imaging Study', *Journal of the American Academy of Child and Adolescent Psychiatry*, 35(4), pp. 530–536. doi: 10.1097/00004583-199604000-00020.

Plaisted, K., O'Riordan, M. and Baron-Cohen, S. (1998) 'Enhanced Visual Search for a Conjunctive Target in Autism : A Research Note', *J. Child Psychol. Psychiat*, 39(5), pp. 777–783.

Podleśny-Drabiniok, A. *et al.* (2017) 'Distinct retinoic acid receptor (RAR) isotypes control differentiation of embryonal carcinoma cells to dopaminergic or

striatopallidal medium spiny neurons', *Scientific Reports*, 7(1), pp. 1–14. doi: 10.1038/s41598-017-13826-x.

Pohl-Guimaraes, F., Krahe, T. E. and Medina, A. E. (2011) 'Early valproic acid exposure alters functional organization in the primary visual cortex', *Experimental Neurology*, 228(1), pp. 138–148. doi: 10.1016/j.expneurol.2010.12.025.

Polo-Castillo, L. E. *et al.* (2019) 'Reimplantable Microdrive for Long-Term Chronic Extracellular Recordings in Freely Moving Rats', *Frontiers in Neuroscience*, 13(128), pp. 1–15. doi: 10.3389/fnins.2019.00128.

Posey, D. J. *et al.* (2008) 'Antipsychotics in the treatment of autism', *Journal of Clinical Investigation*, 118(1), pp. 6–14. doi: 10.1172/JCI32483.

Potashner, S. J., Dymczyk, L. and Deangelis, M. M. (1988) 'D-Aspartate Uptake and Release in the Guinea Pig Spinal Cord After Partial Ablation of the Cerebral Cortex', *Journal of Neurochemistry*, 50(1), pp. 103–111. doi: 10.1111/j.1471-4159.1988.tb13236.x.

Prasad, B. C. and Clark, S. G. (2006) 'Wnt signaling establishes anteroposterior neuronal polarity and requires retromer in C. elegans', *Development*, 133(9), pp. 1757–1766. doi: 10.1242/dev.02357.

Prat, C. S. (2011) 'The Brain Basis of Individual Differences in Language Comprehension Abilities', *Language and Linguistics Compass*, 5, pp. 635–649. doi: 10.1111/j.1749-818x.2011.00303.x.

Prieto, J. J., Peterson, B. A. and Winer, J. A. (1994) 'Morphology and spatial distribution of GABAergic neurons in cat primary auditory cortex (AI)', *Journal of Comparative Neurology*, 344(3), pp. 349–382. doi: 10.1002/cne.903440304.

Puts, N. A. J. *et al.* (2013) 'A vibrotactile behavioral battery for investigating somatosensory processing in children and adults', *Journal of Neuroscience Methods*, 218(1), pp. 39–47. doi: 10.1016/j.jneumeth.2013.04.012.

Puts, N. A. J. *et al.* (2014) 'Impaired tactile processing in children with autism spectrum disorder', *Journal of Neurophysiology*, 111(9), pp. 1803–1811. doi: 10.1152/jn.00890.2013.

Qiu, A., Mori, S. and Miller, M. I. (2015) 'Diffusion Tensor Imaging for Understanding Brain Development in Early Life', *Annual Review of Psychology*, 66(1), pp. 853–876. doi: 10.1146/annurev-psych-010814-015340.

Quaresima, V. and Ferrari, M. (2019) 'Functional Near-Infrared Spectroscopy (fNIRS) for Assessing Cerebral Cortex Function During Human Behavior in Natural/Social Situations: A Concise Review', *Organizational Research Methods*, 22(1), pp. 46–68. doi: 10.1177/1094428116658959.

Quartz, S. R. and Sejnowski, T. J. (1997) 'The neural basis of cognitive development: A constructivist manifesto', *Behavioral and Brain Sciences*, 20(4), pp. 537–596. doi: 10.1017/S0140525X97001581.

Rabaneda, L. G. *et al.* (2014) 'Neurexin Dysfunction in Adult Neurons Results in Autistic-like Behavior in Mice', *Cell Reports*, 8(2), pp. 338–346. doi: 10.1016/j.celrep.2014.06.022.

Rakic, P. (1995) 'A small step for the cell, a giant leap for mankind: a hypothesis of neocortical expansion during evolution', *Trends in Neurosciences*, 18(9), pp. 383–388.

Ranson, S. W. and Clark, S. L. (1959) *The anatomy of the nervous system: its development and function.* 10th Ed. W.B. Saunders Company.

Rapin, I. (1997) 'Autism', *New England Journal of Medicine*, 337(2), pp. 97–104. doi: 10.1056/NEJM199707103370206.

Rapin, I. and Dunn, M. (2003) 'Update on the language disorders of individuals on the autistic spectrum', *Brain and Development*, 25(3), pp. 166–172. doi: 10.1016/S0387-7604(02)00191-2.

Raposo, D. *et al.* (2012) 'Multisensory Decision-Making in Rats and Humans', *Journal of Neuroscience*, 32(11), pp. 3726–3735. doi: 10.1523/JNEUROSCI.4998-11.2012.

Rasalam, A. D. *et al.* (2005) 'Characteristics of fetal anticonvulsant syndrome associated autistic disorder', *Developmental Medicine and Child Neurology*, 47(8), pp. 551–555. doi: 10.1017/S0012162205001076.

Rasmussen, G. L. (1946) 'The olivary peduncle and other fiber projections of the superior olivary complex', *The Journal of Comparative Neurology*, 84(2), pp. 141–219. doi: 10.1002/cne.900840204.

Reale, R. A. and Imig, T. J. (1980) 'Tonotopic organization in auditory cortex of the cat', *The Journal of Comparative Neurology*, 192(2), pp. 265–291. doi: 10.1002/cne.901920207.

Redcay, E. (2008) 'The superior temporal sulcus performs a common function for social and speech perception: Implications for the emergence of autism', *Neuroscience and Biobehavioral Reviews*. Neurosci Biobehav Rev, pp. 123–142. doi: 10.1016/j.neubiorev.2007.06.004.

Reimer, J. *et al.* (2014) 'Pupil Fluctuations Track Fast Switching of Cortical States during Quiet Wakefulness', *Neuron*, 84(2), pp. 355–362. doi: 10.1016/j.neuron.2014.09.033.

Reisinger, S. *et al.* (2015) 'The Poly(I:C)-induced maternal immune activation model in preclinical neuropsychiatric drug discovery', *Pharmacology and Therapeutics*,

149, pp. 213–226. doi: 10.1016/j.pharmthera.2015.01.001.

Remington, A. *et al.* (2009) 'Selective attention and perceptual load in autism spectrum disorder', *Psychological Science*, 20(11), pp. 1388–1393. doi: 10.1111/j.1467-9280.2009.02454.x.

Rhode, W. S. and Greenberg, S. (1992) 'Physiology of the Cochlear Nuclei', in Popper, A. N. and Fay, R. R. (eds) *The Mammalian Auditory Pathway: Neurophysiology*. Springer, New York, NY, pp. 94–152. doi: 10.1007/978-1-4612-2838-7_3.

Richler, J. *et al.* (2007) 'Restricted and Repetitive Behaviors in Young Children with Autism Spectrum Disorders', *J Autism Dev Disord*, 37, pp. 73–85. doi: 10.1007/s10803-006-0332-6.

Rinaldi, T., Perrodin, C. and Markram, H. (2008) 'Hyper-connectivity and hyper-plasticity in the medial prefrontal cortex in the valproic acid animal model of autism', *Frontiers in Neural Circuits*, 2(4), pp. 1–7. doi: 10.3389/neuro.04.004.2008.

Rinaldi, T., Silberberg, G. and Markram, H. (2007) 'Hyperconnectivity of local neocortical microcircuitry induced by prenatal exposure to valproic acid', *Cerebral Cortex*, 18(4), pp. 763–770. doi: 10.1093/cercor/bhm117.

Ring, H. A. *et al.* (1999) 'Cerebral correlates of preserved cognitive skills in autism. A functional MRI study of Embedded Figures Task performance', *Brain*, 122(7), pp. 1305–1315. doi: 10.1093/brain/122.7.1305.

Roberts, T. P. L. *et al.* (2010) 'MEG detection of delayed auditory evoked responses in autism spectrum disorders: Towards an imaging biomarker for autism', *Autism Research*, 3(1), pp. 8–18. doi: 10.1002/aur.111.

Roberts, T. P. L. *et al.* (2011) 'Auditory magnetic mismatch field latency: A biomarker for language impairment in autism', *Biological Psychiatry*, 70(3), pp. 263–269. doi: 10.1016/j.biopsych.2011.01.015.

Robertson, C. E. *et al.* (2012) 'Atypical Integration of Motion Signals in Autism Spectrum Conditions', *PLoS ONE*. Edited by J. J. S. Barton, 7(11), p. e48173. doi: 10.1371/journal.pone.0048173.

Robertson, C. E. *et al.* (2014) 'Global motion perception deficits in autism are reflected as early as primary visual cortex', *Brain*, 137(9), pp. 2588–2599. doi: 10.1093/brain/awu189.

Robertson, C. E. and Baron-Cohen, S. (2017) 'Sensory perception in autism', *Nature Reviews Neuroscience*, 18(11), pp. 671–684. doi: 10.1038/nrn.2017.112.

Robertson, C. E., Ratai, E. M. and Kanwisher, N. (2016) 'Reduced GABAergic Action in the Autistic Brain', *Current Biology*, 26(1), pp. 80–85. doi:

10.1016/j.cub.2015.11.019.

Rodrigues-Dagaeff, C. *et al.* (1989) 'Functional organization of the ventral division of the medial geniculate body of the cat: Evidence for a rostro-caudal gradient of response properties and cortical projections', *Hearing Research*, 39(1–2), pp. 103–125. doi: 10.1016/0378-5955(89)90085-3.

Rogers, S. J., Hepburn, S. and Wehner, E. (2003) 'Parent Reports of Sensory Symptoms in Toddlers with Autism and Those with Other Developmental Disorders', *Journal of Autism and Developmental Disorders*, 33(6), pp. 631–642. doi: 10.1023/B:JADD.0000006000.38991.a7.

Rojas, D. C. *et al.* (2002) 'Smaller left hemisphere planum temporale in adults with autistic disorder', *Neuroscience Letters*, 328(3), pp. 237–240. doi: 10.1016/S0304-3940(02)00521-9.

Rojas, D. C. *et al.* (2005) 'Planum temporale volume in children and adolescents with autism', *Journal of Autism and Developmental Disorders*, 35(4), pp. 479–486. doi: 10.1007/s10803-005-5038-7.

Rojas, D. C. *et al.* (2008) 'Reduced neural synchronization of gamma-band MEG oscillations in first-degree relatives of children with autism', *BMC Psychiatry*, 8(1), p. 66. doi: 10.1186/1471-244X-8-66.

Rommelse, N. *et al.* (2015) 'Intelligence May Moderate the Cognitive Profile of Patients with ASD', *PLOS ONE*. Edited by S. Gilbert, 10(10), p. e0138698. doi: 10.1371/journal.pone.0138698.

Rosenberg, R. E. *et al.* (2009) 'Characteristics and concordance of autism spectrum disorders among 277 twin pairs', *Archives of Pediatrics and Adolescent Medicine*, 163(10), pp. 907–914. doi: 10.1001/archpediatrics.2009.98.

Rosenhall, U. *et al.* (1999) 'Autism and hearing loss', *Journal of Autism and Developmental Disorders*, 29(5), pp. 349–357. doi: 10.1023/A:1023022709710.

Rosenhall, U. *et al.* (2003) 'Autism and auditory brain stem responses', *Ear and Hearing*, 24(3), pp. 206–214. doi: 10.1097/01.AUD.0000069326.11466.7E.

Roth, G. and Dicke, U. (2005) 'Evolution of the brain and intelligence', *Trends in Cognitive Sciences*, 9(5), pp. 250–257.

Roth, G. and Dicke, U. (2012) 'Evolution of the brain and intelligence in primates', *Progress in Brain Research*, 195, pp. 413–430. doi: 10.1016/B978-0-444-53860-4.00020-9.

Rouiller, E. M. *et al.* (1989) 'Functional organization of the medial division of the medial geniculate body of the cat: Tonotopic organization, spatial distribution of response properties and cortical connections', *Hearing Research*, 39(1–2), pp. 127–

142. doi: 10.1016/0378-5955(89)90086-5.

Rouiller, E. M. (1997) 'Functional Organization of the Auditory Pathways', in Ehret, G. and Romand, R. (eds) *The Central Auditory System*. Oxford University Press.

Roullet, F. I. *et al.* (2010) 'Behavioral and molecular changes in the mouse in response to prenatal exposure to the anti-epileptic drug valproic acid', *Neuroscience*, 170(2), pp. 514–522. doi: 10.1016/j.neuroscience.2010.06.069.

Rubenstein, J. L. R. and Merzenich, M. M. (2003) 'Model of autism: increased ratio of excitation/inhibition in key neural systems', *Genes Brain Behav.*, 2(5), pp. 255–267.

Rudy, B. *et al.* (2011) 'Three groups of interneurons account for nearly 100% of neocortical GABAergic neurons', *Developmental Neurobiology*, 71(1), pp. 45–61. doi: 10.1002/dneu.20853.

Rumyantsev, O. I. *et al.* (2020) 'Fundamental bounds on the fidelity of sensory cortical coding', *Nature*, 580(7801), pp. 100–105. doi: 10.1038/s41586-020-2130-2.

Russell, G., Steer, C. and Golding, J. (2011) 'Social and demographic factors that influence the diagnosis of autistic spectrum disorders', *Soc Psychiatry Psychiatr Epidemiol*, 46, pp. 1283–1293. doi: 10.1007/s00127-010-0294-z.

Russell, I. J. (1987) 'The physiology of the organ of corti', *British Medical Bulletin*, 43(4), pp. 802–820. doi: 10.1093/oxfordjournals.bmb.a072219.

Russell, J. T. (2011) 'Imaging calcium signals in vivo: A powerful tool in physiology and pharmacology', *British Journal of Pharmacology*, 163(8), pp. 1605–1625. doi: 10.1111/j.1476-5381.2010.00988.x.

Russo, N. *et al.* (2009) 'Brainstem transcription of speech is disrupted in children with autism spectrum disorders', *Developmental Science*, 12(4), pp. 557–567. doi: 10.1111/j.1467-7687.2008.00790.x.

Russo, N. *et al.* (2010) 'Multisensory processing in children with autism: high-density electrical mapping of auditory-somatosensory integration', *Autism Research*, 3(5), pp. 253–267. doi: 10.1002/aur.152.

Russo, N. *et al.* (2012) 'Parameters of semantic multisensory integration depend on timing and modality order among people on the autism spectrum: Evidence from event-related potentials', *Neuropsychologia*, 50(9), pp. 2131–2141. doi: 10.1016/j.neuropsychologia.2012.05.003.

Russo, N. M. *et al.* (2008) 'Deficient brainstem encoding of pitch in children with Autism Spectrum Disorders', *Clinical Neurophysiology*, 119(8), pp. 1720–1731. doi: 10.1016/j.clinph.2008.01.108.

Rymar, V. V. and Sadikot, A. F. (2007) 'Laminar fate of cortical GABAergic interneurons is dependent on both birthdate and phenotype', *Journal of Comparative Neurology*, 501(3), pp. 369–380. doi: 10.1002/cne.21250.

Ryugo, D. K. and Weinberger, N. M. (1976) 'Corticofugal modulation of the medial geniculate body', *Experimental Neurology*, 51(2), pp. 377–391. doi: 10.1016/0014-4886(76)90262-4.

Sabers, A. *et al.* (2014) 'Long-term valproic acid exposure increases the number of neocortical neurons in the developing rat brain. A possible new animal model of autism', *Neuroscience Letters*, 580, pp. 12–16. doi: 10.1016/j.neulet.2014.07.036.

Sacco, R., Gabriele, S. and Persico, A. M. (2015) 'Head circumference and brain size in autism spectrum disorder: A systematic review and meta-analysis', *Psychiatry Research - Neuroimaging*, 234(2), pp. 239–251. doi: 10.1016/j.pscychresns.2015.08.016.

Saenz, M. and Langers, D. R. M. (2014) 'Tonotopic mapping of human auditory cortex', *Hearing Research*. Elsevier, pp. 42–52. doi: 10.1016/j.heares.2013.07.016.

Sahin, M. and Sur, M. (2015) 'Genes, circuits, and precision therapies for autism and related neurodevelopmental disorders', *Science*, 350(6263). doi: 10.1126/science.aab3897.

Sakata, S. and Harris, K. D. (2009) 'Laminar structure of spontaneous and sensory-evoked population activity in auditory cortex', *Neuron*, 64(3), pp. 404–418.

Saldaña, E. (1993) 'Descending Projections from the Inferior Colliculus to the Cochlear Nuclei in Mammals', in *The Mammalian Cochlear Nuclei*. Springer US, pp. 153–165. doi: 10.1007/978-1-4615-2932-3_13.

Saldaña, E. *et al.* (2009) 'Connections of the superior paraolivary nucleus of the rat: projections to the inferior colliculus', *Neuroscience*, 163(1), pp. 372–387. doi: 10.1016/j.neuroscience.2009.06.030.

Sanchez-Marin, F. J. and Padilla-Medina, J. A. (2008) 'A psychophysical test of the visual pathway of children with autism', *Journal of Autism and Developmental Disorders*, 38(7), pp. 1270–1277. doi: 10.1007/s10803-007-0507-9.

Sarachana, T. and Hu, V. W. (2013) 'Genome-wide identification of transcriptional targets of RORA reveals direct regulation of multiple genes associated with autism spectrum disorder', *Molecular Autism*, 4(1). doi: 10.1186/2040-2392-4-14.

Satterstrom, F. K. *et al.* (2020) 'Large-Scale Exome Sequencing Study Implicates Both Developmental and Functional Changes in the Neurobiology of Autism', *Cell*, 180(3), pp. 568-584.e23. doi: 10.1016/j.cell.2019.12.036.

Sayad, A. *et al.* (2017) 'Retinoic acid-related orphan receptor alpha (RORA) variants

are associated with autism spectrum disorder', *Metabolic Brain Disease*, 32(5), pp. 1595–1601. doi: 10.1007/s11011-017-0049-6.

Schmitzer-Torbert, N. *et al.* (2005) 'Quantitative measures of cluster quality for use in extracellular recordings', *Neuroscience*, 131(1), pp. 1–11. doi: 10.1016/j.neuroscience.2004.09.066.

Schneider, T. and Przewłocki, R. (2005) 'Behavioral alterations in rats prenatally to valproic acid: Animal model of autism', *Neuropsychopharmacology*, 30(1), pp. 80–89. doi: 10.1038/sj.npp.1300518.

Schoenemann, P. T., Sheehan, M. J. and Glotzer, L. D. (2005) 'Prefrontal white matter volume is disproportionately larger in humans than in other primates', *Nature Neuroscience*, 8(2), pp. 242–252. doi: 10.1038/nn1394.

Schreiner, C. E. and Langner, G. (1997) 'Laminar fine structure of frequency organization in auditory midbrain', *Nature*, 388(6640), pp. 383–386. doi: 10.1038/41106.

Schultz, R. T. *et al.* (2000) 'Abnormal ventral temporal cortical activity during face discrimination among individuals with autism and Asperger syndrome', *Archives of General Psychiatry*, 57(4), pp. 331–340. doi: 10.1001/archpsyc.57.4.331.

Schwartz, I. R. (1992) 'The Superior Olivary Complex and Lateral Lemniscal Nuclei', in Webster, D. B. and Fay, R. R. (eds) *The Mammalian Auditory Pathway: Neuroanatomy*. Springer, pp. 117–167.

Schwartzer, J. J. *et al.* (2013) 'Maternal immune activation and strain specific interactions in the development of autism-like behaviors in mice', *Translational Psychiatry*, 3(3), pp. e240–e240. doi: 10.1038/tp.2013.16.

Scott, S. K. and Johnsrude, I. S. (2003) 'The neuroanatomical and functional organization of speech perception', *Trends in Neurosciences*, 26(2), pp. 100–107. doi: 10.1016/S0166-2236(02)00037-1.

Seldon, H. L. (1981) 'Structure of human auditory cortex. I. Cytoarchitectonics and dendritic distributions', *Brain Research*, 229(2), pp. 277–294. doi: 10.1016/0006-8993(81)90994-X.

Semënov, M., Tamai, K. and He, X. (2005) 'SOST is a ligand for LRP5/LRP6 and a Wnt signaling inhibitor', *Journal of Biological Chemistry*, 280(29), pp. 26770–26775. doi: 10.1074/jbc.M504308200.

Semple, B. D. *et al.* (2013) 'Brain development in rodents and humans: Identifying benchmarks of maturation and vulnerability to injury across species', *Progress in Neurobiology*. NIH Public Access, pp. 1–16. doi: 10.1016/j.pneurobio.2013.04.001.

Semple, M. N. and Scott, B. H. (2003) 'Cortical mechanisms in hearing', *Current*

Opinion in Neurobiology, 13(2), pp. 167–173. doi: 10.1016/S0959-4388(03)00048-5.

Shah, A. and Frith, U. (1983) 'An Islet of Ability in Autistic Children: A Research Note', *Journal of Child Psychology and Psychiatry*, 24(4), pp. 613–620. doi: 10.1111/j.1469-7610.1983.tb00137.x.

Shah, A. and Frith, U. (1993) 'Why Do Autistic Individuals Show Superior Performance on the Block Design Task?', *Journal of Child Psychology and Psychiatry*, 34(8), pp. 1351–1364. doi: 10.1111/j.1469-7610.1993.tb02095.x.

Shallcross, R. *et al.* (2011) 'Child development following in utero exposure: Levetiracetam vs sodium valproate', *Neurology*, 76(4), pp. 383–389. doi: 10.1212/WNL.0b013e3182088297.

Shao, Y. *et al.* (2003) 'Fine mapping of autistic disorder to chromosome 15q11-q13 by use of phenotypic subtypes', *American Journal of Human Genetics*, 72(3), pp. 539–548. doi: 10.1086/367846.

Shoham, S., O'Connor, D. H. and Segev, R. (2006) 'How silent is the brain: Is there a "dark matter" problem in neuroscience?', *Journal of Comparative Physiology A*, 192(8), pp. 777–784. doi: 10.1007/s00359-006-0117-6.

Siegenthaler, J. A. *et al.* (2009) 'Retinoic Acid from the Meninges Regulates Cortical Neuron Generation', *Cell*, 139(3), pp. 597–609. doi: 10.1016/j.cell.2009.10.004.

Simms, M. L. *et al.* (2009) 'The anterior cingulate cortex in autism: Heterogeneity of qualitative and quantitative cytoarchitectonic features suggests possible subgroups', *Acta Neuropathologica*, 118(5), pp. 673–684. doi: 10.1007/s00401-009-0568-2.

Simonoff, E. *et al.* (2008) 'Psychiatric disorders in children with autism spectrum disorders: Prevalence, comorbidity, and associated factors in a population-derived sample', *Journal of the American Academy of Child and Adolescent Psychiatry*, 47(8), pp. 921–929. doi: 10.1097/CHI.0b013e318179964f.

Singh, S. P. (2014) 'Magnetoencephalography: Basic principles', *Annals of Indian Academy of Neurology*, 17, pp. 107–112. doi: 10.4103/0972-2327.128676.

Smart, I. H. M. (2002) 'Unique Morphological Features of the Proliferative Zones and Postmitotic Compartments of the Neural Epithelium Giving Rise to Striate and Extrastriate Cortex in the Monkey', *Cerebral Cortex*, 12(1), pp. 37–53.

Smith, K. S. and Graybiel, A. M. (2013) 'A dual operator view of habitual behavior reflecting cortical and striatal dynamics', *Neuron*, 79(2), pp. 361–374. doi: 10.1016/j.neuron.2013.05.038.

Smith, P. H. and Populin, L. C. (2001) 'Fundamental differences between the thalamocortical recipient layers of the cat auditory and visual cortices', *The Journal*

of Comparative Neurology, 436(4), pp. 508–519. doi: 10.1002/cne.1084.

Smith, S. E. P., Elliott, R. M. and Anderson, M. P. (2012) 'Maternal immune activation increases neonatal mouse cortex thickness and cell density', *Journal of Neuroimmune Pharmacology*, 7(3), pp. 529–532. doi: 10.1007/s11481-012-9372-1.

Snow, W. M., Hartle, K. and Ivanco, T. L. (2008) 'Altered morphology of motor cortex neurons in the VPA rat model of autism', *Developmental Psychobiology*, 50(7), pp. 633–639. doi: 10.1002/dev.20337.

Sohal, V. S. *et al.* (2009) 'Parvalbumin neurons and gamma rhythms enhance cortical circuit performance', *Nature*, 459(7247), pp. 698–702. doi: 10.1038/nature07991.

Sohal, V. S. and Rubenstein, J. L. R. (2019) 'Excitation-inhibition balance as a framework for investigating mechanisms in neuropsychiatric disorders', *Mol Psychiatry*, 24(9), pp. 1248–1257.

Song, Y.-H. *et al.* (2017) 'A Neural Circuit for Auditory Dominance over Visual Perception', *Neuron*, 93, pp. 940–954.

Soulières, I. *et al.* (2009) 'Enhanced visual processing contributes to matrix reasoning in autism', *Human Brain Mapping*, 30(12), pp. 4082–4107. doi: 10.1002/hbm.20831.

Soumiya, H., Fukumitsu, H. and Furukawa, S. (2011a) 'Prenatal immune challenge compromises development of upper-layer but not deeper-layer neurons of the mouse cerebral cortex', *Journal of Neuroscience Research*, 89(9), pp. 1342–1350. doi: 10.1002/jnr.22636.

Soumiya, H., Fukumitsu, H. and Furukawa, S. (2011b) 'Prenatal immune challenge compromises the normal course of neurogenesis during development of the mouse cerebral cortex', *Journal of Neuroscience Research*, 89(10), pp. 1575–1585. doi: 10.1002/jnr.22704.

Sowers, L. P. *et al.* (2013) 'Disruption of the non-canonical Wnt gene PRICKLE2 leads to autism-like behaviors with evidence for hippocampal synaptic dysfunction', *Molecular Psychiatry*, 18(10), pp. 1077–1089. doi: 10.1038/mp.2013.71.

Sparks, B. F. *et al.* (2002) 'Brain structural abnormalities in young children with autism spectrum disorder', *Neurology*, 59(2), pp. 184–192. doi: 10.1212/WNL.59.2.184.

Speed, A. *et al.* (2019) 'Cortical State Fluctuations across Layers of V1 during Visual Spatial Perception', *Cell Reports*, 26(11), pp. 2868-2874.e3. doi: 10.1016/J.CELREP.2019.02.045.

Spencer, J. *et al.* (2000) 'Motion processing in autism: Evidence for a dorsal stream

deficiency', *NeuroReport*, 11(12), pp. 2765–2767. doi: 10.1097/00001756-200008210-00031.

Srahna, M. *et al.* (2006) 'A Signaling Network for Patterning of Neuronal Connectivity in the Drosophila Brain', *PLoS Biology*. Edited by Y. N. Jan, 4(11), p. e348. doi: 10.1371/journal.pbio.0040348.

Srinivasan, R. and Nunez, P. L. (2012) 'Electroencephalography', in *Encyclopedia of Human Behavior: Second Edition*. Elsevier Inc., pp. 15–23. doi: 10.1016/B978-0-12-375000-6.00395-5.

Stein, B. E., Wilkinson, L. K. and Price, D. D. (1962) *Enhancement of Perceived Visual Intensity by Auditory Stimuli: A Psychophysical Analysis*. Simon & Craft.

Steinmetz, N. A. *et al.* (2019) 'Distributed coding of choice, action and engagement across the mouse brain', *Nature*, 576, pp. 266–273. doi: 10.1038/s41586-019-1787-x.

Steinmetz, N. A. *et al.* (2020) 'Neuropixels 2.0: A miniaturized high-density probe for stable, long-term brain recordings', *bioRxiv*, p. 2020.10.27.358291. doi: 10.1101/2020.10.27.358291.

Stevenson, R. A. *et al.* (2011) 'Discrete neural substrates underlie complementary audiovisual speech integration processes', *NeuroImage*, 55(3), pp. 1339–1345. doi: 10.1016/j.neuroimage.2010.12.063.

Stevenson, R. A. *et al.* (2014a) 'Evidence for Diminished Multisensory Integration in Autism Spectrum Disorders', *Journal of Autism and Developmental Disorders*, 44(12), pp. 3161–3167. doi: 10.1007/s10803-014-2179-6.

Stevenson, R. A. *et al.* (2014b) 'Multisensory temporal integration in autism spectrum disorders', *Journal of Neuroscience*, 34(3), pp. 691–697. doi: 10.1523/JNEUROSCI.3615-13.2014.

Stevenson, R. A. *et al.* (2016) 'Keeping time in the brain: Autism spectrum disorder and audiovisual temporal processing', *Autism Research*, 9(7), pp. 720–738. doi: 10.1002/aur.1566.

Stiebler, I. *et al.* (1997) 'The auditory cortex of the house mouse: Left-right differences, tonotopic organization and quantitative analysis of frequency representation', *Journal of Comparative Physiology - A Sensory, Neural, and Behavioral Physiology*, 181(6), pp. 559–571. doi: 10.1007/s003590050140.

Stiles, J. and Jernigan, T. L. (2010) 'The Basics of Brain Development', *Neurophychol Rev*, 20, pp. 327–348. doi: 10.1007/s11065-010-9148-4.

Stricanne, B., Andersen, R. A. and Mazzoni, P. (1996) 'Eye-centered, head-centered, and intermediate coding of remembered sound locations in area LIP', *Journal of*

Neurophysiology, 76(3), pp. 2071–2076. doi: 10.1152/jn.1996.76.3.2071.

Suga, N. (2008) 'Role of corticofugal feedback in hearing', *Journal of Comparative Physiology A: Neuroethology, Sensory, Neural, and Behavioral Physiology*. J Comp Physiol A Neuroethol Sens Neural Behav Physiol, pp. 169–183. doi: 10.1007/s00359-007-0274-2.

Suga, N. and Jen, P. H. S. (1976) 'Disproportionate tonotopic representation for processing CF-FM sonar signals in the mustache bat auditory cortex', *Science*, 194(4264), pp. 542–544. doi: 10.1126/science.973140.

Sumby, W. H. and Pollack, I. (1954) 'Visual Contribution to Speech Intelligibility in Noise', *Journal of the Acoustical Society of America*, 26(2), pp. 212–215. doi: 10.1121/1.1907309.

Svoboda, K. *et al.* (1997) 'In vivo dendritic calcium dynamics in neocortical pyramidal neurons', *Nature*, 385(6612), pp. 161–165. doi: 10.1038/385161a0.

Szelag, E. *et al.* (2004) 'Temporal processing deficits in high-functioning children with autism', *British Journal of Psychology*, 95(3), pp. 269–282. doi: 10.1348/0007126041528167.

Talwar, S. K., Musial, P. G. and Gerstein, G. L. (2001) 'Role of Mammalian Auditory Cortex in the Perception of Elementary Sound Properties', *Journal of Neurophysiology*, 85(6), pp. 2350–2358. doi: 10.1152/jn.2001.85.6.2350.

Tao, C. *et al.* (2015) 'Functional dissection of synaptic circuits: In vivo patch-clamp recording in neuroscience', *Frontiers in Neural Circuits*, 9(23), pp. 1–8. doi: 10.3389/fncir.2015.00023.

Tavassoli, T. *et al.* (2011) 'Psychophysical measures of visual acuity in autism spectrum conditions', *Vision Research*, 51(15), pp. 1778–1780. doi: 10.1016/j.visres.2011.06.004.

Tavassoli, T. *et al.* (2016) 'Altered tactile processing in children with autism spectrum disorder', *Autism Research*, 9(6), pp. 616–620. doi: 10.1002/aur.1563.

Tavassoli, T., Hoekstra, R. A. and Baron-Cohen, S. (2014) 'The Sensory Perception Quotient (SPQ): Development and validation of a new sensory questionnaire for adults with and without autism', *Molecular Autism*, 5(1), p. 29. doi: 10.1186/2040-2392-5-29.

Teder-Sälejärvi, W. A. *et al.* (2005) 'Auditory spatial localization and attention deficits in autistic adults', *Cognitive Brain Research*, 23(2–3), pp. 221–234. doi: 10.1016/j.cogbrainres.2004.10.021.

Teffer, K. and Semendeferi, K. (2012) 'Human prefrontal cortex: Evolution, development, and pathology.', in Hofman, M. A. and Falk, D. (eds) *Progress in Brain*

Research. Elsevier B.V., pp. 191–218. doi: 10.1016/B978-0-444-53860-4.00009-X.

Teo, J. L. *et al.* (2005) 'Specific inhibition of CBP/β-catenin interaction rescues defects in neuronal differentiation caused by a presenilin-1 mutation', *Proceedings of the National Academy of Sciences of the United States of America*, 102(34), pp. 12171–12176. doi: 10.1073/pnas.0504600102.

The Jackson Laboratory (2009) 'Breeding Strategies for Maintaining Colonies of Laboratory Mice - A Jackson Laboratory Resource Manual'.

The Jackson Laboratory (2021) *Body Weight Information for C57BL/6J*. Available at: https://www.jax.org/jax-mice-and-services/strain-data-sheet-pages/body-weight-chart-000664.

Thompson, A. *et al.* (2017) 'Impaired Communication Between the Motor and Somatosensory Homunculus Is Associated With Poor Manual Dexterity in Autism Spectrum Disorder', *Biological psychiatry*, 81, pp. 211–219. doi: 10.1016/j.biopsych.2016.06.020.

Thomson, A. M. (2010) 'Neocortical layer 6, a review', *Frontiers in Neuroanatomy*, 4(13), pp. 1–14.

Thorne, C. A. *et al.* (2010) 'Small-molecule inhibition of Wnt signaling through activation of casein kinase 1α', *Nature Chemical Biology*, 6(11), pp. 829–836. doi: 10.1038/nchembio.453.

Tian, L. *et al.* (2009) 'Imaging neural activity in worms, flies and mice with improved GCaMP calcium indicators', *Nature Methods*, 6(12), pp. 875–881. doi: 10.1038/nmeth.1398.

Tomchek, S. D. and Dunn, W. (2007) 'Sensory processing in children with and without autism: a comparative study using the short sensory profile', *American Journal of Occupational Therapy*, 61(2), pp. 190–200. doi: 10.5014/ajot.61.2.190.

Tommerdahl, M. *et al.* (2008) 'Absence of stimulus-driven synchronization effects on sensory perception in autism: Evidence for local underconnectivity?', *Behavioral and Brain Functions*, 4(19). doi: 10.1186/1744-9081-4-19.

Tora, D. *et al.* (2017) 'Cellular functions of the autism risk factor PTCHD1 in mice', *Journal of Neuroscience*, 37(49), pp. 11993–12005. doi: 10.1523/JNEUROSCI.1393-17.2017.

Torres-Reveron, J. and Friedlander, M. J. (2007) 'Properties of persistent postnatal cortical subplate neurons', *Journal of Neuroscience*, 27(37), pp. 9962–9974. doi: 10.1523/JNEUROSCI.1536-07.2007.

Traub, R. D. *et al.* (1996) 'A mechanism for generation of long-range synchronous fast oscillations in the cortex', *Nature*, 383(6601), pp. 621–224. doi:

10.1038/383621a0.

Tremblay, R., Lee, S. and Rudy, B. (2016) 'GABAergic Interneurons in the Neocortex: From Cellular Properties to Circuits', *Neuron*, 91, pp. 260–292. doi: 10.1016/j.neuron.2016.06.033.

Turner, J. N. *et al.* (1999) 'Cerebral astrocyte response to micromachined silicon implants', *Experimental Neurology*, 156(1), pp. 33–49. doi: 10.1006/exnr.1998.6983.

Uchida, N. and Mainen, Z. F. (2003) 'Speed and accuracy of olfactory discrimination in the rat', *Nature Neuroscience*, 6(11), pp. 1224–1229.

Ueno, Y. *et al.* (2019) 'A novel missense PTEN mutation identified in a patient with macrocephaly and developmental delay', *Human Genome Variation*, 6(1), pp. 1–4. doi: 10.1038/s41439-019-0056-8.

Ung, D. C. *et al.* (2017) 'Ptchd1 deficiency induces excitatory synaptic and cognitive dysfunctions in mouse', *Molecular Psychiatry*, 23(5). doi: 10.1038/mp.2017.39.

Vaccarino, F. M. *et al.* (2009) 'Regulation of Cerebral Cortical Size And Neuron Number by Fibroblast Growth Factors: Implications For Autism', *Journal of Autism and Developmental Disorders*, 39(3), pp. 511–520. doi: 10.1007/s10803-008-0653-8.

Valcanis, H. and Tan, S. S. (2003) 'Layer specification of transplanted interneurons in developing mouse neocortex', *Journal of Neuroscience*, 23(12), pp. 5113–5122. doi: 10.1523/jneurosci.23-12-05113.2003.

Vandenbroucke, M. W. G. *et al.* (2008) 'A neural substrate for atypical low-level visual processing in autism spectrum disorder', *Brain*, 131(4), pp. 1013–1024. doi: 10.1093/brain/awm321.

Varela-Nallar, L. and Inestrosa, N. C. (2013) 'Wnt signaling in the regulation of adult hippocampal neurogenesis', *Frontiers in Cellular Neuroscience*, 7(100), pp. 1–11. doi: 10.3389/fncel.2013.00100.

Velmeshev, D. *et al.* (2019) 'Single-cell genomics identifies cell type–specific molecular changes in autism', *Science*, 364(6441), pp. 685–689. doi: 10.1126/science.aav8130.

Verkhratsky, A., Krishtal, O. A. and Petersen, O. H. (2006) 'From Galvani to patch clamp: The development of electrophysiology', *Pflugers Archiv European Journal of Physiology*, 453(3), pp. 233–247. doi: 10.1007/s00424-006-0169-z.

Verly, M. *et al.* (2014) 'Altered functional connectivity of the language network in ASD: Role of classical language areas and cerebellum', *NeuroImage: Clinical*, 4, pp. 374–382. doi: 10.1016/j.nicl.2014.01.008.

Vignoli, A. *et al.* (2015) 'Autism spectrum disorder in tuberous sclerosis complex:

Searching for risk markers', *Orphanet Journal of Rare Diseases*, 10(1). doi: 10.1186/s13023-015-0371-1.

Voigts, J. *et al.* (2013) 'The flexDrive: an ultra-light implant for optical control and highly parallel chronic recording of neuronal ensembles in freely moving mice', *Frontiers in Systems Neuroscience*, 7(8), pp. 1–9. doi: 10.3389/fnsys.2013.00008.

Vulchanova, M. *et al.* (2012) 'Morphology in autism spectrum disorders: Local processing bias and language', *Cognitive Neuropsychology*, 29(7–8), pp. 584–600. doi: 10.1080/02643294.2012.762350.

Wagner, G. C. *et al.* (2006) 'A new neurobehavioral model of autism in mice: Pre- and postnatal exposure to sodium valproate', *Journal of Autism and Developmental Disorders*, 36(6), pp. 779–793. doi: 10.1007/s10803-006-0117-y.

Walcott, E. C., Higgins, E. A. and Desai, N. S. (2011) 'Synaptic and intrinsic balancing during postnatal development in rat pups exposed to valproic acid in utero', *Journal of Neuroscience*, 31(37), pp. 13097–13109. doi: 10.1523/JNEUROSCI.1341-11.2011.

Wang, J. *et al.* (2002) 'Gamma-aminobutyric acid circuits shape response properties of auditory cortex neurons', *Brain Research*, 944(1–2), pp. 219–231. doi: 10.1016/S0006-8993(02)02926-8.

Wang, J. *et al.* (2017) 'Increased Gray Matter Volume and Resting-State Functional Connectivity in Somatosensory Cortex and their Relationship with Autistic Symptoms in Young Boys with Autism Spectrum Disorder', *Frontiers in Physiology*, 8(588), pp. 1–10. doi: 10.3389/fphys.2017.00588.

Wang, Z. *et al.* (2010) 'Demethylation of Specific Wnt/β-Catenin Pathway Genes and its Upregulation in Rat Brain Induced by Prenatal Valproate Exposure', *The Anatomical Record: Advances in Integrative Anatomy and Evolutionary Biology*, 293(11), pp. 1947–1953. doi: 10.1002/ar.21232.

Webb, S. (2009) 'How retinoic acid makes motor neurons', *Nature Reports Stem Cells*. doi: 10.1038/stemcells.2009.86.

Wegiel, J. *et al.* (2010) 'The neuropathology of autism: Defects of neurogenesis and neuronal migration, and dysplastic changes', *Acta Neuropathologica*, 119(6), pp. 755–770. doi: 10.1007/s00401-010-0655-4.

Wehr, M. and Zador, A. M. (2003) 'Balanced inhibition underlies tuning and sharpens spike timing in auditory cortex', *Nature*, 426(6965), pp. 442–446. doi: 10.1038/nature02116.

Weisz, C. J. C. *et al.* (2012) 'Synaptic transfer from outer hair cells to type II afferent fibers in the rat cochlea', *Journal of Neuroscience*, 32(28), pp. 9528–9536. doi: 10.1523/JNEUROSCI.6194-11.2012.

Wen, Z. *et al.* (2017) 'Identification of autism-related MECP2 mutations by whole-exome sequencing and functional validation', *Molecular Autism*, 8(1), p. 43. doi: 10.1186/s13229-017-0157-5.

Wexler, E. M., Geschwind, D. H. and Palmer, T. D. (2008) 'Lithium regulates adult hippocampal progenitor development through canonical Wnt pathway activation', *Molecular Psychiatry*, 13(3), pp. 285–292. doi: 10.1038/sj.mp.4002093.

White, S., O'Reilly, H. and Frith, U. (2009) 'Big heads, small details and autism', *Neuropsychologia*, 47(5), pp. 1274–1281. doi: 10.1016/J.NEUROPSYCHOLOGIA.2009.01.012.

Whitehouse, A. J. O. and Bishop, D. V. M. (2008) 'Do children with autism "switch off" to speech sounds? An investigation using event-related potentials', *Developmental Science*, 11(4), pp. 516–524. doi: 10.1111/j.1467-7687.2008.00697.x.

Wichterle, H. *et al.* (2001) 'In utero fate mapping reveals distinct migratory pathways and fates of neurons born in the mammalian basal forebrain', *Development*, 128, pp. 3759–3771.

Wiebe, S. *et al.* (2019) 'Inhibitory interneurons mediate autism-associated behaviors via 4E-BP2', *Proceedings of the National Academy of Sciences of the United States of America*, 116(36), pp. 18060–18067. doi: 10.1073/pnas.1908126116.

Wilson, M. A. and McNaughton, B. L. (1993) 'Dynamics of the hippocampal ensemble code for space', *Science*, 261(5124), pp. 1055–1058. doi: 10.1126/science.8351520.

Wilson, T. W. *et al.* (2007) 'Children and Adolescents with Autism Exhibit Reduced MEG Steady-State Gamma Responses', *Biological Psychiatry*, 62(3), pp. 192–197. doi: 10.1016/j.biopsych.2006.07.002.

Winer, J. A. (1984a) 'Anatomy of layer IV in cat primary auditory cortex (AI)', *The Journal of Comparative Neurology*, 224(4), pp. 535–567. doi: 10.1002/cne.902240405.

Winer, J. A. (1984b) 'The non-pyramidal cells in layer III of cat primary auditory cortex (AI)', *The Journal of Comparative Neurology*, 229(4), pp. 512–530. doi: 10.1002/cne.902290406.

Winer, J. A. (1984c) 'The pyramidal neurons in layer III of cat primary auditory cortex (AI)', *The Journal of Comparative Neurology*, 229(4), pp. 476–496. doi: 10.1002/cne.902290404.

Winer, J. A. (1985) 'Structure of layer II in cat primary auditory cortex (AI)', *The Journal of Comparative Neurology*, 238(1), pp. 10–37. doi: 10.1002/cne.902380103.

Winer, J. A. *et al.* (2005) 'Auditory thalamocortical transformation: Structure and function', *Trends in Neurosciences*, 28(5), pp. 255–263. doi: 10.1016/j.tins.2005.03.009.

Winer, J. A. (2005) 'Decoding the auditory corticofugal systems', *Hearing Research*, 207, pp. 1–9. doi: 10.1016/j.heares.2005.06.007.

Winer, J. A., Diehl, J. J. and Larue, D. T. (2001) 'Projections of auditory cortex to the medial geniculate body of the cat', *J Comp Neurol*, 430(1), pp. 27–55.

Winer, J. A. and Larue, D. T. (1996) 'Evolution of GABAergic circuitry in the mammalian medial geniculate body', *Proceedings of the National Academy of Sciences of the United States of America*, 93(7), pp. 3083–3087. doi: 10.1073/pnas.93.7.3083.

Winer, J. A. and Schreiner, C. E. (2005) 'The central auditory system: A functional analysis', in *The Inferior Colliculus*. Springer New York, pp. 1–68. doi: 10.1007/0-387-27083-3_1.

Wolff, J. J. *et al.* (2012) 'Differences in white matter fiber tract development present from 6 to 24 months in infants with autism', *American Journal of Psychiatry*, 169(6), pp. 589–600. doi: 10.1176/appi.ajp.2011.11091447.

Wong, A. B. and Borst, J. G. G. (2019) 'Tonotopic and non-auditory organization of the mouse dorsal inferior colliculus revealed by two-photon imaging', *eLife*, 8, pp. 1–50. doi: 10.7554/eLife.49091.

Wong, F. K. *et al.* (2018) 'Pyramidal cell regulation of interneuron survival sculpts cortical networks', *Nature*, 557(7707), pp. 668–673. doi: 10.1038/s41586-018-0139-6.

Wood, A. G. *et al.* (2014) 'Altered cortical thickness following prenatal sodium valproate exposure', *Annals of Clinical and Translational Neurology*, 1(7), pp. 497–501. doi: 10.1002/acn3.74.

Workman, A. D. *et al.* (2013) 'Modeling Transformations of Neurodevelopmental Sequences across Mammalian Species', *Journal of Neuroscience*, 33(17), pp. 7368–7383. doi: 10.1523/JNEUROSCI.5746-12.2013.

Worrell, G. A., Stead, M. and Cascino, G. D. (2008) 'Electrocorticography', in *Handbook of Clinical Neurophysiology*. Elsevier, pp. 141–149. doi: 10.1016/S1567-4231(07)08007-0.

Wright, B. *et al.* (2012) 'Gamma activation in young people with autism spectrum disorders and typically-developing controls when viewing emotions on faces', *PLoS ONE*, 7(7). doi: 10.1371/journal.pone.0041326.

Xu, Q. *et al.* (2004) 'Origins of Cortical Interneuron Subtypes', *Journal of*

Neuroscience, 24(11), pp. 2612–2622. doi: 10.1523/JNEUROSCI.5667-03.2004.

Xu, X., Roby, K. D. and Callaway, E. M. (2010) 'Immunochemical characterization of inhibitory mouse cortical neurons: Three chemically distinct classes of inhibitory cells', *Journal of Comparative Neurology*, 518(3), pp. 389–404. doi: 10.1002/cne.22229.

Yamaguchi, M. *et al.* (2016) 'Neural stem cells and neuro/gliogenesis in the central nervous system: understanding the structural and functional plasticity of the developing, mature, and diseased brain', *Journal of Physiological Sciences*. Springer Tokyo, pp. 197–206. doi: 10.1007/s12576-015-0421-4.

Ye, T. *et al.* (2015) 'Emerging roles of axin in cerebral cortical development', *Frontiers in Cellular Neuroscience*, 9(217), pp. 1–8.

Zdebik, A. A., Wangemann, P. and Jentsch, T. J. (2009) 'Potassium ion movement in the inner ear: Insights from genetic disease and mouse models', *Physiology*, 24(5), pp. 307–316. doi: 10.1152/physiol.00018.2009.

Zechner, D. *et al.* (2007) 'Bmp and Wnt/β-catenin signals control expression of the transcription factor Olig3 and the specification of spinal cord neurons', *Developmental Biology*, 303(1), pp. 181–190. doi: 10.1016/j.ydbio.2006.10.045.

Zerbo, O. *et al.* (2015) 'Maternal Infection During Pregnancy and Autism Spectrum Disorders', *Journal of Autism and Developmental Disorders*, 45(12), pp. 4015–4025. doi: 10.1007/s10803-013-2016-3.

Zhang, K. and Sejnowski, T. J. (2000) 'A universal scaling law between gray matter and white matter of cerebral cortex', *Proceedings of the National Academy of Sciences of the United States of America*, 97(10), pp. 5621–5626. doi: 10.1073/pnas.090504197.

Zhang, M. *et al.* (2010) 'Smad3 prevents β-catenin degradation and facilitates β-catenin nuclear translocation in chondrocytes', *Journal of Biological Chemistry*, 285(12), pp. 8703–8710.

Zhao, H. *et al.* (2019) 'Maternal valproic acid exposure leads to neurogenesis defects and autism-like behaviors in non-human primates', *Translational Psychiatry*, 9(1), pp. 1–13. doi: 10.1038/s41398-019-0608-1.

Zheng, Z. *et al.* (2016) 'Blood Glutamate Levels in Autism Spectrum Disorder: A Systematic Review and Meta-Analysis', *PLOS ONE*. Edited by K. Hashimoto, 11(7), p. e0158688. doi: 10.1371/journal.pone.0158688.

Zhou, X. L. *et al.* (2007) 'Association of adenomatous polyposis coli (APC) gene polymorphisms with autism spectrum disorder (ASD)', *American Journal of Medical Genetics, Part B: Neuropsychiatric Genetics*, 144(3), pp. 351–354. doi:

10.1002/ajmg.b.30415.

Zieger, E. and Schubert, M. (2017) ‘New Insights Into the Roles of Retinoic Acid Signaling in Nervous System Development and the Establishment of Neurotransmitter Systems’, *International Review of Cell and Molecular Biology*, 330, pp. 1–84. doi: 10.1016/bs.ircmb.2016.09.001.

Zikopoulos, B. and Barbas, H. (2010) ‘Changes in prefrontal axons may disrupt the network in autism’, *Journal of Neuroscience*, 30(44), pp. 14595–14609. doi: 10.1523/JNEUROSCI.2257-10.2010.